CZECH TECHNICAL UNIVERSITY IN PRAGUE

Faculty of Electrical Engineering

Department of Radioelectronics

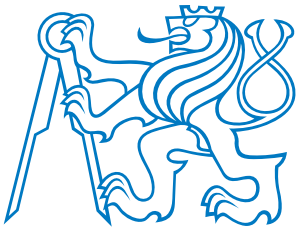

Wireless (Physical Layer) Network Coding Design for Parametric Channels and Systems with Partial Hierarchical Side-Information

Doctoral Thesis

Ing. Tomáš Uřičář

Prague, 2013

Ph.D. Programme: Electrical Engineering and Information Technology
Branch of Study: Radioelectronics

Supervisor: Prof. Ing. Jan Sýkora, CSc.

Abstract

Physical layer (PHY) processing algorithms (including modulation, coding, signal processing etc.) are undoubtedly the real driving force of wireless communication systems. Only these algorithms interact directly with the physical world, trying to fully exploit the available natural resources in wireless communication channels. Consequently, it is not surprising that every improvement in performance of contemporary communication systems is usually tightly connected with a particular advance in physical layer processing algorithms.

During the last few decades, the progress in the physical layer processing research has already pushed the achievable performance of single-link (point-to-point) communication towards the capacity limits forecasted by Claude Shannon in his pioneering work. Development of turbo coding principles, together with sophisticated iterative decoding techniques and space-time coding for Multiple-Input Multiple-Output channels has indeed reduced the gap to the fundamental capacity of wireless channels to an almost negligible value. Taking this fact into account, it could create a false feeling that the research in PHY processing has already exhausted its potential, reaching the limits imposed by the physical world, and thus having no space for further enhancement. Obviously, such conclusion is justified only if we limit our scope to the point-to-point communication. However, if we extend the scope to *wireless communication networks*, where countless nodes, terminals or devices are mutually interacting and communicating in a complicated multi-source, multi-node environment, a tremendous number of complex research problems, questions and challenges quickly arise. Here the *network multi-user information theory* gives us an important lesson. Contemporary wireless networks based on *orthogonal* sharing (e.g. TDMA, FDMA, etc.) are *not* fully exploiting the potential of shared wireless medium and hence a complete revamp of conventional (point-to-point) PHY processing algorithms and techniques is foreseen to be required to harness all the performance benefits accompanied with the *non-orthogonal* sharing of wireless medium. The up-and-coming *Wireless (Physical layer) Network Coding (WNC) techniques*, implemented directly at PHY, possess undoubtedly a great potential to gather these promising performance improvements.

The power of WNC lies mainly in an efficient exploitation of the *inherent properties of wireless channels* (broadcast nature and inherent combining of electromagnetic waves at receiver antenna(s)), which provide a fertile ground for an extension of conventional (wireline) *network-coding principles* to wireless channels. The interference is no longer considered as harmful in WNC-based systems, and hence it is exploited rather than avoided. Since WNC operates directly at PHY, huge performance gains can be achieved, when compared to conventional routing (e.g. doubled throughput in a simple bi-directional relay channel). Unfortunately, the specific properties of wireless channels are not always only beneficial, as they introduce many novel research problems which makes a direct implementation of WNC in wireless systems quite challenging.

First, the *inherent parametrization* of wireless channels (e.g. channel gain) significanlty influences the achievable performance of WNC systems, and hence the PHY processing algorithms must take the channel parametrization inherently into account, providing solutions robust to parametrization effects. Secondly, the inherent broadcast nature is to be exploited on channels with *potentially significantly different capacities*, forcing the PHY processing to cope with the problems associated with an *imperfect/partial*

transmission of information.

In this thesis we focus on these two specific open problems in WNC research, namely the WNC processing in *parametric channels* and WNC processing with *partial/imperfect hierarchical side information*. After a brief overview of general concepts of cooperative communications and WNC systems processing we provide a detailed discussion of our original contributions to the research in these interesting research areas, including the design of linear modulation schemes for *parameteric Hierarchical Decode & Forward systems* and the design/analysis of various aspects of *partial/imperfect Hierarchical Side Information processing* in WNC systems.

Acknowledgments

I would like to thank my supervisor Prof. Ing. Jan Sýkora, CSc. for giving me the opportunity to join DiRaC research group and perform research in the field of wireless digital communication theory under his invaluable support and supervision. A special gratitude goes to my parents and my fiancée who supported and encouraged me during my PhD study.

Proclamation

The presented thesis "*Wireless (Physical Layer) Network Coding Design for Parametric Channels and Systems with Partial Hierarchical Side-Information*" is based on my research work carried out at the DiRaC Research Group, Department of Radioelectronics, Faculty of Electrical Engineering, Czech Technical University in Prague.

Contents

Contents I

List of Figures VII

List of Tables XI

List of Abbreviations XIII

I Introduction 1

1 Introduction 3
1.1 Thesis outline . . . 4
1.1.1 Aims and scope of the thesis . . . 4
1.1.2 Contents . . . 4
1.2 Publications . . . 4
1.3 Grants . . . 6
1.4 Awards and recognitions . . . 7
1.5 International experience . . . 7
1.6 Other professional activities . . . 7

2 Cooperation in wireless networks 9
2.1 Brief overview of general concepts . . . 10
2.1.1 Relays and relaying . . . 10
2.1.2 Network coding paradigm . . . 11
2.1.3 Capacity bounds . . . 12
2.1.4 Half-duplex constraint . . . 13
2.2 Three-terminal relay channel . . . 13
2.2.1 System model . . . 13
2.2.2 Relaying strategies . . . 14
2.2.3 Capacity bounds of the relay channel . . . 14
2.3 Bi-directional relaying . . . 16
2.3.1 Two-way relay channel . . . 16
2.3.2 Bi-directional relaying strategies . . . 17
2.3.3 Wireless (Physical Layer) Network Coding . . . 18

3 Wireless (Physical Layer) Network Coding 21
3.1 HDF relaying in 2-WRC . . . 21
3.1.1 System model . . . 21

3.1.2 MAC phase – source nodes transmission . . . 22
3.1.3 HDF relay processing . . . 23
3.1.3.1 HDF, DNF, CaF: terminology . . . 24
3.1.4 BC phase and destination decoding . . . 24
3.1.5 Uncoded example . . . 25
3.1.5.1 MAC phase . . . 26
3.1.5.2 eXclusive mapping at the relay and BC phase . . . 26
3.1.5.3 Destination decoding . . . 27
3.2 Selected open research problems in WNC . . . 27
3.2.1 HDF in parametric channels . . . 28
3.2.2 Partial HSI processing . . . 29
3.3 Further reading . . . 30
3.3.1 Adaptive eXclusive mapping . . . 30
3.3.2 Lattice codes . . . 32
3.3.3 Real-world implementation of HDF/WNC . . . 32
3.3.4 Further research directions . . . 33

II WNC in parametric wireless channels 35

4 Introduction 37
4.1 Summary of contributions . . . 37
4.2 System model . . . 39

5 Multi-dimensional constellation design 41
5.1 Design criteria for multi-dimensional HXC with parameter invariant decision regions . . . 41
5.1.1 Introduction . . . 41
5.1.2 Definitions and sytem model . . . 41
5.1.3 Parametric Hierarchical Exclusive Code in 2-WRC . . . 42
5.1.3.1 Relay processing in parametric 2-WRC . . . 42
5.1.3.2 HDF decoder decision regions . . . 42
5.1.3.3 Pairwise PHXC design criteria . . . 43
5.1.4 Design criteria for full PHXC codebooks . . . 44
5.1.4.1 E-PHXC design criteria . . . 44
5.1.4.2 E-PHXC decoder decision regions . . . 45
5.1.4.3 E-PHXC with identical codebooks . . . 47
5.1.4.4 E-PHXC with non-identical codebooks . . . 48
5.1.4.5 Example binary alphabet construction algorithm . . . 49
5.1.5 Min-distance based design criteria for higher-order codebooks . . . 50
5.1.5.1 Minimum hierarchical distance . . . 50
5.1.5.2 Modified design criteria . . . 51
5.1.5.3 Performance evaluation . . . 52
5.1.6 Discussion of results . . . 52
5.2 Geometrical approach to the multi-dimensional HXC design . . . 54
5.2.1 Introduction . . . 54
5.2.2 PI-HXA Design . . . 55
5.2.2.1 Principles of geometrical design . . . 55
5.2.2.2 Two-mode relay processing . . . 55
5.2.2.3 An example of 2-dimensional PI-HXA . . . 56

5.2.3 Numerical Results . . . 58
5.2.3.1 Mutual information (capacity) . . . 58
5.2.3.2 Minimum distance . . . 60
5.2.4 Discussion of results . . . 60

6 Hierarchical distance analysis **61**
6.1 Introduction . . . 61
6.2 Euclidean distance analysis . . . 61
6.2.1 Minimum hierarchical distance . . . 61
6.2.2 Bounds of the hierarchical distance . . . 63
6.3 Parametric HXA design . . . 64
6.3.1 HXA design in $\mathbb{C}^1$ . . . 66
6.3.2 Construction algorithm for 2-dimensional alphabets . . . 67
6.4 Numerical evaluations . . . 68
6.5 Discussion of results . . . 68

7 Non-uniform 2-slot constellations **73**
7.1 Introduction . . . 73
7.1.1 Summary of minimum hierarchical distance analysis . . . 73
7.2 Non-uniform 2-slot alphabets . . . 74
7.2.1 Parabolic behaviour analysis . . . 74
7.2.2 Alphabet design algorithm . . . 76
7.3 Numerical evaluation . . . 77
7.3.1 Minimum hierarchical distance . . . 77
7.3.2 Symbol error rate . . . 77
7.4 Discussion of results . . . 79

III WNC processing with imperfect/partial HSI **81**

8 Introduction **83**
8.1 Summary of contributions . . . 84
8.2 System model . . . 84
8.2.1 MAC phase – source nodes transmission . . . 84
8.2.2 Relay processing . . . 85
8.2.3 BC phase and destination decoding . . . 85

9 Superposition coding for wireless butterfly network with partial HSI **87**
9.1 Introduction . . . 87
9.1.1 Definitions and modification of system model . . . 88
9.2 Superposition coding in wireless butterfly network . . . 89
9.2.1 SC relaying scheme . . . 89
9.2.1.1 Relay processing . . . 89
9.2.1.2 Destination processing . . . 90
9.2.2 Information-theoretic bounds for SC rates . . . 91
9.2.3 Optimization of SC parameter α . . . 92
9.2.4 Reference schemes for perfect & zero HSI . . . 92
9.3 Maximal two-way rates . . . 93
9.4 Discussion of results . . . 93

10 WNC in wireless butterfly network: Maximal sum-rate analysis **101**
10.1 Introduction . . . 101
10.2 Symmetric wireless butterfly network . . . 101
10.2.1 Definitions and assumptions . . . 102
10.2.2 Sum-rate performance . . . 102
10.3 Relaying strategies in WBN with limited HSI . . . 103
10.3.1 WBN with perfect and partial HSI . . . 104
10.3.2 3-step scheme . . . 104
10.3.2.1 Decode & Forward . . . 104
10.3.3 2-step schemes . . . 108
10.3.3.1 Amplify & Forward . . . 109
10.3.3.2 Joint Decode & Forward . . . 110
10.3.3.3 Hierarchical Decode & Forward . . . 112
10.3.4 Performance comparison . . . 113
10.3.4.1 Maximal sum-rates . . . 113
10.3.4.2 Relative length of communication steps . . . 114
10.4 SC-based HDF scheme . . . 114
10.4.1 Implementation of HDF_{SC} in WBN . . . 118
10.4.1.1 HDF_{SC} relaying strategy . . . 119
10.4.1.2 $\text{HDF}_{\text{SC}}^{\text{IC}}$ relaying strategy . . . 122
10.5 Discussion of results . . . 122

11 Design of eXclusive mapper for wireless butterfly network **125**
11.1 Introduction . . . 125
11.2 Summary of definitions and assumptions . . . 125
11.2.1 Relay output eXclusive mapping . . . 126
11.3 The role of HSI . . . 126
11.4 HNC mapper design . . . 128
11.4.1 Source alphabet partitioning . . . 129
11.5 Numerical evaluations . . . 130
11.5.1 Adaptive butterfly network performance . . . 131
11.6 Discussion of results . . . 138

12 NuT constellations for imperfect HSI relaying **139**
12.1 Introduction . . . 139
12.2 WBN with HDF strategy . . . 139
12.2.1 Relay output alphabet cardinality . . . 140
12.3 Non-uniform 2-slot alphabets . . . 140
12.3.1 Performance as the HSI link alphabet . . . 141
12.4 Numerical results . . . 142
12.4.1 Minimal cardinality relaying . . . 143
12.4.2 Extended cardinality relaying . . . 143
12.5 Discussion of results . . . 144

IV Conclusions **145**

13 Conclusions and future research directions **147**
13.1 Summary of contributions . . . 147
13.2 Future research directions . . . 148

Bibliography **150**

Appendix I: IEEE Reviewer Appreciation **159**

List of Figures

Figure 2.1 Simple example of NC. . . . 11
Figure 2.2 Multiple Access Relay Channel with network coding at the relay. . . . 11
Figure 2.3 A network with two sets (S, S^C) of nodes separated by a cut C. . . . 13
Figure 2.4 Three-terminal relay channel. . . . 14
Figure 2.5 Possible models of relaying in the three-terminal relay channel. . . . 15
Figure 2.6 General full-duplex relay channel. . . . 15
Figure 2.7 General half-duplex relay channel (BC and MAC phase). . . . 15
Figure 2.8 Two-way relay channel (2-WRC). . . . 16
Figure 2.9 Bi-directional communication schemes in 2-WRC. . . . 17
Figure 2.10 MAC and BC phase of WNC schemes. . . . 18

Figure 3.1 2-WRC with Hierarchical Side Information (HSI). . . . 22
Figure 3.2 MAC phase: 2-WRC with uncoded QPSK. . . . 25
Figure 3.3 Relay eXclusive mapping: 2-WRC with uncoded QPSK. . . . 26
Figure 3.4 Destination decoding: 2-WRC with uncoded QPSK. . . . 27
Figure 3.5 Impact of channel parametrization: 2-WRC with uncoded QPSK. . . . 28
Figure 3.6 Wireline vs. wireless 5-node Butterfly Network. . . . 29
Figure 3.7 HDF signal flow in Wireless Butterfly Network (WBN). . . . 30
Figure 3.8 Perfect (full) HSI processing in WBN. . . . 31
Figure 3.9 Zero HSI processing in WBN. . . . 31
Figure 3.10 Partial HSI processing in WBN. . . . 32

Figure 4.1 Layered Hierarchical eXclusive Code. . . . 37
Figure 4.2 2-WRC with HSI. . . . 38
Figure 4.3 Basic principle of HDF processing in 2-WRC. . . . 38

Figure 5.1 Visualization of the pairwise boundary in the constellation space. . . . 43
Figure 5.2 HDFD decision regions shape example ($\mathbb{R}^2$ codebook). . . . 43
Figure 5.3 Pairwise boundaries shift ($\mathbb{R}^2$ codebook). . . . 44
Figure 5.4 Impact of E-PHXC design criteria on non-critical ($\mathscr{R}^{kl} \notin \mathscr{S}_{\mathrm{CB}}$) boundaries. . . . 46
Figure 5.5 Min-distance performance (QPSK and 4-ary example codebook). . . . 52
Figure 5.6 Min-distance performance (8-PSK and 8-ary example codebook). . . . 53
Figure 5.7 Min-distance performance (16-QAM and 16-ary example codebook). . . . 53
Figure 5.8 EPHXC vs generalized PI-HXA design. . . . 54
Figure 5.9 Constellation space patterns in 2-mode relay processing. . . . 56
Figure 5.10 Constellation space patterns ($\mathscr{U}_{\mathrm{Re}}^{\prime i}$) for the example PI-HXA. . . . 57
Figure 5.11 Design of a suitable hierarchical eXclusive mapper $\mathscr{X}_s(s_A^i, s_B^j)$ for PI-HXA. . . . 57
Figure 5.12 Capacity (mutual information) of PI-HXA. . . . 59
Figure 5.13 Minimum squared distance performance of PI-HXA. . . . 59

Figure 6.1 Minimum hierarchical distance $d^2_{\min}(|h|)$ for BPSK alphabet. 64
Figure 6.2 Minimum hierarchical distance $d^2_{\min}(|h|)$ for QPSK alphabet. 65
Figure 6.3 Minimum hierarchical distance $d^2_{\min}(|h|)$ for 8-PSK alphabet. 65
Figure 6.4 Minimum hierarchical distance $d^2_{\min}(|h|)$ for 16-QAM alphabet. 66
Figure 6.5 Hierarchical symbol pairs vulnerable to eXclusive law failures. 67
Figure 6.6 Minimum hierarchical distance performance for QPSK and 4-ary P-HXA. . . . 68
Figure 6.7 Minimum hierarchical distance performance for 8-PSK and 8-ary P-HXA. . . . 69
Figure 6.8 Minimum hierarchical distance performance for 16-QAM and 16-ary P-HXA. . 69
Figure 6.9 Minimum hierarchical distance $d^2_{\min}(|h|)$ for P-HXA with QPSK alphabet. . . . 70
Figure 6.10 Minimum hierarchical distance $d^2_{\min}(|h|)$ for P-HXA with 8-PSK alphabet. . . . 70
Figure 6.11 Minimum hierarchical distance $d^2_{\min}(|h|)$ for P-HXA with 16-QAM alphabet. . 71

Figure 7.1 Set of min-distance parabolas (QPSK and NuT$(\mathrm{QPSK};1)$). 75
Figure 7.2 Probability distribution of channel parameter $|h| \leq 1$. 75
Figure 7.3 MHD $d^2_{\min}(|h|)$ and min-distance parabolas (NuT$(\mathrm{QPSK};0.25)$). 75
Figure 7.4 2-source NuT alphabet supersymbols. 76
Figure 7.5 MHD $d^2_{\min}(h)$ of NuT$(\mathrm{QPSK};1)$ and NuT$(\mathrm{QPSK};0.25)$ alphabets. 77
Figure 7.6 MHD $d^2_{\min}(h)$ of NuT$(8\mathrm{PSK};1)$ and NuT$(8\mathrm{PSK};0.1)$ alphabets. 78
Figure 7.7 H-SER of NuT$(\mathrm{QPSK};1)$ and NuT$\left(\mathrm{QPSK};s_f\right)$ alphabets. 78
Figure 7.8 H-SER of NuT$(8\mathrm{PSK};1)$ and NuT$\left(8\mathrm{PSK};s_f\right)$ alphabets. 79

Figure 8.1 HDF signal flow in Wireless Butterfly Network. 83
Figure 8.2 Basic principle of WNC processing in WBN. 86

Figure 9.1 Principle of SC-based relaying in WBN. 88
Figure 9.2 Principles of the decoding process in SC-based WBN. 91
Figure 9.3 Maximal 2-way rate & optimized rates R_b, R_s ($\gamma_1 = 10$ dB, $\gamma_3 = 30$ dB). 94
Figure 9.4 Maximal 2-way rate & optimized rates R_b, R_s ($\gamma_1 = 20$ dB, $\gamma_3 = 30$ dB). 95
Figure 9.5 Maximal 2-way rate & optimized rates R_b, R_s ($\gamma_1 = 30$ dB, $\gamma_3 = 30$ dB). 96
Figure 9.6 Maximal 2-way rate & optimized rates R_b, R_s ($\gamma_1 = 30$ dB, $\gamma_3 = 20$ dB). 97
Figure 9.7 Maximal 2-way rate & optimized rates R_b, R_s ($\gamma_1 = 30$ dB, $\gamma_3 = 10$ dB). 98
Figure 9.8 Comparison of maximal 2-way rates of the SC scheme. 99

Figure 10.1 Half-duplex communication in symmetric WBN. 102
Figure 10.2 Maximal DF sum-rates for perfect ($R^{DF^2}_{\mathrm{sum}}$) and partial ($R^{DF^{2'}}_{\mathrm{sum}}$) HSI processing. . 108
Figure 10.3 Operational regions of HDF strategy. 113
Figure 10.4 DF, AF, JDF and HDF: sum-rates in WBN ($\gamma_1 = 10$ dB, $\gamma_3 = 30$ dB). 115
Figure 10.5 DF, AF, JDF and HDF: sum-rates in WBN ($\gamma_1 = 30$ dB, $\gamma_3 = 10$ dB). 115
Figure 10.6 DF, AF, JDF and HDF: sum-rates in WBN ($\gamma_1 = 30$ dB, $\gamma_3 = 30$ dB). 116
Figure 10.7 DF, AF, JDF and HDF: n_{II} in WBN ($\gamma_1 = 10$ dB, $\gamma_3 = 30$ dB). 116
Figure 10.8 DF, AF, JDF and HDF: n_{II} in WBN ($\gamma_1 = 30$ dB, $\gamma_3 = 10$ dB). 117
Figure 10.9 DF, AF, JDF and HDF: n_{II} in WBN ($\gamma_1 = 30$ dB, $\gamma_3 = 30$ dB). 117
Figure 10.10 Principle of $\mathrm{HDF}_{\mathrm{SC}}$ processing in WBN. 118
Figure 10.11 Optimized values of α, r_b, r_s as a function of γ_2 ($\gamma_1 = \gamma_3 = 30$ dB). 121
Figure 10.12 Comparison of the upper-bound of the $\mathrm{HDF}_{\mathrm{SC}}$ sum-rates with R^{HDF}_{sum}. 121
Figure 10.13 Comparison of the upper-bounds of sum-rates in $\mathrm{HDF}_{\mathrm{SC}}$ and $\mathrm{HDF}^{\mathrm{IC}}_{\mathrm{SC}}$. 122

Figure 11.1 SNRs of individual links in WBN with HDF strategy. 126
Figure 11.2 Butterfly network with perfect HSI links ($c^A_{\mathrm{HSI}} = c^B_{\mathrm{HSI}} = 2$). 127
Figure 11.3 Butterfly network with unreliable/missing HSI links ($c^A_{\mathrm{HSI}} = c^B_{\mathrm{HSI}} = 0$). 127

Figure 11.4 Butterfly network with imperfect HSI links ($c^A_{\mathrm{HSI}} = c^b_{\mathrm{HSI}} = 1$). 127
Figure 11.5 HNC matrix partitioning for $c^A_{\mathrm{HSI}} = 2$, $c^B_{\mathrm{HSI}} = 1$ and $c^A_{\mathrm{HSI}} = c^B_{\mathrm{HSI}} = 1$. 128
Figure 11.6 Partitioning of QPSK source constellation alphabet. 130
Figure 11.7 Partitioning of the 8PSK source constellation alphabet. 131
Figure 11.8 BC phase capacity (min. map, $\mathscr{A}_s = \mathrm{QPSK}$, $\mathscr{A}_s^R = \mathrm{QPSK}$). 132
Figure 11.9 BC phase capacity (full map, $\mathscr{A}_s = \mathrm{QPSK}$, $\mathscr{A}_s^R = \mathrm{16QAM}$). 132
Figure 11.10 BC phase capacity (ext. map, $\mathscr{A}_s = \mathrm{QPSK}$, $\mathscr{A}_s^R = \mathrm{8PSK}$). 133
Figure 11.11 BC phase capacity (ext. map, $\mathscr{A}_s = \mathrm{QPSK}$ & Ungerboeck, $\mathscr{A}_s^R = \mathrm{8PSK}$). . . . 133
Figure 11.12 BC phase capacity (min. map, $\mathscr{A}_s = \mathrm{8PSK}$, $\mathscr{A}_s^R = \mathrm{8PSK}$). 134
Figure 11.13 BC phase capacity (full map, $\mathscr{A}_s = \mathrm{8PSK}$, $\mathscr{A}_s^R = \mathrm{64QAM}$). 134
Figure 11.14 BC phase capacity (ext. map, $\mathscr{A}_s = \mathrm{8PSK}$, $\mathscr{A}_s^R = \mathrm{16QAM}$). 135
Figure 11.15 BC phase capacity (ext. map, $\mathscr{A}_s = \mathrm{8PSK}$ & Ungerboeck, $\mathscr{A}_s^R = \mathrm{16QAM}$). . . 135
Figure 11.16 BC phase capacity (ext. map, $\mathscr{A}_s = \mathrm{8PSK}$, $\mathscr{A}_s^R = \mathrm{32QAM}$). 136
Figure 11.17 BC phas capacity (ext. map, $\mathscr{A}_s = \mathrm{8PSK}$ & Ungerboeck, $\mathscr{A}_s^R = \mathrm{32QAM}$). . . . 136
Figure 11.18 Maximum achievable BC phase capacity ($\mathscr{A}_s = \mathrm{QPSK}$). 137
Figure 11.19 Maximum achievable BC phase capacity ($\mathscr{A}_s = \mathrm{8PSK}$). 137

Figure 12.1 WBN with NuT source constellations and extended cardinality relaying. 140
Figure 12.2 SNRs in WBN with HDF strategy. 141
Figure 12.3 Mutual information of $\mathscr{A}_s^A$ for $\mathrm{NuT}(\mathrm{QPSK}; 1)$ & $\mathrm{NuT}(\mathrm{QPSK}; 0.25)$. 142
Figure 12.4 Destination BER (minimal cardinality relaying ($M_R = 16$, $\mathscr{A}_s^R = \mathrm{16QAM}$)). . . 143
Figure 12.5 Destination BER (extended cardinality relaying ($M_R = 64$, $\mathscr{A}_s^R = \mathrm{64QAM}$)). . . 144

List of Tables

Table 5.1 Example of hierarchical codeword table ($|\mathscr{B}_A| = |\mathscr{B}_B| = N$). 42
Table 5.2 Example binary E-PHXC codebooks 49
Table 5.3 Example (non-orthogonal) binary E-PHXC codebooks 49
Table 5.4 Principles of the 2-mode relay processing 56

Table 6.1 Hierarchical symbol table ($\left|\mathscr{A}_s^A(.)\right| = \left|\mathscr{A}_s^B(.)\right| = M_s$). 62

Table 10.1 DF relaying scheme in perfect and partial HSI cases. 105
Table 10.2 JDF and HDF relaying schemes in perfect and partial HSI cases. 106

Table 11.1 Example HNC matrices $X_4^{(1)}$ and $X_4^{(2)}$. 129
Table 11.2 Example HNC matrices $X_8^{(1)}$ and $X_8^{(2)}$. 130

List of Abbreviations

2-WRC	2-Way Relay Channel / Bi-directional Relay Channel
AF	Amplify and Forward
ARQ	Automatic Repeat Request
AWGN	Additive White Gaussian Noise
BC	Broadcast
BER	Bit Error Rate
BN	Butterfly Network
BPSK	Binary Phase Shift Keying
CaF	Compute and Forward
CBS	Cauchy-Bunyakovskii-Schwartz
CF	Compress and Forward
CSE	Channel State Estimate
C-SI	Complementary-Side Information (see HSI)
DF	Decode and Forward
DNF	Denoise and Forward
EF	Estimate and Forward
E-PHXC	Extended Parametric Hierarchical eXclusive Code
FDMA	Frequency Division Multiple Access
HDF	Hierarchical Decode & Forward
HDFD	HDF decoder
HNC	Hierarchical Network Code
H-SER	Hierarchical Symbol Error Rate
HSI	Hierarchical Side Information
HXA	Hierarchical eXclusive Alphabet
HXC	Hierarchical eXclusive Code
IC	Interference Cancellation
JDF	Joint Decode and Forward
LDPC	Low Density Parity Check
LFP	Linear Fractional Programming
L-HXC	Layered Hierarchical eXclusive Code
MAC	Multiple Access
MARC	Multiple Access Relay Channel
MHD	Minimum Hierarchical Distance
MIMO	Multiple-Input Multiple-Output
NC	Network Coding
NuT	Non-uniform 2-slot
OFDM	Orthogonal Frequency Division Multiplexing
P-HXA	Parametric Hierarchical eXclusive Alphabet

PHXC	Parametric Hierarchical eXclusive Code
PHY	Physical layer
PI-HXA	Parameter-Invariant Hierarchical eXclusive Alphabet
PSK	Phase Shift Keying
QAM	Quadrature Amplitude Modulation
QF	Quantize and Forward
QoS	Quality of Service
QPSK	Quaternary Phase Shift Keying
SC	Superposition Coding
SER	Symbol Error Rate
SNR	Signal to Noise Ratio
TDMA	Time Division Multiple Access
WBN	Wireless Butterfly Network
WNC	Wireless (Physical layer) Network Coding
XOR	eXclusive OR

Part I

Introduction

Chapter 1

Introduction

"None is so great that he needs no help, and none is so small that he cannot give it."

King Solomon

Although the fundamental finding that even egoists can sustain cooperation (provided the structure of their environment allows for repeated interactions) was intended originally for the people [1], numerous research results have already shown promising performance benefits of cooperation and cooperative techniques also in the realm of wireless communication systems. Cooperation can be generally understood as a joint action for mutual benefit or as the action of obtaining some advantage by giving, sharing or allowing something. Particularly, in wireless communications it can be viewed from the *communicational* perspective as a number of techniques taking advantage of the synergetic interaction of entities (signals, processing elements, building blocks or even the complete nodes) as well as the collaborative use of resources (e.g. sharing). Apart of this, the *social* or *collective* aspect of cooperation as a process of establishing (and maintaining) a network of collaborating nodes is of key importance from the perspective of the entire communication network [2].

There are numerous potential performance benefits of cooperation in wireless networks including data throughput, Quality of Service (QoS), network coverage or power and spectral efficiency. It is obvious that not only users, but also operators, manufacturers and service providers can benefit from the cooperation. On the other hand, exploitation of cooperative techniques could result into more complicated scheduling in network, increased interference (relay traffic) and moreover, a comprehensive network state information (e.g. local channel estimates, queue and battery state of particular nodes) could become mandatory for implementation of some advanced cooperative processing algorithms in wireless networks [3, 4]. But obviously, only a perpetual progress in this cutting-edge research area can guarantee that the ever-growing requirements of fast and reliable communication and omnipresent connectivity in future wireless networks could be met.

In this thesis we focus purely on the *Physical layer (PHY) aspects of cooperation*. Undoubtedly, the PHY processing algorithms (including modulation, coding, signal processing etc.) are the real driving force of wireless communication systems, since only these algorithms interact directly with the physical world, trying to fully exploit the available natural resources in wireless communication channels. Although the progress in the PHY processing research has already pushed the achievable performance of single-link (point-to-point) communication towards the capacity limits (forecasted by Claude Shannon in his pioneering work [5]), the same cannot be said about the multi-node wireless communication networks. Interestingly, some fundamental questions (e.g. channel capacity) remain unanswered even for the most primitive multi-node network scenario – general 3-node relay channel [6, 7] (even after more than 40 years from the first results from van der Meulen [8] and Cover and El Gamal [9]).

During the last decade researchers over the world demonstrated that allowing a *non-orthogonal sharing* of channel resources (time/frequency/space) and implementation of *cooperative processing* directly at PHY can substantially improve the performance of wireless networks (see e.g. [10, 11]). The emerging PHY technique called usually as the *Wireless (Physical layer) Network Coding (WNC)* [12, 13] is (under some conditions) capable to double the throughput in the wireless 2-Way Relay Channel (2-WRC) and similar (or even larger) gains are envisaged in more complicated wireless networks. However, implementation of WNC in real wireless systems is still connected with an immense number of complex research problems, questions and challenges and there are only very few rigorous research results available up to this day. During my PhD studies I have tried to identify some of these "blank spots" in WNC research to provide generally applicable principles, concepts, algorithms and results which have a potential to push the current state-of-the-art a few steps beyond the limits induced by the conventional point-to-point interpretation of PHY.

1.1 Thesis outline

1.1.1 Aims and scope of the thesis

The scope of this thesis is basically three-fold:

1. It serves as a very brief overview of the basic PHY techniques and principles applicable in wireless cooperative networks (Chapter 2).
2. It introduces the fundamental principles of WNC processing in context of relevant scientific publications and provides some important references for a more in-depth study of the WNC-related problems (Chapter 3).
3. It provides a detailed overview of my up-to-date research work as a PhD candidate at the Czech Technical University in Prague and summarizes my original results on *WNC processing in parametic channel* (Part II) and *imperfec/partial side information WNC* (Part III).

1.1.2 Contents

The rest of this thesis is organized as follows. First we present a brief overview of some fundamental PHY aspects of wireless cooperative networks in Chapter 2, where mainly the use of relays and principles of the Network Coding (NC) [14] are introduced. A short section about the wireless 3-node relay channel and basic relaying and bi-directional relaying techniques, which are closely related to our WNC research, is also included. Chapter 3 is devoted solely to an overview of fundamental WNC principles and techniques, together with an identification of some interesting research questions related to the WNC-based systems. Two particular WNC research challenges, namely the *WNC processing in parametric channels* and implementation of *WNC in networks with partial side information* are discussed in Parts II, III, which together form the *core of this thesis*. Materials contained in Parts II, III cover our original contributions in the field of WNC systems research. A majority of these results have been already published in the scientific journals [15–19] and in the proceedings of international conferences [20–28]. A list of our original publications is provided in the following section.

1.2 Publications

The core of our research results has been published in the following journals:

- **Journals ranked by impact:**

  - T. Uricar and J. Sykora, “Design criteria for hierarchical exclusive code with parameter-invariant decision regions for wireless 2-way relay channel,” *EURASIP J. on Wireless Comm. and Netw.*, vol. 2010, pp. 1–13, 2010. doi:10.1155/2010/921427.
  - T. Uricar and J. Sykora, “Non-uniform 2-slot constellations for bidirectional relaying in fading channels,” *IEEE Commun. Lett.*, vol. 15, no. 8, pp. 795–797, 2011.
  - T. Uricar and J. Sykora, “Non-uniform 2-slot constellations for relaying in butterfly network with imperfect side information,” *IEEE Commun. Lett.*, vol. 16, no. 9, pp. 1369–1372, 2012.
  - T. Uricar, B. Qian, J. Sykora and W. H. Mow, “Wireless (Physical Layer) Network Coding with Limited Side-Information: Maximal Sum-Rates in 5-Node Butterfly Network", *submitted for publication*, 2013.

- **Refereed journals:**

  - T. Uricar, “Parameter-invariant hierarchical eXclusive alphabet design for 2-WRC with HDF strategy,” *Acta Polytechnica*, vol. 50, no. 4, pp. 79–86, 2010.

The following list summarizes our international conference publications, written and published during my PhD study:

- **International conferences:**

  - T. Uricar, “Rateless codes and network coding in two-way wireless relay channels,” in *Proc. POSTER 2009 - 13th International Student Conference on Electrical Engineering*, (Prague, Czech Republic), pp. 1–6, May 2009.
  - T. Uricar and J. Sykora, “Extended design criteria for hierarchical eXclusive code with pair-wise parameter-invariant boundaries for wireless 2-way relay channel,” in *COST 2100 MCM*, (Vienna, Austria), pp. 1–8, Sept. 2009. TD-09-952.
  - T. Uricar, J. Sykora, and M. Hekrdla, “Example design of multi-dimensional parameter-invariant hierarchical eXclusive alphabet for layered HXC design in 2-WRC,” in *COST 2100 MCM*, (Athens, Greece), pp. 1–8, Feb. 2010. TD-10-10088.
  - T. Uricar, “Parameter-invariant hierarchical eXclusive alphabet design for 2-WRC with HDF strategy,” in *Proc. POSTER 2010 - 14th International Student Conference on Electrical Engineering*, (Prague, Czech Republic), pp. 1–8, May 2010.
  - T. Uricar and J. Sykora, “Hierarchical eXclusive alphabet in parametric 2-WRC - Euclidean distance analysis and alphabet construction algorithm,” in *COST 2100 MCM*, (Aalborg, Denmark), pp. 1–9, June 2010. TD-10-11051.
  - M. Hekrdla, T. Uricar, P. Prochazka, M. Masek, T. Hynek, and J. Sykora, “Cooperative communication in wireless relay networks,” in *Proc. WORKSHOP 2011*, (Prague, Czech Republic), pp. 1–18, Feb. 2011.
  - T. Uricar, “Constellation alphabets for hierarchical relaying in multiple-access relay channel,” in *Proc. POSTER 2011 - 15th International Student Conference on Electrical Engineering*, (Prague, Czech Republic), pp. 1–5, May 2011.
  - T. Uricar and J. Sykora, “Hierarchical network code mapper design for adaptive relaying in butterfly network,” in *COST IC1004 MCM*, (Barcelona, Spain), pp. 1–9, Feb. 2012. TD-12-03048.
  - T. Uricar and J. Sykora, “Systematic design of hierarchical network code mapper for butterfly network relaying,” in *Proc. European Wireless Conf. (EW)*, (Poznan, Poland), pp. 1–8, Apr. 2012.

– T. Uricar and J. Sykora, "Non-uniform 2-slot constellations: Design algorithm and 2-way relay channel performance," in *COST IC1004 MCM*, (Lyon, France), pp. 1–7, May 2012. TD-12-04041.

– T. Uricar and J. Sykora, "Wireless (Physical Layer) Network Coding in 5-node butterfly network: Superposition coding approach," in *COST IC1004 MCM*, (Malaga, Spain), pp. 1–9, Feb. 2013. TD-13-06026.

– T. Uricar, B. Qian, J. Sykora, and W. H. Mow, "Superposition coding for wireless butterfly network with partial network side-information," in *Proc. IEEE Wireless Commun. Network. Conf. (WCNC)*, (Shanghai, China), pp. 1–6, Apr. 2013.

– T. Uricar, T. Hynek, P. Prochazka, and J. Sykora, "Wireless-aware network coding: Solving a puzzle in acyclic multi-stage cloud networks," in *Proc. Int. Symp. of Wireless Communication Systems (ISWCS)*, (Ilmenau, Germany), pp. 612–616, Aug. 2013.

1.3 Grants

My research efforts were supported by the following international and local projects, in which I have participated as a co-investigator:

- FP7 ICT/STREP (INFSO-ICT-248001): SAPHYRE — **Sharing Physical Resources Mechanisms and Implementations for Wireless Networks**, 2010-2012
- FP7 ICT/STREP (INFSO-ICT-215669): EUWB — **Coexisting Short Range Radio by Advanced Ultra-WideBand Radio Technology**, 2010-2011
- FP7-ICT-2011-8/ICT-2009.1.1: DIWINE — **Dense Cooperative Wireless Cloud Network**, 2013-2015
- Grant Agency of Czech Republic (GACR 102/09/1624): **Mobile radio communication systems with distributed, cooperative and MIMO processing**, 2009-2012
- Ministry of Education, Youth and Sports (OC 188): **Signal Processing and Air-Interface Technique for MIMO radio communication systems**, 2007-2010
- Ministry of Education, Youth and Sports (LD12062): **Wireless Network Coding and Processing in Cooperative and Distributed Multi-Terminal and Multi-Node Communications Systems**, 2012-2015
- EU COST 2100: **Pervasive Mobile & Ambient Wireless Communications**, 2006-2010
- EU COST IC1004: **Cooperative Radio Communications for Green Smart Environments**, 2011-2014
- Grant Agency of the Czech Technical University in Prague (SGS10/287/OHK3/3T/13): **Distributed, Cooperative and MIMO (Multiple-Input Multiple-Output) Physical Layer Processing in General Multi-Source Multi-Node Mobile Wireless Network**, 2010-2012
- Grant Agency of the Czech Technical University in Prague (SGS13/083/OHK3/1T/13): **Wireless Network Coding based Multi-node Dense Networks**, 2013

1.4 Awards and recognitions

- **Exemplary reviewer of the *IEEE Communications Letters*** (2012)[1)]
- **Dean award for the best paper in section *Communications***: (T. Uricar, "Parameter-invariant hierarchical eXclusive alphabet design for 2-WRC with HDF strategy," in *Proc. POSTER 2010 - 14th International Student Conference on Electrical Engineering*, (Prague, Czech Republic), pp. 1–8, May 2010)

1.5 International experience

- **Visiting postgraduate internship** at the Department of Electronic and Computer Engineering, School of Engineering, *Hong Kong University of Science and Technology* – HKUST (Oct. 2012 – Dec. 2012)

1.6 Other professional activities

Apart of the main research and publishing activities I have also served as a reviewer in several international journals and also as a Technical Program Committee (TPC) member and designated reviewer at international conferences.

Reviewer

Journals

- IEEE Communications Letters
- Radioengineering

Conferences

- IEEE Global Communications Conference (GlobeCom)
- IEEE Vehicular Technology Conference (VTC spring/fall)
- IEEE International Symposium on Personal, Indoor and Mobile Radio Communications (PIMRC)
- International Conference on Computer Communications and Networks (ICCCN)
- International Symposium on Wireless Communications Systems (ISWCS)

Conference Technical Program Committee

- IEEE Student Conference on Research and Development (SCOReD), 2012
- IEEE International Symposium on Personal, Indoor and Mobile Radio Communications (PIMRC), 2013

[1)] See Appendix I

Chapter 2

Cooperation in wireless networks

"If you want to be incrementally better: Be competitive. If you want to be exponentially better: Be cooperative."

Anonymous

Wireless channels possess inherently some specific features which do not have any counterpart in wireline systems. Firstly, it is the *broadcast nature* of the wireless medium – signal broadcast from one node can reach several other nodes in its vicinity at no cost. And secondly, it is an *inherent combining of simultaneously received signals* (electromagnetic waves) at the receiver antenna. Both these distinctive properties evidently leverage the potential of cooperation among the nodes in the wireless network.

Existing wireless network architectures based on the hot-spot and cellular structures fail to take the advantage of cooperation possibilities offered by the adjacent nodes in the network [4]. A concurrent transmission of signals is usually considered harmful in the contemporary wireless systems (purely as an interference), and it is avoided rather than exploited. By employing sophisticated signal processing algorithms, scheduling and medium-access techniques any wireless network is thus nowadays reverted to a set of islolated (orthogonal) point-to-point connections (bit-pipes) that provide virtual error-free channels for the higher layers in the protocol stack. It has been proved that this orthogonal slicing of resources is strongly sub-optimal [7], since it leads to diminishing transmission rates as the network size increases [13]. Obviously, this approach also makes the implementation of cooperation directly at PHY impossible.

In [3] the cooperation is referred to as any architecture that deviates from the traditional approach of users individually communicating with the associated base stations and vice versa. Cooperative systems should exploit adjacent nodes to enhance the user links in a supportive way by relays or in a cooperative way by other users. It is obvious that there is an enormous amount of different ways in which supportive relays and cooperative users can be deployed.

Research of cooperative communication strategies is generally trying to pursue two different goals. The first is the *reliability* of communication in terms of outage probability, or a symbol/bit error probability for a given transmission rate. The spatial diversity available among the distributed nodes can be exploited to emulate the antenna array and thereby increase the reliability of communication. This principle is sometimes called *cooperative diversity* [2]. The second goal is the increase of *transmission rate*. For various processing algorithms and transmission protocols/strategies, significant performance improvements in terms of transmission rate and reliability have been already demonstrated (see e.g. [2,3,10,11,29] and references therein). Typical cooperative gains of wireless networks are summarized in [3] as follows:

- *Pathloss gain*: By splitting the source-destination propagation path into smaller parts (by exploiting the relay) significant gains can be achieved. The aggregate pathloss of the split path is less than the

pathloss of the full path, resulting in transmit power gain. This remains true even if we consider allocating half of the power to each part (source and relay).

- *Diversity gain*: Providing additional independent copies of the same information via independent (relay) channels results in diversity gains, since the probability of all paths being simultaneously illegible decreases.

- *Multiplexing gain*: Using a relay, there is a potential (under a certain conditions) of creating a second independent channel between the source and the destination. This can be viewed as a distributed extension of the well-known principles from the Multiple-Input Multiple-Output (MIMO) systems, although this gain can be achieved even if all the transmitting nodes use only a single antenna. Note that throughput/capacity gain provided by WNC techniques can be also interpreted as the mutliplexing gain.

Cooperation is evidently possible whenever the number of communicating nodes exceeds two. A *3-node network* captures many important aspects of user cooperation and hence it can be viewed as one of the *primary building blocks* of the cooperative system. A vast amount of research was devoted (especially in the realm of information theory) to this special 3-terminal channel, generally called the *relay channel*. The relay channel was introduced by van der Meulen in 1968 in his PhD thesis [30] (and later in [8]) and since then several hundreds of papers devoted to the communication in the relay channel already appeared. Interested reader should check the references in [2–4,29] for further information. More recently a problem of *bi-directional flow of information* in this 3-node relay channel (called usually as 2-WRC when the communication is bi-directional) has attracted a huge interest of the research community, since it represents the most primitive wireless network model where the application of WNC techniques is possible (see e.g. [10, 31] and references therein).

In the rest of this chapter we briefly overview the general concepts employed in cooperative wireless systems, including the relaying and network coding techniques [14]. Application of these basic cooperative principles is demonstrated on the example 3-terminal relay channel, including an overview of relaying strategies and disussion of some information-theoretical aspects of relaying. The chapter is concluded with a notion of the bi-directional transmission of information in 2-WRC, where the requirement of multiple information flows traversing the wireless network allows to employ the WNC technique. A more detailed overview of the principles of WNC processing is presented separately in Chapter 3.

2.1 Brief overview of general concepts

2.1.1 Relays and relaying

We have already mentioned the potential benefits of cooperation in wireless networks. It is important to note that the use of relay(s) is the prevailing assumption in the design of new cooperative techniques. Genereally the relays can be deployed as standalone nodes in the network, but virtually any user in the network can serve as a relaying node from time to time. Considering the number of idle terminals in the present-day cellular networks and the broadcast nature of the wireless medium, it is quite obvious that the number of potential relays could be relatively large.

The function of the relay can be either *supportive* (relay has not own data to transmit) or *cooperative* (relay has own data to transfer). The design of relaying techniques is further influenced by several other characteristics – e.g. absence/availability of the direct link between the source and the destination, number of cooperating relays (dual-hop versus multi-hop networks) etc. Discussion about these characteristics and the resulting canonical architectures of relaying systems is out of the scope of this thesis and can be found e.g. in [3]. Here we only summarize one of the possible classifications of the relaying techniques, which is also available in [3]:

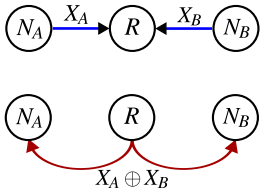

Figure 2.1: Simple example of NC.

- *Transparent relaying*: No digital operations are performed on the signal received by the relay. Relay usually only amplifies the signal before retransmission or performs some linear (e.g. phase shifting) or non-linear operations on the signal in the *analog* domain.
- *Regenerative relaying*: Relays are allowed to change the waveform and/or the information contents of the received signal by performing some processing in the *digital* domain.

2.1.2 Network coding paradigm

NC [14] was originally proposed as a means to faciliate the information multicast (source to a set of receivers) in a communication network [32]. With NC, intermediate nodes in the network are allowed to send combinations of previously received information (packets), instead of simply forwarding (routing) data [33]. This allows to reduce the total amount of packets which must be sent by the intermediate relay nodes in the network, which in turn leads to great throughput gains.

A simple example of NC principle in the 3-node topology is in Fig. 2.1. Two nodes (N_A, N_B) want to exchange information through a common relay R. The relay decodes packets from both sources (X_A, X_B), combines them using simple bit-wise XOR operation and broadcasts the combined packet ($X_R = X_A \oplus X_B$). Node A then decodes the packet X_B from X_R by a simple bit-wise XOR operation (note that packet X_A is known by the node A a-priori):

$$X_R \oplus X_A = (X_A \oplus X_B) \oplus X_A = X_B, \tag{2.1}$$

and similarly for node B.

There are two main benefits of the NC approach: a potential *throughput improvement* and a *high degree of robustness*. The capability to boost the capacity of a network for multicast flows is discussed e.g. in [32, 33]. The potential to improve the robustness of a system by a proper application of NC is observed e.g. in [34], where an additional diversity gain is obtained by employing NC in the Wireless Multiple Access Relay Channel (MARC) – see Fig. 2.2. In MARC the single destination can decode both packets, provided that at least two (out of three) packets are correctly received. The outage probability of the MARC scheme with NC is analyzed in [35].

The broadcast nature of wireless medium is recognized as a desirable characteristic that facilitates a direct application of conventional NC in wireless systems [34]. In wireless systems an NC-encoded

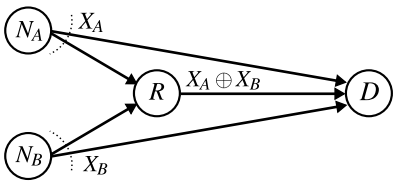

Figure 2.2: Multiple Access Relay Channel with network coding at the relay.

packet can be broadcast by the relay to all destinations in a single transmission, and hence less network resources (power, use of channels) are required for a successful communication (as compared to the system without NC). Obviously, NC can be used jointly with traditional channel coding to further improve the reliability of a transmission. Joint network-channel coding is discussed e.g. in [36] for a 3-node relay network and in [37] (joint network-LDPC[2)] code) and [39] (joint network-turbo code) for MARC. Practical implementation of NC in the wireless network can be found e.g. in [40, 41]. The experimental measurements from the 802.11 testbed [41] confirm the potential gains of NC in the wireless network setup.

Since NC is basically a wire-line technique, which usually operates with the whole data packets in the wire-line network, a detailed description of this interesting technique is out of the scope of this thesis. Interested reader can find more details in [14, 32, 42–45] and references therein.

2.1.3 Capacity bounds

Unlike for the traditional single (source-destination) link, which capacity is well known for decades (e.g. [6]), the capacity of a general multi-source multi-node network is not known even today. In fact, even the capacity of the general relay channel [8, 9] still have not been found. Although the information-theoretical analysis of the capacity of general multi-node wireless channels is out of the scope of this thesis, here we restate the theorem, which bounds the rate of information transfer between two sets in a multi-node network (Fig. 2.3) by a conditional mutual information.

The network consist of N nodes. Node i is characterized by the input-output pair $\left(X^{(i)}, Y^{(i)}\right)$, and sends information at a rate $R^{(ij)}$ to node j. The nodes are divided in two sets S and S^C (the complement of S), and a cut C conceptually separates the nodes in these two sets. The channel is represented by the conditional probability mass function $p(y(1), y(2), \ldots y(N) \mid x(1), x(2), \ldots x(N))$.

Theorem 1 (Cut-set theorem)**.** *If the information rates* $\left\{R^{(ij)}\right\}$ *are achievable, then there exists a joint input probability distribution* $p(x(1), x(2), \ldots x(N))$ *such that*

$$\sum_{i \in S, j \in S^C} R^{(ij)} \leq I\left(X^{(S)}; Y^{(S^C)} \mid X^{(S^C)}\right) \tag{2.2}$$

for all $S \subset 1, 2, \ldots N$.

Proof can be found e.g. in [6]. Theorem 1 says that the rate of information flow across any cut (boundary) dividing the set of nodes in the network in two parts (the transmitter and receiver sides) cannot exceed the mutual information between the channel inputs on the transmitter side and the channel outputs on the receiver side, conditioned on the knowledge of inputs on the receiver side. The problem of information flow in general networks [6] would be solved if the bounds of Theorem 1 were achievable. But unfortunately, these *bounds are not achievable* even for some simple channel models like the general relay channel [2, 6].

As noted in [11], it is unlikely that the capacity regions (in Shannon's sense) of general wireless networks can be obtained, especially when the network dynamics and feedback are incorporated. Unfortunately, separation theorems[3)] [6] which usually guide the wireless network protocol design are also absent due to the lack of capacity results [11].

Due to the high complexity of the *capacity evaluation* in general multi-node wireless networks some authors focus only on the evaluation of the *approximate capacity* to provide capacity bounds which are

[2)] LDPC is a commonly used acronym for the Low Density Parity Check Codes [38].

[3)] Shannon's separation theorem shows that separate design of source (compression) and channel coding does not cause any performance loss if the underlying communication channel is point-to-point and static.

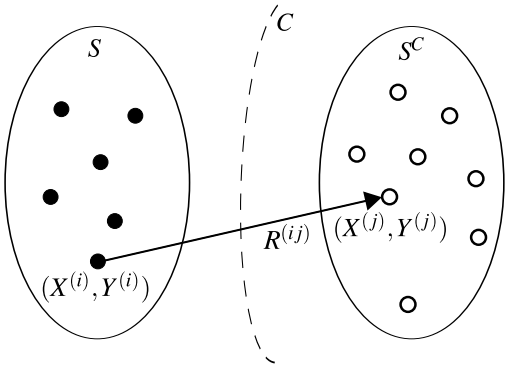

Figure 2.3: A network with multiple nodes divided in two sets (S, S^C) and separated by a cut C.

at least more tight than those suggested in Theorem 1. Quite recently, Avestimehr, Diggavi and Tse presented a novel approach to the evaluation of approximate capacity of wireless networks with single source and single/multiple destinations (including some basic multi-source scenarios). Their idea is based on the observation that signal interactions become more important than noise in the high Signal to Noise Ratio (SNR) region, and hence that wireless networks operate in an interference-limited (rather than noise-limited) regime in this SNR region. This allows (if the specific broadcast and superposition properties of wireless medium are incorporated) to model the whole wireless network as a set of deterministic wire-line bit-pipes, providing a tighter bound of the achievable capacity than that available in Theorem 1. Interested reader can find more details in [46–49].

2.1.4 Half-duplex constraint

The deployment of relays in practical systems puts an emphasis on the half-duplex limitations of current radios. If the relay would transmit and receive simultaneously in the same frequency band, than the transmitted signal will interfere with the received signal. Considering the large difference between the received and transmitted signal (typically 100-150 dB [2]), it is obvious that this interference could degrade the received signal significantly. Although it is theoretically possible to cancel out the interference at the relay by interference cancellation techniques (since the relay knows the transmitted signal), it is still problematic for the state-of-the-art radios to avoid the errors in the interference cancellation for the signal of such a large difference [2]. The full-duplex radios are hence not commonly used and *half-duplex constraints* are usually considered as an integral part of the system model. The information theoretic analysis of the half-duplex networks can be found e.g. in [50], where the cut-set theorem (Theorem 1) has been extended to networks with multiple states.

2.2 Three-terminal relay channel

2.2.1 System model

The relay channel is the 3-terminal communication channel [8] shown in Fig. 2.4. The source S wants to transmit information to the destination D. The relay R has no own information to transmit, and hence only supports the communicating nodes (S,D). The signal being transmitted from node i, $i \in \{S,R\}$ is labeled X_i and the signal received by node j, $j \in \{R,D\}$ is labeled Y_j.

Conceptually, information is relayed in two phases (modes). The first is the broadcast (BC) mode, when S transmits and R,D receive. The second mode, when S,R transmit and D receives is known as

the multiple-access mode (MAC). This differentiation is only conceptual since it is theoretically possible that the communication in both modes proceeds simultaneously [2]. However, the half-duplex constraint discussed in the previous section essentially prevents the simultaneous transmission of both modes for current state-of-the-art radios. Four different models (setups) of relaying (based on the two aforementioned modes) are depicted in Fig. 2.5.

2.2.2 Relaying strategies

Two fundamental relaying strategies (protocols) for the 3-terminal relay channel can be distinguished, based on the fact whether the relay decodes the received information or not. In the first strategy, called usually *Decode and Forward* (DF), the relay decodes the signal transmitted from the source and retransmits the decoded signal (after possibly compressing and/or adding redundancy). This strategy is close to optimal when the source-relay channel is perfect, since in this case the relay channel virtually becomes a 2 x 1 multiple-antenna system [2]. The second strategy refers to the case, where the relay is not able to decode the signal from the source. Nevertheless even in this case it has an independent observation of the information transmitted from the source, which can be effectively exploited by the destination in the decoding process. The relay sends an estimate of the source transmission to the destination and hence the strategy is often called *Estimate and Forward* (EF)[4)]. Both protocols which are now commonly known as DF and EF have been introduced in [9]. A special case of the EF strategy, called *Amplify and Forward* (AF) has gained a lot of attention, mainly due to its simplicity [2, 3]. In this strategy, the estimated signal is simply the analog signal received by the relay antenna and the relay simply amplifies this signal before retransmission.

Slight modifications/combinations of these basic strategies can be found in the literature. *Adaptive* relaying [3] (called selection relaying in [2]) refers to the strategy where the relay chooses whether to use DF or AF, according to the fact whether it is able to decode the received data (DF strategy used) or not (AF strategy used). In contrast, in the *Dynamic* relaying [3] the relay uses DF if the received data were decoded correctly, but otherwise stays idle.

DF and EF strategies are thoroughly examined in [51]. Further details about the uni-directional relaying strategies can be found e.g. in [2, 3, 9, 52, 53]. While these references discuss the relaying problem mainly from the information-theoretical point of view, some examples of practical coding strategies for uni-directional relaying have been already proposed in [53] (based on the LDPC codes) and in [54] (based on the rateless-codes [55–57]).

2.2.3 Capacity bounds of the relay channel

As we have already mentioned, the capacity of the general 3-terminal relay channel is still not know (even after more than 40 years from the first results from van der Meulen [8] and Cover and El Gamal [9]). Although the capacity of the degraded relay channel [6] has been completely solved in [9], the channel degradedness is an unrealistic assumption for the wireless systems (as noted e.g. in [2]).

[4)] Note that terms Compress and Forward (CF) and Quantize and Forward (QF) generally refer to the identical principle [2].

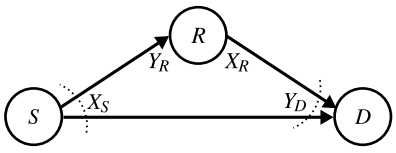

Figure 2.4: Three-terminal relay channel.

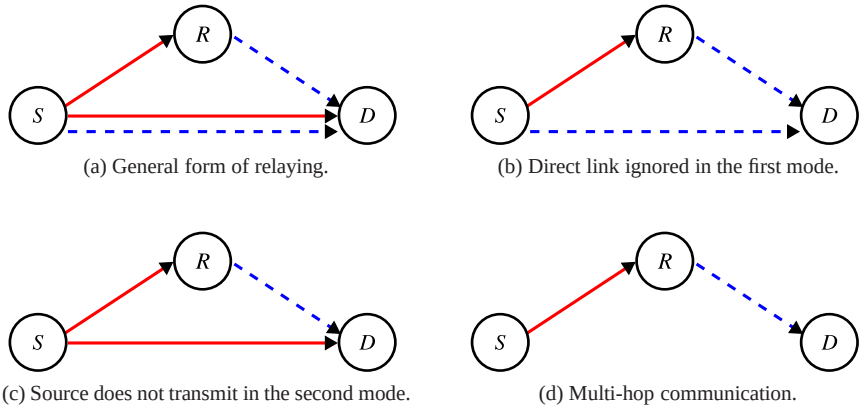

(a) General form of relaying.

(b) Direct link ignored in the first mode.

(c) Source does not transmit in the second mode.

(d) Multi-hop communication.

Figure 2.5: Possible models of relaying in the three-terminal relay channel. The BC mode/phase (solid red) and the MAC mode/phase (dashed blue) are distinguished by different colour and line style.

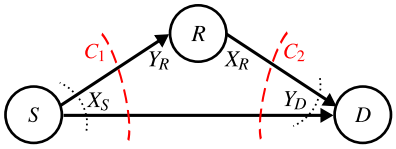

Figure 2.6: General full-duplex relay channel.

In addition to the capacity of the degraded channel, also the capacities of the reversely degraded channel and the feedback relay channel are discussed in [9]. It is important to note that the analysis therein has been performed for Gaussian communication channels only, therefore neither the fading channel was considered, nor the pathloss gains were incorporated into the analysis [3]. Information-theoretical analysis of the relaying strategies in the context of wireless channels is available in [51], where the capacity results are generalized to multi-antenna transmission with Rayleigh fading and extended to multi-source and multi-destination networks.

Further information about the information-theoretical aspects of relaying can be found mainly in [6, 9, 51]. Here we introduce only the upper-bound for the capacity of the general *full-duplex* relay channel (Fig. 2.6) [9] and the upper-bound for the capacity of the general *half-duplex* relay channel (Fig. 2.7) [50]. These upper-bounds are derived as consequences of the general cut-set theorem (Theorem 1) [6] and its half-duplex extension [50]. The proofs of both Theorems can be found in [9] and [50].

Theorem 2 (Capacity upper-bound (full-duplex relay))**.** *The capacity C of the general relay channel is bounded above as follows*

$$C \leq \sup_{p(x_S,x_R)} \min\left(I\left(X_S;Y_R,Y_D \mid X_R\right), I\left(X_S,X_R;Y_D\right)\right). \tag{2.3}$$

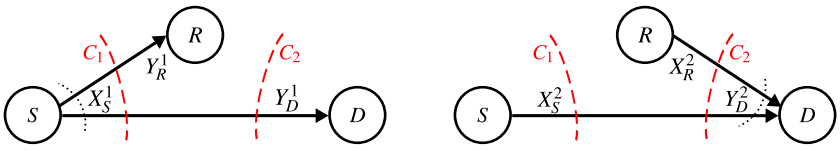

Figure 2.7: General half-duplex relay channel (BC and MAC phase).

Theorem 3 (Capacity upper-bound (half-duplex relay))**.** *The capacity of the general half-duplex relay channel is upper bounded as follows*

$$C_{hd} \leq \sup_{t:0<t<1} \min\left(tI\left(X_S^1;Y_R^1,Y_D^1\right)+(1-t)I\left(X_S^2;Y_D^2 \mid X_R^2\right), tI\left(X_S^1;Y_D^1\right)+(1-t)I\left(X_S^2,X_R^2;Y_D^2\right)\right), \quad (2.4)$$

where the superscript 1 stands for the BC phase, the superscript 2 stands for the MAC phase and t is a portion of the time in which the network is in the BC phase.

2.3 Bi-directional relaying

Many examples of bi-directional traffic flows can be found in present wireless networks, including voice conversations, video conferencing (between two users), instant messaging and routing of information in ad-hoc networks, just to name a few. Moreover, future cellular networks will probably deploy inexpensive bi-directional relays to expand their coverage area [58]. These relay nodes will intervene between the mobile device and the base station. All these facts increase the interest in bi-directional relaying scenarios.

In the bi-directional relay channel (2-WRC) two sources (nodes A, B) want to mutually exchange the information with the potential help of the relay terminal R (see Fig. 2.8). Such mutual exchange of information between two nodes can follow various schemes. Since both nodes have knowledge of their own (previously sent) data, this case calls naturally for the exploitation of the NC principles (compare the system model from Fig. 2.8 with the NC example in Fig. 2.1). Together with the signal received from the relay, the a-priori known own data (visualized in Fig. 2.8 as the Hierarchical Side Information (HSI) [19]) can be used at both nodes to decode the desired information.

First notes about the utilization of NC for bi-directional relaying in wireless systems can be found in [33, 59] and in [60] (also a bi-directional multi-hop is addressed in this paper). The joint network-channel coding principle from [39] is extended to the bi-directional relay channel in [61].

2.3.1 Two-way relay channel

Three possible bi-directional relaying schemes are summarized in Fig. 2.9. Traditional routing (Fig. 2.9a) requires four steps to successfully deliver the data in both directions. Utilization of NC coding principles together with the inherent broadcast nature of the wireless medium allows to reduce the required number of steps to three (see Fig. 2.9b). This raises the potential to achieve a sum-rate gain of about 33,3% (e.g. [59]), compared to the traditional 4-step routing. Moreover, if an appropriate processing is used, it is possible to exploit the inherent physical combining of the communication flows over the wireless multiple access channel to achieve a sum-rate gain of 100% (e.g. [31, 62, 63]), compared again to the traditional 4-step routing. In this case, the number of required steps reduces to two (see Fig. 2.9c).

Note that while the 4-step and 3-step schemes allow theoretically to exploit the direct channels between nodes A, B, in the 2-step scheme the utilization of direct channels is naturally prohibited by the half-duplex constraint. Since the 4-step scheme corresponds to the traditional routing, in the following section we focus on the bi-directional relaying strategies for the 3-step (2.9b) and 2-step (2.9c) schemes.

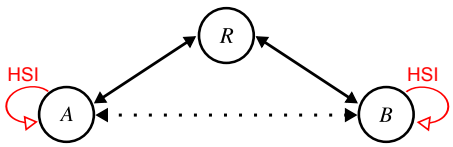

Figure 2.8: Two-way relay channel (2-WRC).

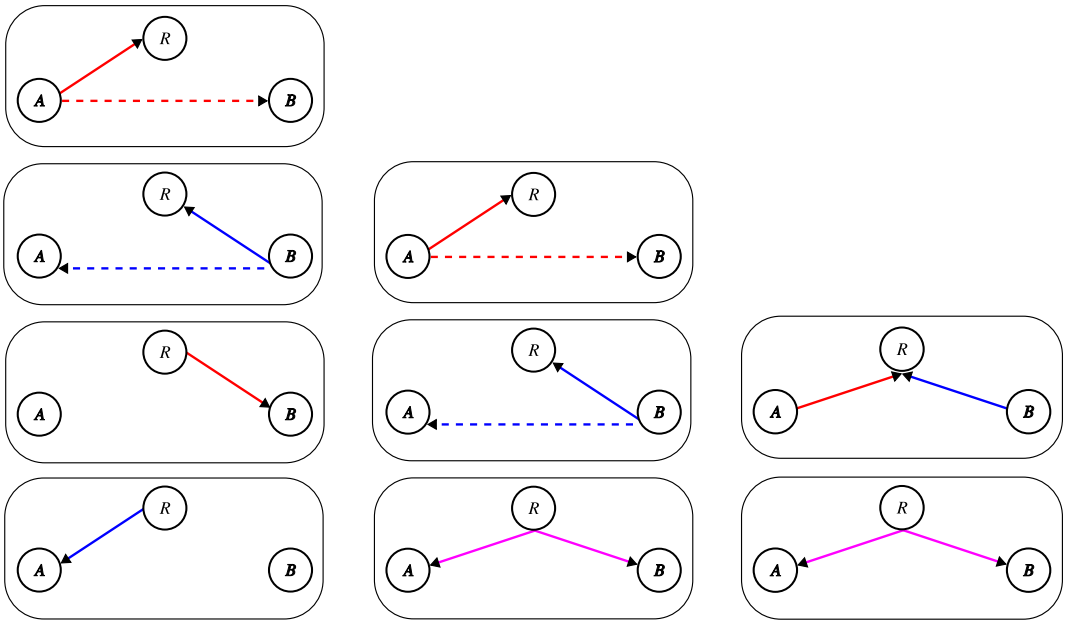

(a) Traditional routing. (b) 3-step scheme. (DF strategy) (c) 2-step scheme. (JDF, AF, DNF/HDF)

Figure 2.9: Bi-directional communication schemes in 2-WRC.

2.3.2 Bi-directional relaying strategies

In the 3-step scheme (Fig. 2.9b) the relay receives information from the sources in two separate steps (e.g. time slots). The relay decodes the data, combines them using NC and broadcast them to both destinations in a single transmission. Since both data streams are decoded by the relay, this strategy is usually called *Decode and Forward* (DF). In simple 3-step DF schemes [59, 60, 62], the direct link between sources is ignored. In [61], the direct link is not ignored and a joint network-channel coding is utilized to process the information received from the direct and relay links.

In a similar strategy, called *Joint Decode and Forward* (JDF) [31, 64], the relay again decodes both data streams, but the sources are allowed to transmit simultaneously in the first step (hence only two steps are sufficient for this scheme). Since both data streams must be decoded by the relay, both nodes have to select their date rates *within the Multiple Access (MAC) sum-rate region* [6]. In both DF and JDF strategies, the network coding is performed on the received data streams, hence a simple bit-wise XOR NC operation on the received data packets can be used.

The 2-step relaying strategies, where the relay does not decode the data from both sources are often commonly referred to as *Wireless (Physical Layer) Network Coding* (WNC or PLNC) (e.g. [31, 63, 65]). These strategies were inspired by the observation that it is unnecessary for the relay to decode the exact source information [63, 66–68], as it is not the final destination of any of the two data streams. This allows both nodes to select their data rates *outside the relay MAC sum-rate region* and thus improve markedly spectrum efficiency. Basically two such strategies can be found in the literature (see e.g. [67]). The first strategy is a bi-directional counterpart of the (uni-directional) AF strategy. In this strategy the relay again only amplifies the received analog signal and hence this strategy is again called *Amplify and Forward* (AF) (see e.g. [31, 62, 67, 69, 70]) or Analog Network Coding [58]. The second strategy, whose principles were independently introduced in [63, 66] is usually called *Denoise and Forward* (DNF) [66], *Hierarchical Decode and Forward* (HDF) [71] or *Compute and Forward* (CaF) [13], although some less

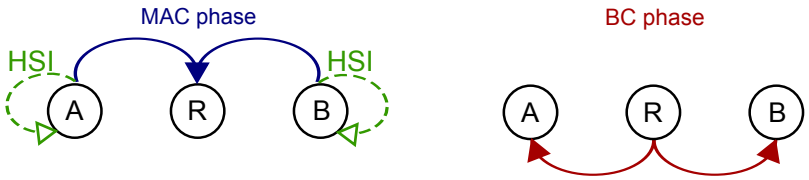

Figure 2.10: MAC and BC phase of WNC schemes.

common names like *Partial Decoding* [72] can be found in the literature as well.

Achievable rate regions of the 2-WRC channel were analyzed e.g. in [64] (full-duplex assumption), [70] (half-duplex assumption) and [73]. Two-way rates for DF, JDF, AF and an upper-bound of the achievable rate for DNF were analyzed in [31] (sub-optimal broadcast strategies assumed). Broadcast capacity region of the 2-WRC is dealt with in [74], where the optimal broadcast strategy for the relay which has decoded data from both sources (DF, JDF strategies) is analyzed.

We briefly overview the basic concepts of the WNC techniques in the last sub-section of this chaper. Subseqently, in Chapter 3 we discuss solely the HDF-like WNC processing, since the majority of our own research results (as presented in Parts II, III) is focused on this family of WNC relaying strategies.

2.3.3 Wireless (Physical Layer) Network Coding

The WNC strategies (AF, HDF) offer the best potential performance among all the bi-directional relaying strategies in 2-WRC, as they require only 2-steps (called usually MAC and BC phase - see Fig. 2.10) to bi-directionally relay the data, and they are not limited by the relay MAC capacity region (unlike JDF). Although the AF strategy is quite simple to implement, it suffers from severe limitations. First of all, the noise received by the relay in the MAC phase is amplified together with the useful signal and hence this strategy suffers from the *noise accumulation* [62, 75]. Moreover, the knowledge of both source-relay channels is usually required at both destinations to extract the desired data from the relay signal [31], which inevitably raises the communication overhead[5)]. The last significant limitation of AF is a direct consequnce of the layered architecture of contemporary wireless systems. These systems use the error-correcting codes and Automatic Repeat Request (ARQ) mechanisms to *mimic error-free PHY* to higher layers. This cannot be done in AF since no decoding is essentially performed at the intermediate relay nodes and hence potentially erroneous data (packets) are forwarded through the network [10]. Nevertheless, promising performance improvements of a practical implementation of AF have been already shown in [58], where the throughput improvements of 70% (compared to traditional routing) and 30% (compared to traditional NC) have been observed in a testbed of software radios.

To the best of our knowledge, the principles equivalent to the HDF (DNF/CaF) strategy, which avoids the typical problem of noise amplification in AF and simultaneously allows to exploit the power of error correction coding even on a “per-hop" basis (more details will be given later), have been independently introduced in [63] and [66].

In DNF the relay performs an estimate of the pair of received symbols (codewords) and maps the estimate to the symbol (codeword) from the discrete set [31], which is then broadcast by the relay. Since the impact of the noise is eliminated from the received signal, the relay processing is described as “de-noising” in [31, 66], which gives the name to the whole strategy (DNF). HDF and CaF follow essentially an almost identical idea. In HDF the relay decodes directly the compound *“hierarchical" data* from the observed signal, and then broadcasts (after potential re-encoding) this hierarchical data/codeword to the destinations [71]. Similarly, the relay processing is described as a direct decoding of some function of source data at the relay in the CaF strategy [13]. The underlying principle of all HDF, DNF and CaF

[5)] Global channel state estimates must be relayed to respective destinations.

strategies is quite similar to the traditional NC coding[6], but note that here the relay output signal is obtained directly from the observation in the MAC phase, separate source packets *are not decoded* by the relay. In all these strategies both destinations are able to decode the desired data from the relay signal and own (previously sent) data iff the *eXclusive law* (see e.g. [31]) of NC is not violated (more details will be given later). In the following chapter we focus in somewhat more detail on the basic concepts, principles and research challenges in the HDF-family of WNC processing.

[6] A fundamental idea of HDF/DNF/CaF can be described as an attempt to generalize the finite field NC principles to the continuously valued constellation space.

Chapter 3

Wireless (Physical Layer) Network Coding

"To be happy in this world, first you need a cell phone and then you need an airplane. Then you're truly wireless."

Ted Turner

As we have already mentioned in the previous chapters, WNC is a promising technique which possesses a great potential to significantly increase the achievable throughput in wireless networks. In this chapter we focus solely on the HDF-family (DNF [31, 65], CaF [13, 76]) of WNC processing. Readers interested in AF processing should refer e.g. to [31, 62, 67, 69, 70].

We demonstrate the basic concepts of HDF[7)] on the simple 2-WRC model, which, despite of its simplicity, allows to clearly describe the basic principles of HDF [71], together with all the research and design challenges naturally accompanied with this technique. We focus solely on the core principles of HDF which are neccessary for introduction of our own research results (as presented in Parts II, III).

Following the adage, *"A picture is worth a thousand words"*, we try to explain the HDF principles as simply and illustratively as possible, without diving deep into the detailed and rigorous mathematical descriptions. A rigorous description of HDF, DNF and CaF strategies is available in the excellent papers [10, 12, 13, 71].

3.1 HDF relaying in 2-WRC

3.1.1 System model

The 2-WRC system contains three physically separated nodes (nodes A, B and relay R). Nodes A and B would like to mutually (bi-directionally) exchange data. Data A source is hence co-located with the destination for data B (and vice-versa). Since A, B are not in a radio visibility (direct link is missing), a support of a common shared relay node R is required (Fig. 3.1). The transmission from each source serves also as the Hierarchical Side Information[8)] (HSI) [19, 26] for the reverse link (more details will be given later).

[7)] Since the core idea of the HDF, DNF and CaF strategies is essentially identical, from now on we will use the acronym HDF to refer to all these WNC strategies.

[8)] This specific form of side information is sometimes also called as the Complementary-Side Information (C-SI) [71] or simply as the self-information [12].

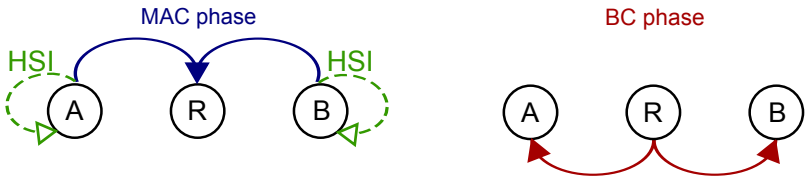

Figure 3.1: 2-WRC with Hierarchical Side Information (HSI).

A wireless system is considered, and hence all transmitted and received symbols are signal space symbols. Channels are modeled as linear frequency flat with Additive White Gaussian Noise (AWGN) and all nodes are half-duplex (one node cannot simultaneously receive and transmit). The nodes operate with synchronized symbol timing and Channel State Estimates (CSE) are available only at the receiving nodes (unless stated otherwise). Due to the half-duplex constraint each bi-directional communication round can be divided into the MAC and BC phase (Fig. 3.1).

3.1.2 MAC phase – source nodes transmission

In the MAC phase both nodes A, B simultaneously transmit their messages (data words) $\mathbf{d}_A$,$\mathbf{d}_B$ to the relay R. If a channel coding (error-correction) is employed in the system, the sources encode their data messages prior to the transmission to obtain the codewords $\mathbf{c}_A = \mathscr{C}^A(\mathbf{d}_A)$, $\mathbf{c}_B = \mathscr{C}^B(\mathbf{d}_B)$, where $\mathscr{C}^i$, $i \in \{A,B\}$ is the channel coding operation. A signal space representation (with an *orthonormal* basis) of the $n-$th transmitted channel symbol[9] is $s_A(c_A)$, $s_B(c_B)$ ($s_i \in \mathscr{A}_s^i \subset \mathbb{C}^{N_s}$, $\left|\mathscr{A}_s^i\right| = M_s$), where c_A, c_B are source node code symbols, $\mathscr{A}_s^i(.)$ is the channel symbol memoryless mapper at node $i \in (A,B)$, N_s is the complex dimensionality of channel symbols s_A, s_B and M_s is the source alphabet cardinality.

The constellation space signal received at the relay in MAC phase is

$$\mathbf{x} = h_A\mathbf{s}_A + h_B\mathbf{s}_B + \mathbf{w}, \tag{3.1}$$

and hence the n-th constellation space symbol received at the relay can be evaluated as

$$x = h_A s_A + h_B s_B + w, \tag{3.2}$$

where w is AWGN[10] and h_A, h_B are scalar complex channel coefficients (constant during the observation and known at the relay). Note that $\mathbf{s}_i$ is generally a vector of vectors since $s_i \subset \mathbb{C}^{N_s}$.

For some subsequent analysis, it is convenient to equivalently express the useful signal ($h_A\mathbf{s}_A + h_B\mathbf{s}_B$) after a rescaling by $1/h_A$ as

$$\mathbf{u} = \mathbf{s}_A + h\mathbf{s}_B. \tag{3.3}$$

where $h = h_B/h_A$, $h_A, h_B, h \in \mathbb{C}^1$. The only purpose of this "rescaling" is an attempt to simplify the signal analysis in parametric MAC channel [15] by introducing a model of useful signal which incorporates the influence of both channel parameters (h_A, h_B) in the single one (relative) channel parameter h. Since the useful signal (3.3) is in fact a superimposed (compound) symbol in the signal space, it it sometimes called the *hierarchical signal* (and similarly u is called the *hierarchical symbol*). The received signal at the relay hence can be evaluated also as

$$\mathbf{x} = h_A\mathbf{u} + \mathbf{w}'. \tag{3.4}$$

Both nodes A, B are assumed to have sufficiently large buffers to store their own transmitted messages for subsequent processing. This process is visualized as a *virtual transmission* of HSI in Fig. 3.1.

[9] We will omit the symbol time variable n from the following expressions to improve the readability.

[10] w is assumed to be circularly symmetric complex Gaussian noise with variance σ_w^2 per complex dimension.

3.1.3 HDF relay processing

In 2-WRC both destinations have naturally available their previously sent data (HSI). Without HSI, it would be necessary to decode both separate data messages at the relay and then broadcast both these decoded messages to secure an end-to-end information exchange between nodes A, B. However, in 2-WRC this would be strongly sub-optimal, since HSI is available there virtually at no cost (only sufficiently large buffers are required) and hence it can be utilized to "compress" the relay output similarly as in the conventional wire-line NC [42].

In 2-WRC the relay can always perform a traditional multi-user decoding to decode both separate source messages $\mathbf{d}_A, \mathbf{d}_B$. Since HSI is available at both nodes, the relay can simply create its output message as $\mathbf{d}_R = \mathbf{d}_A \oplus \mathbf{d}_B$ ($\oplus$ is a convetional NC operation – e.g. bit-wise XOR) and broadcast this message (after channel coding and modulation) to both destinations. Note that this processing corresponds to the JDF strategy (as mentioned in Chapter 2). Node B is then able to decode the desired message $\mathbf{d}_A$ from the relay signal and HSI (own data $\mathbf{d}_B$) as:

$$\begin{aligned} \hat{\mathbf{d}}_A &= \hat{\mathbf{d}}_R \oplus \mathbf{d}_B \\ &= \widehat{(\mathbf{d}_A \oplus \mathbf{d}_B)} \oplus \mathbf{d}_B \end{aligned} \tag{3.5}$$

and similarly for the decoding of message $\mathbf{d}_B$ at node A.

Although the aforementioned principle is nearly optimal at low SNR (see e.g. [77]), it is possible to show that even better performance can be achieved when the WNC relaying strategies (see a brief overview in Chapter 2) are employed in 2-WRC. The fundamental underlying principle of WNC strategies is grounded in the fact that the relay does not have to decode the individual source messages $\mathbf{d}_A, \mathbf{d}_B$, since it is not the final destination of the communication. Moreover, as noted e.g. in [10, 12, 13, 71] the inherent superposition property of wireless channels can be interpreted as a *natural NC operation*. The relay hence must only map its observation (3.1) to a valid output message, which will secure that both destinations are able to decode the desired data similarly as in (3.5). The relay operation in any WNC system[11] hence can be described by the following mapping:

$$\mathscr{X}_d : \quad \mathbf{x}(\mathbf{d}_A, \mathbf{d}_B) \overset{(\mathrm{HDF})}{\longmapsto} \mathbf{d}_R \tag{3.6}$$

or

$$\mathscr{X}_c : \quad \mathbf{x}(\mathbf{c}_A, \mathbf{c}_B) \overset{(\mathrm{HDF})}{\longmapsto} \mathbf{c}_R \tag{3.7}$$

Mapping $\mathscr{X}_d$ (respectively $\mathscr{X}_c$) describes the relay operation which assigns a discrete relay message (respectively codeword) to the received constellation space signal $\mathbf{x}$. A particular implementation of this operation can have various forms [10, 12, 65, 67, 71, 72, 78], including a sub-optimal symbol-wise processing [65, 79–81] (which ignores the structure of the underlying channel codes), a modulo-lattice operation [13, 78] (nested-lattice codes must be employed at both sources) or a processing which exploits the linearity (group structure)[12] of the underlying channel codes [71, 82, 83]. As noted e.g. in [12, 83, 84], the performance of a particular HDF processing depends also on the *decoding metric* employed at the relay node[13].

It is obvious that $\mathscr{X}_c$ (equivalently $\mathscr{X}_d$) must fulfil some requirements to guaratee that successful decoding of the desired data can be performed at both destinations. The first fundamental property is

[11] In AF the relay output signal $\mathbf{s}_R$ is simply an amplified version of the received analogue signal, i.e. $\mathbf{s}_R = \beta\mathbf{x}$, where β is the AF amplification factor (see e.g. [31]).

[12] Thanks to the linearity of the underlying channel codes any linear combination of codewords is again a valid codeword.

[13] Apart of the optimal metric (sum of exponentials [71]), it is possible to use some approximate metrics (e.g. codeword Euclidean distance [84]) with a sub-optimal (but often near-optimum) performance to reduce the complexity of the decoding process.

usually termed *eXclusive law* [71, 79]:

$$\mathscr{X}_c(\mathbf{c}_A, \mathbf{c}_B) \neq \mathscr{X}_c(\mathbf{c}'_A, \mathbf{c}_B) \Leftrightarrow \mathbf{c}_A \neq \mathbf{c}'_A, \tag{3.8}$$
$$\mathscr{X}_c(\mathbf{c}_A, \mathbf{c}_B) \neq \mathscr{X}_c(\mathbf{c}_A, \mathbf{c}'_B) \Leftrightarrow \mathbf{c}_B \neq \mathbf{c}'_B, \tag{3.9}$$

and hence the mapping operation is simply called as the *eXclusive mapping* [71]. The second fundamental property of the eXclusive mapping is given by the existence of an *inverse mapping operation* $\mathscr{X}^{-1}$ which allows to retrieve the desired data message (from the relay singnal and HSI) at both destinations:

$$\mathscr{X}_c^{-1}(\mathbf{c}_R, \mathbf{c}_A) = \mathbf{c}_B, \tag{3.10}$$
$$\mathscr{X}_c^{-1}(\mathbf{c}_R, \mathbf{c}_B) = \mathbf{c}_A. \tag{3.11}$$

Note that even though the eXclusive mapping is described as a function of individual source data $\mathbf{d}_A, \mathbf{d}_B$ (or equivalently codewords $\mathbf{c}_A, \mathbf{c}_B$) none of these are decoded by the relay in the HDF strategy. This expression is used usually only to simplify the analysis [85].

3.1.3.1 HDF, DNF, CaF: terminology

As we have already mentioned, the principles of HDF, DNF and CaF relaying strategies follow essentially the same basic idea. Here we briefly review the terminology used in the literature to help the reader to get acquainted with the basic concepts of these relaying strategies:

- **HDF**: The eXclusive mapping operation (3.6) is described as the (hierarchical) decoding of the *hierarchical data* message $\mathbf{d}_R = \mathbf{d}_{AB}$ (equivalently hierarchical codeword $\mathbf{c}_R = \mathbf{c}_{AB}$). The hierarchical data are a joint representation of the data from both sources such that they uniquely represent one data source given a full knowledge of the other one [86]. For the successful decoding at the destination, a specific Side Information (SI) on the complementary data must be available. Since this specific SI enables a decoding of the desired data from the hierarchical signal, it is usually denoted as the *hierarchical SI* (HSI) [19, 26].

- **DNF**: In DNF, the eXclusive mapping operation (3.6) is denoted as *denoising*, to stress the fact that the effect of noise is eliminated by the mapping operation and only useful signal is transmistted by the relay (unlike in the AF astrategy). Destinations must have HSI available to decode the desired data. Although some papers focus on the per-sybol operation (per-symbol denoising) [79–81], DNF has been originally introduced as an operation on the whole codewords [31, 62]. Example implementation of the per-codeword denoising[14)] can be found e.g. in [72, 87].

- **CaF**: The eXclusive mapping operation (3.6) is described as a *computation* of some function of the source codewords $\mathbf{c}_R = f(\mathbf{c}_A, \mathbf{c}_B)$ in the CaF strategy. Again, both destinations must have HSI available to decode the desired data. The key idea is to decode the linear functions of the transmitted messages at the relay node, rather than ignoring the interference as noise [13]. The CaF principles are usually demonstrated on the *lattice codes* [88] which are well suited to map the finite field operations (codeword space) to the complex field (constellation space) [13, 77].

3.1.4 BC phase and destination decoding

The output of the eXclusive mapping function (either $\mathbf{d}_R$ or $\mathbf{c}_R$) is further processed by the relay using standard PHY algorithms (channel coding and modulation), and hence it is (after a potential re-encoding)

[14)] Convolutional [87] or LDPC codes [72] are employed at both sources.

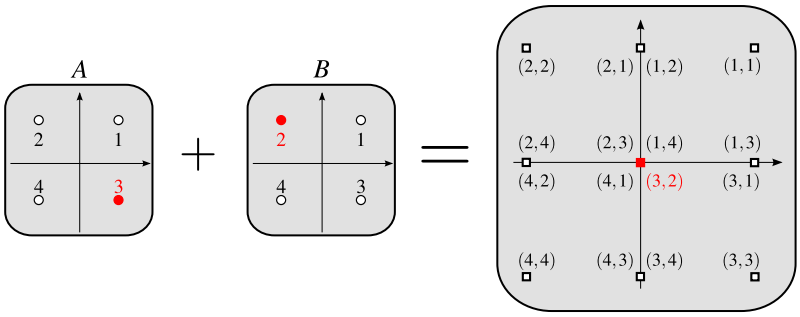

Figure 3.2: MAC phase: 2-WRC with uncoded QPSK ($s_A = s_A^{(3)}$ and $s_B = s_B^{(2)}$ sent).

mapped into the signal space channel symbols $s_R \in \mathscr{A}_s^R$ and broadcast to destinations A and B in the BC phase. The n-th received signal space symbol at node A (the destination for data B) is

$$y_A = h_{RA} s_R + w_A, \tag{3.12}$$

where the complex circularly symmetric AWGN (w_A) has the variance σ_A^2 per complex dimension. Similarly we denote the n-th received signal space symbol at node B (the destination for data A) as

$$y_B = h_{RB} s_R + w_B, \tag{3.13}$$

where the complex circularly symmetric AWGN (w_B) has the variance σ_B^2 per complex dimension.

As noted e.g. [12], the key idea of any WNC system is based on the existence of the "network decoding" (inverse) function which allows to decode the desired message at each destination from the observed relay signal and HSI. The existence of this inverse mapping function is guaranteed by the inverse property of the eXclusive mapping (3.10), (3.11) and hence the desired codeword can be retrieved from the relay signal iff the eXclusive mapping operation employed by the relay fulfills this property.

The complete HDF decoding process at node A can be simply summarized as an inverse mapping operation which maps the received constellation space signal from the relay ($\mathbf{y}_A$) to the desired data/codeword ($\mathbf{c}_B$), using the own (previously sent) data ($\mathbf{d}_A$) as HSI:

$$\mathscr{D}_{\text{HDF}}^A: \quad (\mathbf{y}_A(\mathbf{c}_R), \mathbf{c}_A(\mathbf{d}_A)) \longmapsto \mathbf{c}_B(\mathbf{d}_B), \tag{3.14}$$

and similarly for the node B:

$$\mathscr{D}_{\text{HDF}}^B: \quad (\mathbf{y}_B(\mathbf{c}_R), \mathbf{c}_B(\mathbf{d}_B)) \longmapsto \mathbf{c}_A(\mathbf{d}_A). \tag{3.15}$$

Standard channel decoding algorithms can be used to decode the desired data $\mathbf{d}_i$ from the codeword $\mathbf{c}_i$, $i \in \{A,B\}$ at each destination. Obviously, there are again numerous ways how to implement the decoding operation (3.14), (3.15) in the 2-WRC system, including a 2-step processing (decoding of the relay codeword $\mathbf{c}_R$ followed by the inverse mapping operation (3.10), (3.11)) or a more general decoder implementation, where HSI and relay observations are fed directly into the source data decoder and hence the relay codeword $\mathbf{c}_R$ is not explicitly decoded at the destination.

3.1.5 Uncoded example

To visualize the basics of the HDF operation we overview the processing of particular nodes in a single communication round (MAC and BC phase) in the uncoded 2-WRC system with QPSK modulation.

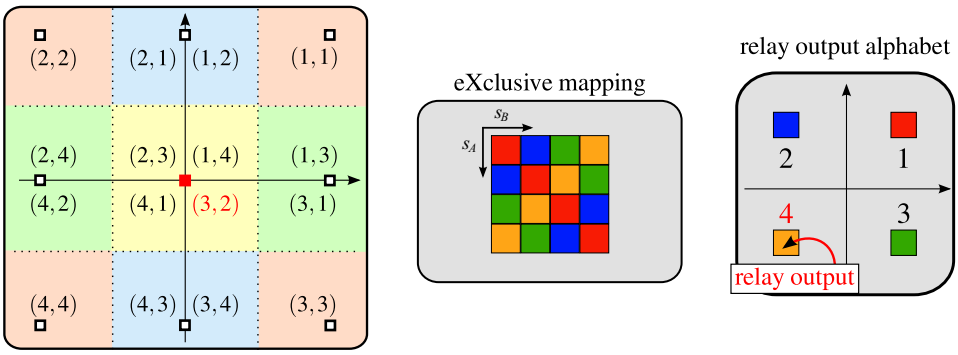

Figure 3.3: Relay eXclusive mapping: 2-WRC with uncoded QPSK ($s_A = s_A^{(3)}$ and $s_B = s_B^{(2)}$ sent).

3.1.5.1 MAC phase

The source messages are mapped directly to constellation symbols[15] s_A, s_B, which are then simultaneously transmited towards the relay. The *compound (hierarchical) constellation* observed at the relay node is visualized in Fig. 3.2 (for the sake of simplicity we assume that $h_A = h_B$).

3.1.5.2 eXclusive mapping at the relay and BC phase

As it is obvious from Fig. 3.2, the relay cannot unambiguously infer the actual transmitted pair of source symbols $s_A^{(3)}, s_B^{(2)}$, since the corresponding point in the constellation space belongs to multiple (overlapped) pairs of source symbols. Fortunately, even in this case it is still possible to map the received signal to the relay output in such a way that both destinations would be able to retrieve the desired symbol from the relay signal.

In HDF the relay maps the received constellation space signal to the output signal using the eXclusive mapping operation as in (3.6), (3.7). Since we analyze the uncoded system, this mapping produces directly the relay symbol $\mathscr{X}_s(s_A, s_B) = s_R$. To demonstrate the principle of the mapping operation[16] $s_R^{k_{ij}} = \mathscr{X}_s\left(s_A^i, s_B^j\right)$, it is useful to describe it in a matrix form [24]:

$$X_s = \begin{bmatrix} k_{11} & \cdots & k_{1M_s} \\ \vdots & \ddots & \vdots \\ k_{M_s1} & \cdots & k_{M_sM_s} \end{bmatrix}, \tag{3.16}$$

where $k_{ij} = X_s(i,j)$, $i,j \in \{1,2,\ldots M_s\}$ is the index of the relay output symbol $s_R^{k_{ij}}$ and M_s is the source alphabet cardinality.

In the uncoded system the eXclusive mapping operation can be simply visualized (see Fig. 3.3) as a "colouring" process, where the particular colour (i.e. relay output symbol s_R) is assigned to the particular region in the continuous constellation space. As it is also obvious from Fig. 3.3, this corresponds to the assignment of indices k_{ij} (colours) of relay symbols to particular elements of the eXclusive mapping

[15] The channel coding operation $\mathscr{C}^i$, $i \in \{A,B\}$ is simply an identity operation ($\mathbf{c}_i = \mathscr{C}^i(\mathbf{b}_i) = \mathbf{b}_i$) in the uncoded system.

[16] Note again that even though the eXclusive mapping $\mathscr{X}_s$ is described as a function of individual source symbols s_A, s_B, none of these are decoded by the relay in the HDF strategy and this expression is used again only to simplify the analysis [85].

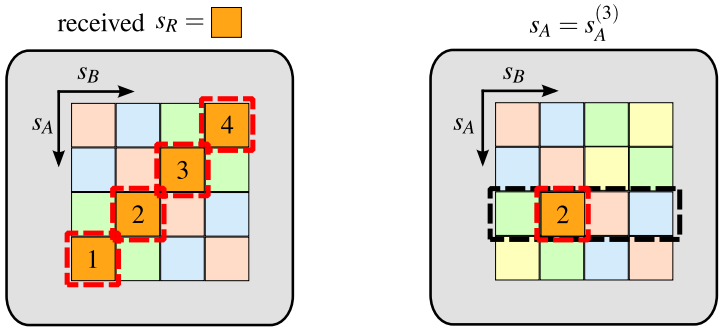

Figure 3.4: Destination decoding: 2-WRC with uncoded QPSK ($s_A = s_A^{(3)}$ and $s_B = s_B^{(2)}$ sent).

matrix. The mapping operation visualized in Fig. 3.3 can be explicitly evaluated as:

$$X_s = \begin{bmatrix} 1 & 2 & 3 & 4 \\ 2 & 1 & 4 & 3 \\ 3 & 4 & 1 & 2 \\ 4 & 3 & 2 & 1 \end{bmatrix}.$$

As already said, the eXclusive mapping operation must not break the eXclusive law (3.8), (3.9) to guarantee the decodability of the desired data from the relay signal at both destinations. It is quite straightforward to show that in this simple example this is equivalent to securing that each particular relay output symbol s_R (colour) occurs only once in every row and every column of the eXclusive mapping matrix[17]. Note also that even in this simple uncoded example the “compression" of relay output information (induced by the eXclusive mapping operation) is clearly demonstrated. Although there are M_s^2 total combinations of M_s-ary source symbols, the relay output is “compressed" to the M_s-ary symbol by the eXclusive mapping operation, as it is also aparent from Fig. 3.3.

3.1.5.3 Destination decoding

The decoding operation (3.14), (3.15) reduces to a simple inverse mapping operation $\mathscr{X}_s^{-1}(s_R, s_i) = s_j$ ($i, j \in \{A, B\}$ and $i \neq j$) in the uncoded system. Without loss of generality we describe the decoding process at node A. As it is visualized in Fig. 3.4, the decoding operation is a two step process in the observed example. Firstly, the estimate of the relay output signal $\hat{s_R} = s_R^{(4)}$ (“yellow" symbol) is inferred and subsequently this estimate is used together with the own (previously sent) symbol $s_A = s_A^{(3)}$ (HSI) to retrieve the desired symbol:

$$\mathscr{X}_s^{-1}\left(s_R^{(4)}, s_A^{(3)}\right) = s_B^{(2)}.$$

Note that if HSI would be unavailable at destination, there will remain an ambiguity about the desired symbol s_B after obtaining $\hat{s}_R$ (as it is also visualized in Fig. 3.4).

3.2 Selected open research problems in WNC

Although the fundamental idea of HDF processing is relatively straightforward, there is still a great number of research challenges which quickly arise when more complicated models of channels and networks are to be analyzed. In this section we briefly overview two specific open problems in the WNC research,

[17] Equivalently it can be said that the mapping must form a Latin square – see e.g. [81]

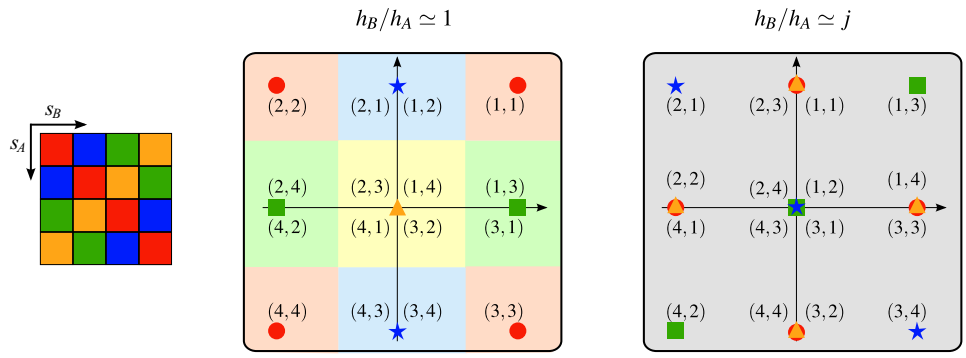

Figure 3.5: Impact of channel parametrization: 2-WRC with uncoded QPSK.

namely the WNC processing in *parametric channels* and WNC processing with *partial/imperfect HSI*. Since both these problems are currently under a heavy investigation in the research community we also provide an overview of the state-of-the-art solutions in these interesting research areas.

3.2.1 HDF in parametric channels

While the HDF strategies are mature in the traditional AWGN channel, their performance in *fading channels* can be seriously degraded due to the inherent wireless channel *parametrization* (e.g. complex channel gain) [65, 71]. As noted also in [79, 89], the fixed eXclusive mapping operation (e.g. bit-wise XOR) does not work always well due to the undesired phase and amplitude offset between the source-relay channels h_A, h_B.

In a parametric system, channel coefficients h_A, h_B in the MAC stage determine how the two source signals overlap in the compound constellation observed at the relay node [65]. If the eXclusive mapping operation is kept fixed at the relay, some specific values of channel parameters can directly invoke *failures of the eXclusive law* (3.8), (3.9), resulting in a decreased performance of the overall system[18)]. The impact of channel parametrization on the shape of compound constellation in the uncoded system is shown in Fig. 3.5. As it is obvious from this Figure, the eXclusive mapping operation designed in Fig. 3.3 for $h_A \simeq h_B$ does not work well for $h_B/h_A \simeq \mathrm{j}$, since in this case some symbols belonging to the different relay output symbol s_R are overlapped in the constellation space, preventing the relay to perform unambiguous decision about its output. This detrimental effect of channel parametrization is specific for HDF systems and it has been identified as a *major problem* of the WNC-based bi-directional relaying strategies already in [63, 66].

Generally, such performance degradation of a parametric HDF system can be avoided by phase pre-rotation (and power control) of both source node transmissions [65, 68, 75] or by adapting the relay eXclusive mapping operation to the actual channel conditions [65]. While the first aproach virtually reverts the fading channel into the conventional (non-parametric) AWGN, the second one aims on the *adaptive design of eXclusive mapping* operation (adaptation to the actual value of channel parameters h_A, h_B), which can also prevent the occurance of eXclusive law failures. However, both these approaches have several drawbacks, including a practical infeasibility of the (synchronized) multi-node transmission phase pre-rotation or a sensitivity to channel estimation errors of adaptive solutions (inaccurate channel estimates results in an improper choice of the relay eXclusive symbol mapper) [90].

Due to the aforementioned drawbacks of HDF with phase-synchronization or adaptive eXclusive mapping, some authors try to attack the problem from a different angle. In [91] a simple multi-level

[18)] This detrimental effect of channel parametrization affects the performance of the system even if the relay has perfect estimates of source-relay channels available.

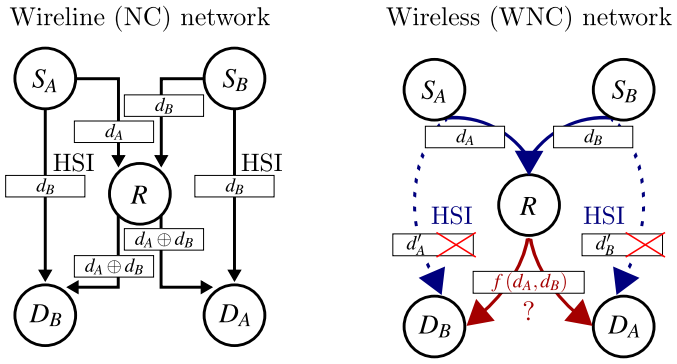

Figure 3.6: Wireline vs. wireless 5-node Butterfly Network. Since HSI channels are generally unreliable in wireless butterfly network, the particular amount of information which must be broadcast by the relay (denoted as $f(d_A, d_B)$ in the figure) depends on the quality of both HSI links $S_A \to D_B$ and $S_B \to D_A$ (see e.g. [24]).

coding scheme over QPSK modulation is presented which allows to adaptively change the decoding of hierarchical codewords at the relay according to the actual channel conditions. However, this approch is limited only to the QPSK modulation scheme, and moreover, it avoids the performance degradation only for some specific values of channel parameters. In [92] the authors try to avoid the occurance of *singular fade states* (eXclusive law failures) by the design of a distributed space-time coding technique (single antenna at both sources and relay node is assumed). Another approach is based on the design of new modulation schemes which can essentialy avoid (or at least decrease) the impact of channel parametrization on the system performance. Some novel *non-linear modulation schemes* for parametric HDF systems are introduced in [93, 94]. The design of *linear modulation schemes* for parameteric HDF systems represents one of the two major areas of our own research and it is covered separately in Part II. A core of our results in this field has been already published in [15, 16, 18, 20–22, 25, 95].

3.2.2 Partial HSI processing

Although the principles of WNC profit from the specific nature of wireless channels (inherent combining of electromagnetic waves and its broadcast nature), they still remain partially grounded in the essentials of conventional Network Coding (NC) [14, 32].

In wireline NC-based networks, the information packets are sent through orthogonal links with identical capacity and intermediate relay nodes combine the received packets before re-transmission (instead of purely relaying them) to boost the system performance. While this packet-based NC processing is natural in wireline networks, in wireless networks the *inherent broadcast property* is to be exploited on channels with potentially *significantly different capacities*. Consequently, even though each node's transmission can be potentially overheard by several nodes in its vicinity, the same (perfect) information cannot be always retrieved by all these nodes due to the varying capacities of related wireless channels. The legacy of NC principles is hence partially broken in wireless (WNC-based) networks, yielding several significant and novel research challenges [19].

One example of this phenomenon can be demonstrated in a *5-node Butterfly Network* (BN) topology (see Fig. 3.6), where, similarly as in 2-WRC, HSI is required to decode the desired data from a common (NC/WNC-coded) data stream. While this information can be perfectly delivered to both destinations through orthogonal links in the wired BN, no dedicated orthogonal channels for transmission of HSI are required in the *Wireless BN (WBN)*, where both destinations can obtain HSI directly from the overheard

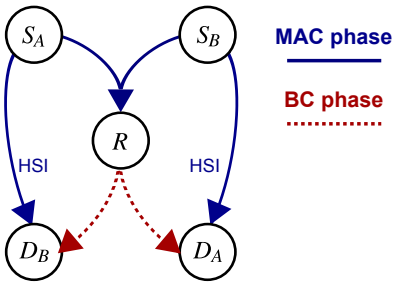

Figure 3.7: HDF signal flow in Wireless Butterfly Network (WBN).

source node transmission (Fig. 3.7). Unfortunately, when channel conditions on such "overheard" HSI link(s) are not favourable, only *limited (partial/imperfect) HSI* can be received at destinations, making the conventional (perfect HSI) decoding impossible [24, 96, 97].

To the best of our knowledge, there are still only very limited results considering the problem of *imperfect HSI processing*. As shown in [96], the performance of WBN with *minimal cardinality HDF* relaying[19] is limited by the *HSI link capacity*. Fortunately, it is possible to overcome this limitation by employing the *extended cardinality* processing (see e.g. [24, 97]). Although the increased cardinality of the relay output is required in this case, only *partial HSI* becomes sufficient to guarantee a successful decoding at both destinations. As shown in [24], this approach can outperform (for some specific channel conditions) the conventional processing with minimal cardinality HDF relaying.

The basic principles of HDF processing in the *uncoded WBN system* with QPSK source alphabet constellation are summarized in Figs. 3.8 (perfect/full HSI), 3.9 (no HSI) and 3.10 (partial HSI). The decoding process is visualized only for destination D_B (for the sake of clarity).

The analysis of *partial/imperfect HSI* processing represents one of the two major areas of our own research and it is covered separately in Part III. A core of our results in this field has been already published in [17, 23, 24, 26, 27], [19] has been submitted for publication.

3.3 Further reading

To help the reader get acquainted with another interesting areas of WNC processing research we conclude this section with an overview of some further relevant references.

3.3.1 Adaptive eXclusive mapping

As already noted, some authors try to avoid the performance degradation of HDF in 2-WRC by the adaptation of eXclusive mapping [65, 75, 79]. A design of adaptive relay output mapping was originally proposed in the paper by Koike et al. [79], where a brute-force search algorithm which identifies the optimal mapping operation[20] for a given value of the *relative channel parameter* ($h = {}^{h_B}/_{h_A}$) was presented. This technique was later extended to the adaptive modulation case in [98].

An analytical treatment of the eXclusive law failure events (singular fade states) is presented in [80], where the fact that only some singular fade states contribute dominantely to the average Symbol Error Rate (SER) in Rician channels is presented[21]. Koike's design of adaptive mapping was revised in [81],

[19] The cardinality of the relay output alphabet $\mathscr{A}_s^R$ is given by $\left|\mathscr{A}_s^R\right| = \max\left\{\left|\mathscr{A}_s^A\right|, \left|\mathscr{A}_s^B\right|\right\}$ in the minimal cardinality HDF.

[20] The goal was to find the mapping which has the best Euclidean distance profile of the compound constellation received at the relay (unocoded QPSK modulation is assumed at both sources).

[21] Such behaviour was not observed in Rayleigh channels. Similar conclusions have been drawn already in [22].

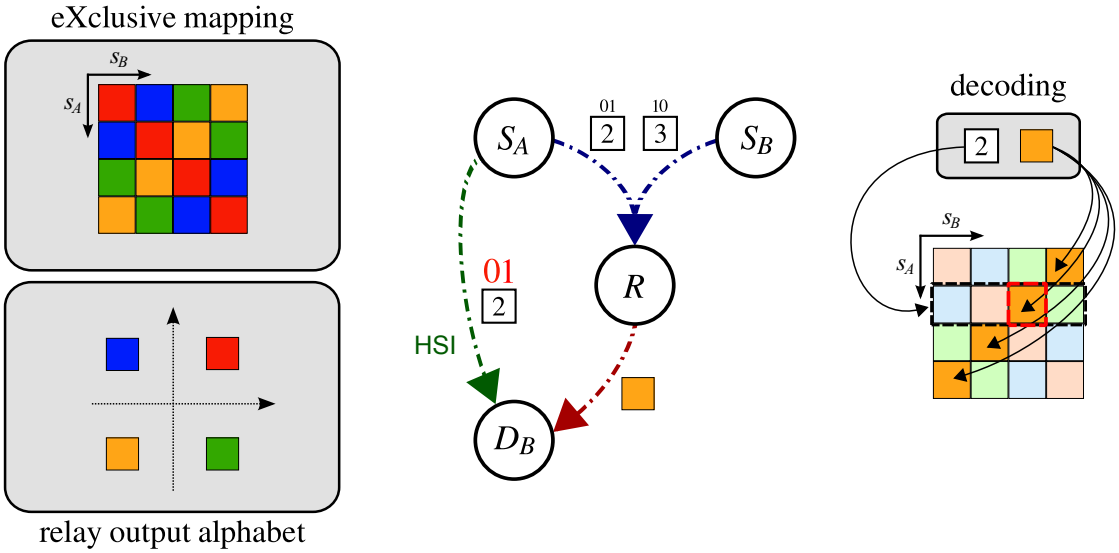

Figure 3.8: Perfect (full) HSI processing in WBN. Relay output has *minimal cardinality* ($\left|\mathscr{A}_s^R\right| = \max\left\{\left|\mathscr{A}_s^A\right|, \left|\mathscr{A}_s^B\right|\right\}$).

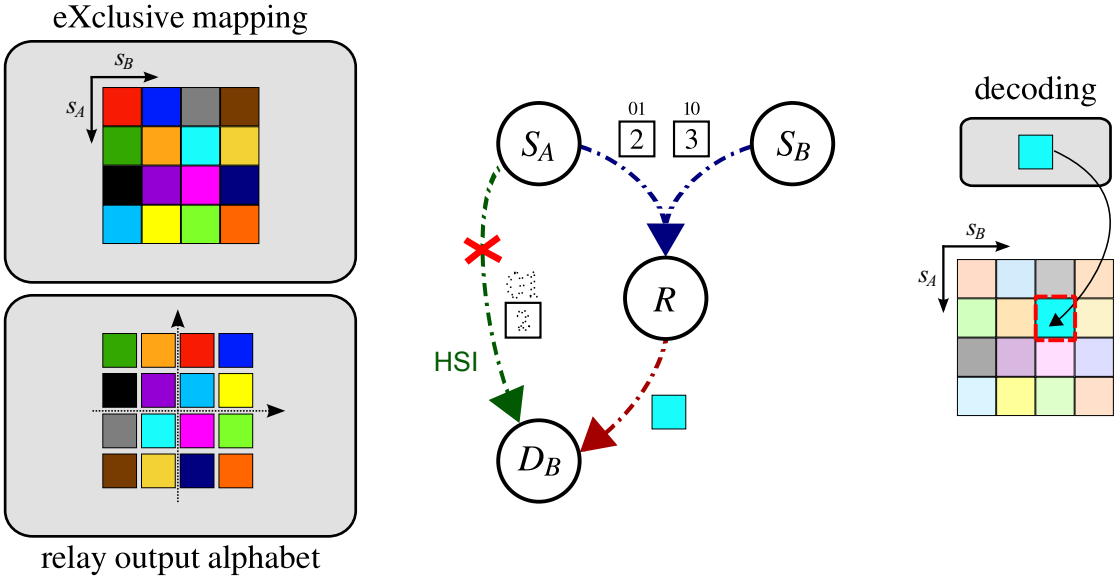

Figure 3.9: Zero HSI processing in WBN. Relay output has *full cardinality* ($\left|\mathscr{A}_s^R\right| = \left|\mathscr{A}_s^A\right| \cdot \left|\mathscr{A}_s^B\right|$).

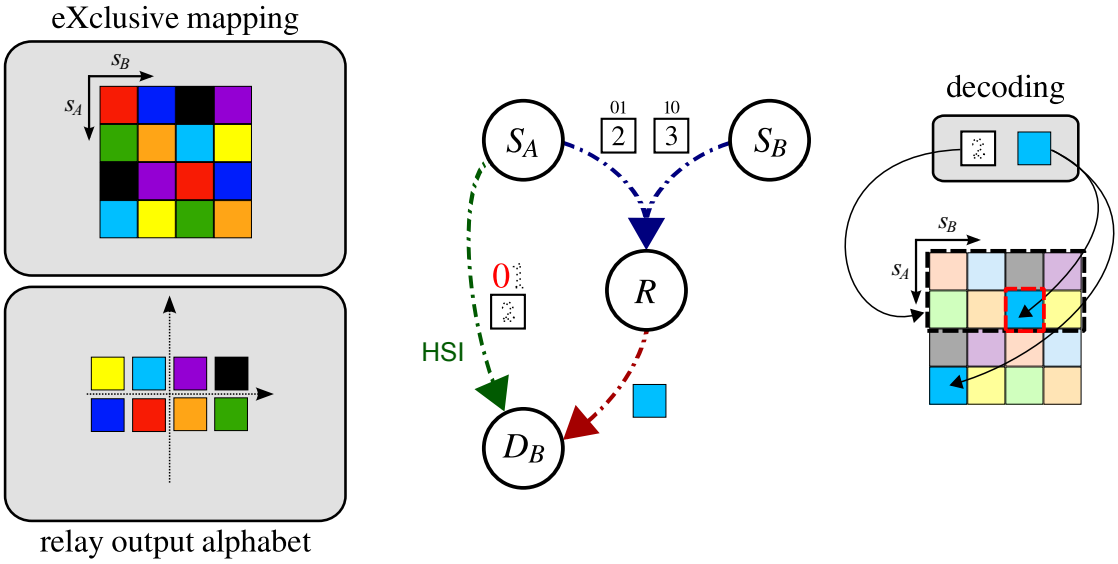

Figure 3.10: Partial HSI processing in WBN. Relay output has *extended cardinality* ($\max\{|\mathscr{A}_s^A|, |\mathscr{A}_s^B|\} < |\mathscr{A}_s^R| < |\mathscr{A}_s^A| \cdot |\mathscr{A}_s^B|$).

where a novel construction of adaptive mapping operation (based on the Latin squares) is introduced. The Latin squares-based design of adaptive mapping was further extended to 2-WRC with multiple source and relay node antennas [99].

While most of the authors focus only on the *uncoded 2-WRC* case, there are already some results available also for the convolutionally-coded [87] and LDPC-coded [72] 2-WRC systems.

3.3.2 Lattice codes

Structured codes (e.g. the lattice codes [88]) are more and more preferred over the random codes in capacity analyses of multinode wireless networks. In the realm of HDF systems, the inherent linearity (group structure) of lattice codes can be favourably exploited, since they perfectly suite the requirement that any linear combination (sum) of codewords (performed by the channel) is again a valid codeword. This group structure of lattices (with respect to real vector addition) is pointed out e.g. in [77] and it is exploited later as the basis for the capacity evaluation of the CaF relaying strategy [13, 76]. More details about the lattice code construction can be found e.g. in [10, 100–103] and references therein.

3.3.3 Real-world implementation of HDF/WNC

Practical implementation of HDF/WNC systems introduces several new research challenges which do not have its counterpart in the convetional point-to-point systems. First of all, one of the prevailing assumptions in the research of HDF system is the perfect synchronization of symbol timing among all simultaneously transmitting nodes. Unfortunately, there are still only very few papers discussing the issues associated with the symbol-time synchronization in HDF systems (see e.g. [104–106]).

As already noted in Section 3.2.1, performance of HDF systems faces a serious perfromance degradation in fading channels, which could be potentially avoided if a synchronization of source nodes transmission phases is employed in the system. Although this phase-level synchronization is often considered as unfeasible, Huang et al. introduced a *phase synchronization scheme* for the 2-WRC with uncoded QAM

constellation[22] [107], providing some promising initial results which encourage an implementation of phase-synchronous HDF processing.

To the best of our knowledge, there are still very few papers investigating real-world implementations of WNC processing. These papers include [58] (AF), [108] (3-step DF scheme based on the modified 802.11 MAC/PHY) and [109] (HDF implemented on USRP-ETTUS [110]). The implementation in [109] (so-called frequency domain WNC) requires only moderate modification of packet preamble design for 802.11 a/g, and it also efficiently exploits the cyclic prefix of OFDM modulation to combat the symbol asynchronism. The experimental results show that synchronous and asynchronous frequency domain WNC have nearly the same Bit Error Rate (BER) performance (for both channel coded and uncoded system).

3.3.4 Further research directions

Design of a suitable processing for channel-coded HDF (joint network-channel coding strategies) represents another important direction in the research of HDF systems. Some practical design of joint-network channel coding schemes can be found in [111] (fountain codes [55]), [83] (repeat-accumulate codes) or [72, 89] (LDPC codes).

As noted e.g. in [24], even the mapping of source information bits to the constellation symbols can have a significant impact on the HDF system performance [107,112]. A non-uniform constellation design (including the bit mapping) for binary WNC system is presented in [113], where the goal is to lower the complexity of HDF with higher-order constellation by utilizing the binary codes (lattice codes or non-binary schemes have higher decoding complexity). The fact that non-binary codes over the finite field $\mathbb{F} = \mathrm{GF}(q)$ allow to decode the hierarchical data from a larger set of linear network combinations is discussed e.g. in [82].

The optimization of BC phase transmission in the HDF systems represents an another poorly investigated research area. In the 2-WRC systems with full relay decoding (DF or JDF strategy) the optimal relay BC processing depends on the symmetry of BC channels. While the conventional bit-wise XOR operation applied on the decoded source data is considered as optimal when the BC channels are symmetric, the assymetric case calls for novel BC schemes, based e.g. on the superposition coding approach (see e.g. [114] for more details). The broadcast capacity region of 2-WRC with the DF relay is investigated e.g. in [74].

[22] Even better performance of the proposed synchronization scheme is expected in the channel coded systems.

Part II

WNC in parametric wireless channels

Chapter 4

Introduction

"The best way to predict the future is to invent it."

Alan Curtis Kay

As noted in Section 3.1.3, the feasibility of HDF is conditioned by the satisfaction of the eXclusive law (3.10), (3.11). Moreover, it can be shown that this law must hold alongside the complete signal path (MAC and BC) [86] to guarantee that both destinations can decode the desired data.

A code (codebook) satisfying the eXclusive law at the signal space codeword level is sometimes called the Hierarchical eXclusive Code (HXC) [71, 86]. While a direct design of HXC codebooks is highly complex [86], an alternative approach based on the Layered HXC (L-HXC) design was introduced in [86, 115]. L-HXC consists (in the simplest case) of the error correcting code (outer layer) and the alphabet memoryless mapper (inner layer). The inner layer (closer to channel symbols) provides the *eXclusive property* of the hierarchical symbols and the outer layer code can be arbitrary state-of-the-art capacity achieving code (e.g. turbo code or LDPC). The alphabet memoryless mapper ($\mathscr{A}_s^i(.), i \in (A,B)$) fulfilling the eXclusive law is then called the Hierarchical eXclusive Alphabet (HXA) [115] (see Fig. 4.1).

Theorems showing the viability of the L-HXC design in 2-WRC with HDF strategy can be found in [71, 115]. The complexity of the proper HXA design increases in case of the *parametric* channel (see Section 3.2.1), where a specific channel parametrization can invoke the *eXclusive law failures*, resulting in a significant performance degradation (see e.g. [79, 86]). Note again that these eXclusive law failures occur whenever a specific pair of hierarchical symbols $u^{i,j}\left(s_A^i, s_B^j\right)$, $u^{i',j'}\left(s_A^{i'}, s_B^{j'}\right)$, such that $\mathscr{X}_s(u^{i,j}) \neq \mathscr{X}_s(u^{i',j'})$, falls into the same point (or close to each other) in the constellation space, thus increasing the probability of erroneous decision at the relay (see Fig. 3.5).

4.1 Summary of contributions

In this part of the thesis we overview our contributions to the design of *linear modulation schemes* for parameteric HDF systems (*Parametric HXC* (PHXC) design). Our first approach to the design of PHXC for

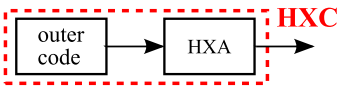

Figure 4.1: Layered Hierarchical eXclusive Code.

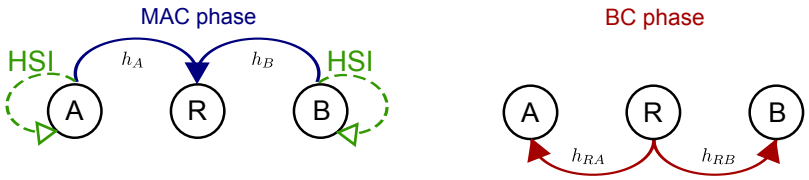

Figure 4.2: 2-WRC with HSI.

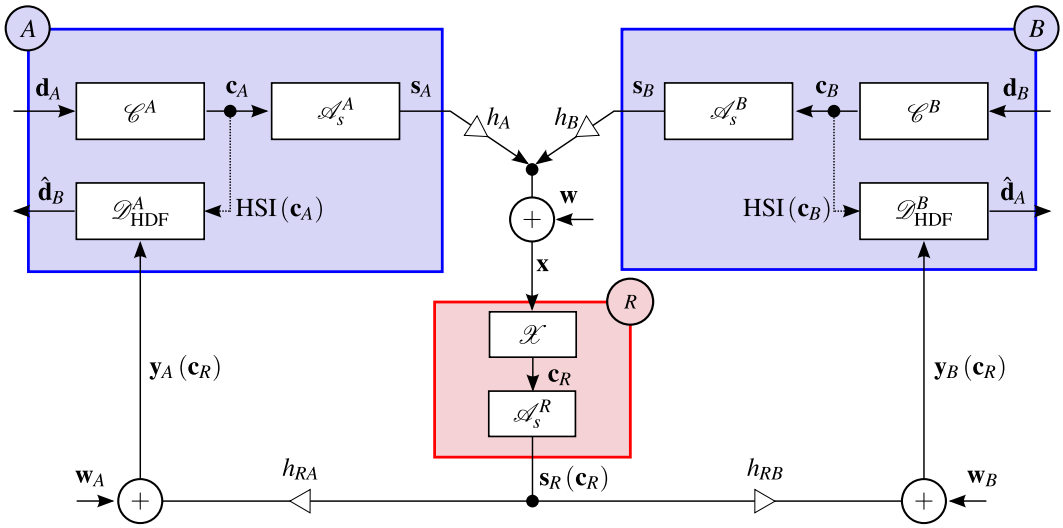

Figure 4.3: Basic principle of HDF processing in 2-WRC.

parametric 2-WRC is presented in [20], where, based on the criterion for parameter-invariant constellation space boundary [116], the design criteria for *constellation space source node codebooks* with *channel parameter-invariant decision regions* at the relay are derived. However (as discussed later in [15]), requirements of these design criteria are relatively strict, preventing the design of codebooks with higher than binary cardinality in $\mathbb{C}^2$. To overcome this inconvenience, a relaxed version of these design criteria is introduced in [15], and a construction algorithm for codebooks with arbitrary cardinality in $\mathbb{C}^2$ is presented. An alternative approach (based on a geometrical interpretation of the design problem) to the design of multi-dimenisonal HXC (respective HXA) is available in [18, 21, 117]. The principles of these two multi-dimensional constellation design approaches are summarized in Chapter 5.

Although the novel $\mathbb{C}^2$ constellation alphabets (Chapter 5) are quite robust to channel parametrization, this robustness is unfortunately accompanied with a reduction of achievable throughput (a direct consequence of the increased alphabet dimensionality). Naturally, the goal of the follow-up work was to find a suitable constellations in $\mathbb{C}^1$ to avoid this inherent drawback of multi-dimensional constellations. Unfortunately, based on the analysis of (squared) *Euclidean distance properties* of hierarchical symbols, the fact that only binary HXA can avoid violation of the eXclusive law (for arbitrary parametrization) in $\mathbb{C}^1$ is proved in [22]. The analysis of the Euclidean distance of hierarchical symbols is restated in Chapter 6.

Although the occurance of eXclusive law failures cannot be prevented in case of conventional modulation schemes in $\mathbb{C}^1$ (excepting the binary alphabets), it can be shown that in *Rician fading channels* it is possible to suppress this harmful behaviour of channel parametrization by a design of novel 2-slot constellation alphabets. The proposed *Non-uniform 2-slot (NuT)* alphabets [16, 25] are robust to channel

parametrization effects in Rician channels, outperforming the traditional linear modulation schemes without sacrificing the overall system throughput. The design principles of NuT constellations are discussed in Chapter 7.

4.2 System model

For the purpose of this Chapter we adopt the 2-WRC system model presented in Section 3.1 (see Fig. 4.2). Nodes A and B would like to mutually (bi-directionally) exchange data. Since A, B are not in a radio visibility (direct link is missing), a support of a common shared relay node R is required. The transmission from each source serves also as HSI for the reverse link.

The basic principle of HDF processing in 2-WRC is summarized in Fig. 4.3. Relay R maps the received constellation space signal $\mathbf{x}$ to the discrete relay output message $\hat{\mathbf{c}}_R$, which carries a joint information about source A, B data. If HSI (own, previously sent data in 2-WRC) is available at both sources, the desired information can be decoded from the relay signal and HSI. Note again that a particular implementation of the relay eXclusive mapping ($\mathscr{X}$) and destination decoding operations ($\mathscr{D}^A_{\text{HDF}}$, $\mathscr{D}^B_{\text{HDF}}$) can have various forms (as discussed also in Section 3.1).

Chapter 5

Multi-dimensional constellation design

"Science never solves a problem without creating ten more."

George Bernard Shaw

5.1 Design criteria for multi-dimensional HXC with parameter invariant decision regions

5.1.1 Introduction

One of the first attempts to find a suitable HXC for HDF processing in parametric 2-WRC was based on the idea to design the source alphabets (codewords) in such a way that the resulting hierarchical codeword visible at the relay has *parameter-invariant decision regions* [15, 20]. Based on the analysis of conditions which guarantee parameter-invariant decision regions for a particular pair of hierarchical codewords (PHXC design criteria – see [116] for details), we introduce a design algorithm for complete *PHXC codebooks*.

PHXC codebooks are designed by applying the pairwise PHXC design criteria on all *"critical" hierarchical codeword pairs*, i.e. on all pairs of hierarchical codeword pairs which must follow the eXclusive law. Such an approach will force all corresponding pairwise boundaries (i.e. not only the ones which are directly affecting the decision regions shape) to be parameter-invariant. Although this requirement could be relatively strict, it allows us to express the codebook design criteria in a compact set of required conditions. In this section we present the design criteria for the PHXC codebook and show that all requirements of these design criteria can be satisfied at once only if the nodes use different individual codebooks.

5.1.2 Definitions and sytem model

We adopt the 2-WRC system model presented in Section 3.1 (see Fig. 4.2). For the purpose of this section we assume that signal space codewords $\mathbf{s}_i$ ($i \in \{A,B\}$) are drawn directly from individual source codebooks $\mathscr{B}_A$, $\mathscr{B}_B$ (source codebooks can be different in general). The equivalent hierarchical signal $\mathbf{u} = \mathbf{s}_A + h\mathbf{s}_B$ (as seen by the relay) can be interpreted as an element of the equivalent hierarchical codebook $\mathbf{u} \in \mathscr{B}_u$. The number of individual codewords in $\mathscr{B}_A$ and $\mathscr{B}_B$ is assumed to be equal, i.e. $|\mathscr{B}_A| = |\mathscr{B}_B| = N$ and the number of hierarchical codewords is $|\mathscr{B}_u(h)| \leq N^2$. Throughout this section we assume only a *minimal* cardinality of the hierarchical codebook $|\mathscr{B}_u(h)| = N$. For a general discussion on hierarchical codebook cardinality see [86].

	i_{B1}	i_{B2}	$\dots$	i_{BN}
i_{A1}	$\mathbf{u}^{(i_{A1},i_{B1})}$	$\mathbf{u}^{(i_{A1},i_{B2})}$	$\dots$	$\mathbf{u}^{(i_{A1},i_{BN})}$
i_{A2}	$\mathbf{u}^{(i_{A2},i_{B1})}$	$\mathbf{u}^{(i_{A2},i_{B2})}$	$\dots$	$\mathbf{u}^{(i_{A2},i_{BN})}$
$\vdots$	$\vdots$	$\vdots$	$\ddots$	$\vdots$
i_{AN}	$\mathbf{u}^{(i_{AN},i_{B1})}$	$\mathbf{u}^{(i_{AN},i_{B2})}$	$\dots$	$\mathbf{u}^{(i_{AN},i_{BN})}$

Table 5.1: Example of hierarchical codeword table ($|\mathscr{B}_A| = |\mathscr{B}_B| = N$).

5.1.3 Parametric Hierarchical Exclusive Code in 2-WRC

5.1.3.1 Relay processing in parametric 2-WRC

In parametric 2-WRC the codewords visible at the relay $\mathbf{u}(h) \in \mathscr{B}_u(h)$ are parametrized by the relative channel parameter $h = h_A/h_B$, making the decision regions of the relay HDF re-encoder to be also dependent on h. Consequently, the exclusive law must be generalized in *parametric* channel [116]:

$$\mathscr{X}_s(\mathbf{s}_A, \mathbf{s}_B, h) \neq \mathscr{X}_s(\mathbf{s}'_A, \mathbf{s}_B, h) \Leftrightarrow \mathbf{s}_A \neq \mathbf{s}'_A, \tag{5.1}$$

$$\mathscr{X}_s(\mathbf{s}_A, \mathbf{s}_B, h) \neq \mathscr{X}_s(\mathbf{s}_A, \mathbf{s}'_B, h) \Leftrightarrow \mathbf{s}_B \neq \mathbf{s}'_B, \tag{5.2}$$

and it must hold for all permissible values of h.

The code which has the relay processing invariant to the channel parametrization is usually called PHXC [116]. PHXC generally comprises source codebooks $\mathscr{B}_A$, $\mathscr{B}_B$, the relay output codebook $\mathscr{B}_R$ and particular relay processing functions. In the following sections we introduce a design criteria for $\mathscr{B}_A$ and $\mathscr{B}_B$ which can guarantee that the relay decoding function does not depend on h, i.e. the relay decision regions are *parameter-invariant* [116].

5.1.3.2 HDF decoder decision regions

We denote the particular signal space codewords in codebooks as follows: $\mathscr{B}_A = \{\mathbf{s}^{i_A}\}_{i_A}$, $\mathscr{B}_B = \{\mathbf{s}^{i_B}\}_{i_B}$ and $\mathscr{B}_u = \{\mathbf{u}^k\}_k$. Let $\mathbf{u}^{k(i_A,i_B)}(h) = \mathbf{s}^{i_A} + h\mathbf{s}^{i_B}$ be the equivalent hierarchical codeword received at the relay. Codeword indices k, i_A, i_B must follow the exclusive law (5.1), (5.2). Note that the index of hierarchical codeword (k) is a function of the pair of individual codeword indices (i_A, i_B), hence it is useful to list all permissible combinations of individual codewords $\mathbf{s}^{i_A}$, $\mathbf{s}^{i_B}$ (and corresponding hierarchical codewords $\mathbf{u}^{k(i_A,i_B)}$) in a "hierarchical codeword table" (Table 5.1). We generally assume that all codebooks are subsets of 2-dimensional vector space over the field $\mathbb{C}$ ($\mathscr{B}_A, \mathscr{B}_B, \mathscr{B}_u, \mathscr{B}_R \subset \mathbb{C}^2$) and that the parameter is a scalar in $\mathbb{C}$, $h \in \mathbb{C}$. The field is typically the set of real or complex numbers.

For the subsequent analysis, we need to define a *pairwise boundary* as a set of points which have the same constellation space distance to a pair of hierarchical codewords $\mathbf{u}^k(h)$ and $\mathbf{u}^l(h)$.

Definition 4. Pairwise boundary $\mathscr{R}^{kl}(h)$ is the set of points having the same (constellation space) Euclidean distance to a pair of hierarchical codewords $\mathbf{u}^{k(i_A,i_B)}(h)$ and $\mathbf{u}^{l(i'_A,i'_B)}(h)$ for any $k \neq l$. The *pairwise boundaries set* $\mathscr{S}_{\mathrm{PB}}$ is the union of all pairwise boundaries $\mathscr{R}^{kl}(h)$.

The pairwise boundary (see the example in Fig. 5.1) is defined for every permissible pair of hierarchical codewords ($\mathbf{u}^k(h)$,$\mathbf{u}^l(h)$). It is obvious that, from the perspective of the codebook design, the most critical are those pairs of hierarchical codewords, which have one of the comprising individual codewords identical ($\mathbf{s}_A = \mathbf{s}'_A$ or $\mathbf{s}_B = \mathbf{s}'_B$). These hierarchical codeword pairs may directly violate the exclusive law (5.1), (5.2), if some specific value of parametrization cause them to fall into an identical decision region of the relay decoder. The codewords from such pair must hence be designed appropriately to ensure

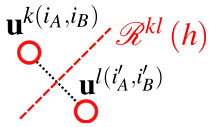

Figure 5.1: Visualization of the pairwise boundary in the constellation space.

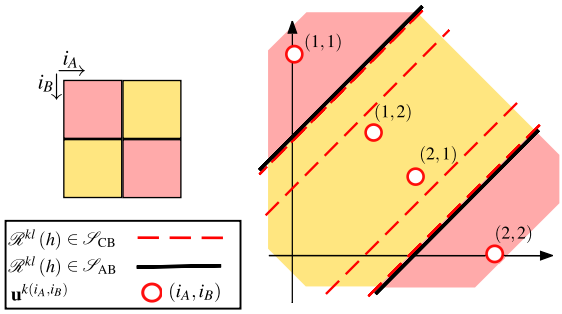

Figure 5.2: HDFD decision regions shape example ($\mathbb{R}^2$ codebook). Note that some boundaries lie *inside* the decision region corresponding to *one hierarchical codeword* (given by the same region colour). Such boundaries *do not* affect the final decision region shape an hence can be considered as "masked".

that they always fall into two *distinct mapping regions* of the output HDF codebook $\mathscr{B}_R$, otherwise the error-less communication would be impossible. As it is noted in the following Definition, the particular pairwise boundaries between all such pairs of hierarchical codewords constitute some subset of $\mathscr{S}_{\mathrm{PB}}$.

Definition 5. *Critical boundaries subset* $\mathscr{S}_{\mathrm{CB}} \subset \mathscr{S}_{\mathrm{PB}}$ is the set of all pairwise boundaries $\mathscr{R}^{kl}(h)$ between all permissible hierarchical codewords pairs $\mathbf{u}^{k(i_A,i_B)}(h)$, $\mathbf{u}^{l\left(i'_A,i'_B\right)}(h)$ such that $i_A = i'_A$ or $i_B = i'_B$.

Pairwise boundary $\mathscr{R}^{kl}$ between the hierarchical codewords pair $\mathbf{u}^{k(i_A,i_B)}(h)$, $\mathbf{u}^{l\left(i'_A,i'_B\right)}(h)$ is hence classified as critical ($\mathscr{R}^{kl}_{\mathrm{CB}}$) by Definition 5, if the corresponding hierarchical codewords reside in the same row ($i_A = i'_A$) or column ($i_B = i'_B$) of the hierarchical codeword table (Table 5.1).

5.1.3.3 Pairwise PHXC design criteria

As already mentioned, one of the possible ways how to design PHXC is to design the codebooks $\mathscr{B}_A$ and $\mathscr{B}_B$ in such a way that the relay decoding function would not depend on h, i.e. the HDF decoder (HDFD) decision regions are *h-invariant*. The shape of the HDFD decision regions is given directly by some subset of pairwise boundaries, the so-called *active boundaries subset*[23] ($\mathscr{S}_{\mathrm{AB}} \subset \mathscr{S}_{\mathrm{PB}}$) - see the example in Fig. 5.2. As it is also obvious from this figure, the final shape of the HDFD decision regions generally does not have to be formed by all boundaries from $\mathscr{S}_{\mathrm{CB}}$. Boundaries for some index pairs could be overlapped by other decision boundaries. E.g., boundaries between two neigbouring hierarchical codewords (in one column or row of the hierarchical codeword table) do not have to appear as a true decision boundaries of the overall hierarchical codebook. However, considering all, even the "masked" ones, enables simplified parametric codebook construction at the expense of fulfilling stricter criterion than actually required. Such code design rules are thus sufficient but not necessary ones.

The pairwise design criterion for the *h-invariant pairwise boundary* $\mathscr{R}^{kl}$ (i.e. for the *h*-invariant

[23] In general, the active boundaries subset $\mathscr{S}_{\mathrm{AB}}$ does not have to comprise solely the boundaries from $\mathscr{S}_{\mathrm{CB}}$ ($\mathscr{S}_{\mathrm{AB}} \nsubseteq \mathscr{S}_{\mathrm{CB}}$).

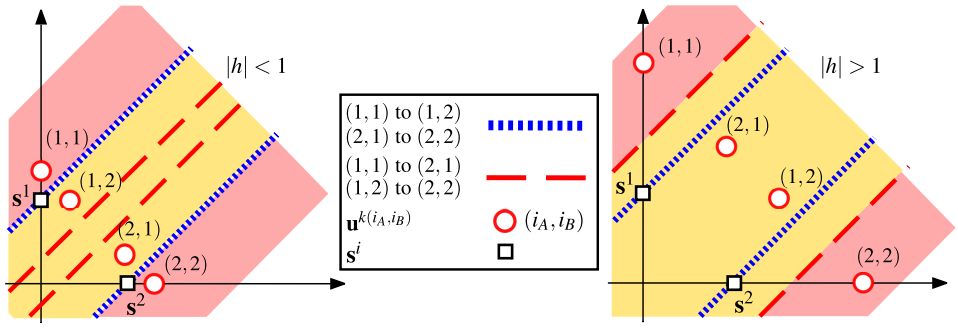

Figure 5.3: Shift of pairwise boundaries affects the HDFD decision regions shape ($\mathbb{R}^2$ codebook).

hierarchical codeword pair $\mathbf{u}^{k(i_A,i_B)}$ and $\mathbf{u}^{l\left(i'_A,i'_B\right)}$) in $\mathbb{C}^2$ isderived as a pair of required conditions in [116]:

$$\left\langle \mathbf{s}^{i_A} - \mathbf{s}^{i'_A}; \mathbf{s}^{i_B} + \mathbf{s}^{i'_B} \right\rangle = 0, \tag{5.3}$$

$$\left\langle \mathbf{s}^{i_B} - \mathbf{s}^{i'_B}; \mathbf{s}^{i_B} + \mathbf{s}^{i'_B} \right\rangle = 0. \tag{5.4}$$

5.1.4 Design criteria for full PHXC codebooks

The *final shape* of the HDFD decision regions is given entirely by active boundaries ($\mathscr{R}^{kl}_{\mathrm{AB}}(h) \in \mathscr{S}_{\mathrm{AB}}$) and hence it could seem quite reasonable to apply the pairwise design criteria (5.3), (5.4) only to these boundaries in $\mathscr{S}_{\mathrm{AB}}$. In this case the design criteria would ensure that the constellation space "position" of all boundaries from $\mathscr{S}_{\mathrm{AB}}$ will remain fixed, however some other boundaries could potentially "move" along with the varying channel parameter h.

This "boundary movement" could (for some values of h) change the HDFD decision regions shape and hence break the requirement of parameter-invariant HDFD decision regions (Fig. 5.3). One way how to potentially avoid this undesirable behavior is to apply the design criteria on *all critical boundaries* ($\mathscr{R}^{kl}_{\mathrm{CB}}(h) \in \mathscr{S}_{\mathrm{CB}}$), thus requiring all pairwise boundaries in $\mathscr{S}_{\mathrm{CB}}$ to be h-invariant. As we prove later in this section, this condition is sufficient to force the entire set $\mathscr{S}_{\mathrm{PB}}$ to be parameter-invariant.

5.1.4.1 E-PHXC design criteria

Forcing all critical pairwise boundaries to be h-invariant is a relatively strict requirement, nevertheless it allows us to express the design criteria in a compact set of required conditions and it avoids the movement of all critical boundaries (complete set $\mathscr{S}_{\mathrm{CB}}$), which are dominantly responsible for the final shape of the HDFD decision regions. We apply the design criteria (5.3), (5.4) for the parameter-invariant pairwise boundary to *all critical boundaries*, resulting in the set of *extended design criteria* for *complete PHXC codebooks*.

A code which has all the *critical* boundaries ($\mathscr{R}^{kl}_{\mathrm{CB}}(h) \in \mathscr{S}_{\mathrm{CB}}$) invariant to the channel parameter will be called *Extended Parametric Hierarchical eXclusive Code* (E-PHXC). Now we will formally define the E-PHXC codebooks and introduce the necessary conditions for the codebooks design in Lemma 7.

Definition 6. The codebooks $\mathscr{B}_A = \left\{\mathbf{s}^{i_A}\right\}_{i_A}$, $\mathscr{B}_B = \left\{\mathbf{s}^{i_B}\right\}_{i_B}$ are *E-PHXC* when all the critical boundaries $\mathscr{R}^{kl}_{\mathrm{CB}}(h) \in \mathscr{S}_{\mathrm{CB}}$ for hierarchical codebook $\mathscr{B}_u(h)$ at the relay are h-invariant.

Lemma 7. *Codebooks* $\mathscr{B}_A = \left\{\mathbf{s}^{i_A}\right\}_{i_A}$, $\mathscr{B}_B = \left\{\mathbf{s}^{i_B}\right\}_{i_B}$ *are* E-PHXC *if the following conditions hold:*

$$\left\langle \mathbf{s}^{i_A} - \mathbf{s}^{i'_A}; \mathbf{s}^{i_B} \right\rangle = 0 \;\; \forall i_A < i'_A, \tag{5.5}$$

$$\left\langle \mathbf{s}^{i_B} - \mathbf{s}^{i'_B}; \mathbf{s}^{i_B} + \mathbf{s}^{i'_B} \right\rangle = 0 \;\; \forall i_B < i'_B, \tag{5.6}$$

for all $i_A, i_B, i'_A, i'_B \in \{1,2,\ldots N\}$, *where* $N = |\mathscr{B}_A| = |\mathscr{B}_B|$.

Proof. We apply the PHXC design criteria (5.3), (5.4) to all critical boundaries. The critical boundary $\mathscr{R}^{kl}_{\mathrm{CB}}(h)$ is the pairwise boundary between hierarchical codewords $\mathbf{u}^{k(i_A,i_B)}(h)$ and $\mathbf{u}^{l\left(i'_A,i'_B\right)}(h)$ where $i_A = i'_A$ or $i_B = i'_B$ (from Definition 5).

Now we have (from (5.3)):

$$0 = \left\langle \mathbf{s}^{i_A} - \mathbf{s}^{i_A}; \mathbf{s}^{i_B} + \mathbf{s}^{i'_B} \right\rangle = \left\langle \mathbf{0}; \mathbf{s}^{i_B} + \mathbf{s}^{i'_B} \right\rangle, \tag{5.7}$$

for all $i_A = i'_A$, $i_B \neq i'_B$, $i_A, i_B, i'_B \in \{1,2,\ldots N\}$ and

$$0 = \left\langle \mathbf{s}^{i_A} - \mathbf{s}^{i'_A}; \mathbf{s}^{i_B} + \mathbf{s}^{i_B} \right\rangle = \left\langle \mathbf{s}^{i_A} - \mathbf{s}^{i'_A}; 2\mathbf{s}^{i_B} \right\rangle, \tag{5.8}$$

for all $i_B = i'_B$, $i_A \neq i'_A$, $i_A, i'_A, i_B \in \{1,2,\ldots N\}$.

From (5.4) we have:

$$0 = \left\langle \mathbf{s}^{i_B} - \mathbf{s}^{i'_B}; \mathbf{s}^{i_B} + \mathbf{s}^{i'_B} \right\rangle, \tag{5.9}$$

for all $i_B \neq i'_B$, $i_B, i'_B \in \{1,2,\ldots N\}$ and

$$0 = \left\langle \mathbf{s}^{i_B} - \mathbf{s}^{i_B}; \mathbf{s}^{i_B} + \mathbf{s}^{i_B} \right\rangle = \left\langle \mathbf{0}; 2\mathbf{s}^{i_B} \right\rangle, \tag{5.10}$$

for all $i_B = i'_B$, $i_B, i'_B \in \{1,2,\ldots N\}$.

It is obvious that the inner products in (5.7) and (5.10) are always zero, and hence these conditions are always satisfied for all the required individual codeword indices. From the remaining two inner products (5.8) and (5.9) we have the following criteria for the E-PHXC design:

$$\left\langle \mathbf{s}^{i_A} - \mathbf{s}^{i'_A}; \mathbf{s}^{i_B} \right\rangle = 0 \;\; \forall i_A, i'_A, i_B \in \{1,2,\ldots N\}, \;\; i_A \neq i'_A, \tag{5.11}$$

$$\left\langle \mathbf{s}^{i_B} - \mathbf{s}^{i'_B}; \mathbf{s}^{i_B} + \mathbf{s}^{i'_B} \right\rangle = 0 \;\; \forall i_B, i'_B \in \{1,2,\ldots N\}, \;\; i_B \neq i'_B. \tag{5.12}$$

Furthermore the condition (5.11) for a given pair of indices (i_A, i'_A) is equivalent to the same condition for a "reversed" pair of these indices (i'_A, i_A), because $\left\langle \mathbf{s}^{i'_A} - \mathbf{s}^{i_A}; \mathbf{s}^{i_B} \right\rangle = -1 \left\langle \mathbf{s}^{i_A} - \mathbf{s}^{i'_A}; \mathbf{s}^{i_B} \right\rangle$ (and similarly for (5.12)). Hence it is sufficient to check (5.11) only for $i_A < i'_A$ (and (5.12) for $i_B < i'_B$). □

5.1.4.2 E-PHXC decoder decision regions

Design criteria for E-PHXC codebooks (5.5), (5.6) force all critical boundaries (set $\mathscr{S}_{\mathrm{CB}}$) to be invariant to the channel parameter. Hence, all pairs of hierarchical codewords which are in the same row (or column) of the hierarchical codeword table (Table 5.1) have the corresponding pairwise boundary invariant to the channel parameter. Moreover, the design criteria are sufficient to force the *entire set* of pairwise boundaries ($\mathscr{S}_{\mathrm{PB}}$) to be parameter-invariant, i.e. the constellation space boundary $\mathscr{R}^{kl}$ between any permissible pair of hierarchical codewords is forced to be parameter-invariant by the E-PHXC design criteria (5.5), (5.6). We prove this proposition in the following Lemma:

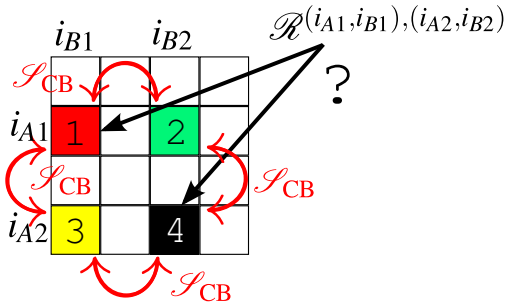

Figure 5.4: Impact of E-PHXC design criteria on non-critical ($\mathscr{R}^{kl} \notin \mathscr{S}_{\mathrm{CB}}$) boundaries.

Lemma 8. *If the codebook fulfills E-PHXC design criteria then it has* all permissible pairwise boundaries *($\mathscr{R}^{kl} \in \mathscr{S}_{PB}$)* invariant *to the channel parameter.*

Proof. We choose (without loss of generality) two hierarchical codewords ($\mathbf{u}^{(i_{A1},i_{B1})}$ and $\mathbf{u}^{(i_{A2},i_{B2})}$) which have different both indices ($i_{A1} \neq i_{A2}$ and $i_{B1} \neq i_{B2}$). These hierarchical codewords reside in a different row and column of the hierarchical codeword table (Table 5.1). The corresponding pairwise boundary is not considered as critical by Definition 5 ($\mathscr{R}^{(i_{A1},i_{B1}),(i_{A2},i_{B2})} \notin \mathscr{S}_{\mathrm{CB}}$), hence it is not directly forced to be parameter-invariant by the E-PHXC design criteria (see Fig. 5.4). We prove that $\mathscr{R}^{(i_{A1},i_{B1}),(i_{A2},i_{B2})}$ is parameter-invariant if the E-PHXC design criteria are satisfied.

Assume that codebooks $\mathscr{B}_A$, $\mathscr{B}_B$ are E-PHXC. Then any hierarchical codeword pair residing in the same row or column of the corresponding hierarchical codeword table has the pairwise boundary invariant to channel parameter (corresponding boundary is considered as critical by Definition 5 and required to be parameter-invariant by Definition 6). All such boundaries satisfy the PHXC pairwise criteria (5.3), (5.4). The following four boundaries are hence parameter-invariant (marked as $\mathscr{S}_{\mathrm{CB}}$ in Fig. 5.4)

$$\mathscr{R}^{(i_{A1},i_{B1}),(i_{A2},i_{B1})} = \mathscr{R}^{13}, \tag{5.13}$$
$$\mathscr{R}^{(i_{A1},i_{B1}),(i_{A1},i_{B2})} = \mathscr{R}^{12}, \tag{5.14}$$
$$\mathscr{R}^{(i_{A1},i_{B2}),(i_{A2},i_{B2})} = \mathscr{R}^{24}, \tag{5.15}$$
$$\mathscr{R}^{(i_{A2},i_{B1}),(i_{A2},i_{B2})} = \mathscr{R}^{34}. \tag{5.16}$$

Boundaries $\mathscr{R}^{13},\mathscr{R}^{12},\mathscr{R}^{24},\mathscr{R}^{34}$ satisfy the PHXC design criteria (5.3), (5.4), and hence the following three inner products (conditions for $\mathscr{R}^{12}$ and $\mathscr{R}^{34}$ are identical) are forced to be zero:

$$\left\langle \mathbf{s}^{i_{A1}} - \mathbf{s}^{i_{A2}}; \mathbf{s}^{i_{B1}} \right\rangle = 0, \tag{5.17}$$
$$\left\langle \mathbf{s}^{i_{B1}} - \mathbf{s}^{i_{B2}}; \mathbf{s}^{i_{B1}} + \mathbf{s}^{i_{B2}} \right\rangle = 0, \tag{5.18}$$
$$\left\langle \mathbf{s}^{i_{A1}} - \mathbf{s}^{i_{A2}}; \mathbf{s}^{i_{B2}} \right\rangle = 0. \tag{5.19}$$

The examined pairwise boundary ($\mathscr{R}^{(i_{A1},i_{B1}),(i_{A2},i_{B2})} = \mathscr{R}^{14}$) are parameter-invariant if the following two inner products are zero:

$$\left\langle \mathbf{s}^{i_{A1}} - \mathbf{s}^{i_{A2}}; \mathbf{s}^{i_{B1}} + \mathbf{s}^{i_{B2}} \right\rangle = 0, \tag{5.20}$$
$$\left\langle \mathbf{s}^{i_{B1}} - \mathbf{s}^{i_{B2}}; \mathbf{s}^{i_{B1}} + \mathbf{s}^{i_{B2}} \right\rangle = 0. \tag{5.21}$$

Now it is obvious that (5.21) is identical with (5.18) and (5.20) is forced to be zero by (5.17) and (5.19):

$$\left\langle \mathbf{s}^{i_{A1}} - \mathbf{s}^{i_{A2}}; \mathbf{s}^{i_{B1}} + \mathbf{s}^{i_{B2}} \right\rangle = \left\langle \mathbf{s}^{i_{A1}} - \mathbf{s}^{i_{A2}}; \mathbf{s}^{i_{B1}} \right\rangle + \left\langle \mathbf{s}^{i_{A1}} - \mathbf{s}^{i_{A2}}; \mathbf{s}^{i_{B2}} \right\rangle$$
$$\left\langle \mathbf{s}^{i_{A1}} - \mathbf{s}^{i_{A2}}; \mathbf{s}^{i_{B1}} + \mathbf{s}^{i_{B2}} \right\rangle = 0. \tag{5.22}$$

The pairwise boundary $\mathscr{R}^{(i_{A1},i_{B1}),(i_{A2},i_{B2})}$ satisfies both (5.20), (5.21), and hence it is indirectly forced to be parameter-invariant by the E-PHXC design criteria (5.5), (5.6). In the same way we can prove that any permissible pairwise boundary ($\mathscr{R}^{kl} \in \mathscr{S}_{\mathrm{PB}}$) with arbitrary indices k,l is forced to be parameter-invariant by the E-PHXC design criteria. □

5.1.4.3 E-PHXC with identical codebooks

Here we analyze the design criteria for a special case of identical codebooks ($\mathscr{B}_A = \mathscr{B}_B = \mathscr{B}$) to show that E-PHXC does not exist if the sources are limited to have identical codebooks. Note that by "identical codebooks" we mean codebooks which have completely identical all codewords[24] (i.e. including the indexing of codewords in the codebook). In this case both codebooks contain the same codewords, so we may omit the subscripts (A,B) from indices.

Theorem 9 (E-PHXC with identical codebooks)**.** *Codebook* $\mathscr{B} = \left\{\mathbf{s}^i\right\}_i$ *is* E-PHXC *if the following conditions hold:*

$$\left\|\mathbf{s}^i\right\| = \left\|\mathbf{s}^{i'}\right\| \ \ \forall i < i', \tag{5.23}$$

$$\left\|\mathbf{s}^1\right\|^2 = \left\langle \mathbf{s}^i; \mathbf{s}^{i'} \right\rangle \ \ \forall i < i', \tag{5.24}$$

for all $i,i' \in \{1,2,\ldots N\}$*, where* $N = |\mathscr{B}|$.

Proof. We start with (5.6), from which we get for the two pairs of codeword indices (i,j) and (i',j')

$$\left\langle \mathbf{s}^i - \mathbf{s}^{i'}; \mathbf{s}^i + \mathbf{s}^{i'} \right\rangle = 0,$$

$$\left\|\mathbf{s}^i\right\|^2 - \left\|\mathbf{s}^{i'}\right\|^2 + \mathrm{j}2\Im\left\{\left\langle \mathbf{s}^i; \mathbf{s}^{i'} \right\rangle\right\} = 0 \ \ \forall i < i', \tag{5.25}$$

where j is an imaginary unit. Should this hold for all $i < i'$, the inner products $\left\langle \mathbf{s}^i; \mathbf{s}^{i'} \right\rangle$ must be real-valued and all norms $\left\|\mathbf{s}^i\right\|, \left\|\mathbf{s}^{i'}\right\|$ must have same magnitude. Thus, the condition (5.6) is equivalent to a pair of conditions $\left\langle \mathbf{s}^i; \mathbf{s}^{i'} \right\rangle \in \mathbb{R}$ and $\|\mathbf{s}^i\| = \text{const}$.

From (5.5) we get

$$\left\langle \mathbf{s}^i - \mathbf{s}^{i'}; \mathbf{s}^j \right\rangle = 0,$$

$$\left\langle \mathbf{s}^i; \mathbf{s}^j \right\rangle = \left\langle \mathbf{s}^{i'}; \mathbf{s}^j \right\rangle \ \ \forall i < i', \tag{5.26}$$

for all $i,i',j \in \{1,2,\ldots N\}$. Considering the symmetry, this is equivalent to

$$\left\langle \mathbf{s}^i; \mathbf{s}^j \right\rangle = \left\langle \mathbf{s}^{i'}; \mathbf{s}^j \right\rangle \ \ \forall i,i',j, \tag{5.27}$$

which is in turn equivalent to

$$\left\langle \mathbf{s}^i; \mathbf{s}^{i'} \right\rangle = \text{const} = \|\mathbf{s}^1\|^2, \forall i,i'. \tag{5.28}$$

And thus the condition (5.5) is equivalent to $\left\langle \mathbf{s}^i; \mathbf{s}^{i'} \right\rangle = \|\mathbf{s}^1\|^2$. □

Theorem 10. *E-PHXC does not exist for identical* binary *codebooks (*$\mathscr{B}_A = \mathscr{B}_B = \mathscr{B}$*,* $|\mathscr{B}| = 2$*).*

[24] Two mutually rotated BPSK are hence not considered as identical codebooks.

Proof. The binary codebook contains two individual codewords $\mathscr{B} = \{\mathbf{s}^1, \mathbf{s}^2\}$. Each codeword is a vector over $\mathbb{C}^2$. The design criteria for the E-PHXC with identical binary codebooks require (from (5.23) and (5.24)):

$$\|\mathbf{s}^1\| = \|\mathbf{s}^2\|, \tag{5.29}$$

$$\|\mathbf{s}^1\|^2 = \langle \mathbf{s}^1; \mathbf{s}^2 \rangle. \tag{5.30}$$

We assume that there exist $\mathbf{s}^1 \neq \mathbf{s}^2$ such that both conditions are satisfied.

The *Cauchy-Bunyakovskii-Schwartz inequality* (CBS) [118] states that for all vectors $\mathbf{x}$,$\mathbf{y}$ holds

$$|\langle \mathbf{x}, \mathbf{y} \rangle| \leq \|\mathbf{x}\| \cdot \|\mathbf{y}\|, \tag{5.31}$$

where the equality is achieved iff $\mathbf{x} = \gamma \mathbf{y}$ for $\gamma = \frac{\langle \mathbf{x}, \mathbf{y} \rangle}{\|\mathbf{x}\|^2}$. Since the inner product $\langle \mathbf{s}^1; \mathbf{s}^2 \rangle$ must be positive and real-valued (from (5.30)) it is obvious that $|\langle \mathbf{s}^1; \mathbf{s}^2 \rangle| = \langle \mathbf{s}^1; \mathbf{s}^2 \rangle$. Now we apply the CBS inequality (5.31) on vectors $\mathbf{s}^1, \mathbf{s}^2$:

$$|\langle \mathbf{s}^1; \mathbf{s}^2 \rangle| \leq \|\mathbf{s}^1\| \cdot \|\mathbf{s}^2\|,$$

$$\langle \mathbf{s}^1; \mathbf{s}^2 \rangle \leq \|\mathbf{s}^1\|^2, \tag{5.32}$$

because $\|\mathbf{s}^1\| = \|\mathbf{s}^2\|$ (from (5.29)). Condition (5.30) requires the equality in (5.32). This equality is achieved iff $\mathbf{s}^1 = \gamma \mathbf{s}^2$, where $\gamma = \frac{\langle \mathbf{s}^1; \mathbf{s}^2 \rangle}{\|\mathbf{s}^1\|^2} = 1$, i.e. the equality is achieved iff $\mathbf{s}^1 = \mathbf{s}^2$, which is a contradiction with the assumption $\mathbf{s}^1 \neq \mathbf{s}^2$. □

Corollary 11. *E-PHXC does not exist for any identical individual codebooks ($\mathscr{B}_A = \mathscr{B}_B = \mathscr{B}$, $|\mathscr{B}| = N$).*

Proof. Conditions (5.29) and (5.30) form a subset of all required conditions for any individual codebook with cardinality greater than two ($|\mathscr{B}| > 2$). As shown in a proof of Theorem 10, it is impossible to find two different codewords satisfying this condition. □

5.1.4.4 E-PHXC with non-identical codebooks

We proved that source codebooks satisfying all the required E-PHCS design criteria does not exist if we limit both codebooks to be identical. In this section we derive the E-PHXC design criteria for the assumption of two non-identical individual codebooks ($\mathscr{B}_A \neq \mathscr{B}_B$).

Theorem 12 (E-PHXC with different codebooks)**.** *Codebooks $\mathscr{B}_A = \{\mathbf{s}^{i_A}\}_{i_A}$, $\mathscr{B}_B = \{\mathbf{s}^{i_B}\}_{i_B}$ are* E-PHXC *if the following conditions hold:*

$$\|\mathbf{s}^{i_B}\| = \left\|\mathbf{s}^{i'_B}\right\| \ \forall i_B < i'_B, \tag{5.33}$$

$$\Im\left\langle \mathbf{s}^{i_B}; \mathbf{s}^{i'_B} \right\rangle = 0 \ \forall i_B < i'_B, \tag{5.34}$$

$$\left\langle \mathbf{s}^{i_A} - \mathbf{s}^{i'_A}; \mathbf{s}^{j_B} \right\rangle = 0 \ \forall i_A < i'_A, \tag{5.35}$$

for all $i_A, i'_A, i_B, i'_B, j_B \in \{1, 2, \ldots, N\}$.

Proof. We start again with (5.6) from which we get:

$$\left\langle \mathbf{s}^{i_B} - \mathbf{s}^{i'_B}; \mathbf{s}^{i_B} + \mathbf{s}^{i'_B} \right\rangle = 0,$$

$$\|\mathbf{s}^{i_B}\|^2 - \left\|\mathbf{s}^{i'_B}\right\|^2 + \mathrm{j}2\Im\left\{\left\langle \mathbf{s}^{i_B}; \mathbf{s}^{i'_B} \right\rangle\right\} = 0 \ \forall i_B < i'_B, \tag{5.36}$$

for all $i_B, i'_B \in \{1, 2, \ldots, N\}$, which gives us directly (5.33) and (5.34). From (5.5) we get immediately the last condition (5.35). □

	$\mathbf{s}^{1_A}$	$\mathbf{s}^{2_A}$	$\mathbf{s}^{1_B}$	$\mathbf{s}^{2_B}$
codebook I	$(-1,1)$	$(1,-1)$	$(1,1)$	$(-1,-1)$
codebook II	$(0,1)$	$(0,-1)$	$(1,0)$	$(-1,0)$
codebook III	$(-1+\mathrm{j},1-\mathrm{j})$	$(1-\mathrm{j},-1+\mathrm{j})$	$(1+\mathrm{j},1+\mathrm{j})$	$(-1-\mathrm{j},-1-\mathrm{j})$

Table 5.2: Example binary E-PHXC codebooks

	$\mathbf{s}^{1_A}$	$\mathbf{s}^{2_A}$	$\mathbf{s}^{1_B}$	$\mathbf{s}^{2_B}$
codebook IV	$(2,1)$	$(1,2)$	$(1,1)$	$(-1,-1)$
codebook V	$(1,2)$	$(1,1)$	$(1,0)$	$(-1,0)$
codebook VI	$(1,\mathrm{j})$	$(\mathrm{j},1)$	$(1+\mathrm{j},1+\mathrm{j})$	$(-1-\mathrm{j},-1-\mathrm{j})$
codebook VII	$(2,1+\mathrm{j})$	$(1+\mathrm{j},2)$	$(1+\mathrm{j},1+\mathrm{j})$	$(-1-\mathrm{j},-1-\mathrm{j})$
codebook VIII	$(2+\mathrm{j},1)$	$(1+2\mathrm{j},2-\mathrm{j})$	$(1+\mathrm{j},1+\mathrm{j})$	$(-1-\mathrm{j},-1-\mathrm{j})$

Table 5.3: Example (non-orthogonal) binary E-PHXC codebooks

5.1.4.5 Example binary alphabet construction algorithm

We showed that E-PHXC codebooks have all pairwise boundaries invariant to the channel parameter and that they could be designed only if the sources use two different individual codebooks ($\mathscr{B}_A \neq \mathscr{B}_B$). Here we exemplify the E-PHXC design criteria for this case ((5.33), (5.34), (5.35)) on a few simple cases.

Assume two different binary codebooks $|\mathscr{B}_A| = |\mathscr{B}_B| = 2$ in $\mathbb{C}^2$ with code indices $i_A, i_B \in \{1,2\}$ and scalar relative channel parameter $h \in \mathbb{C}^1$. Considering these assumptions, the design criteria for a binary E-PHXC (from Theorem 12) are:

$$\left\|\mathbf{s}^{1_B}\right\| = \left\|\mathbf{s}^{2_B}\right\|, \tag{5.37}$$

$$\Im\left\{\left\langle \mathbf{s}^{1_B}; \mathbf{s}^{2_B}\right\rangle\right\} = 0, \tag{5.38}$$

$$\left\langle \mathbf{s}^{1_A} - \mathbf{s}^{2_A}; \mathbf{s}^{1_B}\right\rangle = 0, \tag{5.39}$$

$$\left\langle \mathbf{s}^{1_A} - \mathbf{s}^{2_A}; \mathbf{s}^{2_B}\right\rangle = 0. \tag{5.40}$$

As it is obvious from (5.39) and (5.40), a trivial example of E-PHXC are codebooks $\mathscr{B}_A, \mathscr{B}_B$ with mutually *orthogonal* codewords ($\left\langle \mathbf{s}^{i_A}; \mathbf{s}^{i_B}\right\rangle = 0$ for all $\mathbf{s}^{i_A}, \mathbf{s}^{i_B}$), provided that also (5.37) and (5.38) are not violated. Some examples of these "orthogonal" binary codebooks are presented in Table 5.2. Codebooks $\mathscr{B}_A, \mathscr{B}_B$ spanning mutually orthogonal subspaces have additional advantage of providing unitary-parameter-invariant performance (e.g. with respect to the phase rotation). The decision sub-spaces for both source codebooks are independent (orthogonal) and thus an unitary rotation of one subspace cannot affect the overall performance. Despite of the fact that the orthogonality itself puts the HXC (in MAC phase) on the same level as the classical MAC with joint decoding of both data streams, the HDF strategy with such HXC can still utilize all the BC phase benefits of network coding principles (see e.g. [65] for details), regardless of the MAC phase channel parametrization.

Example design process for *non-orthogonal* E-PHXC codebooks $\mathscr{B}_A, \mathscr{B}_B$ is presented in Algorithm 5.1. Some examples of non-orthogonal binary codebooks are presented in Table 5.3. The construction algorithm however does not guarantee zero-mean nor equal distance (Gram matrix) codebooks $\mathscr{B}_A, \mathscr{B}_B$. However, it is obvious that if alphabet $\mathscr{B}_i$ satisfies the design criteria from Theorem 12, then codebook

Algorithm 5.1 Binary E-PHXC codebook - Example design

1. Choose arbitrarily $\mathbf{s}^{1_B} \in \mathbb{C}^2$.
2. Choose $\mathbf{s}^{2_B} \in \mathbb{C}^2$, $\mathbf{s}^{2_B} = \delta_1 \mathbf{s}^{1_B}$, where $\delta_1 \in \mathbb{C}^1$ is arbitrary scaling constant such that (5.37), (5.38) are satisfied.
3. Find $\mathbf{v} \in \mathbb{C}^2$ such that $\left\langle \mathbf{v}; \mathbf{s}^{1_B} \right\rangle = 0$.
4. Choose arbitrarily $\mathbf{s}^{1_A} \in \mathbb{C}^2$.
5. Find $\mathbf{s}^{2_A} \in \mathbb{C}^2$ such that $\mathbf{s}^{2_A} = \mathbf{s}^{1_A} - \delta_2 \mathbf{v}$, where $\delta_2 \in \mathbb{C}^1$ is arbitrary scaling constant.
6. $\mathscr{B}_A = \left\{ \mathbf{s}^{1_A}, \mathbf{s}^{2_A} \right\}$, $\mathscr{B}_B = \left\{ \mathbf{s}^{1_B}, \mathbf{s}^{2_B} \right\}$

$\mathscr{B}'_i = -\mathscr{B}_i$ (all codewords have inverted signs) satisfies the design criteria as well (this holds for any alphabet cardinality). The non-zero mean of any codebook hence can be quite easily adjusted by sequential swapping of the codebooks $\mathscr{B}_i$ and $-\mathscr{B}_i$ at the particular source, since the resulting "compound" codebook will be zero-mean.

5.1.5 Min-distance based design criteria for higher-order codebooks

The new challenge in the codebook design arises when we need to design a codebook with higher cardinality. It can be shown that the strictness of the complete E-PHXC design criteria ((5.33), (5.34) and (5.35)) disable the codebook design in $\mathbb{C}^2$ for higher than binary cardinality. To overcome this inconvenience, we will slightly "relax" the E-PHXC design criteria and propose a new codebook design algorithm which provides a feasible tool for the construction of codebooks with arbitrary cardinality. By relaxing the proposed design criteria we lose the parameter-invariant shape of the decision regions at the relay HDF decoder, but nevertheless the overall system performance does not have to be negatively influenced. As we will show in this section, the performance analysis of the codebooks constructed according to the modified design algorithm shows some promising performance (compared to the traditional linear modulation schemes - e.g. PSK, QAM).

5.1.5.1 Minimum hierarchical distance

As we have already mentioned, the eXclusive law failure occurs whenever the channel parametrization cause that some pair of useful signals $(\mathbf{u}(h), \mathbf{u}'(h))$ which corresponds to a distinct eXclusive relay output codeword $(\mathscr{X}_s(\mathbf{u}(\mathbf{s}_A, \mathbf{s}_B, h)) \neq \mathscr{X}_s(\mathbf{u}'(\mathbf{s}'_A, \mathbf{s}'_B, h)))$ falls in (or close) to each other in the constellation space, thus increasing the probability of erroneous decision at the relay. It is useful to analyze these eXclusive law failures by observing the (squared) Euclidean distance of useful signals in the constellation space:

$$d^2_{(\mathbf{u},\mathbf{u}')}(h) = \left\| \mathbf{u}(h) - \mathbf{u}'(h) \right\|^2. \tag{5.41}$$

For a general pair of useful signals $(\mathbf{u}^{(i_A,i_B)}, \mathbf{u}^{\left(i'_A,i'_B\right)})$ it becomes

$$d^2_{\mathbf{u}^{(i_A,i_B)},\mathbf{u}^{\left(i'_A,i'_B\right)}}(h) = \left\| \left(\mathbf{s}^{i_A} - \mathbf{s}^{i'_A} \right) + h \left(\mathbf{s}^{i_B} - \mathbf{s}^{i'_B} \right) \right\|^2. \tag{5.42}$$

The minimum hierarchical distance represents an approximation of the hierarchical decoder exact metric (as discussed e.g. in [65]) and its performance is quite closely connected with the error rate

Algorithm 5.2 Higher-order codebook - Relaxed (min-distance based) design

1. Choose $\mathbf{x}, \mathbf{y} \in \mathbb{C}^2$ such that $\langle \mathbf{x}; \mathbf{y} \rangle = 0$.
2. $\mathscr{B}_B = \{q^{i_B} \cdot \mathbf{x}\}_{i_B=0}^{N-1}; \quad q^{i_B} \in \mathbb{C}$
3. Pick $\mathbf{v} \in \mathbb{C}^2$.
4. $\mathscr{B}_A = \{\mathbf{v} - q^{i_A} \cdot \mathbf{y}\}_{i_A=0}^{N-1}; \quad q^{i_A} \in \mathbb{C}$.

performance of the whole system [65]. The minimum hierarchical distance for the HDF strategy can be defined as[25]:

$$d^2_{\min}(h) = \min_{\mathscr{X}_S(\mathbf{u}) \neq \mathscr{X}_S(\mathbf{u}')} d^2_{(\mathbf{u},\mathbf{u}')}(h). \tag{5.43}$$

The eXclusive law failures cause $d^2_{\min}(h) \to 0$, which in turn results into a faulty decision of the relay decoder, and consequently a performance degradation. In the following subsection we show that the fulfillment of (5.35) from the E-PHXC design criteria (Theorem 12) are sufficient to completly avoid the eccurance of eXclusive law failures for arbitrary channel parametrization.

5.1.5.2 Modified design criteria

The following Theorem shows that (5.35) is sufficient to avoid the significant performance degradation of the system by avoiding the eXclusive law failures ($d^2_{\min}(h) = 0$).

Theorem 13. *The codebooks $\mathscr{B}_A = \left\{\mathbf{s}^{i_A}\right\}_{i_A}$, $\mathscr{B}_B = \left\{\mathbf{s}^{i_B}\right\}_{i_B}$ are resistant to eXclusive law failures (for $|h| > 0$) if the following condition holds:*

$$\left\langle \mathbf{s}^{i_A} - \mathbf{s}^{i'_A}; \mathbf{s}^{j_B} \right\rangle \quad = \quad 0 \ \ \forall i_A < i'_A, \tag{5.44}$$

for all $i_A, i'_A, j_B \in \{1, 2, \ldots, N\}$.

Proof. It is obvious that (5.44) forces the following inner product to be always equal to zero:

$$\left\langle \left(\mathbf{s}^{i_A} - \mathbf{s}^{i'_A}\right); \left(\mathbf{s}^{j_B} - \mathbf{s}^{j'_B}\right) \right\rangle = 0, \tag{5.45}$$

and hence vectors $\Delta\mathbf{s}^{i_A,i'_A} = \left(\mathbf{s}^{i_A} - \mathbf{s}^{i'_A}\right)$ and $\Delta\mathbf{s}^{i_B,i'_B} = \left(\mathbf{s}^{j_B} - \mathbf{s}^{j'_B}\right)$ are mutually orthogonal. Now since the pairs of mutually orthogonal vectors are always linearly independent (e.g. [118]) and the norm of the vector is equal to zero iff the vector is a zero vector ($\|\mathbf{x}\| = 0 \Leftrightarrow \mathbf{x} = \mathbf{o}$), we can conclude that the minimum distance (5.42) is non-zero for any $h \neq 0$, because $\left(\mathbf{s}^{i_A} - \mathbf{s}^{i'_A}\right) + h\left(\mathbf{s}^{i_B} - \mathbf{s}^{i'_B}\right)$ is a linear combination of the linearly independent vectors. The eXclusive law failures $d^2_{\min}(h) = 0$ are hence avoided for any $h \neq 0$. □

The "relaxed" design criteria (5.44) guarantee that the eXclusive law failures are avoided for any permissible value of the channel parametrization (excluding the singular case $h = 0$). The Algorithm 5.2 presents an example design process for codebooks of generally arbitrary cardinality.

Vector $\mathbf{v}$ defines the mean of the codebook $\mathscr{B}_A$. For $\mathbf{v} = \mathbf{o}$ we obtain a trivial solution with mutually *orthogonal* codewords ($\langle \mathbf{s}^{i_A}; \mathbf{s}^{i_B} \rangle = 0$ for all $\mathbf{s}^{i_A}, \mathbf{s}^{i_B}$). In this case the main benefits of the HDF strategy are again mainly in the BC phase. For $\mathbf{v} \neq \mathbf{o}$ we have the codebook with a non-zero mean, which can be

[25] A detailed analysis of minimum hierarchical distance is available in Chapter 6.

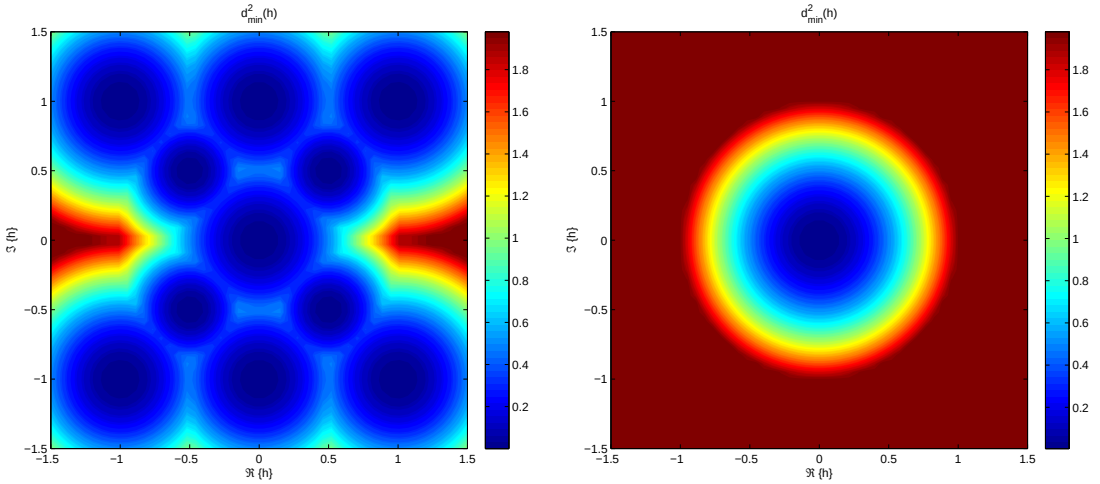

Figure 5.5: Minimum hierarchical distance performance for QPSK and 4-ary example codebook (zero-mean).

again easily adjusted by sequential swapping of the codebooks $\mathscr{B}_A$ and $-\mathscr{B}_A$. The coefficients q^{i_A}, q^{i_B} can be chosen from the classical linear modulation constellation (e.g. PSK or QAM) and can be generally identical ($q^{i_A} = q^{i_B}$) for both codebooks.

5.1.5.3 Performance evaluation

We analyze the minimum hierarchical distance performance of the codebooks designed according to the Algorithm 5.2. Figures 5.5, 5.6 and 5.7 present the performance comparison of the example codebooks (with zero mean ($\mathbf{v} = \mathbf{o}$)) and classical linear modulation constellations (for various channel parametrization). All codebooks are scaled to have identical mean symbol energy. Note that the distance shortening at $|h| \to 0$ is generally inevitable [65].

5.1.6 Discussion of results

Utilizing the criterion for parameter-invariant constellation space boundary [116], *construction criteria* for E-PHXC codebooks are derived in this Section. Unfortunately, these criteria require to have two non-identical source node codebooks and moreover, their strict nature disables the possibility of designing the codebooks with higher than binary cardinality in $\mathbb{C}^2$. Fortunately, the modified codebook construction algorithm (Algorithm 5.2), based on the relaxed version of the full E-PHXC design criteria, provides a feasible way for the design of arbitrary cardinality codebooks in $\mathbb{C}^2$.

Although neither of the construction algorithms require mutual orthogonality of the codebooks, it appears to be the simplest way how to fulfill their requirements. Despite of the fact that the orthogonality itself puts the HXC (in MAC phase) on the same level as the classical MAC with joint decoding of both data streams, the performance gain of the HDF strategy is in this case given by the increased reliability of the BC phase (similarly as in the conventional NC).

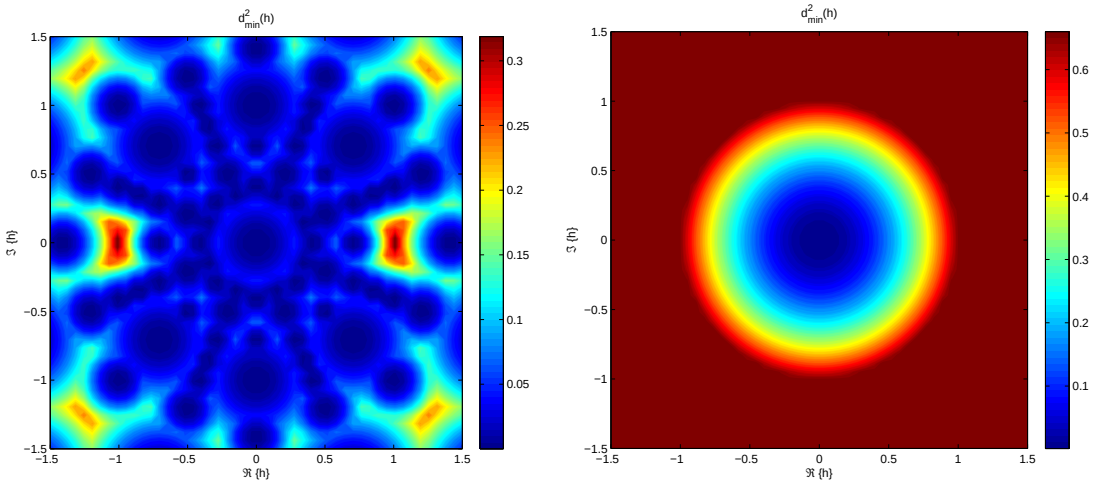

Figure 5.6: Minimum hierarchical distance performance for 8-PSK and 8-ary example codebook (zero-mean).

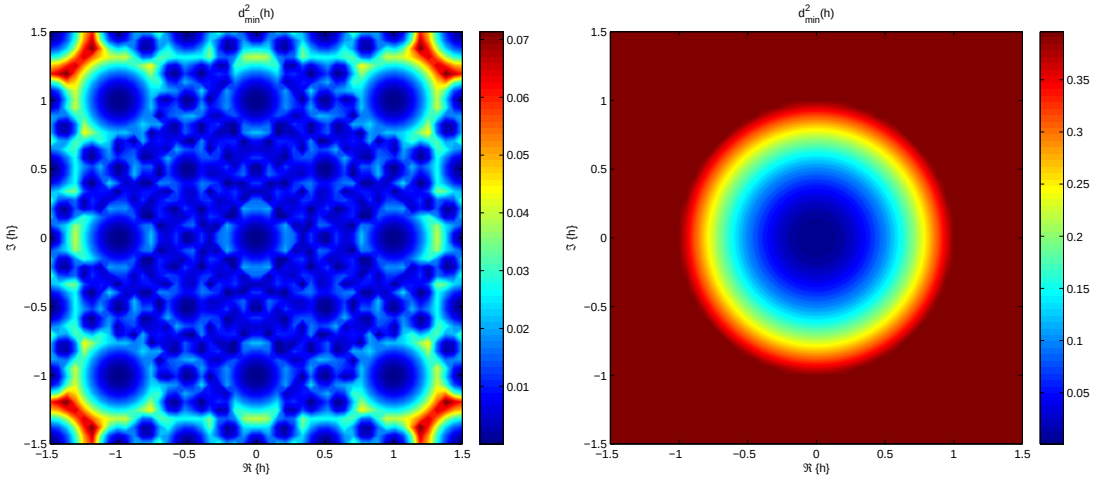

Figure 5.7: Minimum hierarchical distance performance for 16-QAM and 16-ary example codebook (zero-mean).

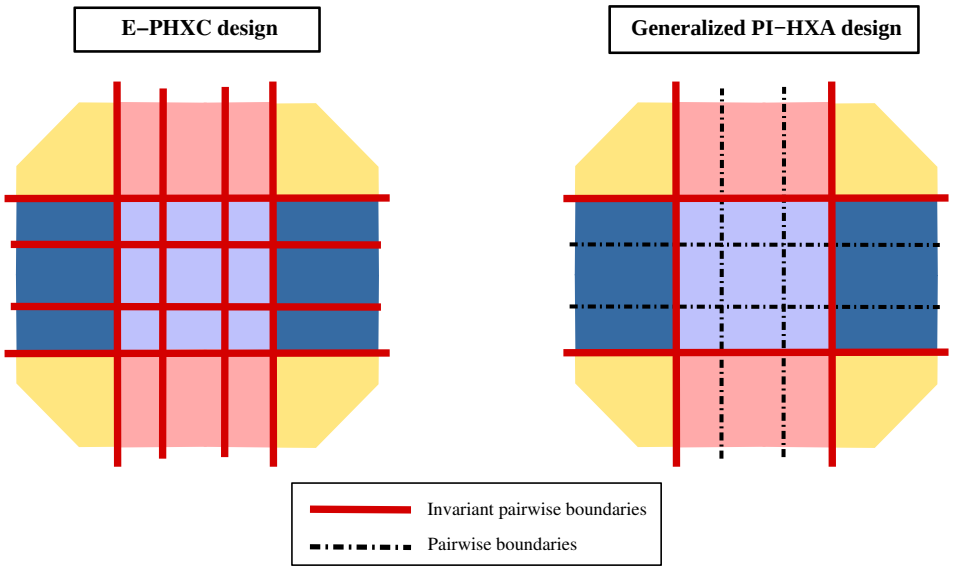

Figure 5.8: The final shape of the relay decision regions is affected only by the pairwise boundaries between different hierarchical codewords (given by a different colour of the region in the figure). The generalized approach to the PI-HXA design requires only these particular boundaries to be *invariant* to the channel parametrization (unlike E-PHXC).

5.2 Geometrical approach to the multi-dimensional HXC design

5.2.1 Introduction

An alternative approach (based on a geometrical interpretation of the design problem) to the design of multi-dimenisonal HXC (respective HXA) is introduced in [18, 21, 117]. Similarly like in the case of E-PHXC design, the goal is to take the channel parametrization into account inherently from the beginning of the HXA design by forcing the relay decision regions to be invariant to the relative channel parameter h:

$$\mathscr{X}_{s(h)}(s_A, s_B) = \mathscr{X}_s(s_A, s_B), \quad \forall h \in \mathbb{C} \tag{5.46}$$

HXAs that have the relay decision regions invariant to channel parametrization are called Parameter-Invariant HXAs (PI-HXA) in [18].

A first attempt to design PI-HXA for layered HXC in 2-WRC was given by the E-PHXC design criteria [20] (see Section 5.1). The strictness of the E-PHXC design criteria (which in turn essentially causes only the orthogonal solution to PI-HXA design to be feasible) is due to the fact that *all* permissible pairwise boundaries (in the relay decision regions) are forced to be parameter invariant. This is obviously not necessary since some of these boundaries can be "overlaid" by other boundaries or remain somehow "hidden" inside the relay decision region. In such cases, the resulting final shape of relay decision regions remains unaffected by these boundaries and hence these boundaries do not have to be considered by the PI-HXA design criteria. This approach to PI-HXA design should relax the strictness of the design criteria (compared to E-PHXC) and hence non-orthogonal PI-HXAs with the rate region extending the classical MAC region can possibly be found. A comparison of this "generalized" design approach with E-PHXC based design is shown in Fig. 5.8.

5.2.2 PI-HXA Design

5.2.2.1 Principles of geometrical design

The derivation of the systematic design criteria (design algorithm) for PI-HXA is still relatively complex. The particular constellation space boundaries of the relay decision regions result from the selected PI-HXA constellation (i.e. alphabet mapper $\mathscr{A}_s$), and the design criteria for invariant decision region boundaries directly affect the requirements given on the PI-HXA constellation. This mutual relationship increases the complexity of the systematic solution to PI-HXA design.

We show the viability of the layered HXC solution in parametric channels (i.e. the possibility to find PI-HXA) by introducing some major simplifications which allow a *geometric* interpretation of the PI-HXA design problem. The idea of the geometric approach to PI-HXA design is based on the "constellation space patterns" of the useful signal $u = s_A + hs_B$.

Definition 14. A constellation space pattern $\mathscr{U}^{i_A}$ is the subspace spanned by the useful signal $u = s_A + hs_B$ for $s_A = s_{i_A}$, $\forall s_B \in \mathscr{A}_s^B$ and $\forall h \in \mathbb{C}$.

The absolute value of the channel parameter $|h| \in (0;\infty)$ causes the constellation space patterns to be potentially unbounded. This is the only remaining inconvenience for a simple geometric interpretation of PI-HXA design. As we will show in the following subsection, the constellation space patterns can be effectively bounded by simple processing at the relay.

5.2.2.2 Two-mode relay processing

The received (useful) signal u is obtained by rescaling the true channel response ($h_A s_A + h_B s_B$) by $1/h_A$. Note again that the only purpose of this rescaling is to obtain a simplified expression of the useful signal (3.3), which is (after rescaling) parametrized only by a single complex channel parameter $h = h_B/h_A$. It is obvious that the true channel response can alternatively be rescaled by $1/h_B$, hence we can obtain two alternative models of the useful signal u:

$$M_1: \qquad u_{M_1} = s_A + hs_B, \tag{5.47}$$

$$M_2: \qquad u_{M_2} = \frac{1}{h}s_A + s_B. \tag{5.48}$$

This corresponds to two alternative models of the received signal at the relay:

$$x_{M_1} = h_A u_{M_1} + w', \tag{5.49}$$

$$x_{M_2} = h_B u_{M_2} + w''. \tag{5.50}$$

The relay can potentially swap these two channel models (respective models of the useful signal) in such a way that the absolute value of the channel parameter (h for model M_1 and $\frac{1}{h}$ for M_2) is always less than (or equal to) one. This processing at the relay will be called *2-mode relay processing*. If the hierarchical mapping at the relay is "symmetric":

$$s_R(c_{AB}) = \mathscr{X}_s(s_A^i, s_B^j) = \mathscr{X}_s(s_A^j, s_B^i),' \quad \forall i,j \in \{1,\dots|\mathscr{A}_s|\} \tag{5.51}$$

(where $|\mathscr{A}_s| = \left|\mathscr{A}_s^A\right| = \left|\mathscr{A}_s^B\right|$ is the source alphabet carindality), then 2-mode relay processing can be used transparently to both sources A,B (i.e. the sources are not aware which channel model is in use at the relay for the current transmission), and hence it is feasible for the HDF strategy with HXC.

The symmetry of the relay hierarchical mapper (5.51) allows the relay to swap these two equivalent models of the useful signal (5.47), (5.48) transparently to both sources. In this way the relay can ensure that the value of the channel parameter in the useful signal model remains bounded, which in turn affects the subspaces spanned by the useful signals u_{M_1}, u_{M_2}, i.e. the constellation space patterns.

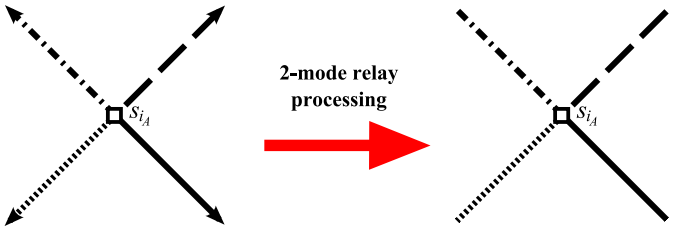

Figure 5.9: Example of the constellation space patterns for 2-mode relay processing ($|\mathscr{A}_s| = 4$). The particular line style corresponds to the particular hs_B, $\forall s_B \in \mathscr{A}_s^B$.

channel	$\lvert h\rvert$	$\lvert\frac{1}{h}\rvert$	u	$\mathscr{U}'^i$
$\lvert h_A\rvert \geq \lvert h_B\rvert$	≤ 1	≥ 1	u_{M_1}	$\mathscr{U}^{i_A}$
$\lvert h_A\rvert < \lvert h_B\rvert$	> 1	< 1	u_{M_2}	$\mathscr{U}^{i_B}$

Table 5.4: Principles of the 2-mode relay processing

Definition 15. A constellation space pattern $\mathscr{U}^{i_B}$ is the subspace spanned by the useful signal $u_{M_2} = \frac{1}{h}s_A + s_B$ for $s_B = s_{i_B}$, $\forall s_A \in \mathscr{A}_s^A$ and $\forall h \in \mathbb{C}$.

Definition 16. A bounded constellation space pattern $\mathscr{U}'^i$ is the subspace given by:

$$\mathscr{U}'^i = \begin{cases} \mathscr{U}^{i_A} & \text{for } |h| \leq 1 \\ \mathscr{U}^{i_B} & \text{for } |h| > 1 \end{cases}. \tag{5.52}$$

Constellation space patterns $\mathscr{U}'^i$ are effectively bounded (Fig. 5.9) by simple swapping of the useful signal models at the relay. The only requirement for this 2-mode relay processing is symmetry of the relay hierarchical output mapper (5.51). We summarize the principles of 2-mode relay processing in Table 5.4.

5.2.2.3 An example of 2-dimensional PI-HXA

We assume a real-valued channel symbol memoryless mapper $\mathscr{A}_s \subset \mathbb{R}^2$ (common to both sources). The channel parameter is complex $h \in \mathbb{C}$, and the useful signals are $u_{M_1}, u_{M_2} \in \mathbb{C}^2$. The assumption of a real-valued alphabet ($\mathscr{A}_s \subset \mathbb{R}^2$) allows the following simple interpretation of the real and imaginary part of the received useful signal $u_{M_1} \in \mathbb{C}^2$ (similarly for u_{M_2}):

$$\Re\{u_{M_1}\} = s_A + \Re\{h\}s_B, \tag{5.53}$$
$$\Im\{u_{M_1}\} = \Im\{h\}s_B, \tag{5.54}$$

which corresponds to the following vector notation:

$$\Re\left\{\begin{bmatrix} u_{M_1,1} \\ u_{M_1,2} \end{bmatrix}\right\} = \begin{bmatrix} s_{A,1} \\ s_{A,2} \end{bmatrix} + \Re\{h\}\begin{bmatrix} s_{B,1} \\ s_{B,2} \end{bmatrix}, \tag{5.55}$$
$$\Im\left\{\begin{bmatrix} u_{M_1,1} \\ u_{M_1,2} \end{bmatrix}\right\} = \Im\{h\}\begin{bmatrix} s_{B,1} \\ s_{B,2} \end{bmatrix}. \tag{5.56}$$

It is obvious that the imaginary part of the useful signal $\Im\{u_{M_i}\}$ depends solely on the channel symbols from one source (source B for mode M_1 (5.47) and source A for mode M_2 (5.48)). This can be viewed as an additional side information transmission from the corresponding source.

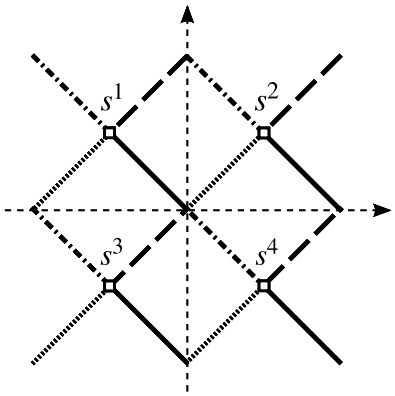

	s^1	s^2	s^3	s^4
$\mathscr{A}_s$	$(-1,1)$	$(1,1)$	$(-1,-1)$	$(1,-1)$

Figure 5.10: Channel symbol mapper ($\mathscr{A}_s$) and the resulting constellation space patterns ($\mathscr{U}'^{i}_{\mathrm{Re}}$) for the example of PI-HXA.

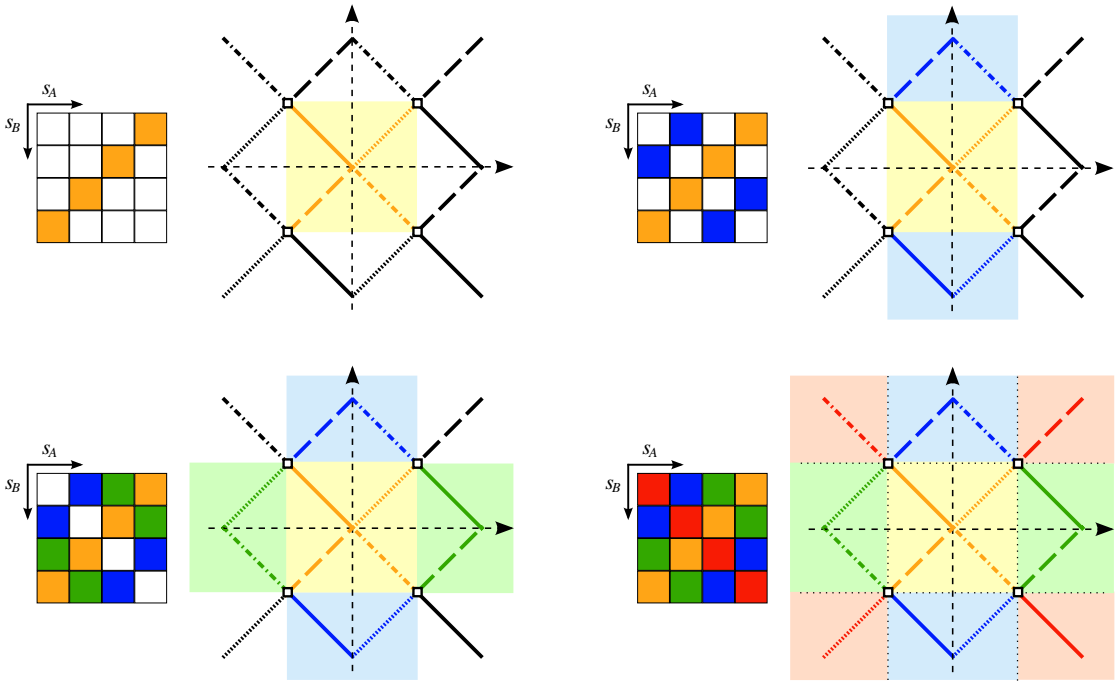

Figure 5.11: Design of a suitable hierarchical eXclusive mapper $\mathscr{X}_s(s_A^i, s_B^j)$ for the example of PI-HXA from Fig. 5.10. The resulting hierarchical eXclusive mapper corresponds to a bit-wise XOR of the symbol indices ($i, j \in \{1,2,\ldots|\mathscr{A}_s|\}$).

The relay employs 2-mode processing, hence the corresponding constellation space patterns $\mathscr{U}'^{i}$ are bounded. To simplify the design example even more, only the real part of the constellation space patterns ($\mathscr{U}'^{i}_{\mathrm{Re}} = \Re\left\{\mathscr{U}'^{i}\right\}$) will be considered here. These assumptions allow a simple geometric interpretation of the PI-HXA design problem in $\mathbb{R}^2$. The common channel symbol mapper $\mathscr{A}_s$ cause that for $i_A = i_B$ the corresponding patterns $\mathscr{U}^{i_A}$ and $\mathscr{U}^{i_B}$ define identical subspaces. Hence it is sufficient to consider only $\mathscr{U}^{i_A}$ for the case $|h| \leq 1$ (it is equivalent to the analysis of $\mathscr{U}^{i_B}$ for the case $\left|\frac{1}{h}\right| < 1$).

By defining the particular channel symbol mapper ($\mathscr{A}_s$) we also directly define the corresponding constellation space patterns $\mathscr{U}^{i_A}$. In this case, the geometrical PI-HXA design example turns into a puzzle-like problem of the constellations space pattern ($\mathscr{U}^{i_A}_{\mathrm{Re}}$ for $i_A \in \{1,2,\ldots|\mathscr{A}_s|\}$) arrangement in $\mathbb{R}^2$. The main goal of this "puzzle" is to find a suitable channel symbol mapper $\mathscr{A}_s$ and a proper hierarchical eXclusive mapper $s_R(c_{AB}) = \mathscr{X}_s(s^i_A, s^j_B)$, which will jointly prevent the possibility of violation of the exclusive law for arbitrary channel parameter h.

Here we show an example of a two-dimensional 4-ary ($|\mathscr{A}_s| = 4$) PI-HXA, designed according to the assumptions given in this section. The selected constellation space symbols (i.e. the chosen channel symbol mapper $\mathscr{A}_s$) and the resulting constellation space patterns ($\mathscr{U}'^{i}_{\mathrm{Re}}$) are depicted in Fig. 5.10. The final task of the example of geometrical PI-HXA design is a proper choice of the hierarchical eXclusive mapper. The selection of a suitable hierarchical eXclusive mapper can be visualized as a "colouring" (partitioning) process of the constellation space patterns. A visualization of this colouring process for the example of PI-HXA from Fig. 5.10 is presented in Fig. 5.11. The resulting hierarchical eXclusive mapper $\mathscr{X}_s(s^i_A, s^j_B)$ corresponds to a bit-wise XOR of the symbol indices ($i \in \{1,2,\ldots|\mathscr{A}_s|\}$).

5.2.3 Numerical Results

To show the viability of the layered HXC design in a parametric 2-WRC with HDF strategy we present some numerical evaluations of the mutual information (capacity) and the minimum squared distance of the example of PI-HXA design from Fig. 5.10.

5.2.3.1 Mutual information (capacity)

We evaluate the hierarchical and single-user (alphabet limited cut-set bound) rates (Fig. 5.12) for an example alphabet $\mathscr{A}_s$ (see Fig. 5.10) and various channel parametrization. The Signal-to-Noise Ratio (SNR) is defined as the ratio of the real base-band symbol energy of one source (e.g. A, to have a fair comparison for reference cases) to the noise power spectrum density ratio $\gamma_x = \left(\mathscr{E}_{\mathbf{s}_A}/2\right)/N_0$. Assuming orthonormal basis signal space complex envelope representation of the AWGN, we have $\sigma_w^2 = 2N_0$ and thus $\gamma_x = \mathrm{E}\left[\|\mathbf{s}_A\|^2\right]/\sigma_w^2$. The alphabet $\mathscr{A}_s$ is indexed by symbols $s_A, s_B \in \{0,\ldots,M_s-1\}$. The exclusive hierarchical mapping corresponds to a bit-wise XOR of the symbol indices (Fig. 5.11).

The graph (Fig. 5.12) shows the classical MAC cut-set bounds (1st and 2nd order) related to one user in comparison to the capacity of the HDF strategy with the example PI-HXA. The HDF capacity is parametrized by actual relative phase shift of the source-relay channels, while the amplitude is kept constant $|h|$ in our setup (to respect the symmetry of the rates from A and B). We show the minimal, maximal and mean values of the HDF capacity. The results were obtained using the technique shown in [86].

It is obvious from Fig. 5.12 that the HDF capacity approaches the alphabet constrained cut-set bound limit for medium to high SNR. For SNR values above approximately2 dB the capacity outperforms the classical MAC capacity, irrespective of the channel parametrization (relative phase shift of the source-relay channel), which has only a minor impact on the resulting performance.

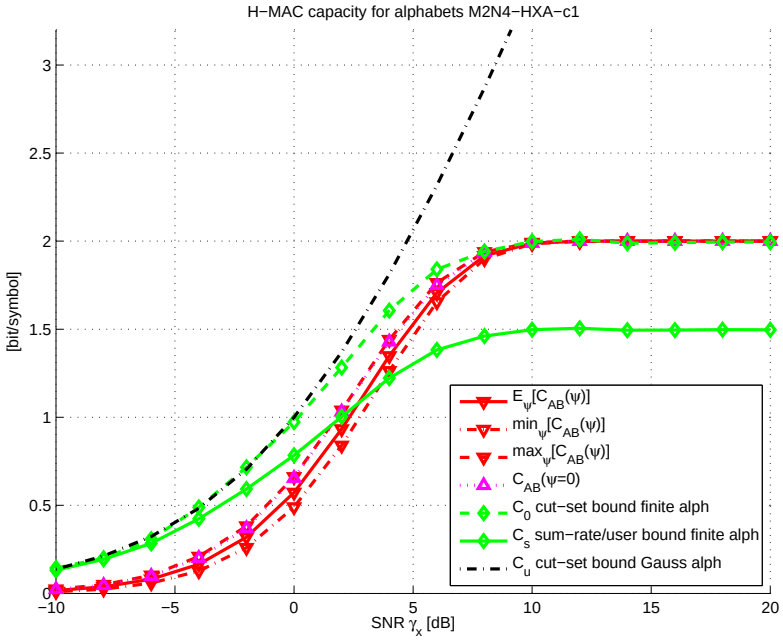

Figure 5.12: Capacity (mutual information) for the example of PI-HXA from Fig. 5.10.

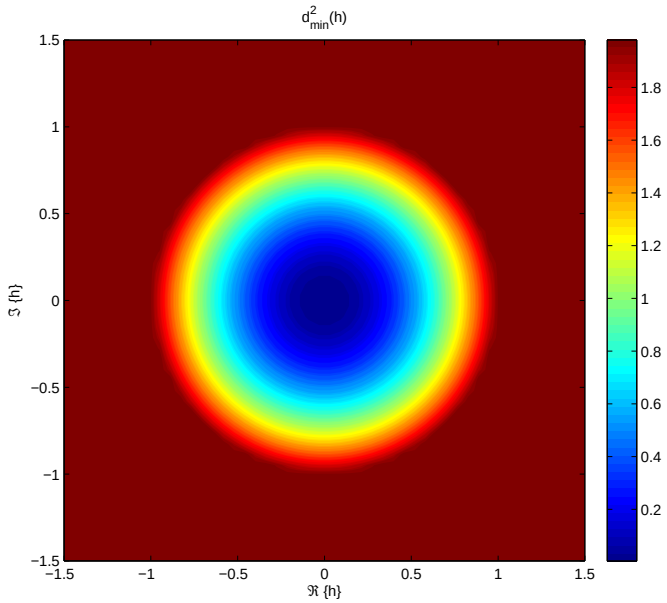

Figure 5.13: Minimum squared distance as a function of the channel parameter (for the example of PI-HXA from Fig. 5.10).

5.2.3.2 Minimum distance

We conclude the discussion of multi-dimensional constellation design by an analysis of the minimum squared Euclidean distance of the proposed alphabet. Fig. 5.13 depicts the squared minimum distance as a function of channel parameter h. It is obvious from this figure, that the minimum squared distance is again highly resistant to the relative phase shift ($\angle h$) of the source-relay channels. Note that distance shortening at $|h| \to 0$ is inevitable. Interestingly, the min-distance performance of the proposed alphabet is identical to that of the example 4-ary codebook shown in Fig. 5.5. However, the geometrical design introduced in this Section allows to employ identical alphabets at both sources, while the relaxed E-PHXC design criteria (Algorithm 5.2) forces the sources to use non-identical alphabets.

5.2.4 Discussion of results

The geometrical approach to PI-HXA design was presented in this Section. Alhough this design approach is based on many simplifying assumptions, the numerical results show relatively high resistance of both the capacity (Fig. 5.12) and the minimum distance (Fig. 5.13) to the channel parametrization. In addition, our setup requires no adaptation of the hierarchical exclusive mapping (unlike [65, 79]) and hence the processing at the relay can always be kept transparent to both sources. Nevertheless, similarly like in the case of the relaxed E-PHXC design criteria, the presented geometrical design approach requires multi-dimensional alphabets at source nodes, resulting again in a reduction of the maximal potential throughput (a direct consequence of the increased alphabet dimensionality).

Chapter 6

Hierarchical distance analysis

"Success is a science; if you have the conditions, you get the result."

Oscar Wilde

6.1 Introduction

In this chapter we investigate the impact of channel parametrization on the HDF system processing. We analyse the *Euclidean distance of hierarchical symbols* observed by the relay node to reveal the relation between channel parametrization and achievable performance of the system. Based on this analysis, we prove that it is impossible to fully avoid the occurance of eXclusive law failure events, if the source alphabets are restricted to $\mathbb{C}^1$.

6.2 Euclidean distance analysis

The *minimum hierarchical distance* represents an approximation of the exact per-symbol measure decoding metric for hierarchical symbols received at the relay (as discussed e.g. in [65, 84, 86]) and its performance is quite closely connected with the error-rate performance of the whole system [65]. In the following text we analyze the hierarchical distance as a function of the actual channel parametrization in 2-WRC (given by the relative channel parameter $h = {}^{h_B}/_{h_A} \in \mathbb{C}$).

6.2.1 Minimum hierarchical distance

The (squared) Euclidean distance ($d^2_{u^{i,j},u^{i',j'}}(h)$) of a general pair of hierarchical symbols ($u^{i,j} = s_A^i + hs_B^j$ and $u^{i',j'} = s_A^{i'} + hs_B^{j'}$) can be defined as:

$$\begin{aligned} d^2(h) &= \left\| \left(s_A^i + hs_B^j\right) - \left(s_A^{i'} + hs_B^{j'}\right) \right\|^2 \\ &= \left\| \Delta s_A^{i,i'} + h\Delta s_B^{j,j'} \right\|^2 \\ &= \left\| \Delta s_A^{i,i'} \right\|^2 + |h|^2 \left\| \Delta s_B^{j,j'} \right\|^2 + 2\Re\left\{h^* z\right\}, \end{aligned} \tag{6.1}$$

where $z = \left\langle \Delta s_A^{i,i'}; \Delta s_B^{j,j'} \right\rangle$, $\Delta s^{i,i'} = s^i - s^{i'}$ and $i, i', j, j' \in \{1, 2, \ldots M_s\}$.

Table 6.1: Hierarchical symbol table ($\left|\mathscr{A}_s^A(\cdot)\right| = \left|\mathscr{A}_s^B(\cdot)\right| = M_s$).

	j_1	j_2	$\dots$	j_M
i_1	$u^{(i_1,j_1)}$	$u^{(i_1,j_2)}$	$\dots$	$u^{(i_1,j_M)}$
i_2	$u^{(i_2,j_1)}$	$u^{(i_2,j_2)}$	$\dots$	$u^{(i_2,j_M)}$
$\vdots$	$\vdots$	$\vdots$	$\ddots$	$\vdots$
i_M	$u^{(i_M,j_1)}$	$u^{(i_M,j_2)}$	$\dots$	$u^{(i_M,j_M)}$

If some pair of hierarchical symbols (u,u') belongs to the same eXclusive relay output ($\mathscr{X}_s(u^{i,j}) = \mathscr{X}_s(u^{i',j'})$), it will be "clustered" by the relay decoder and such pair does not affect the final *minimum hierarchical* distance. The minimum hierarchical distance ($d^2_{\min}(h)$) is hence given by:

$$d^2_{\min}(h) = \min_{\mathscr{X}_s(u^{i,j}) \neq \mathscr{X}_s(u^{i',j'})} d^2_{u^{i,j},u^{i',j'}}(h). \tag{6.2}$$

Note that the eXclusive law failures cause $d^2_{\min}(h) \to 0$, which in turn results into a faulty decision of the relay decoder (and consequently the performance degradation). To provide a better insight into the following discussion, we introduce the *hierarchical symbol table* (Table 6.1), which illustrates the relation between the source (A,B) output symbols s_A^i, s_B^j (given by the indices $i,\, j \in \{1,2,\dots M_s\}$) and the corresponding hierarchical symbols u^{i_A,j_B}.

The eXclusive law constraints, together with the assumption of minimal cardinality of L-HXC (see [71] for details), prevents the mapping of hierarchical symbols ($u^{i,j}$, $u^{i',j'}$) which have one index in common (i.e. $i = i'$ or $j = j'$) to the same relay output. All such hierarchical symbol pairs lie in the same row ($i = i'$) or column ($j = j'$) of the hierarchical symbol table (Table 6.1). Since only the L-HXC with minimal cardinality is considered in this Chapter, the search of the minimum Euclidean distance in (6.2) can be divided into the following three cases:

1. $i = i'$ (rows):

$$\begin{aligned} d^2_{\text{row}}(h) &= \min_{u^{i,j} \neq u^{i,j'}} d^2_{u^{i,j},u^{i,,j'}}(h) \\ &= |h|^2 \min_{j \neq j'} \left\| \Delta s_B^{j,j'} \right\|^2 \end{aligned} \tag{6.3}$$

2. $j = j'$ (columns):

$$\begin{aligned} d^2_{\text{col}} &= \min_{u^{i,j} \neq u^{i',j}} d^2_{u^{i,j},u^{i',j}}(h) \\ &= \min_{i \neq i'} \left\| \Delta s_A^{i,i'} \right\|^2 \end{aligned} \tag{6.4}$$

3. $i \neq i'$ and $j \neq j'$ (general case). In this case the Euclidean distance remains in the "full" form of (6.1):

$$d^2_g(h) = \min_{\mathscr{X}_s(u^{i,j}) \neq \mathscr{X}_s(u^{i',j'})} d^2_{u^{i,j},u^{i',j'}}(h). \tag{6.5}$$

The minimum distance (6.2) of the hierarchical symbols (as observed by the relay) hence can be equivalently defined as:

$$d^2_{\min}(h) = \min\left\{ d^2_{\text{row}}(h), d^2_{\text{col}}, d^2_g(h) \right\}. \tag{6.6}$$

6.2.2 Bounds of the hierarchical distance

Those hierarchical symbol pairs $(u^{i,j}, u^{i',j'})$ which have one index in common (i.e. $i = i'$ or $j = j'$) cannot be clustered by a common $\mathscr{X}_s(.)$ (minimal cardinality assumption). The corresponding Euclidean distances ((6.3) and (6.4)) hence always (for arbitrary HXA and relay output eXclusive mapper $\mathscr{X}_s(.)$) form the upper bound of the minimum hierarchical distance:

$$d^2_{\min,\mathrm{UB}}(h) = \min\left\{d^2_{\mathrm{row}}(h), d^2_{\mathrm{col}}\right\}. \tag{6.7}$$

And consequently:

$$d^2_{\min}(h) = d^2_{\min,\mathrm{UB}}(h), \quad \text{for} \quad d^2_g(h) \geq d^2_{\min,\mathrm{UB}}(h), \tag{6.8}$$

$$d^2_{\min}(h) < d^2_{\min,\mathrm{UB}}(h), \quad \text{for} \quad d^2_g(h) < d^2_{\min,\mathrm{UB}}(h). \tag{6.9}$$

As we will show in the following discussion, the min-distance upper bound given by (6.7) is not tight in general (for a considerable range of channel parameter (h) values). However, it defines an upper bound for the overall min-distance performance, since it is given solely by the properties of the HXA mappers at sources ($\mathscr{A}^A_s(.), \mathscr{A}^B_s(.)$) and it is not affected by the choice of the relay output eXclusive mapper $\mathscr{X}_s(.)$. Note that the min-distance upper bound (6.7) does not depend on $\angle h$.

The reason why the hierarchical min-distance upper bound (as given by (6.7)) could be quite broad is given by the last term in the search of the min-distance in (6.6). This term (given by (6.5)) depends generally on both HXA mappers ($\mathscr{A}^A_s(.), \mathscr{A}^B_s(.)$), the relay output eXclusive mapper $\mathscr{X}_s(.)$ and also on the value of channel parameter $h \in \mathbb{C}$. Even for the fixed HXA and eXclusive mappers, the value of $d^2_g(h)$ could change significantly with the varying channel parameter h. As we will show in the following Lemma, the search of the minimum in (6.5) can be bounded, if we consider the worst case value of $\angle h$ and focus only on the varying absolute value of the channel parameter ($|h|$).

Lemma 17. *The Euclidean distance $d^2_g(h)$ of the general pair of hierarchical symbols $u^{i,j}, u^{i',j'}$ is lower bounded by*

$$d^2_{g,LB}(h) = \min_{i\neq i',\, j\neq j'} \left\{ \left\|\Delta s^{i,i'}_A\right\|^2 + |h|^2 \left\|\Delta s^{j,j'}_B\right\|^2 - 2|h||z| \right\}, \tag{6.10}$$

where $z = \left\langle \Delta s^{i,i'}_A ; \Delta s^{j,j'}_B \right\rangle$, $\Delta s^{i,i'} = s^i - s^{i'}$ and $i, i', j, j' \in \{1,2,\ldots M_s\}$, such that $\mathscr{X}_s\left(u^{i,j}\right) \neq \mathscr{X}_s\left(u^{i',j'}\right)$.

Proof. The minimum of $d^2_{u^{i,j},u^{i',j'}}(h)$ in (6.5) is taken over all permissible hierarchical symbol pairs $u^{i,j}, u^{i',j'}$ (such that $\mathscr{X}_s\left(u^{i,j}\right) \neq \mathscr{X}_s\left(u^{i',j'}\right)$). The general form of $d^2_{u^{i,j},u^{i',j'}}(h)$ is given by (6.1), where $\Re\{h^* z\} = \Re\{|h||z|\exp(j(\angle h^* + \angle z))\}$. Now since $h \in \mathbb{C}$ and consequently $(\angle h^* + \angle z) \in (-\Pi;\Pi\rangle$, there can always be found h'^* such that $(\angle h'^* + \angle z) = \Pi$. This gives us $\Re\{h^* z\} \geq -|h||z|$, where the minimum is achieved for h'^*. By applying the minimum of $\Re\{h^* z\}$ to (6.1) we immediately obtain (6.10). □

The min-distance lower bound in (6.10) is always achievable, since the complex channel parameter h can have arbitrary phase ($\angle h$) and hence it can achieve the value of h'^* as in the proof of Lemma 17. Now it can be easily shown that (6.10) is equivalent to the search of minimum over the set of parabolas given by

$$\left\|\Delta s^{i,i'}_A\right\|^2 + |h|^2 \left\|\Delta s^{j,j'}_B\right\|^2 - 2|h||z| \tag{6.11}$$

for each of the particular $i, i', j, j' \in \{1,2,\ldots M_s\}$, such that $\mathscr{X}_s\left(u^{i,j}\right) \neq \mathscr{X}_s\left(u^{i',j'}\right)$.

To illustrate the influence of the derived bounds (6.7), (6.10) on the the overall hierarchical min-distance performance, we will observe the $d^2_{\min}(|h|)$, i.e. the minimum Euclidean distance as a function of

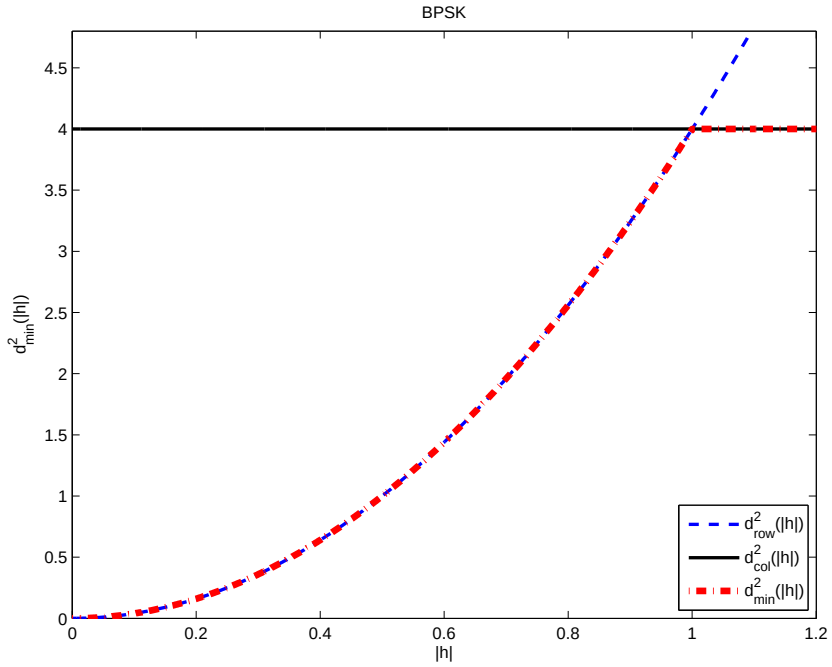

Figure 6.1: Minimum hierarchical distance $d^2_{\min}(|h|)$ for BPSK alphabet.

the absolute value of the channel parameter $|h|$. The results for some classical linear modulation schemes are available in Figs. 6.1, 6.2, 6.3 and 6.4. Standard Gray mapping of alphabet indices ($i \in \{1,2,\dots M_s\}$) to constellation space symbols (s^i) was used and the eXclusive hierarchical mapping ($\mathscr{X}_s(.)$) was defined by the bit-wise XOR operation of the symbol indices. All alphabets were scaled to have identical mean symbol energy. All parabolas defined by (6.11) are included in the figures, to show their influence on the search of minimum in (6.10). Note that since it is possible to employ the 2-mode relay processing (see [21]), which effectively bounds the range of channel parameter values, it could be sufficient to observe only the interval bounded by $|h| \leq 1$.

Many important conclusions can be stated by observing the Figs. 6.1, 6.2, 6.3 and 6.4. Since $d^2_g(h)$ essentially does not exist for binary alphabets (e.g. BPSK) the hierarchical min-distance is always equal to the bound given by (6.7) and hence the binary alphabets are highly resistant to the channel parametrization. For higher alphabet cardinality (QPSK, 8-PSK and 16-QAM in our Figures) an increasing number of parabolas (given by (6.11)) quickly emerge and significantly affect the resulting values of $d^2_{\min}(|h|)$.

Note again that for some specific value of channel parametrization (respective specific value of $\angle h$) the minimum hierarchical distance will achieve the lower bound ($d^2_{\min}(h) = d^2_{g,LB}(h)$). Hence the observations presented in the Figs. 6.1, 6.2, 6.3 and 6.4 can help us to identify the eXclusive law failures ($d^2_{\min}(h) \to 0$) for any alphabet mapper.

6.3 Parametric HXA design

In this section we focus on the possibility to construct *Parametric HXA*[26] (P-HXA), which is able to prevent the occurance of eXclusive law failures ($d^2_{\min}(h) \to 0$) for arbitrary parametrization ($h \in \mathbb{C}$). We

[26] *Note that P-HXA (source alphabet which prevents the occurance of eXclusive law failures) and PI-HXA (source alphabet with parameter-invariant decision regions at the relay) refer to the two different approaches to the source alphabet design.*

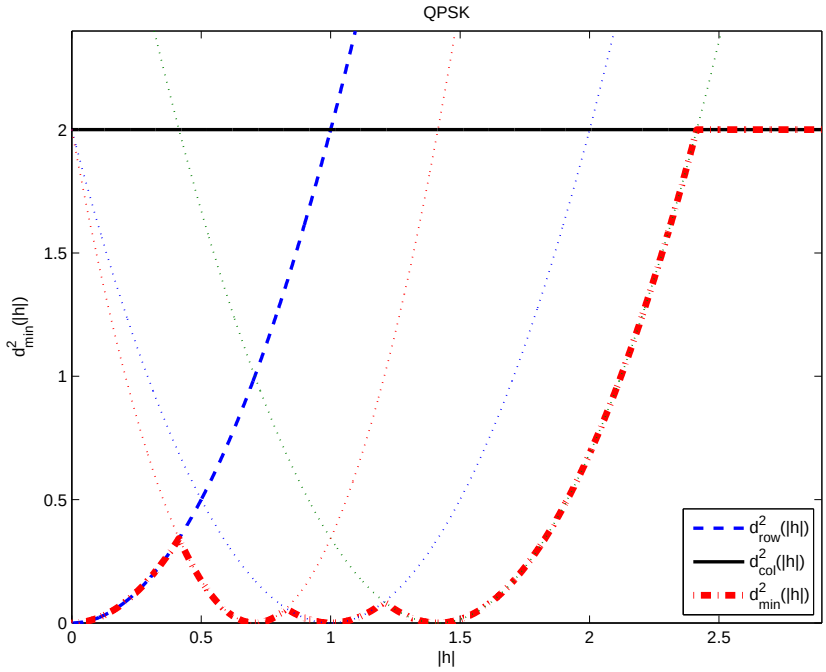

Figure 6.2: Minimum hierarchical distance $d^2_{\min}(|h|)$ for QPSK alphabet.

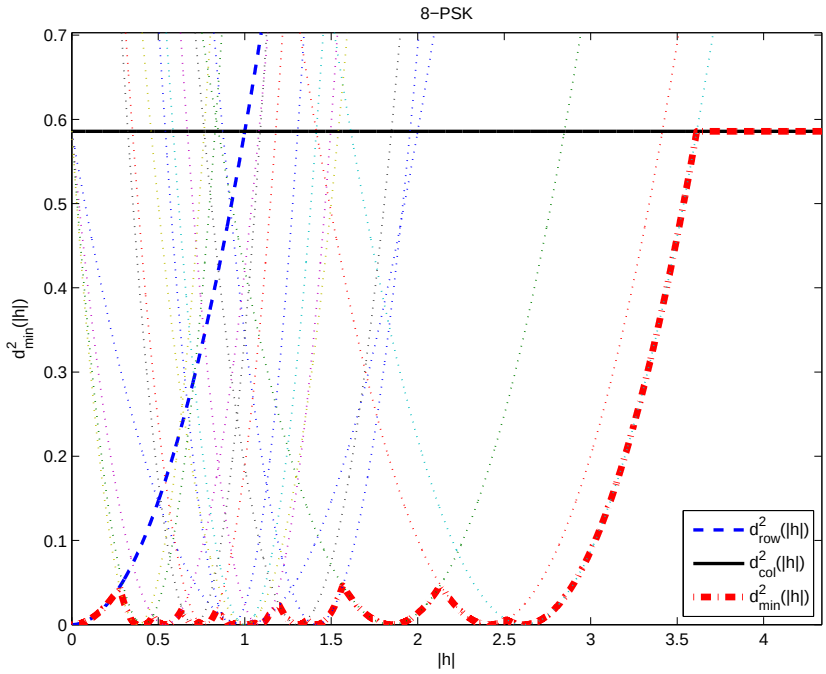

Figure 6.3: Minimum hierarchical distance $d^2_{\min}(|h|)$ for 8-PSK alphabet.

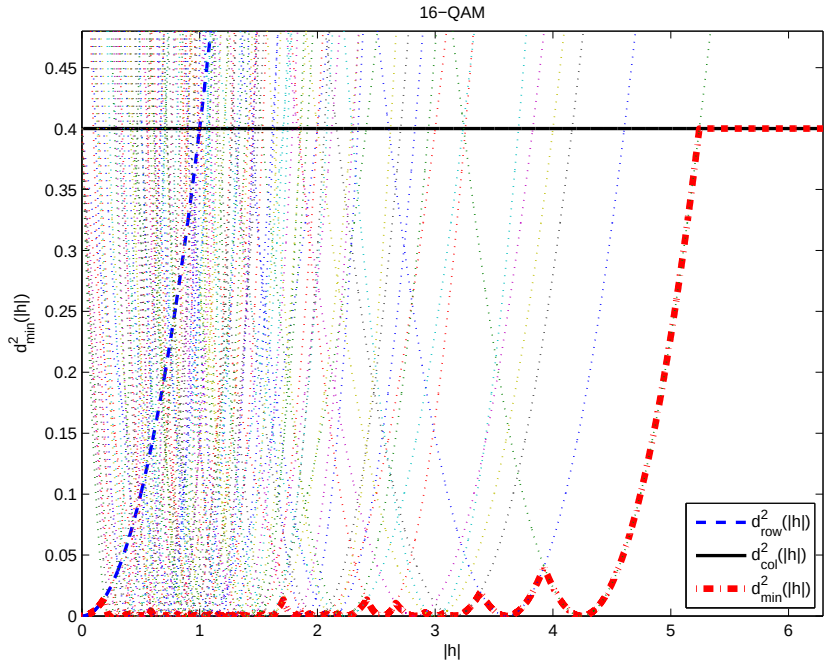

Figure 6.4: Minimum hierarchical distance $d^2_{\min}(|h|)$ for 16-QAM alphabet.

prove that only binary P-HXA can be constructed in $\mathbb{C}^1$, while $\mathbb{C}^2$ is sufficient to design P-HXA with arbitrary cardinality.

6.3.1 HXA design in $\mathbb{C}^1$

In the following Lemma we show that it is impossible to design P-HXA in $\mathbb{C}^1$ (with $M_s > 2$) if we require the eXclusive law failures ($d^2_{\min}(h) \to 0$) to be avoided for arbitrary channel parametrization.

Lemma 18. *The eXclusive law failures $d^2_{\min}(h) \to 0$ ($h \neq 0$, $h \in \mathbb{C}^1$) cannot be avoided for any alphabets $\mathscr{A}_s^A(.), \mathscr{A}_s^B(.)$ such that $\mathscr{A}_s^A(.), \mathscr{A}_s^B(.) \in \mathbb{C}^1$ and $|\mathscr{A}_s(.)| = M_s > 2$.*

Proof. The eXclusive law failure occur whenever $d^2_{u^{i,j},u^{i',j'}}(h) = 0$ for any hierarchical symbol pair $u^{i,j}, u^{i',j'}$ such that $\mathscr{X}_s\left(u^{i,j}\right) \neq \mathscr{X}_s\left(u^{i',j'}\right)$. We focus on the (squared) Euclidean distance (as defined in (6.1)) in the following form:

$$d^2(h) = \left\| \Delta s_A^{i,i'} + h \Delta s_B^{j,j'} \right\|^2. \tag{6.12}$$

Now since for a general vector $\mathbf{a}$ holds $\|\mathbf{a}\| = 0 \Leftrightarrow \mathbf{a} = \mathbf{o}$, it is obvious from (6.12) that $d^2(h) = 0 \Leftrightarrow \Delta s_A^{i,i'} + h\Delta s_B^{j,j'} = 0$. If this linear combination of vectors $\Delta s_A^{i,i'}, \Delta s_B^{j,j'}$ should be non-zero for any $h \neq 0$, these vectors must be linearly independent. However, it is impossible to find two (non-zero) linearly independent vectors in $\mathbb{C}^1$, and hence the assumption of $\mathscr{A}_s^A(.), \mathscr{A}_s^B(.) \in \mathbb{C}^1$ forces the vectors $\Delta s_A^{i,i'}, \Delta s_B^{j,j'}$ to be always linearly dependent. Consequently, for any pair of hierarchical symbols $u^{i,j}, u^{i',j'}$ in $\mathbb{C}^1$ (such that $\mathscr{X}_s\left(u^{i,j}\right) \neq \mathscr{X}_s\left(u^{i',j'}\right)$) it can always be found some $h' \neq 0$ resulting in a failure of the eXclusive law.

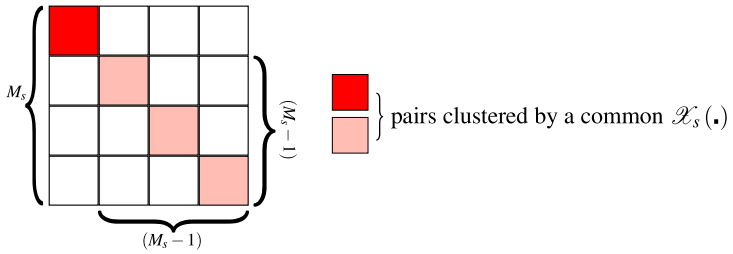

Figure 6.5: Visualization of hierarchical symbol pairs vulnerable to eXclusive law failures.

For a given $u^{i,j}$ there is a total of $\left[(M_s-1)^2-(M_s-1)\right]=\left(M_s^2-3M_s+2\right)$ such pairs of $u^{i,j}$, $u^{i',j'}$ (see Fig. 6.5) and each of these pairs can consequently violate the eXclusive law. It is obvious that $\left(M_s^2-3M_s+2\right)$ is always nonzero for cardinality $M_s>2$, and hence for $M_s>2$ there always exists some pair of hierarchical symbols $u^{i,j}$, $u^{i',j'}$, which can invoke the eXclusive law failure. Note that for $M_s=2$ such pair of hierarchical symbols never exists (since all such pairs are clustered by a common $\mathscr{X}_s(.)$ - see Fig. 6.5), which corresponds to the fact the $d_g^2(h)$ essentially does not exist for binary alphabets. □

6.3.2 Construction algorithm for 2-dimensional alphabets

Since it is impossible to find P-HXA in $\mathbb{C}^1$ we conclude this Chapter with an example design of two-dimensional alphabet mappers $\mathscr{A}_s^A(.),\mathscr{A}_s^B(.)\in\mathbb{C}^2$. The following orthogonality

$$\left\langle \Delta s_A^{i,i'};\Delta s_B^{j,j'}\right\rangle=0 \tag{6.13}$$

guarantees the linear independence of vectors $\Delta s_A^{i,i'}$, $\Delta s_B^{j,j'}$, which in turn prevents the occurance of eXclusive law failures for a corresponding pair of hierarchical symbols $u^{i,j}$, $u^{i',j'}$ (see the proof of Lemma 18). Moreover, if the source alphabets fullfil this orthogonality condition (6.13) for all $i,j,i',j'\in\{1,\dots M_s\}$, Euclidean distance of the corresponding hierarchical symbols (6.1) reduces to:

$$d_{\text{orth}}^2(h)=\left\|\Delta s_A^{i,i'}\right\|^2+|h|^2\left\|\Delta s_B^{j,j'}\right\|^2, \tag{6.14}$$

and consequently, the minimum hierarchical distance achieves the upper bound given by (6.7) for arbitrary parametrization.

It is obvious that the orthogonality of vectors $\Delta s_A^{i,i'}$, $\Delta s_B^{j,j'}$ can be simply achieved by forcing all individual constellation symbols (given by the alphabet mappers $\mathscr{A}_s^A(.),\mathscr{A}_s^B(.)$) to be mutually orthogonal

$$\left\langle s_A^i;s_B^j\right\rangle=0, \tag{6.15}$$

for all $i,j\in\{1,2,\dots M\}$. Please note that such (orthogonal) solution does not have to be optimal in general. We introduce it only as an example solution to the P-HXA design problem.

An example alphabet construction (based on the aforementioned discussion) is available in Algorithm 6.1, which enables a design of P-HXA with arbitrary cardinality. Coefficients q^{i_A}, q^{i_B} can be chosen from a conventional linear modulation constellation, and even identical coefficients for both alphabets ($\left\{q^{i_A}\right\}_{i_A=0}^{M_s-1}=\left\{q^{i_B}\right\}_{i_B=0}^{M_s-1}$) can be chosen. The resulting alphabets are then denoted as P-HXA-QPSK, P-HXA-8-PSK etc.

Algorithm 6.1 Higher-order codebook - Example design

1. Choose $\mathbf{x}, \mathbf{y} \in \mathbb{C}^2$ such that $\langle \mathbf{x}; \mathbf{y} \rangle = 0$.
2. $\mathscr{A}_s^A = \{q^{i_A} \cdot \mathbf{x}\}_{i_A=0}^{M_s-1}; \quad q^{i_A} \in \mathbb{C}$
3. $\mathscr{A}_s^B = \{q^{i_B} \cdot \mathbf{y}\}_{i_B=0}^{M_s-1}; \quad q^{i_B} \in \mathbb{C}$

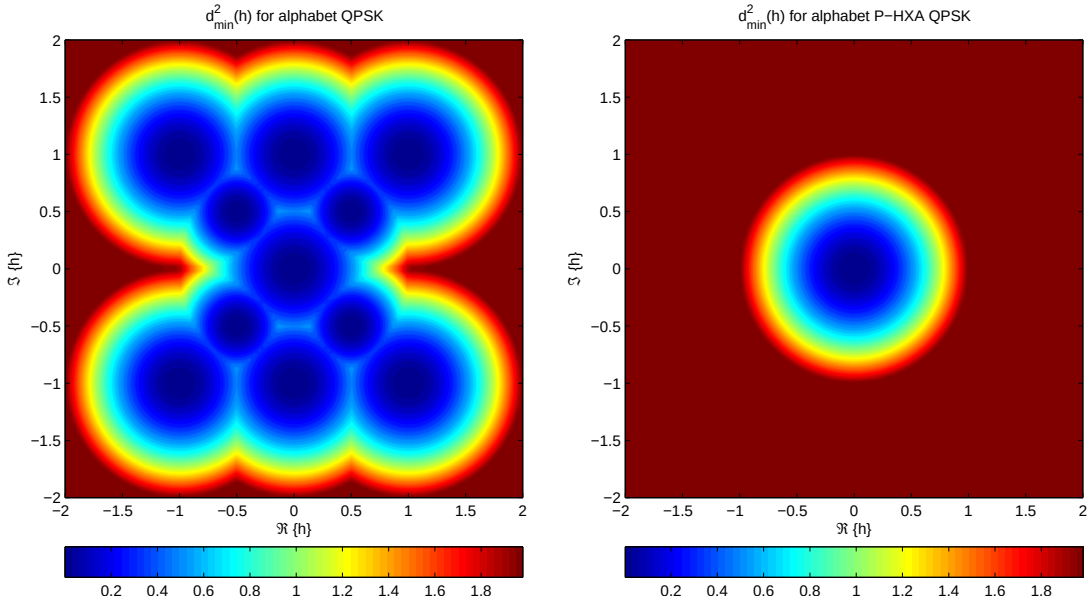

Figure 6.6: Minimum hierarchical distance performance for QPSK and 4-ary P-HXA.

6.4 Numerical evaluations

It is obvious that Algorithm 6.1 is a zero-mean equivalent of Algorithm 5.2 (relaxed E-PHXC design criteria) and hence the alphabets designed according to these two design Algorithms have identical min-distance performance. This is obvious also from a comparison of Figs. 6.6, 6.7, 6.8) with Figs. 5.5, 5.6 and 5.7 in Chapter 5. A numerical evaluation of hierarchical distance $d^2_{\min}(|h|)$ of some example alphabets is presented in Figs. 6.9, 6.10 and 6.11 (compare with Figs. 6.2, 6.3 and 6.4).

6.5 Discussion of results

The impact of channel parametrization on the Euclidean distance performance of compound constellation (hierarchical distance) in 2-WRC with HDF strategy is analyzed in this Chapter. Based on this analysis, the bounds of hierarchical distance are identified and the fact that occurance of eXclusive law failures cannot be completly prevented (if the source alphabets are restricted to $\mathbb{C}^1$) is proved. A simple construction Algorithm for the design of source alphabets in $\mathbb{C}^2$ is then presented. The presented Algorithm 6.1 appears to be a simplified (zero-mean) version of Algorithm 5.2. This is a direct consequence of the fact that the relaxed E-PHXC design criteria (Algorithm 5.2) are also based on the min-distance properties of source alphabets.

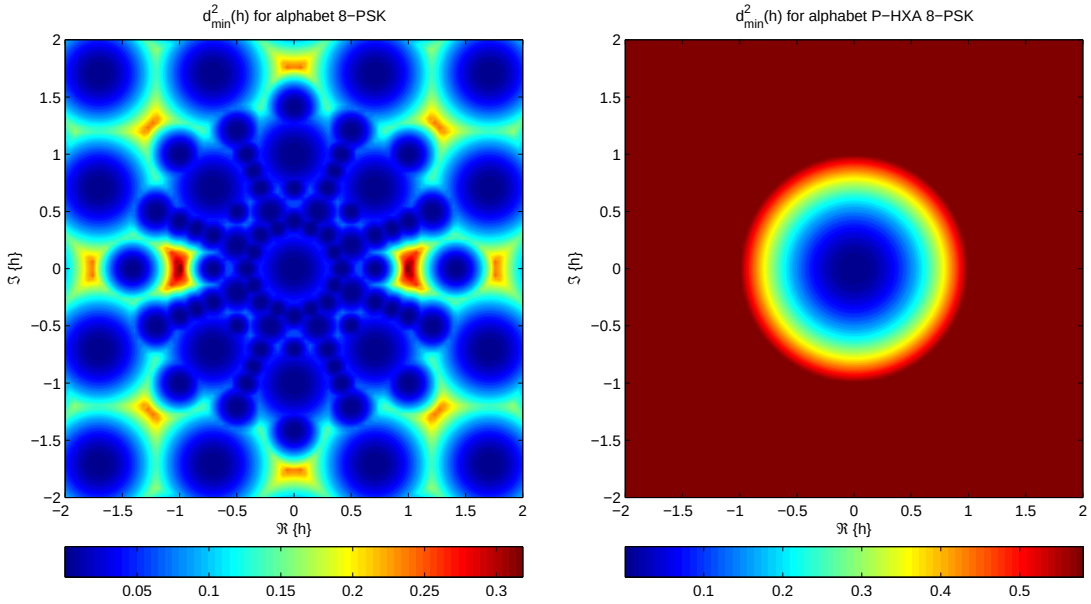

Figure 6.7: Minimum hierarchical distance performance for 8-PSK and 8-ary P-HXA.

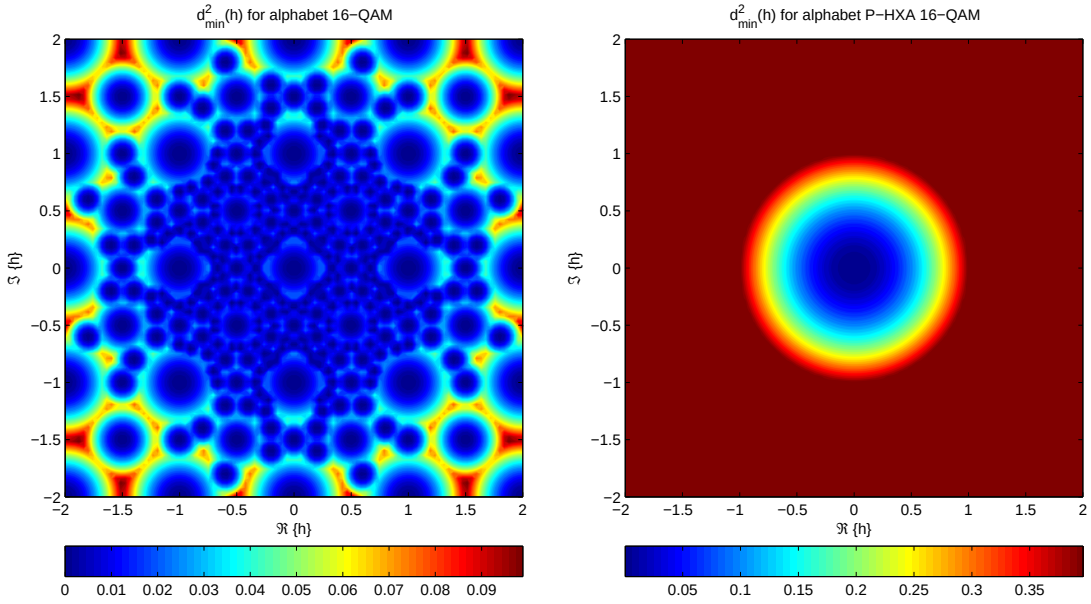

Figure 6.8: Minimum hierarchical distance performance for 16-QAM and 16-ary P-HXA.

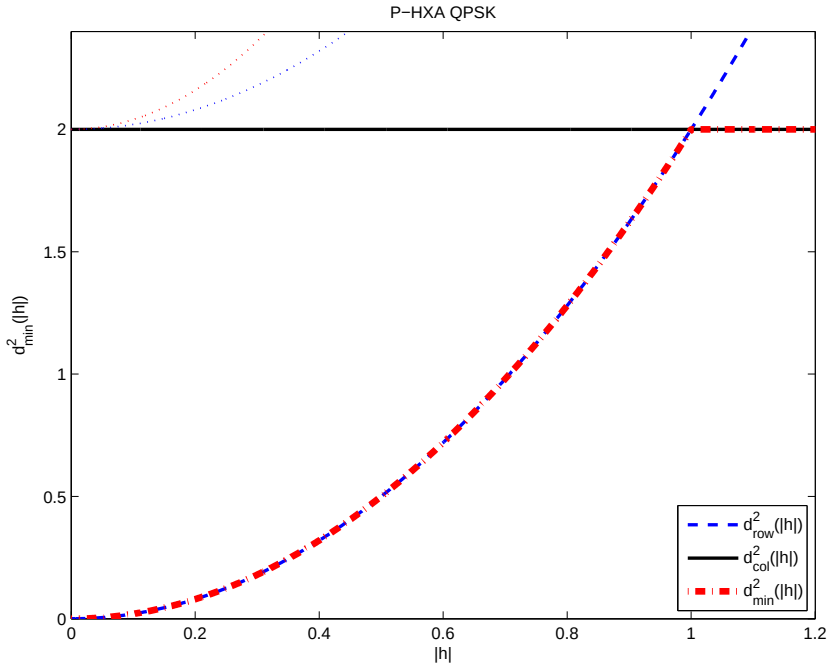

Figure 6.9: Minimum hierarchical distance $d^2_{\min}(|h|)$ for P-HXA with QPSK alphabet.

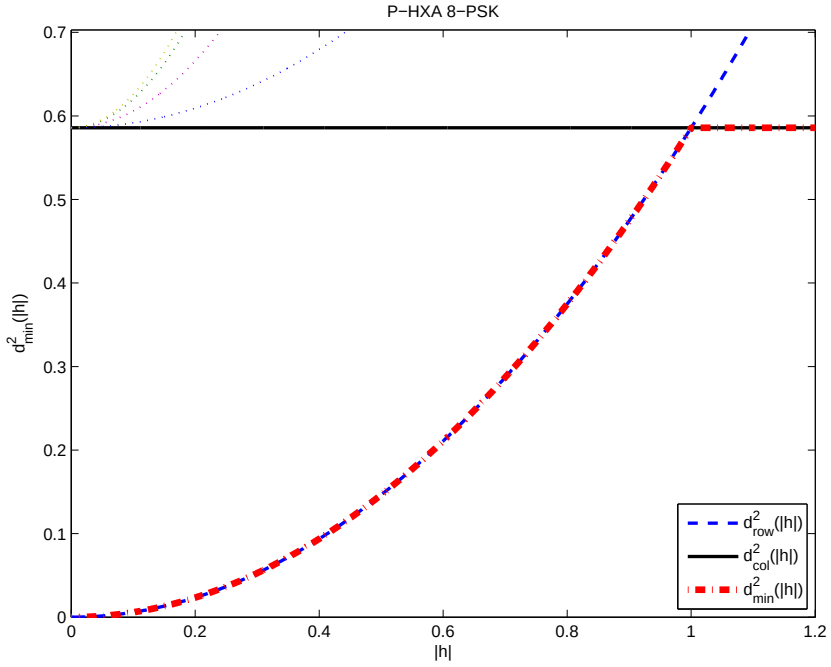

Figure 6.10: Minimum hierarchical distance $d^2_{\min}(|h|)$ for P-HXA with 8-PSK alphabet.

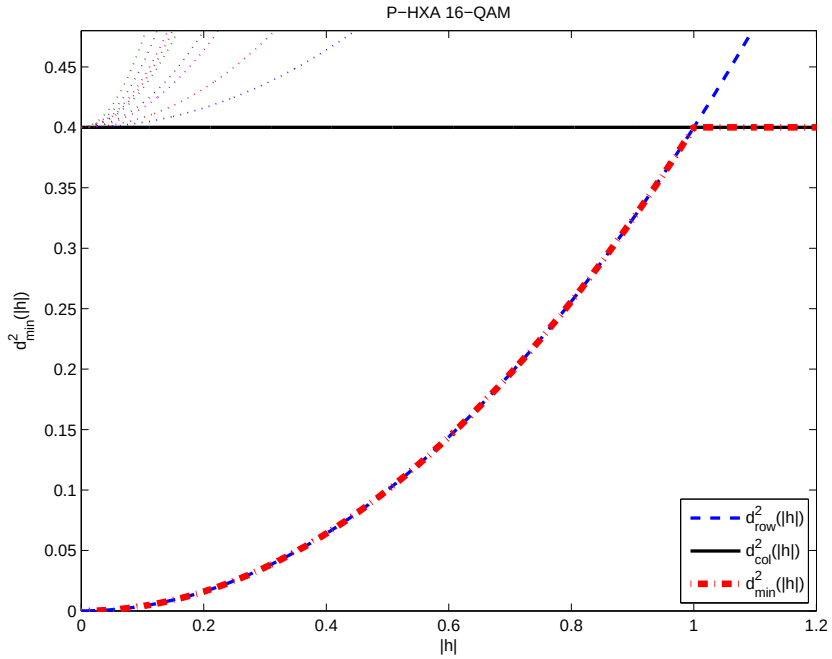

Figure 6.11: Minimum hierarchical distance $d^2_{\min}(|h|)$ for P-HXA with 16-QAM alphabet.

Despite of the fact that again only multi-dimensional alphabets were identified to be resistant to channel parametrization, the *bounds of minimum hierarchical distance* revealed in this Chapter help us to identify the major performance limits invoked by channel parametrization in 2-WRC, and moreover, they provide us some useful hints for the design of *novel constellation alphabets* in $\mathbb{C}^1$. As we show in the following Chapter, these novel alphabets have a potential to outperform the conventional linear modulation schemes in HDF without sacrificing the overall system throughput.

Chapter 7

Non-uniform 2-slot constellations

"The part can never be well unless the whole is well."

Plato

7.1 Introduction

In this Chapter we show that it is possible to improve the performance of the 2-WRC system (in a special case of Rician fading channels) by a *design of novel 2-slot source alphabets.* The proposed *Non-uniform 2-slot (NuT) alphabets* are robust to channel parameterization effects, while avoiding the requirement of phase pre-rotation (or adaptive processing) but still preserving the $\mathbb{C}^1$ (per symbol slot) dimensionality constraint (to avoid the throughput reduction). Based on the analysis of the hierarchical (Euclidean) distance [22] (see Chapter 6), we introduce a design algorithm for NuT alphabets and we compare their Symbol Error Rate (SER) performance to that of the traditional linear modulation constellations.

7.1.1 Summary of minimum hierarchical distance analysis

The (squared) *Minimum Hierarchical Distance* (MHD) is closely connected to the error rate performance of the system (similarly as the minimum Euclidean distance of the single user constellation in a traditional point-to-point communication), and hence the goal of the novel alphabet design is to *maximize the hierarchical distance* for all permissible values of $h = {}^{h_B}/_{h_A} \in \mathbb{C}$. However, this is not an easy task in the parametric MAC channel, since there the minimum Euclidean distance of the compound constellation is strongly influenced by a (mutual) variation of complex channels h_A, h_B (see e.g. [16, 22]).

As noted in the previous Chapter, the (squared) Euclidean distance ($d^2_{u^{i,j},u^{i',j'}}(h)$) of a general pair of compound symbols ($u^{i,j} = s^i_A + hs^j_B$ and $u^{i',j'} = s^{i'}_A + hs^{j'}_B$) can be defined as

$$d^2_{u^{i,j},u^{i',j'}}(h) = \|\Delta s_A\|^2 + |h|^2 \|\Delta s_B\|^2 + 2\Re\{h^* z\} \tag{7.1}$$

where $z = \langle \Delta s_A; \Delta s_B \rangle$, $\Delta s_A = s^i - s^{i'}$, $\Delta s_B = s^j - s^{j'}$ and $i, i', j, j' \in \{1, 2, \ldots M_s\}$.

As shown in [22], the MHD[27)]

$$d^2_{\min}(h) = \min_{(i,j,i',j'):\mathscr{X}_s(i,j)\neq\mathscr{X}_s(i',j')} d^2_{u^{i,j},u^{i',j'}}(h) \tag{7.2}$$

[27)] In the rest of this Chapter we will use a slightly relaxed notation for the eXclusive mapping operation: $\mathscr{X}_s(i,j) = \mathscr{X}_s\left(s^i_A, s^j_B\right)$.

is (for the worst case phase $\angle h'$) lower bounded by a *set of parabolas* $\mathscr{S}_p = \left\{p_{i,j,i',j'}\right\}_{\mathscr{X}_s(i,j)\neq\mathscr{X}_s(i',j')}$, where each particular parabola is given by

$$\begin{aligned} p_{i,j,i',j'}(|h|) &= \min_{\angle h} d^2_{u^{i,j},u^{i',j'}}(h) \\ &= |h|^2 \|\Delta s_B\|^2 - 2|h||z| + \|\Delta s_A\|^2 . \end{aligned} \tag{7.3}$$

The lower bound defined by $\mathscr{S}_p$ is always achieved for some specific $\angle h$ [22] and hence

$$d^2_{\min}(|h|) = \min_{\mathscr{X}_s(i,j)\neq\mathscr{X}_s(i',j')} p_{i,j,i',j'}(|h|) . \tag{7.4}$$

The min-distance parabola $p_{i,j,i',j'}(|h|)$ is hence defined for all permissible 4-tuples of indices i,j,i',j' such that $\mathscr{X}_s(i,j) \neq \mathscr{X}_s(i',j')$ and it virtually describes the min-distance $d^2_{u^{i,j},u^{i',j'}}(|h|)$ of a pair of compound symbols ($u^{i,j} = s^i_A + hs^j_B$ and $u^{i',j'} = s^{i'}_A + hs^{j'}_B$) for the worst case phase $\angle h'$ of the channel parameter $h \in \mathbb{C}$ [22].

This *parabolic behaviour* of the hierarchical min-distance (see an example in Fig. 7.1) results necessarily in eXclusive law failures ($d^2_{\min}(h) \to 0$), and consequently in destination decoding errors, since the relay cannot unambiguously determine the output symbol [22]. The analysis of the complete set of these min-distance parabolas (given by $\mathscr{S}_p$) can help us to identify the eXclusive law failure events ($d^2_{\min}(h) \to 0$) i.e. the values of h, for which the hierarchical min-distance is poor.

7.2 Non-uniform 2-slot alphabets

As proved in [22] (see Lemma 18), the parabolic behaviour of hierarchical min-distance cannot be fully avoided for traditional linear modulation constellations in $\mathbb{C}^1$ (excepting the binary alphabets). However, as we will show in the following section, in case of *Rician fading channels* it is possible to suppress this harmful behaviour by a suitable design of 2-source NuT constellation alphabets.

7.2.1 Parabolic behaviour analysis

It can be shown that for Rician source-relay channels ($|h_A|, |h_B|$), the probability distribution of channel parameter $|h| = {}^{|h_B|}/_{|h_A|}$ is diminishing as $|h| \to 0$ (see Fig. 7.2). Considering the hierarchical min-distance $d^2_{\min}(|h|)$ of QPSK (Fig. 7.1) along with the probability distribution of $|h|$ (Fig. 7.2) it is obvious that the performance of HDF system with QPSK source alphabets is presumably poor. Fortunately, it is possible to decrease the negative impact of this parabolic min-distance behaviour by shifting the min-distance parabolas (7.3) towards the less probable values of $|h|$.

A position of each particular min-distance parabola (7.3) vertex (minimum) is given by

$$\left|h'_{\min}\right| = \arg\min_{|h|} p_{i,j,i',j'}(|h|) = \frac{|\langle \Delta s_A; \Delta s_B\rangle|}{\|\Delta s_B\|^2}. \tag{7.5}$$

In case of constellation alphabets in $\mathbb{C}^1$, this formula can be further simplified to

$$\left|h'_{\min}\right| = \frac{\|\Delta s_A\| \cdot \|\Delta s_B\|}{\|\Delta s_B\|^2} = \frac{\|\Delta s_A\|}{\|\Delta s_B\|}, \tag{7.6}$$

since any pair of vectors in $\mathbb{C}^1$ is always linearly dependent, which gives us the equality in the general *Cauchy-Schwartz inequality* (see e.g. [118]).

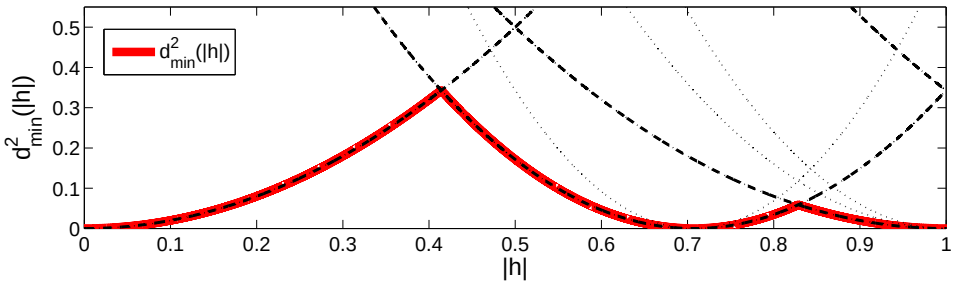

Figure 7.1: Set $\mathscr{S}_p$ of min-distance parabolas for the QPSK alphabet (dashed lines) and NuT$(\mathrm{QPSK};1)$ alphabet (dotted lines). The hierarchical min-distance $d^2_{\min}(|h|)$ of both alphabets coincides.

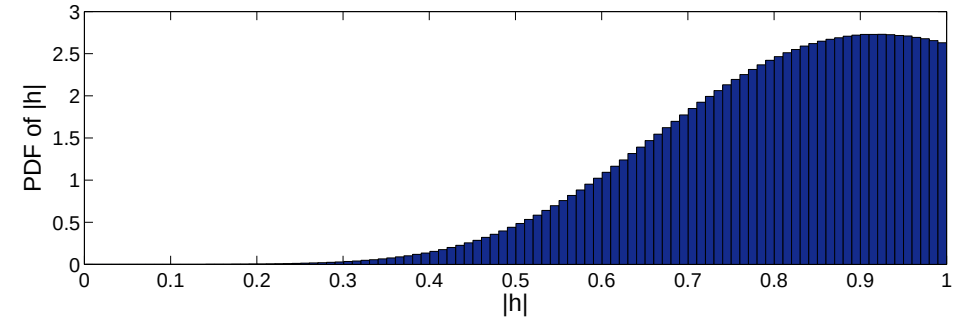

Figure 7.2: Probability distribution of channel parameter $|h| \leq 1$ (Rician fading channels $|h_A|, |h_B|$ with a Rician factor $K = 10\,\mathrm{dB}$).

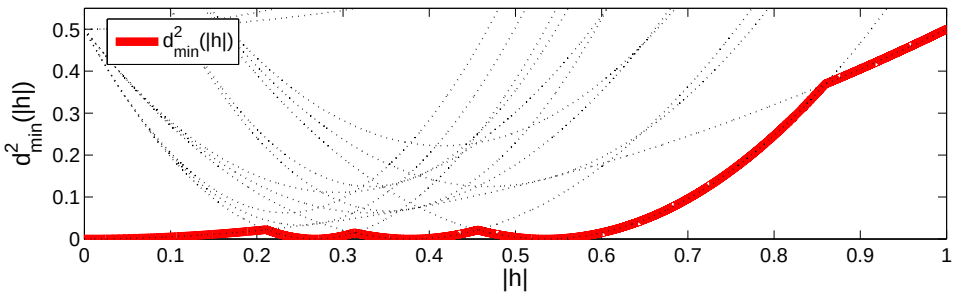

Figure 7.3: Hierarchical min-distance $d^2_{\min}(|h|)$ and the set $\mathscr{S}_p$ of min-distance parabolas for the NuT$(\mathrm{QPSK};0.25)$ alphabet (compare to Fig. 7.1 and distribution of $|h|$ in Fig. 7.2).

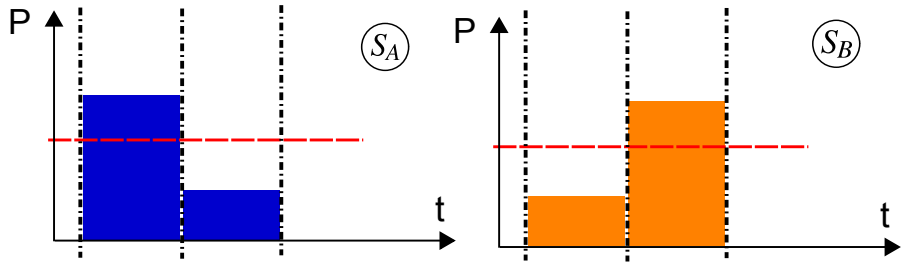

Figure 7.4: Re-distribution of power among the particular slots of 2-source NuT alphabet supersymbols.

Algorithm 7.1 NuT constellation alphabet design.

1. Pick a base alphabet $\mathscr{A}_s$.
2. Choose a power scaling factor $s_f \in (0,2)$.
3. Source A alphabet: $\mathscr{A}_s^A = [\sqrt{s_f}\mathscr{A}_s, \sqrt{2-s_f}\mathscr{A}_s]$.
4. Source B alphabet: $\mathscr{A}_s^B = [\sqrt{2-s_f}\mathscr{A}_s, \sqrt{s_f}\mathscr{A}_s]$.

7.2.2 Alphabet design algorithm

As it is obvious from (7.6), a position of the minimum of each particular min-distance parabola $p_{i,j,i',j'}(|h|)$ is given solely by a ratio of $\left\|\Delta s_A^{i,i'}\right\|$ and $\left\|\Delta s_B^{j,j'}\right\|$, i.e. by the corresponding min-distances of individual source alphabets $\mathscr{A}_s^A, \mathscr{A}_s^B$. Now it seems quite straightforward that it should be possible to control the positions of particular min-distance parabolas directly by the design of source alphabets. Considering the distribution of the channel parameter $|h|$ for Rician $|h_A|, |h_B|$ (Fig. 7.2), the goal is to design $\mathscr{A}_s^A, \mathscr{A}_s^B$ in such a way that all the min-distance parabolas $p_{i,j,i',j'}(|h|) \in \mathscr{S}_p$ will be situated close to $|h| \to 0$. This could be obviously achieved by increasing $\left\|\Delta s_A^{i,i'}\right\|$ relatively to $\left\|\Delta s_B^{j,j'}\right\|$, i.e. by a suitable allocation of output power at both sources.

Since the average power constraint must be taken into account, it is not feasible to purely increase the output power of one source relatively to the other one. However, if we allow pairing of two subsequent source symbols into a *2-slot super-symbol*, we obtain an additional degree of freedom, since the available power can be arbitrarily re-distributed among the two slots of the super-symbol. This principle is visualized in Fig. If we denote this power as $P_{2\text{slot}} = 2P_{1\text{slot}}$, it is obvious that the only restriction is that the power scaling coefficients for both slots in the super-symbol must sum up to 2, which gives us $P_{2\text{slot}} = s_f P_{1\text{slot}} + (2-s_f) P_{1\text{slot}}$, where $s_f \in (0,2)$ defines the *power scaling factor*.

Based on this observation we propose a design algorithm for the *NuT constellation alphabets* (Algorithm 7.1). The NuT constellation (NuT $(\mathscr{A}_s; s_f)$) is a 2-source alphabet ($\mathscr{A}_s^A, \mathscr{A}_s^B$), where the power is re-allocated *non-uniformly* among the 2-slots (see Fig. 7.4). Note that NuT $(\mathscr{A}_s; 1)$ constellation is a pure 2-slot extension of a traditional linear modulation constellation with identical hierarchical min-distance properties as the "base" alphabet $\mathscr{A}_s$ (see Fig. 7.1).

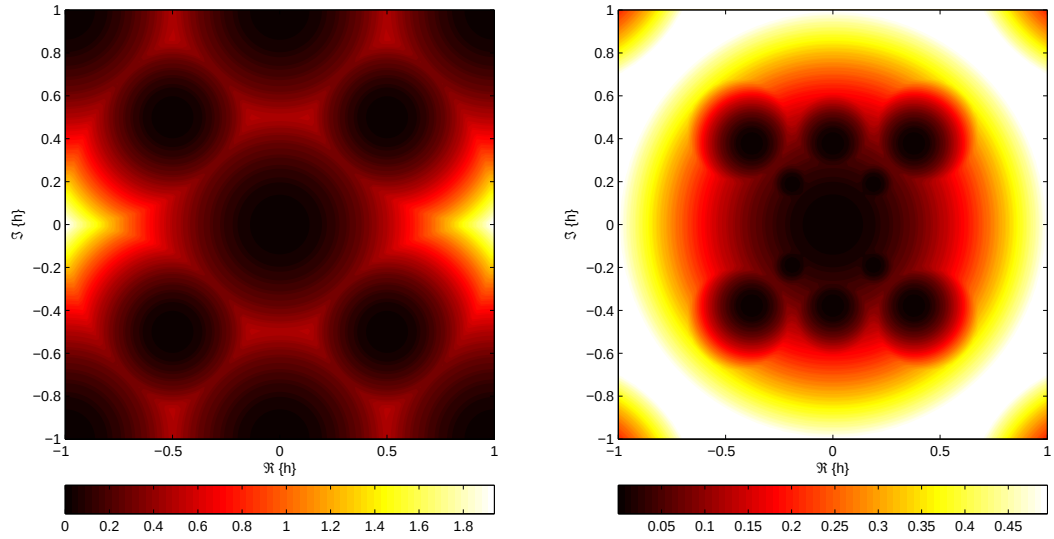

Figure 7.5: MHD $d^2_{\min}(h)$ of NuT$(\text{QPSK};1)$ and NuT$(\text{QPSK};0.25)$ alphabets as a function of channel parameter $h \in \mathbb{C}$.

7.3 Numerical evaluation

In this section we evaluate the performance of some example NuT alphabets. We choose QPSK and 8PSK constellations as the base alphabets $\mathscr{A}_s$ in Algorithm 7.1 and we observe the performance of NuT alphabets for variable values of the power scaling factor s_f. To provide a relevant comparison with the conventional linear modulation schemes, we always compare the proposed NuT alphabets with NuT$(\mathscr{A}_s;1)$ constellation. Note again that the NuT$(\mathscr{A}_s;1)$ constellation is a pure 2-slot extension of a traditional linear modulation constellation with identical hierarchical min-distance properties as the "base" alphabet $\mathscr{A}_s$ (see Fig. 7.1).

7.3.1 Minimum hierarchical distance

The hierarchical min-distance $d^2_{\min}(|h|)$ (together with min-distance parabolas set $\mathscr{S}_p$) of the NuT$(\text{QPSK};0.25)$ constellation is depicted in Fig. 7.3. Considering Figs. 7.1, 7.3 it is obvious that the hierarchical minimum distance of NuT$(\text{QPSK};1)$ alphabet is relatively poor for $0.6 \leq |h| \leq 1$, while the NuT$(\text{QPSK};0.25)$ alphabet has this poor min-distance performance “shifted" towards $|h| \leq 0.6$, i.e. towards the less probable values of $|h|$ (compare this with the distribution of $|h|$ in Fig. 7.2). A comparison of the overall MHD $d^2_{\min}(h)$ properties (i.e. as a function of $h \in \mathbb{C}$) for some examples of NuT alphabets is in Figs. 7.5, 7.6.

7.3.2 Symbol error rate

Evaluation of the SER of the proposed NuT alphabets (with variable s_f) is in Figs. 7.7, 7.8. Since the source alphabets $\mathscr{A}^A_s, \mathscr{A}^B_s$ are used only in the MAC phase, we analyze only the SER of Hierarchical (compound) symbols (H-SER) received by the relay. The decoder of the 2-slot alphabets decodes the compound symbols on a per-slot basis (for a better comparison with traditional linear modulation constellations). Rician fading channels h_A, h_B with a Rician factor $K = 10\,\text{dB}$ are assumed. The average SNR is defined as $\frac{1}{2\sigma^2_w}\mathbb{E}\left[|h_A|^2 + |h_B|^2\right]$. For simplicity reasons we do not use error-correcting codes at the relay.

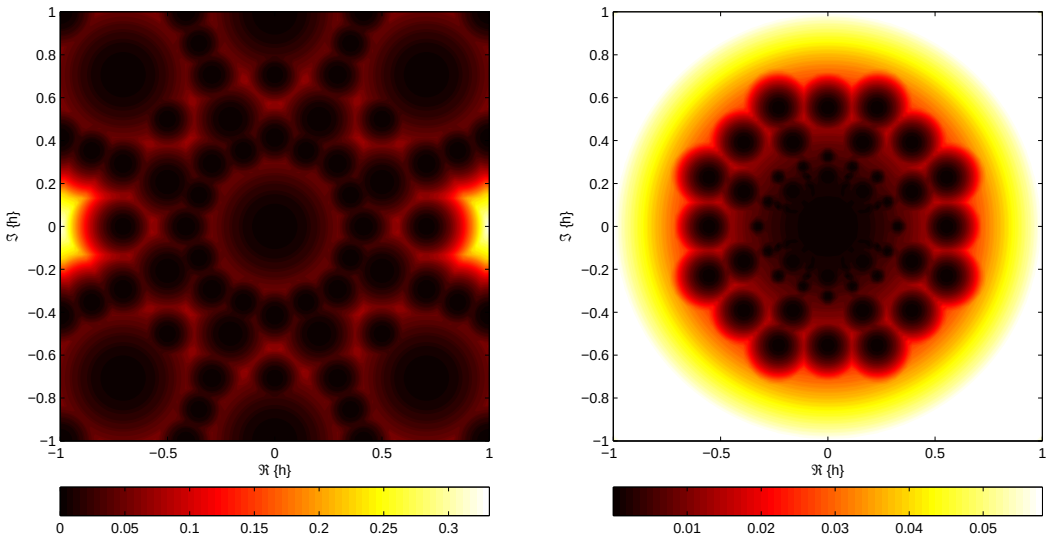

Figure 7.6: MHD $d^2_{\min}(h)$ of NuT$(8\text{PSK};1)$ and NuT$(8\text{PSK};0.1)$ alphabets as a function of channel parameter $h \in \mathbb{C}$.

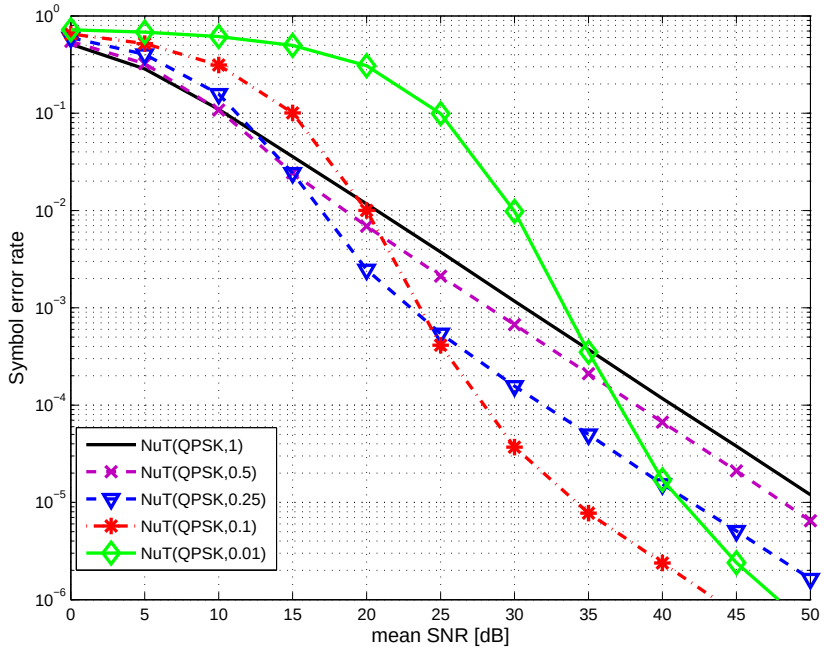

Figure 7.7: H-SER of NuT$(\text{QPSK};1)$ and NuT$\left(\text{QPSK};s_f\right)$ alphabets. It is obvious that a crucial part of the alphabet design (Algorithm 7.1) is a choice of the scaling factor s_f.

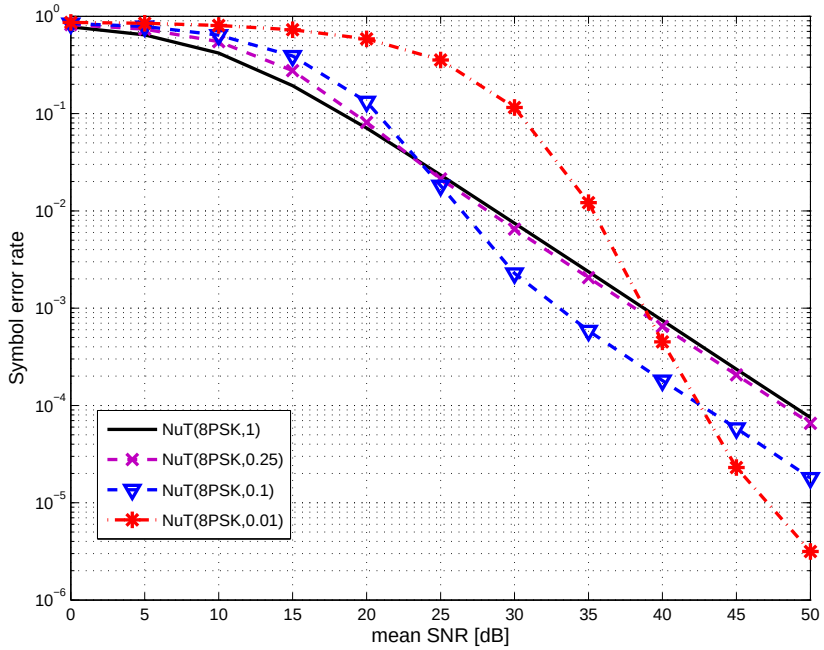

Figure 7.8: H-SER of NuT$(8\text{PSK};1)$ and NuT$\left(8\text{PSK};s_f\right)$ alphabets. It is obvious that the choice of the scaling factor s_f is again a crucial part of the alphabet design (Algorithm 7.1).

Remarkable SNR gains can be observed for the proposed NuT alphabets ($\sim 10-15\,$dB in Fig. 7.7, $\sim 5-7\,$dB in Fig. 7.8) for moderately high SNR. It is important to note that the overall system throughput is not sacrificed, since the cardinality of the NuT alphabet is $\left|\mathscr{A}_s^A\right| = \left|\mathscr{A}_s^B\right| = M_s^2$ for $|\mathscr{A}_s| = M_s$ (see Algorithm 7.1). The promising parametric performance of the proposed 2-slot alphabets is hence not accompanied with a reduction of achievable throughput (inherent for multi-dimensional alphabets).

7.4 Discussion of results

The NuT constellation alphabet design can be generally characterized as an alphabet-diversity technique regarding the hierarchical min-distance. A suitable selection of the scaling factor s_f (in Algorithm 7.1) is evidently critical for alphabet performance, since it allows to *trade-off the vulnerability to eXclusive law failures with the alphabet distance properties*, resulting in an improved performance in the medium to high SNR region. As it is obvious from Figs. 7.7, 7.8, it is not appropriate to purely allocate most of the available source power to a one slot of the 2-slot alphabet ($s_f \ll 0.1$ for $\mathscr{A}_s = \text{QPSK}$), since H-SER performance of such alphabet will be poor (even for a reasonably high SNR).

Part III

WNC processing with imperfect/partial HSI

Chapter 8

Introduction

"Science may set limits to knowledge, but should not set limits to imagination."

Bertrand Russell

As noted in Section 3.2.2, all specific aspects of wireless channels must be properly taken into consideration to efficiently utilize their favourable properties in WNC-based systems. The *inherent broadcast property* of wireless channels allows that each source transmission can be overheard by several nodes in its vicinity, however, it cannot guarantee that all these nodes are facing a channel of sufficient capacity, i.e. that all these nodes are able to perfectly decode the overheard source information. The importance of this phenomenon is even more emphasized in multi-node wireless networks, where a successful decoding of some specific *overheard information* can be required to retrieve the desired data at a given destination. A particular example of this event can be demonstrated in WBN (see Fig. 8.1), where each destination can overhear the “unintended" source transmission (HSI) to enable WNC processing at the relay. Unfortunately, a conventional WNC processing (similar to that in 2-WRC) can be employed in WBN only if the HSI channels have sufficient capacity (allowing a perfect decoding of overheard source information). Whenever the channel conditions on HSI link(s) are not favourable, only *limited (partial/imperfect) HSI* can be received at destinations, thus requiring an appropriate modification of relay and destination processing [24, 96, 97].

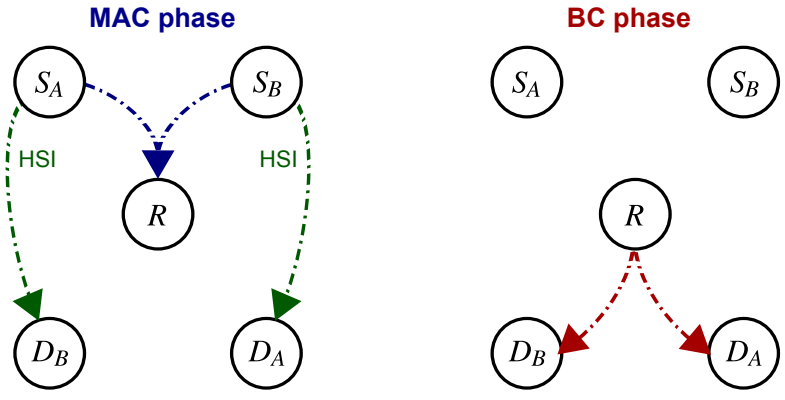

Figure 8.1: HDF signal flow in Wireless Butterfly Network.

8.1 Summary of contributions

In this part of the thesis we overview our contribution to the research of *partial/imperfect HSI processing* in WNC networks. A Superposition Coding (SC) based scheme for relaying in WBN is introduced in [26, 27]. This SC-based scheme is capable to adapt to arbitrary amount of HSI and hence it provides a natural information theoretic tool for the implementation of HDF strategy in WBN. The basic principles of SC-based relaying are summarized in Chapter 9.

A general analysis of *maximal sum-rates* of various WNC strategies in WBN is presented in [19], where the conventional bi-directional 3-step (DF) and 2-step (AF, JDF and HDF) WNC strategies are modified to guarantee that successful decoding at destinations is made possible even if only partial HSI is available. This *partial HSI processing* usually provides a better sum-rate than the straightforward solution, where the availability of perfect HSI is secured by a decrease of the source transmission rate. The analysis of maximal sum-rates of WNC strategies with general imperfect HSI is restated in Chapter 10.

One of the crucial steps in the design of particular HDF processing for partial HSI systems is the choice of a suitable eXclusive mapping operation at the relay. As noted in [23, 24], the unreliable transmission of HSI can be overcome by increasing the cardinality of the relay output [71]. A design of eXclusive mapping operation is quite simple for the *minimal mapping* (perfect HSI assumption) operation, where it is usually given by a simple bit-wise xor operation. However, in case of the *extended cardinality mapping* (see Fig. 3.10), a suitable eXclusive mapper must respect the amount of HSI at destinations to maximize the system throughput. A systematic approach to the design of a *set of eXclusive relay output mappers* for WBN is introduced in Chapter 11.

Since 2-WRC can be viewed as the perfect HSI equivalent of WBN, the promising parametric channel performance of *NuT source alphabets* (see Chapter 7) can be likewise efficiently exploited in the WBN systems [17]. While this favourable parametric MAC channel performance of NuT alphabets induces a *lower error floor* in both minimal and extended cardinality relaying, the increased reliability of *partial one-slot HSI* transforms into an *additional SNR gain* in the extended cardinality case, where the worse aggregate HSI performance is compensated by an increased cardinality of the relay output alphabet. The promising performance of NuT constellations in WBN is discussed in Chapter 12.

8.2 System model

The parametric WBN (Fig. 8.1) contains five physically separated nodes (sources S_A, S_B, destinations D_A, D_B and relay R). Since A, B are not in a radio visibility (direct link is missing), a support of a common shared relay node R is required. The transmission from each source can be overheard by the "unintended" destination as HSI. A wireless system is considered, and hence all transmitted and received symbols are signal space symbols. Channels are modeled as linear frequency flat with AWGN and all nodes are half-duplex (one node cannot simultaneously receive and transmit). The nodes operate with synchronized symbol timing and CSE is available only at the receiving nodes (unless stated otherwise). Due to the relay half-duplex constraint each communication round can be again divided into the MAC and BC phase (Fig. 8.1) with potentially uneven lengths (unless stated otherwise).

8.2.1 MAC phase – source nodes transmission

In the MAC phase sources S_A, S_B simultaneously transmit their messages (data words) $\mathbf{d}_A$,$\mathbf{d}_B$ to the relay R. Due to the broadcast property of wireless transmission, the transmitted signal is overheard at destinations D_A, D_B. If a channel coding (error-correction) is employed in the system, the sources encode their data messages prior to the transmission to obtain the codewords $\mathbf{c}_A = \mathscr{C}^A(\mathbf{d}_A)$, $\mathbf{c}_B = \mathscr{C}^B(\mathbf{d}_B)$, where $\mathscr{C}^i$, $i \in \{A, B\}$ is the channel coding operation. A signal space representation (with an *orthonormal* basis)

of the $n-$th transmitted channel symbol[28] is $s_A(c_A)$, $s_B(c_B)$ ($s_i \in \mathscr{A}_s^i \subset \mathbb{C}^{N_s}$, $\left|\mathscr{A}_s^i\right| = M_s$), where c_A, c_B are source node code symbols, $\mathscr{A}_s^i(.)$ is the channel symbol memoryless mapper at node $i \in (A,B)$, N_s is the complex dimensionality of channel symbols s_A, s_B and M_s is the source alphabet cardinality.

The n-th constellation space symbol received at R in MAC phase is

$$x = h_{S_AR}s_A + h_{S_BR}s_B + w_R, \tag{8.1}$$

where w_R is the circularly symmetric complex Gaussian noise (variance $\sigma_{w_R}^2$ per complex dimension) and h_{S_AR}, h_{S_BR} are scalar complex channel coefficients (constant during the observation and known at the relay). Sources' transmissions in the MAC phase are overheard by destinations D_A, D_B as HSI:

$$z_B = h_{S_AD_B}s_A + w'_B, \tag{8.2}$$

$$z_A = h_{S_BD_A}s_B + w'_A, \tag{8.3}$$

where w'_i, $i \in \{A,B\}$ is the circularly symmetric complex Gaussian noise (variance $\sigma_{w'_i}^2$ per complex dimension) and $h_{S_AD_B}$, $h_{S_BD_A}$ are scalar complex channel coefficients (constant during the observation and known at the respective destination).

8.2.2 Relay processing

Similarly like in the 2-WRC case, the relay must map its observation (signal space signal $\mathbf{x}$) to a valid output message, which ensures that both destinations are able to decode the desired data from the relay signal and observed (generally imperfect) HSI. A particular implementation of this *eXclusive mapping operation* (sometimes also called as the *Hierarchical Network Code* (HNC) [119]) can have various forms (similarly as in 2-WRC), but note that in WBN it must respect also the amount of HSI, which can be reliably decoded at destinations (from the overheard source signal). The relay operation in WBN system hence can be described again by the following mapping[29] :

$$\mathscr{X}: \quad \mathbf{x}(\mathbf{d}_A, \mathbf{d}_B) \overset{(\mathrm{WNC})}{\longmapsto} \mathbf{s}_R(\mathbf{c}_R) \tag{8.4}$$

Note that standard PHY algorithms (channel coding and modulation) can be implemented at the relay. To simplify the description, all these potential PHY operations are assumed to be encapsulated by the eXclusive mapping operation (8.4).

8.2.3 BC phase and destination decoding

In the simplified description (8.4), the relay eXclusive mapping operation is assumed to produce directly the signal space channel symbols $s_R \in \mathscr{A}_s^R$, which are then broadcast to destinations D_A and D_B in the BC phase. The n-th constellation space symbol received at D_i ($i \in \{A,B\}$) is

$$y_i = h_{RD_i}s_R + w''_i. \tag{8.5}$$

where w''_i, $i \in \{A,B\}$ is the circularly symmetric complex Gaussian noise (variance $\sigma_{w''_i}^2$ per complex dimension) and h_{RD_i} is scalar complex channel coefficient (constant during the observation and known at the respective destination). Assuming that a suitable eXclusive mapping (HNC map) is used by the relay, both destinations are able to decode the desired data from the relay signal and observed (partial) HSI.

[28] We will omit the symbol time variable n from the following expressions to improve the readability.

[29] Note again that in AF the relay output signal $\mathbf{s}_R$ is simply an amplified version of the received analogue signal, i.e. $\mathbf{s}_R = \beta\mathbf{x}$, where β is the AF amplification factor (see e.g. [31]).

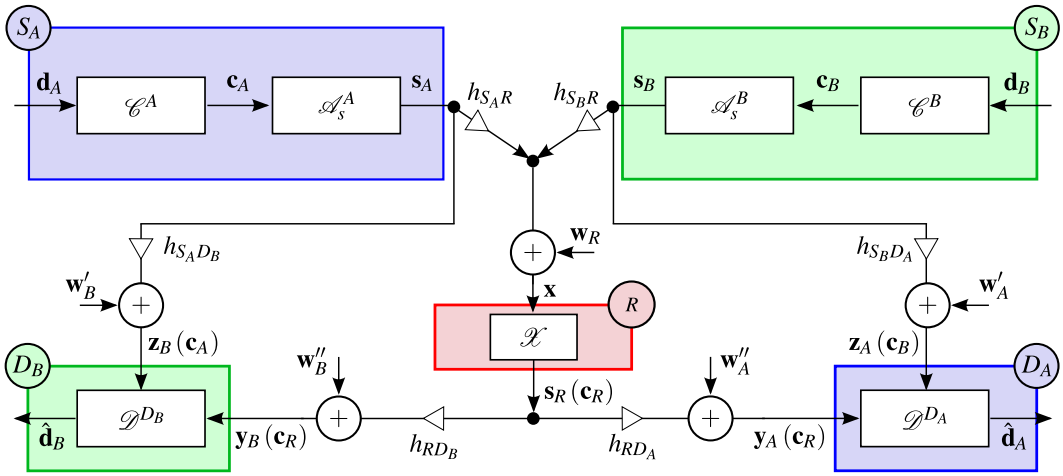

Figure 8.2: Basic principle of WNC processing in WBN.

The complete decoding process at D_A can be simply summarized as an inverse mapping operation which maps the received constellation space signal from the relay ($\mathbf{y}_A$) to the desired data message ($\mathbf{d}_A$), using the overheard data from S_B as (generally) *partial HSI* ($\mathbf{d}'_B$) :

$$\mathscr{D}^{D_A}: \quad \left(\mathbf{y}_A(\mathbf{c}_R), \mathbf{z}_A\left(\mathbf{c}'_B\left(\mathbf{d}'_B\right)\right)\right) \longmapsto \mathbf{c}_A(\mathbf{d}_A), \tag{8.6}$$

and similarly for D_B:

$$\mathscr{D}^{D_B}: \quad \left(\mathbf{y}_B(\mathbf{c}_R), \mathbf{z}_B\left(\mathbf{c}'_A\left(\mathbf{d}'_A\right)\right)\right) \longmapsto \mathbf{c}_B(\mathbf{d}_B). \tag{8.7}$$

As already noted, HSI generally carries only a partial information about the source data in WBN and hence

$$0 \leq \left|\mathbf{d}'_i\right| \leq |\mathbf{d}_i|,$$

where $|\mathbf{d}_i|$ denotes the number of bits in a binary message $\mathbf{d}_i$ (transmitted from source S_i, $i \in \{A,B\}$). Obviously, there are again numerous ways how to implement the decoding operation (8.6), (8.7) in the WBN system, including the most general decoder implementation, where the HSI channel ($\mathbf{z}_i$, $i \in \{A,B\}$) and relay ($\mathbf{y}_i$, $i \in \{A,B\}$) observations are fed directly into a joint decoder. The basic principle of WNC processing in WBN is summarized in Fig. 8.2.

Chapter 9

Superposition coding for wireless butterfly network with partial HSI

"There is nothing in a caterpillar that tells you it's going to be a butterfly."

Richard Buckminster Fuller

9.1 Introduction

An optimal strategy for communication in WBN is to a great extent dependent on the amount of HSI which can be reliably retrieved at both destinations from the overheard source transmission (Fig. 8.1). Considering two special cases (zero & perfect HSI), two (in principle) different kinds of relay processing in WBN can be distinguished:

1. *Zero HSI case:* Destinations are not able to overhear any information from the sources and consequently the relay has to deliver full information to both destinations on its own. Note that network coding-based operations are not allowed due to the lack of HSI and hence both separate data streams must be fully decoded by the relay prior to transmission. The only one constraint for the design of WBN processing for this case is hence given by the convex MAC capacity region [6], which gives the upper-bound for the maximum transmission rates from both sources.

2. *Perfect/full HSI case:* Destinations can decode perfectly the information overheard from the source broadcast, making this case virtually equivalent to the 2-WRC scenario. Consequently, the relay can fully utilize the WNC principles to deliver the information to both destinations. Note that similarly as in the 2-WRC scenario, full decoding of both separate data streams is not required. The design of WBN processing for this case must guarantee full decodability of overheard source signal at both destinations, while the relay processing is no longer limited by the MAC capacity region (see e.g. [10, 65, 71]).

By observing these two special HSI cases, we are one step closer to derive a suitable strategy for WBN relaying. Obviously, the optimal WBN processing could be adapted to any available amount of HSI by a suitable combination of the two principles mentioned above. By splitting the source information into the two separate data streams, we should be able to utilize the available (partial) HSI to exploit all the WNC-related benefits (see e.g. [10]) for the first stream, while the information carried by the second stream has to be fully decoded by the relay and then separately delivered to both destinations (see Fig. 9.1).

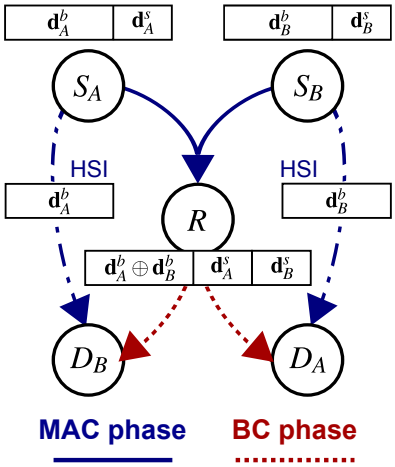

Figure 9.1: Principle of SC-based relaying in WBN.

In this chapter we show that *SC* [6] provides a natural tool for implementation of WBN relaying under an arbitrary HSI assumption. By splitting the source information into two separate data streams (and optimization of rate and power allocated to each particular stream) it is possible to adapt the WBN processing to actual channel conditions (and hence the available HSI at destinations). Under this optimization, SC represents a viable solution for the case where only *partial HSI* is available at both destinations and moreover, it is feasible also for the *zero* and *perfect HSI* cases.

9.1.1 Definitions and modification of system model

Complex channel coefficients of source-relay (h_{S_AR}, h_{S_BR}), source-destination (i.e. HSI – $h_{S_AD_B}$, $h_{S_BD_A}$) and relay-destination links (h_{RS_A}, h_{RS_B}) are assumed to be constant during the observation and perfectly known by all nodes. This enable to adapt the transmission rates of all nodes (allowing an unequal duration of MAC and BC steps) to the actual channel conditions and thus to optimize the rates of basic and superposed messages. Transmitted symbols from all nodes are zero-mean with a power normalized to unity. Consequently, SNR of a particular link can be defined as:

$$\gamma_{ij} = \frac{|h_{ij}|^2}{N_0} \qquad i,j \in \{S_A, S_B, D_A, D_B, R\}\,, \tag{9.1}$$

where N_0 is the variance of the complex additive Gaussian noise ($\mathscr{CN}(0,N_0)$) at the receiving node. Similarly as in [31, 120] we assume that all channels have bandwidth normalized[30] to 1 Hz and hence a rate up to

$$C(\gamma) = \log_2(1+\gamma)\ [\text{bit/s}] \tag{9.2}$$

can be reliably sent through a channel with SNR γ. For the sake of simplicity we assume a symmetric WBN and hence the particular channel SNRs can be summarized as:

$$\begin{array}{rcl} \gamma_{S_AR} = \gamma_{S_BR} & = & \gamma_1, \\ \gamma_{S_AD_B} = \gamma_{S_BD_A} & = & \gamma_2, \\ \gamma_{RD_A} = \gamma_{RD_B} & = & \gamma_3, \end{array} \tag{9.3}$$

[30] The bandwidth normalization allows to express the rates in bits/s [31]. Moreover, it makes also the the terms “rate" and “spectral efficiency" equivalent [120].

Similarly as in [31] we assume that the time is measured in the number of symbols, such that when a packet of N symbols is sent at a rate r, it contains Nr bits. Packet lengths are assumed to be sufficiently large, such that we can use codebooks that offer zero errors if $r \leq C$ (C is the channel capacity). The duration of the MAC phase will be without loss of generality fixed to N_{MAC} symbols. We define the two-way rate in WBN as the total sum of information exchanged between source-destination pairs S_A, D_A and S_B, D_B during one communication round (MAC and BC phase):

Definition 19. *(Two-way rate):* Source S_A (respectively S_B) transmits a packet with the rate R_A (respectively R_B) in the MAC phase. If each destination D_i is able to reliably decode the packet sent from its intended source S_i ($i \in \{A,B\}$) using only the signal received from the relay and signal overheard as HSI, the two-way rate can be defined as:

$$R_{2\mathrm{way}} = \frac{N_{\mathrm{MAC}}\,(R_A + R_B)}{N_{\mathrm{MAC}} + N_{\mathrm{BC}}} \quad [\mathrm{bit/s}]\,, \tag{9.4}$$

where N_{MAC} (respectively N_{BC}) is the length of MAC (respectively BC) phase in symbols. Note that N_{BC} is generally a function of $R_A, R_B, N_{\mathrm{MAC}}$ and γ_3.

9.2 Superposition coding in wireless butterfly network

Source messages $\mathbf{d}_A$, $\mathbf{d}_B$ are divided into basic ($\mathbf{d}_A^b$, $\mathbf{d}_B^b$) and superposed ($\mathbf{d}_A^s$, $\mathbf{d}_B^s$) messages. Only the basic messages are decoded by destinations as HSI (superposed messages cannot be decoded), while the relay needs to decode only some function of the basic messages (e.g. bit-wise XOR - denoted as $\oplus$ in Fig. 9.1). Since there is no additional HSI at destinations, the remaining superposed messages must be individually decoded and broadcast separately by the relay. Note that the perfect HSI case corresponds to a situation where source signals contain only basic messages, while in the zero HSI case source signals comprise solely superposed messages.

9.2.1 SC relaying scheme

We assume that each source S_i, $i \in \{A,B\}$ broadcasts the following signal in the MAC phase:

$$s_i[m] = \sqrt{1-\alpha_i}\, s_i^b[m] + \sqrt{\alpha_i}\, s_i^s[m]\,, \tag{9.5}$$

where $s_i^b[m]$ (respectively $s_i^s[m]$) is the m-th signal space symbol of the basic (respectively superposed) message transmitted from node i, and $0 \leq \alpha_i \leq 1$ is the SC power-division parameter. In the following discussion we omit the time variable m to simplify the notation.

Due to the system symmetry the two-way rate is maximized for symmetric source output rates $R_A = R_B = R$. Consequently, the basic (respectively superposed) messages are sent with identical rate R_b (respectively R_s) from both sources and hence $\alpha_A = \alpha_B = \alpha$. Note that in the following discussion it will be assumed that only basic messages can be decoded by both destinations as HSI.

9.2.1.1 Relay processing

Relay R receives the following signal in the MAC phase:

$$x = h_{S_A R}\left(\sqrt{1-\alpha}\, s_A^b + \sqrt{\alpha}\, s_A^s\right) + h_{S_B R}\left(\sqrt{1-\alpha}\, s_B^b + \sqrt{\alpha}\, s_B^s\right) + w_R, \tag{9.6}$$

where w_R is the complex additive Gaussian noise $\mathscr{CN}(0, N_0)$. Relay performs HDF decoding (see [65, 71] for more details) to decode only some specific function ("hierarchical signal" – e.g. bit-wise

XOR operation) of the basic messages from the received signal (9.6). This hierarchical signal is denoted simply as $\mathbf{d}_A^b \oplus \mathbf{d}_B^b$. Note that individual messages $\mathbf{d}_A^b$, $\mathbf{d}_B^b$ are not separately decoded. After decoding the hierarchical signal, the relay tries to perform Interference Cancellation (IC) to remove the "mixture" of basic messages ($\sqrt{1-\alpha}\left(h_{S_AR}s_A^b + h_{S_BR}s_B^b\right)$) from the received signal[31].

After IC, the relay has the following observation:

$$x_R' = \sqrt{\alpha}\left(h_{S_AR}s_A^s + h_{S_BR}s_B^s\right) + w_R. \tag{9.7}$$

Since there is no additional HSI at destinations (superposed messages cannot be decoded there), the relay must fully decode both individual superposed messages $\mathbf{d}_A^s$, $\mathbf{d}_B^s$.

In the BC phase the relay has to broadcast the following message:

$$\mathbf{d}_R = \begin{bmatrix} \mathbf{d}_A^b \oplus \mathbf{d}_B^b \\ \mathbf{d}_A^s \\ \mathbf{d}_B^s \end{bmatrix}, \tag{9.8}$$

where $\mathbf{d}_A^b \oplus \mathbf{d}_B^b$ is the hierarchical signal. To simplify the analysis, we do not optimize the relay broadcast strategy and hence we assume that all three parts of $\mathbf{d}_R$ in (9.8) are broadcast separately by the relay.

9.2.1.2 Destination processing

We describe the decoding process at destination D_A, decoding at D_B follows identical steps. In the MAC phase, D_A overhears the following signal transmitted by the source S_B:

$$z_A = h_{S_BD_A}\left\{\left(\sqrt{1-\alpha}\right)s_B^b + \sqrt{\alpha}s_B^s\right\} + w_A'. \tag{9.9}$$

Only the basic message $\mathbf{d}_B^b$ is decodable (as HSI) at the destination and hence the signal corresponding to the superposed message ($\mathbf{s}_B^s$) is considered only as an interference. Surprisingly, thanks to the information content of the relay signal (it contains both superposed messages $\mathbf{d}_A^s$, $\mathbf{d}_B^s$) and the symmetry of the system, IC of the superposed message signal $\mathbf{s}_B^s$ from (9.9) can be performed. Consequently, D_A does not perform any decoding after the MAC phase, and only stores the signal (9.9) in its buffer.

In the BC phase D_A decodes the full relay message (9.8) from the received relay signal, and hence it has available the desired superposed message ($\mathbf{d}_A^s$), the superposed message of the unintended source ($\mathbf{d}_B^s$) and the hierarchical basic message ($\mathbf{d}_A^b \oplus \mathbf{d}_B^b$). The superposed message of the unintended source ($\mathbf{d}_B^s$) can be used to generate a local version of $\mathbf{s}_B^s$, and hence IC of this signal from (9.9) can be performed at D_A to obtain the following (interference free) HSI observation:

$$z_A' = h_{S_BD_A}\left(\sqrt{1-\alpha}\right)s_B^b + w_A'. \tag{9.10}$$

The *efficient HSI* ($\mathbf{d}_B^b$) can be then decoded from (9.10) and combined with hierarhical message ($\mathbf{d}_A^b \oplus \mathbf{d}_B^b$) to get the desired basic message $\mathbf{d}_A^b$. This completes the decoding of the full desired message $\mathbf{d}_A = \left[\mathbf{d}_A^b, \mathbf{d}_A^s\right]$ at D_A. The principle of the decoding at both destinations in SC-based WBN is summarized in Fig. 9.2.

[31] The feasibility of such IC should be justified, since constellation space signal ($\sqrt{1-\alpha}\left(h_{S_AR}s_A^b + h_{S_BR}s_B^b\right)$) corresponding to basic messages should be removed from (9.6) after $\mathbf{d}_A^b \oplus \mathbf{d}_B^b$ is decoded. Obviously, this could introduce some constraints on the particular modulation/coding design. For the purpose of this Chapter we assume that perfect IC of the mixture signal can be always performed by the relay. Consequently, the derived two-way rates should be understood as the upper-bounds, conditioned on the possibility of perfect IC of basic messages from the relay observation.

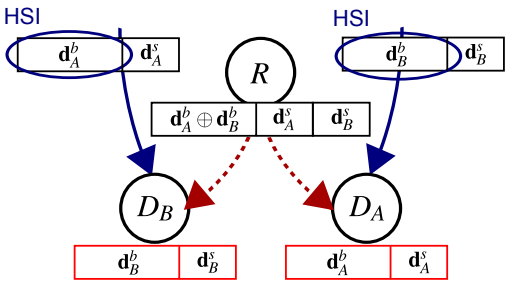

Figure 9.2: Principles of the decoding process in SC-based WBN.

9.2.2 Information-theoretic bounds for SC rates

Apparently, the two-way rate of the proposed scheme depens on the particular choice of parameter α. While conjectures on the optimal value of power division parameter α for the special cases of zero and perfect HSI can be easily drawn (more details will be given later), its value needs to be optimized for the general HSI case.

Lemma 20. *(Bounds for SC-messages rates): Rates of basic (R_b) and superposed messages (R_s) are bounded by:*

$$R_b(\alpha) \leq C\left(\frac{(1-\alpha)\gamma_1}{2\alpha\gamma_1+1}\right) \tag{9.11}$$

$$R_b(\alpha) \leq C((1-\alpha)\gamma_2) \tag{9.12}$$

$$R_s(\alpha) \leq \frac{1}{2}C(2\alpha\gamma_1) \tag{9.13}$$

$$R_b(\alpha)+R_s(\alpha) \leq C(\gamma_1) \tag{9.14}$$

Proof. The first bound for R_b corresponds to the relay decoding of the hierarchical (basic messages) signal from the relay observation (9.6), considering the superposed messages as interference. The second bound for R_b is given by destination decoding of the basic message from the equivalent HSI channel observation (9.10). Rate R_s is bounded by the requirement of full decoding of individual superposed messages from the equivalent relay MAC channel (9.7). It can be easily shown (see e.g. [6]), that the maximal symmetric rate for this equivalent MAC channel with gain $\alpha\gamma_1$ is given by (9.13). The last bound (9.14) is obvious. □

Note that we assume that inequalities in (9.11), (9.14) are not strict. This should be understood only as a conjecture, since the exact proof of achievability of these bounds is still not available (see e.g. [103]). Under the constraints given by Lemma 20, we can easily derive the maximal two-way rate of the SC scheme:

Lemma 21. *(SC-scheme two-way rate): The maximal two-way rate of the SC scheme is given by:*

$$R_{\mathrm{SC}}(\gamma_1,\gamma_2,\gamma_3) \leq \frac{2C(\gamma_3)\left(R_b\left(\alpha_{\mathrm{opt}}\right)+R_s\left(\alpha_{\mathrm{opt}}\right)\right)}{C(\gamma_3)+R_b\left(\alpha_{\mathrm{opt}}\right)+2R_s\left(\alpha_{\mathrm{opt}}\right)}, \tag{9.15}$$

where α_{opt} is the optimal value of SC power division parameter maximizing the two-way rate for a given SNR triplet $\gamma_1,\gamma_2,\gamma_3$.

Proof. Total of $N_{\mathrm{MAC}}(R_A+R_B)=2N_{\mathrm{MAC}}R=2N_{\mathrm{MAC}}(R_b+R_s)$ bits are transmitted from sources in the MAC phase. Since the relay needs to send separately three independent messages (9.8) in the BC phase through the channel with capacity $C(\gamma_3)$, the duration of the BC phase will be at least $N_{\mathrm{BC}}=\frac{R_bN_{\mathrm{MAC}}}{C(\gamma_3)}+\frac{2R_sN_{\mathrm{MAC}}}{C(\gamma_3)}$. Consequently, from (9.4) we have $R_{\mathrm{SC}}\leq\frac{2N_{\mathrm{MAC}}(R_b+R_s)}{N_{\mathrm{MAC}}+N_{BC}}$, which gives us finally (9.15). □

9.2.3 Optimization of SC parameter α

In this section we optimize the value of parameter α to maximize the two-way rate R_{SC} under the constraints given by Lemma 20.

This optimization problem can be rewritten in a compact form as following:

$$\begin{aligned}\underset{\alpha,R_b,R_s}{\text{maximize}} \quad & \frac{2C(\gamma_3)(R_b+R_s)}{C(\gamma_3)+2R_s+R_b}\\ \text{subject to} \quad & R_b\leq C\left(\frac{(1-\alpha)\gamma_1}{2\alpha\gamma_1+1}\right)\\ & R_b\leq C((1-\alpha)\gamma_2)\\ & R_s\leq\frac{1}{2}C(2\alpha\gamma_1)\\ & R_b+R_s\leq C(\gamma_1)\end{aligned}$$

Note that for a fixed α the constraints are linear. Now since $R_b\geq 0$ and $R_s\geq 0$, we can equivalently transfer the maximization of the objective function into the minimization of its inverse. As a result, the objective function can be optimized using Linear Fractional Programming (LFP), which can be transformed into a linear programming [121].

The optimization problem can be thus rewritten equivalantly as

$$\begin{aligned}\underset{\alpha}{\text{minimize}} \quad & f(\alpha)\\ \text{subject to} \quad & 0\leq\alpha\leq 1,\end{aligned}$$

where

$$f(\alpha)=\min_{R_b,R_s}\frac{C(\gamma_3)+2R_s+R_b}{2C(\gamma_3)(R_b+R_s)} \tag{9.16}$$

Hence, the maximal value of the two-way rate R_{SC} can be found by finding the optimal value of parameter α, for which (9.16) is minimized. The minimum of $f(\alpha)$ (under the constraints given by Lemma 20) can be found for a fixed value of α using LFP.

In order to simplify the analysis, we can use LFP to find the optimal SC messages rates R_b, R_s for a fixed α and then perform an exhaustive search to find the optimal value α_{opt} (maximizing the two-way rate). The numerical results of the optimization problem are shown in the next section.

9.2.4 Reference schemes for perfect & zero HSI

Here we introduce the reference scenarios for zero and perfect HSI case and analyze their maximal 2-way rates.

Theorem 22. *(Zero HSI). The maximal two-way rate for WBN with zero HSI at destinations is:*

$$R_{\mathrm{zero}}^{\max}=\frac{C(2\gamma_1)C(\gamma_3)}{C(\gamma_3)+C(2\gamma_1)}. \tag{9.17}$$

Proof. When HSI is unavailable at destinations, the relay must fully decode the received signal in MAC phase. Considering $R_A = R_B = R$, total of $2RN_{\mathrm{MAC}}$ bits are sent by sources in the MAC phase. Maximal R allowing full decoding of both messages is $R \leq \frac{1}{2}C(2\gamma_1)$. In the BC the relay must send separately both decoded messages through a channel with $C(\gamma_3)$ and hence $N_{\mathrm{BC}} = \frac{2N_{\mathrm{MAC}}R}{C(\gamma_3)}$. Under the given assumptions we immediately obtain (9.17) from (9.4) by setting $R = \frac{1}{2}C(2\gamma_1)$. □

Theorem 23. *(Perfect HSI). The maximal two-way rate for the WBN with perfect HSI at destinations is:*

$$R_{\mathrm{perf}}^{\max} = \frac{2C(\gamma_1)C(\gamma_3)}{C(\gamma_3)+C(\gamma_1)}. \tag{9.18}$$

Proof. When perfect HSI is available at destinations, WBN is virtually equivalent to 2-WRC, where $R_A = R_B = R \leq C(\gamma_1)$ (see e.g. [31]). Total of $2RN_{\mathrm{MAC}}$ bits are sent by sources in the MAC phase. In the BC phase the relay sends only the hierarchical (WNC-coded) message of size $N_{\mathrm{MAC}}R$ through a channel with $C(\gamma_3)$ and hence $N_{\mathrm{BC}} = \frac{N_{\mathrm{MAC}}R}{C(\gamma_3)}$. Under the given assumptions we immediately obtain (9.18) from (9.4) by setting $R = C(\gamma_1)$. □

Comparing the rates $R_{\mathrm{zero}}^{\max}$ (9.17) and $R_{\mathrm{perf}}^{\max}$ (9.18) with (9.15), one can easily infer that $R_{\mathrm{SC}} = R_{\mathrm{zero}}^{\max}$ when $\alpha = 1$, $R_b = 0$, $R_s = \frac{1}{2}C(2\gamma_1)$ and $R_{\mathrm{SC}} = R_{\mathrm{perf}}^{\max}$ when $\alpha = 1$ and $R_b = C(\gamma_1)$, $R_s = 0$. As expected, for these special HSI cases the SC scheme reduces to a single message transmission.

9.3 Maximal two-way rates

The rates of basic (R_b) and superposed (R_s) SC-messages maximizing R_{SC} for arbitrary values of $\gamma_1, \gamma_2, \gamma_3$ can be found by optimizing the value of power division parameter α. The maximal 2-way rate of the proposed SC scheme and the optimized values of R_b, R_s are depicted (as a function of γ_2) in Figs. 9.3, 9.4, 9.5, 9.6, 9.7 for various γ_1, γ_3. Maximal rates given by the reference schemes (9.17), (9.18) are also shown in these Figures for a comparison. The optimized parameter α_{opt}, maximal individual source rate $C(\gamma_1)$ and maximal symmetric rate $\frac{1}{2}C(2\gamma_1)$ are also shown. Comparison of the maximal 2-way rates for the complete range of the observed $\gamma_1, \gamma_2, \gamma_3$ is available in Fig. 9.8.

As it is obvious from Figs. 9.3, 9.4, 9.5, 9.6, 9.7, in the low γ_2 region the two-way rate of SC scheme is maximized by allocating all the power to the superposed messages ($\alpha = 1$, $R_b = 0$) and ignoring the weak (unreliable) HSI links. This case is hence equivalent to the zero HSI case. Note that in this region the SC scheme achieves the bound given by (9.17) and the two-way rate does not depend on γ_2. On the other hand, in the high γ_2 region the two-way rate is maximized by allocating all the power to the basic messages ($\alpha = 0$, $R_s = 0$) and thus fully exploiting the favourable quality of HSI links. This case is hence equivalent to the perfect HSI case. Note that in the high γ_2 region the 2-way rate can still depend on γ_2 (e.g. see Fig. 9.7 for $10\,\mathrm{dB} \leq \gamma_2 \leq 30\,\mathrm{dB}$), while the bound given by (9.18) is finally achieved for $\gamma_2 \geq \gamma_1$. The most interesting results have been observed for the partial HSI case (middle γ_2 region). Here the partial available HSI is exploited (by mixing the optimal rates of both SC-messages, i.e. $R_b \neq 0$, $R_s \neq 0$ and $0 < \alpha < 1$) to increase the 2-way rate, and thus to bridge the gap between the zero and perfect HSI cases.

9.4 Discussion of results

The maximal two-way rates of the proposed SC scheme for relaying in WBN under arbitrary HSI assumption is analyzed in this Chapter. Numerical optimization of power division parameter α and SC-messages

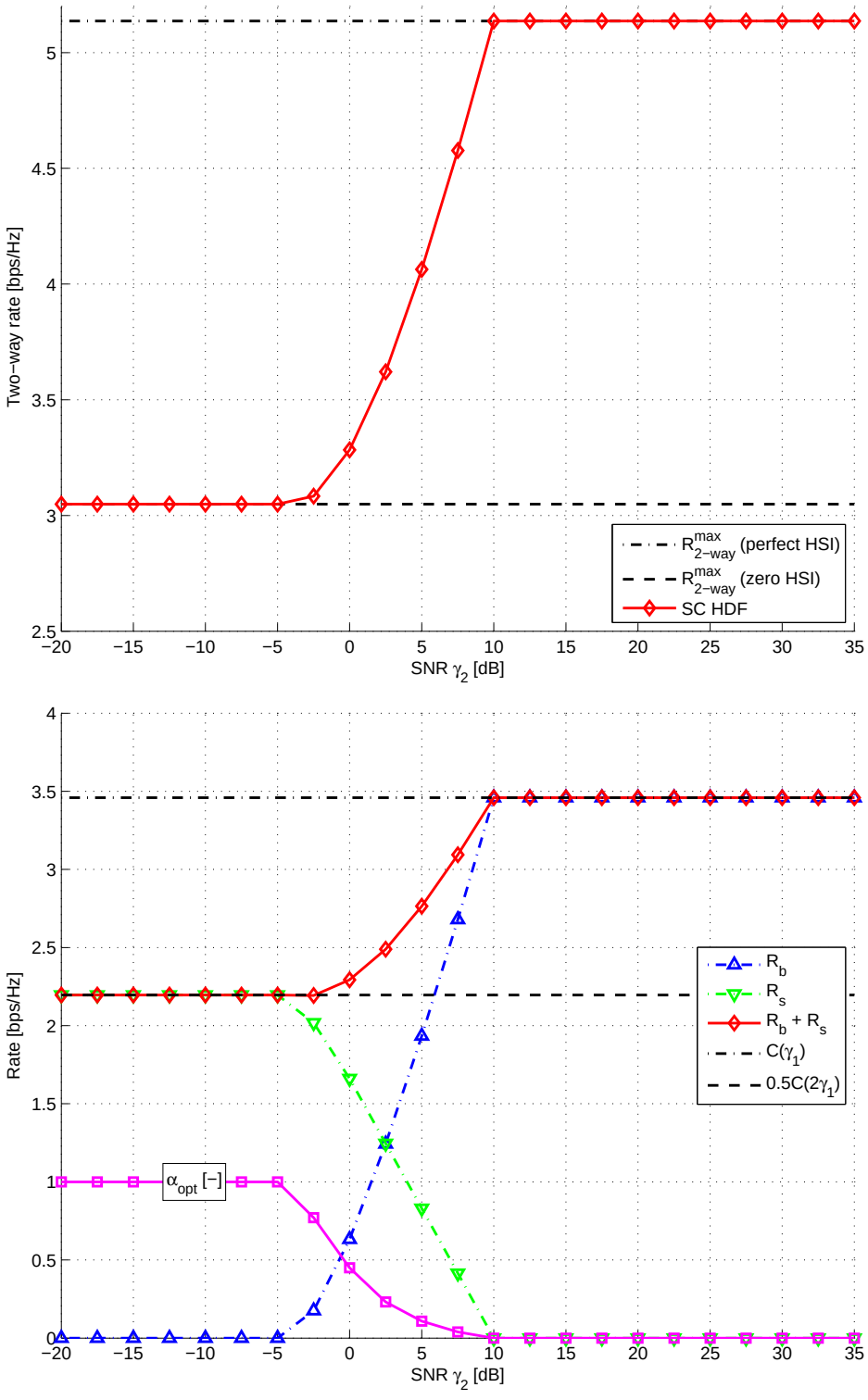

Figure 9.3: Maximal 2-way rate & optimized rates R_b, R_s for the proposed SC scheme ($\gamma_1 = 10$ dB, $\gamma_3 = 30$ dB).

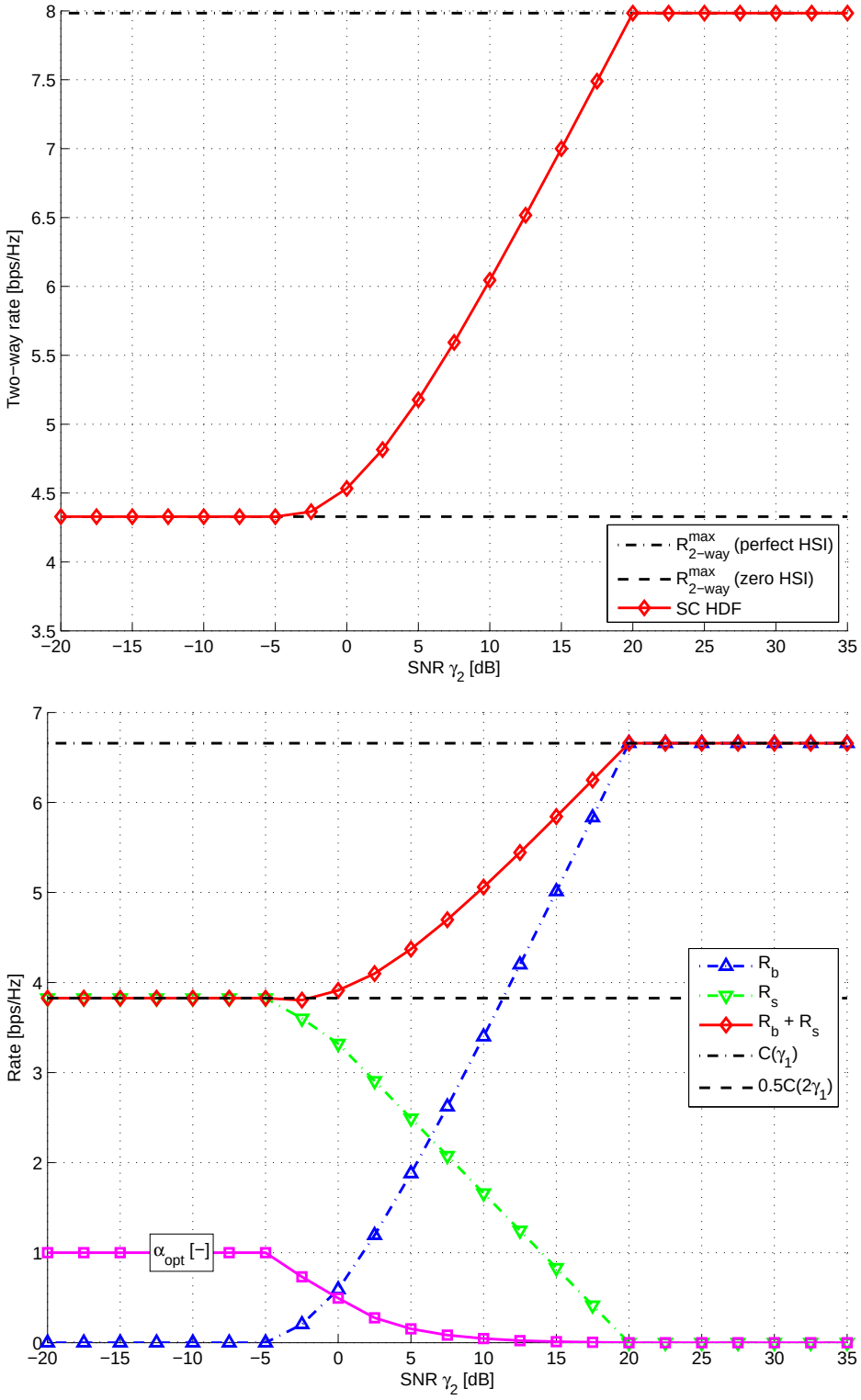

Figure 9.4: Maximal 2-way rate & optimized rates R_b, R_s for the proposed SC scheme ($\gamma_1 = 20$ dB, $\gamma_3 = 30$ dB).

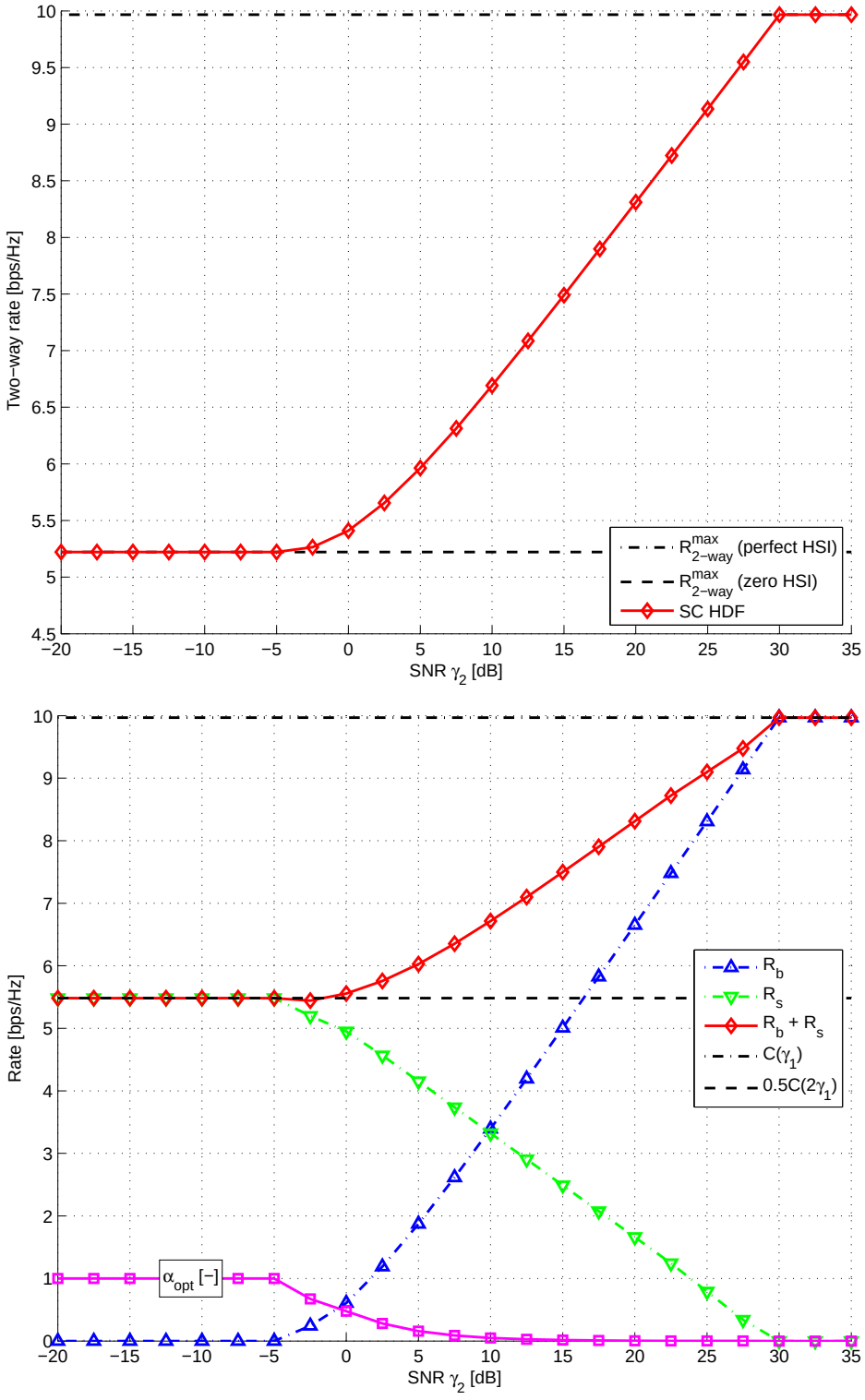

Figure 9.5: Maximal 2-way rate & optimized rates R_b, R_s for the proposed SC scheme ($\gamma_1 = 30$ dB, $\gamma_3 = 30$ dB).

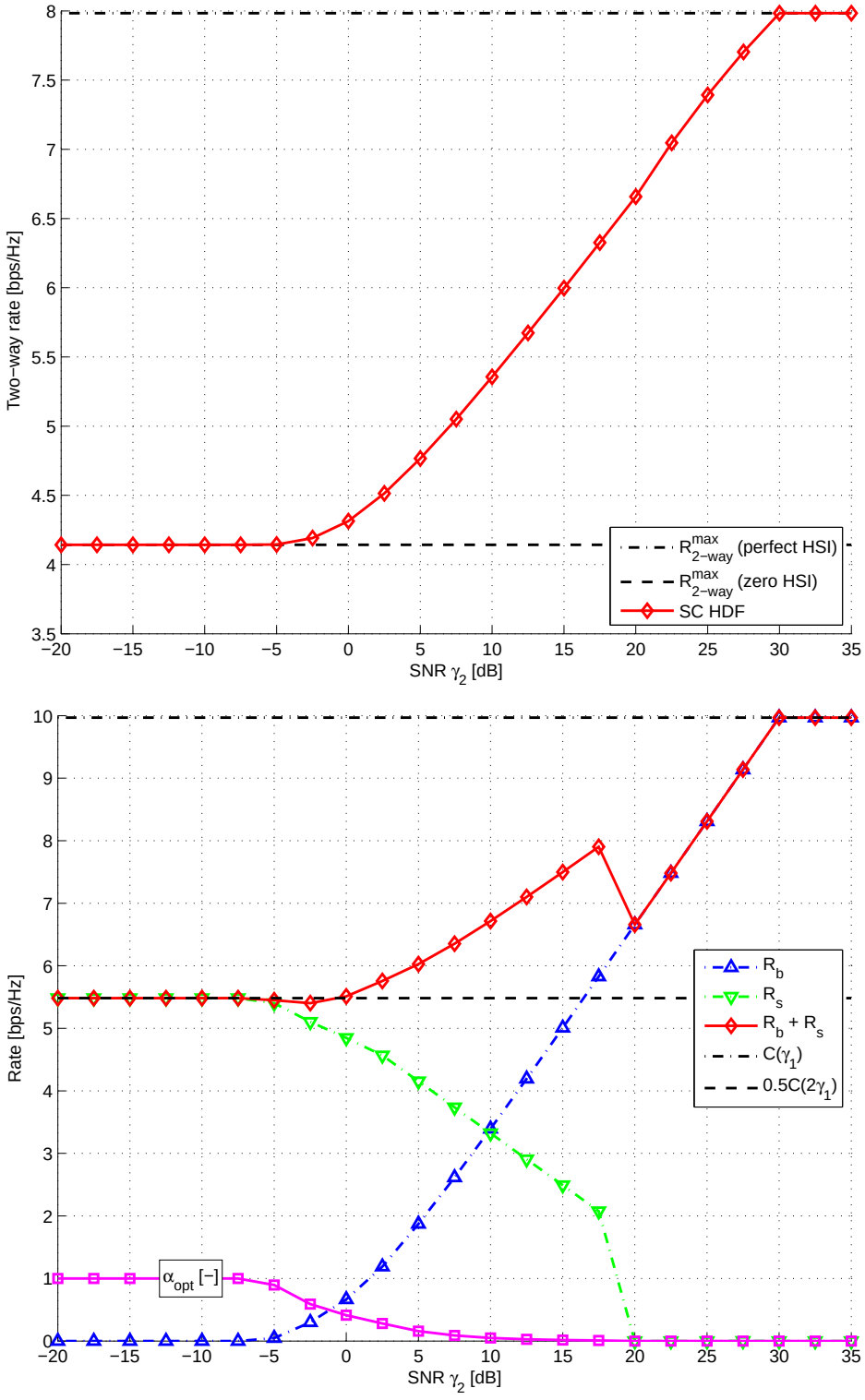

Figure 9.6: Maximal 2-way rate & optimized rates R_b, R_s for the proposed SC scheme ($\gamma_1 = 30$ dB, $\gamma_3 = 20$ dB).

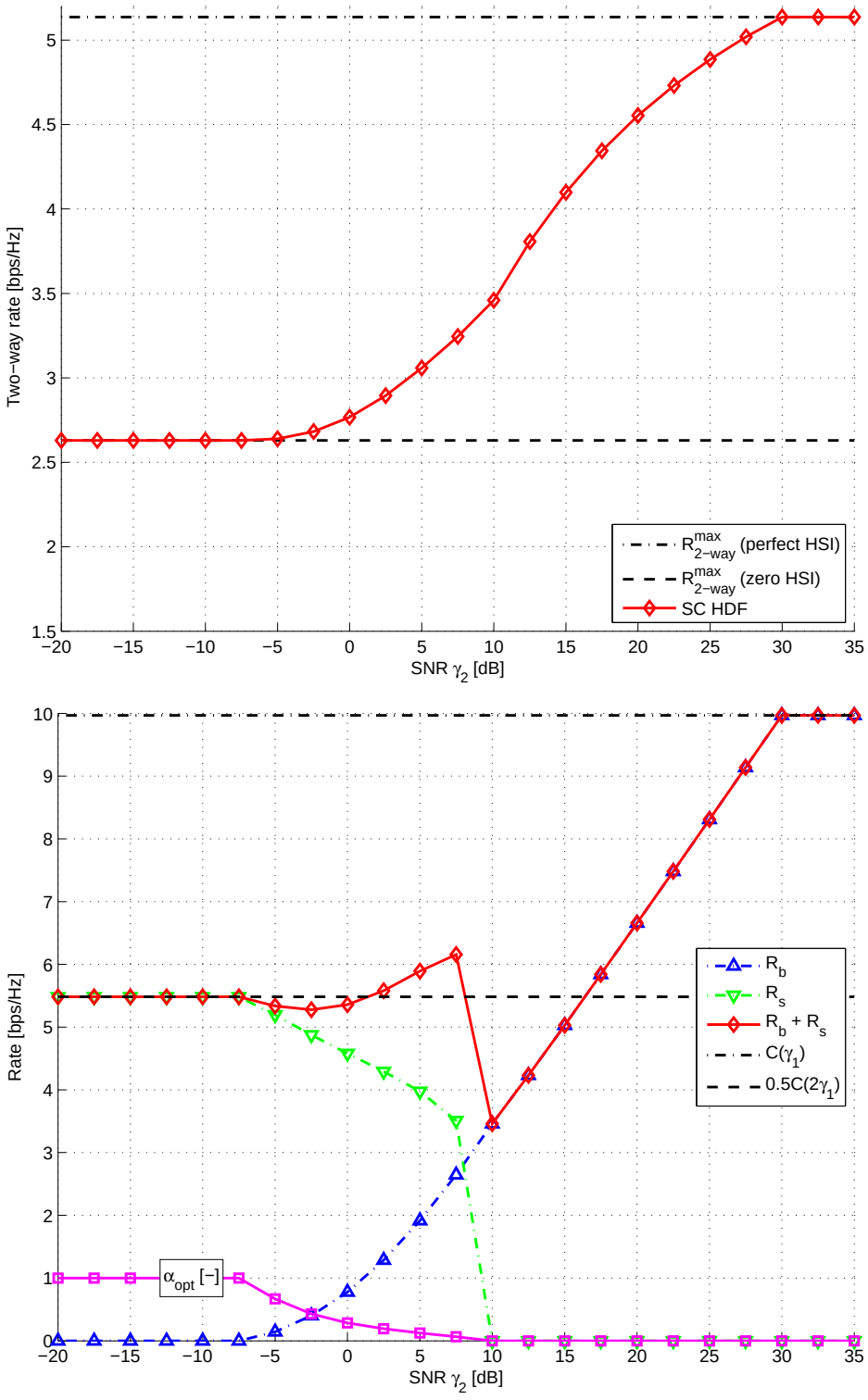

Figure 9.7: Maximal 2-way rate & optimized rates R_b, R_s for the proposed SC scheme ($\gamma_1 = 30$ dB, $\gamma_3 = 10$ dB).

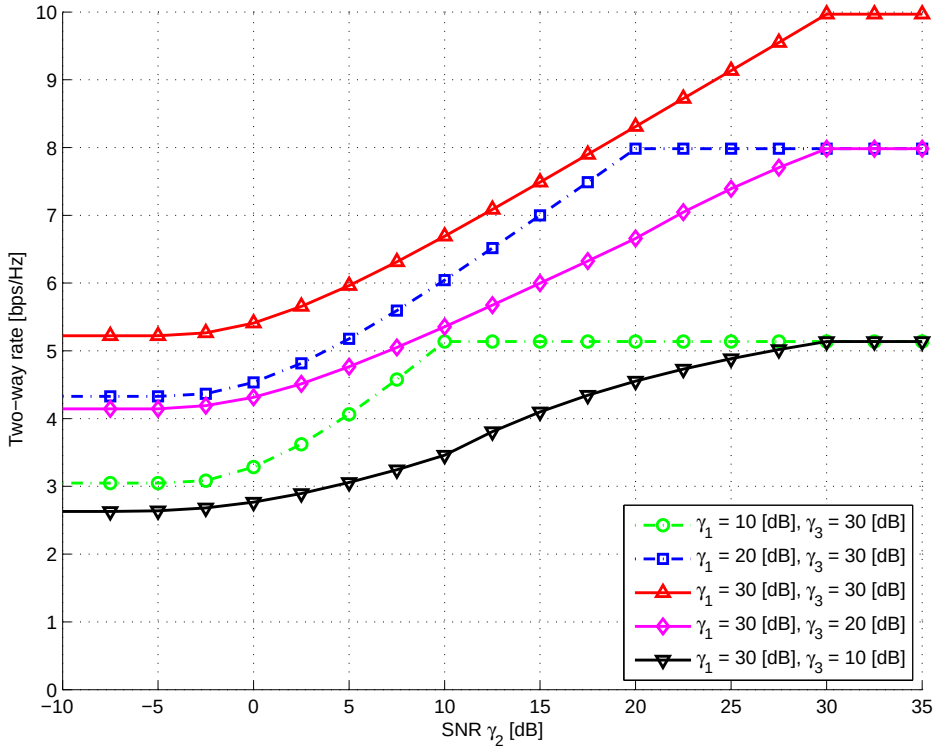

Figure 9.8: Comparison of maximal 2-way rates of the SC scheme.

rates is performed to maximize the two-way rate. The proposed SC scheme achieves the maximal 2-way rates defined in the reference schemes (zero and perfect HSI), and moreover, it is able to adapt its performance to actual SNR conditions and thus utilize even the partially available HSI.

As expected, when only partial HSI is available at destinations, the proposed SC scheme can adapt to the situation by a suitable mixing of the basic and superposed messages, and thereby increase the 2-way rate in the given SNR region. Surprisingly, for some specific SNR values (e.g. check Fig. 9.7 for $5\,\text{dB} \leq \gamma_2 \leq 15\,\text{dB}$) the 2-way rate can be improved by completly removing the transmission of superposed messages ($R_s = 0$), even if this results in a significant decrease of the total source transmission rate ($R_b + R_s$).

Chapter 10

WNC in wireless butterfly network: Maximal sum-rate analysis

"People cannot foresee the future well enough to predict what's going to develop from basic research. If we only did applied research, we would still be making better spears."

George Smoot

10.1 Introduction

In this Chapter we analyse the impact of limited HSI on various state-of-the-art relaying strategies in WBN and determine the maximal sum-rate performance as a function of the quality of HSI channels. Based on the results of this information-theoretic investigation, a modified version of SC-based scheme from [27] (see Chapter 9) is also introduced. We show that the *modified SC-based scheme* is also capable to adapt to arbitrary amount of available HSI, without requiring the implementation of challenging IC of hierarchical signal at the relay (more details will be given later).

The rest of this Chapter is organized as follows. First, we briefly summarize the system model and all the required definitions and assumptions in Section 10.2. Then, an overview of relaying strategies, including a comparison of their performance in WBN is provided in Section 10.3. SC-based relaying scheme is finally introduced in Section 10.4, together with a numerical optimization of its performance.

10.2 Symmetric wireless butterfly network

For simplicity reasons the symmetric WBN is analyzed in this Chapter (see Fig. 10.1). Sources S_A, S_B transmit their data to the relay R in step I. Due to the inherent broadcast nature of wireless channels, transmission of source S_A (respectively S_B) is overheard by its "unintended" destination D_B (respectively D_A). Generally only limited HSI can be gathered from this observation at destinations[32]. The relay node processes the received signal and broadcasts the output signal to both destinations D_A, D_B in step II. A particular relay processing (and the corresponding form of relay output signal) depends on a particular WNC strategy (more details will be provided in the following sections). Since the relay output signal contains always some specific function of source signals (a particular form of this function is given by the

[32] Note that the 2-WRC system where nodes have finite (limited) buffer size for previously sent messages can be also described by this model. There only a part of the previously sent message can be stored in the node's buffer, calling likewise for a modified WNC processing.

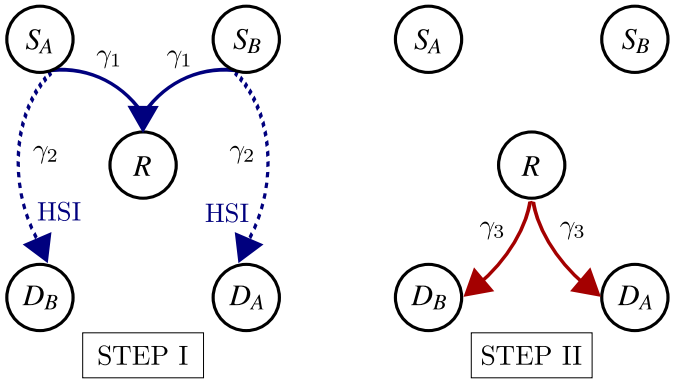

Figure 10.1: Half-duplex communication in symmetric WBN.

specific WNC strategy), the relay output signal is sometimes called generally as the *hierarchical signal* (see e.g. [122]). Destinations D_A, D_B decode the desired information from the hierarchical signal, using HSI overheard in step I as SI.

10.2.1 Definitions and assumptions

A signal space representation of the signal transmitted from node K and observed at node L is:

$$y_L[m] = h_{KL}s_K[m] + w_L[m], \tag{10.1}$$

where $s_K[m]$ denotes the m-th complex constellation symbol from node K to node L, h_{KL} is the complex channel coefficient on link KL and $w[m]$ is the complex additive Gaussian noise $\mathscr{CN}(0,N_0)$. Complex valued vector will be denoted by $\mathbf{x}$. Complex channel coefficients of source-relay (h_{S_AR}, h_{S_BR}), source-destination (i.e. HSI – $h_{S_AD_B}$, $h_{S_BD_A}$) and relay-destination links (h_{RS_A}, h_{RS_B}) are assumed to be constant during the observation and perfectly known by all nodes. This assumption allows us to adapt the transmission rates of all nodes (allowing an unequal duration of steps I, II) to the actual channel conditions and thus evaluate the maximum sum-rate performance of all the analysed WNC strategies.

Transmitted symbols from all nodes are zero-mean with a power normalized to unity. Consequently, Signal-to-Noise Ratio (SNR) of a particular link can be defined as:

$$\gamma_{ij} = \frac{|h_{ij}|^2}{N_0} \qquad i,j \in \{S_A,S_B,D_A,D_B,R\}. \tag{10.2}$$

For simplicity reasons a symmetric WBN is assumed in this Chapter. Hence, the channel SNRs can be summarized as (see also Fig. 10.1):

$$\begin{array}{rclcl} \gamma_{S_AR} & = & \gamma_{S_BR} & = & \gamma_1, \\ \gamma_{S_AD_B} & = & \gamma_{S_BD_A} & = & \gamma_2, \\ \gamma_{RD_A} & = & \gamma_{RD_B} & = & \gamma_3, \end{array} \tag{10.3}$$

10.2.2 Sum-rate performance

We extend the results of the WNC performance investigation presented in [31] to the case with limited HSI at destinations. Similarly as in the previous Chapter we assume that all channels have bandwidth normalized[33)] to 1 Hz and hence a rate up to $C(\gamma) = \log_2(1+\gamma)$ [bit/s] can be reliably sent through a

[33)] Note again that this bandwidth normalization allows to express the rates in bits/s [31] and it makes also the the terms “rate" and “spectral efficiency" equivalent [120].

channel with SNR γ. Time can be expressed in a number of symbols and hence Nr bits are transmitted when N symbols are sent with a rate equal to r. We assume that codewords are sufficiently long, securing a zero error probability for the rates below the channel capacity (i.e. if $r \leq C$).

We evaluate the sum-rate (equivalent to the 2-way rate in 2-WRC) to compare the performance of various WNC relaying schemes in WBN with limited HSI. The sum-rate can be defined as the total sum of bits successfully transmitted between the intended source-destination pairs ($S_A \rightarrow D_A$, $S_B \rightarrow D_B$) during one communication round (step I & step II):

Definition 24. *(Sum-rate):* One communication round comprises step I (length N_I symbols) and step II (length N_{II} symbols). In step I, sources S_A,S_B transmit their messages $\mathbf{d}_A$,$\mathbf{d}_B$ to the relay. If destination D_A (respectively D_B) can reliably decode the desired message $\mathbf{d}_A$ (respectively $\mathbf{d}_B$) from source S_A (respectively S_B) using only HSI (overheard during step I) and the relay message $\mathbf{d}_R$ (received during step II), the sum-rate can be defined as:

$$R_{\text{sum}} = \frac{|\mathbf{d}_A| + |\mathbf{d}_B|}{N_I + N_{II}}, \tag{10.4}$$

where $|\mathbf{d}|$ denotes the number of bits in a binary message $\mathbf{d}$.

10.3 Relaying strategies in WBN with limited HSI

The main goal of this Chapter is the analysis of the impact of limited HSI on the performance of state-of-the-art WNC strategies. In particular, we analyse the *Amplify & Forward* (AF), *Joint Decode & Forward* (JDF) and *Hierarchical Decode & Forward* (HDF) strategies (see [12, 13, 31, 65, 70, 71, 73, 79] and references therein for 2-WRC implementation of these strategies). Apart of these 2-step strategies, we also analyse the 3-step *Decode & Forward* (DF) strategy [31], where step I (Fig. 10.1) is time-shared by both sources (orthogonal source transmissions).

Due to the system symmetry (see Fig. 10.1) the maximum sum-rate can be achieved when both sources transmit at the same rate, i.e. when $r_A = r_B = r$ and hence (10.4) can be rewritten for 2-step strategies (AF, JDF, HDF) as

$$R_{\text{sum}}^{\text{2step}} = \frac{N_I\,(r_A + r_B)}{N_I + N_{II}} = \frac{2rN_I}{N_I + N_{II}} \tag{10.5}$$

and similarly as

$$R_{\text{sum}}^{\text{3step}} = \frac{\frac{1}{2}N_I\,(r_A + r_B)}{N_I + N_{II}} = \frac{rN_I}{N_I + N_{II}}, \tag{10.6}$$

for the 3-step strategy (DF), where equal time-sharing of step I is applied[34]. Note that N_{II}, i.e. the length of step II generally depends on the length of step I (N_I), source rates (r), channel SNRs (γ_1, γ_2, γ_3) and also on the employed WNC strategy. Hence, the choice of source rate r in step I is a key factor for maximizing the sum-rates in all the analysed WNC strategies.

In the following analysis we assume (without loss of generality) that the total length of step I is always kept fixed to N_I symbols in all the relaying strategies, while step II is allowed to have variable length[35]. For the sake of our analysis we also assume that the relay is aware about the information content of the HSI available at destinations after step I. Although this could be viewed as a relatively strong assumption, we will show later that some coding strategies (e.g. *SC* [6]) can naturally guarantee this. To further simplify (and clarify) the analysis, we assume that each destination performs a hard decision on the HSI

[34] In the 3-step DF scheme both sources equally share the available time resources in an orthogonal way and hence each source transmits $\frac{1}{2}N_I$ symbols.

[35] Note that in AF the relay only retransmits each received symbol [70] and hence both steps have always equal length, i.e. $N_I = N_{II}$.

prior to the processing of relay signal. Even though such processing could be sub-optimal, it still allows a fair comparison of WNC relaying strategies in a *limited-HSI network*[36].

10.3.1 WBN with perfect and partial HSI

Before proceeding to the sum-rate analysis we classify the WBN processing according to the amount of available HSI. Since HSI is some specific portion of source information which can be overheard by destinations on the channel with SNR γ_2 (Fig. 10.1), its effective amount depends on the mutual relation between the source rate r and HSI channel capacity $C(\gamma_2)$. Hence, as shown in Tables 10.1, 10.2, the WBN system can be classified into *perfect and partial HSI* cases[37].

It is apparent that the system can be always forced to operate in the perfect HSI region, if the source rates are kept bounded below the HSI channel capacity (i.e. if $r \leq C(\gamma_2)$). However, it can be shown that such approach is usually only sub-optimal (especially in the low γ_2 region) and superior sum-rate performance can be achieved if $r > C(\gamma_2)$ and partial HSI processing is allowed. The particular node operations in both perfect and partial HSI regions are summarized in Table 10.1 for DF and in Table 10.2 for JDF and HDF relaying schemes[38]. Note that the HSI channels become completely unreliable for $C(\gamma_2) \to 0$ and hence separate individual source messages must be decoded and broadcast by the relay (in all DF, JDF and HDF strategies), making the WBN processing equivalent to the conventional routing approach (see Tables 10.1, 10.2 for $C(\gamma_2) = 0$).

In the following sections we derive the maximal sum-rates rates of particular relaying strategies in WBN. Note that since we have defined some operational restrictions to the applied WNC schemes, the provided sum-rates are not the absolute capacities of the WBN. Similarly as in [31] we also do not optimize the relay broadcast strategy.

10.3.2 3-step scheme

Sources S_A, S_B equally share the available time in step I of the 3-step scheme, resulting in two orthogonal source-relay channels ($S_A \to R$, $S_B \to R$). Source signals do not mutually interfere and hence the relay is able to decode both individual source massages if a suitable transmission rate r is set at both sources. The relaying strategy where such separate decoding of orthogonal source transmissions is performed is usually called DF [31].

10.3.2.1 Decode & Forward

The individual source messages $\mathbf{d}_A, \mathbf{d}_B$ are always decoded by the relay (from orthogonal observations), regardless of the amount of HSI which can be gathered at destinations. Since we assume that the relay knows the amount (and information content) of HSI received at destinations, it is always able to compose the output message $\mathbf{d}_R$ from the decoded messages and then broadcast it to D_A, D_B (see Table 10.1). The maximal sum-rate of the DF scheme can be evaluated as shown in the following Theorem:

Theorem 25. *(DF sum-rate):* The maximal sum-rate in WBN with DF relaying strategy is:

$$R_{\text{sum}}^{DF} = \begin{cases} \frac{C(\gamma_1)C(\gamma_3)}{C(\gamma_3)+0.5C(\gamma_1)}, & \gamma_2 \geq \gamma_1 \\ \max\left[R_{\text{sum}}^{DF^2}; R_{\text{sum}}^{DF^{2'}}\right], & \gamma_2 < \gamma_1 \end{cases} \tag{10.7}$$

where $R_{\text{sum}}^{DF^2} = \frac{C(\gamma_2)C(\gamma_3)}{C(\gamma_3)+0.5C(\gamma_2)}$ and $R_{\text{sum}}^{DF^{2'}} = \frac{C(\gamma_1)C(\gamma_3)}{C(\gamma_3)+C(\gamma_1)-0.5C(\gamma_2)}$.

[36] Later in the analysis of the SC-based scheme we show how the potential correlation of HSI and relay messages can be exploited to further boost the sum-rate performance.

[37] Note that WBN with perfect HSI is equivalent to the 2-WRC scenario.

[38] More details about the particular processing in the AF relaying scheme will be provided later.

Available HSI	*Perfect/full*	*Imperfect/partial*
S_A, S_B *broadcast (step I)*	Sources S_A, S_B orthogonally share the available time in step I and hence they successively broadcast their messages $\mathbf{d}_A, \mathbf{d}_B$ ($\lvert\mathbf{d}_A\rvert = \lvert\mathbf{d}_B\rvert = \frac{1}{2}N_I r$) towards the relay and unintended destinations D_B, D_A with rate r.	
HSI channel capacity vs. source rate	$C(\gamma_2) \geq r$	$C(\gamma_2) < r$
D_A: *HSI processing*	Decodes perfectly the information message transmitted by the unintended source S_B, $\left\lvert\mathbf{d}^A_{\text{HSI}}\right\rvert = \frac{1}{2}N_I r$.	Decodes only the partial HSI message, $\left\lvert\mathbf{d}^{(A1)}_{\text{HSI}}\right\rvert = \frac{1}{2}N_I C(\gamma_2)$.
D_B: *HSI processing*	Decodes perfectly the information message transmitted by the unintended source S_A, $\left\lvert\mathbf{d}^B_{\text{HSI}}\right\rvert = \frac{1}{2}N_I r$.	Decodes only the partial HSI message, $\left\lvert\mathbf{d}^{(B1)}_{\text{HSI}}\right\rvert = \frac{1}{2}N_I C(\gamma_2)$.
DF relay decoding	Decodes separate source data $\mathbf{d}_A, \mathbf{d}_B$ ($\lvert\mathbf{d}_A\rvert = \lvert\mathbf{d}_B\rvert = \frac{1}{2}N_I r$) and combines them to form $\lvert\mathbf{d}_{AB}\rvert = \frac{1}{2}N_I r$ (e.g. bitwise XOR of the messages) [12].	Decodes separate source data $\mathbf{d}_A, \mathbf{d}_B$ ($\lvert\mathbf{d}_A\rvert = \lvert\mathbf{d}_B\rvert = \frac{1}{2}N_I r$) and then splits each data message $\mathbf{d}_i$ ($i \in \{A, B\}$) into two separate parts, where $\left\lvert\mathbf{d}^{(1)}_i\right\rvert = \frac{1}{2}N_I C(\gamma_2)$ and $\left\lvert\mathbf{d}^{(2)}_i\right\rvert = \lvert\mathbf{d}_i\rvert - \left\lvert\mathbf{d}^{(1)}_i\right\rvert = \frac{1}{2}N_I(r - C(\gamma_2))$. Subsequently $\mathbf{d}^{(1)}_A$ and $\mathbf{d}^{(1)}_B$ are combined to form the hierarchical message $\mathbf{d}^{(1)}_{AB}$.
Relay broadcast (step II)	Broadcasts (after a potential re-encoding) the hierarchical message $\mathbf{d}_R = \mathbf{d}_{AB}$, $\lvert\mathbf{d}_R\rvert = \frac{1}{2}N_I r$ with rate $r_R = C(\gamma_3)$ to both destinations.	Forms the output message as $\mathbf{d}_R = \left[\mathbf{d}^{(1)}_{AB}, \mathbf{d}^{(2)}_A, \mathbf{d}^{(2)}_B\right]$, $\lvert\mathbf{d}_R\rvert = \frac{1}{2}N_I C(\gamma_2) + N_I(r - C(\gamma_2))$ and broadcasts it (after a potential re-encoding) with rate $r_R = C(\gamma_3)$ to both destinations.
D_A *decoding*	Full HSI $\mathbf{d}^A_{\text{HSI}} = \mathbf{d}_B$ is combined with $\mathbf{d}_{AB}$ to decode $\mathbf{d}_A$.	Partial HSI $\mathbf{d}^{(A1)}_{\text{HSI}} = \mathbf{d}^{(1)}_B$ is combined with $\mathbf{d}^{(1)}_{AB}$ to obtain $\mathbf{d}^{(1)}_A$ and joined with $\mathbf{d}^{(2)}_A$ to get $\mathbf{d}_A$.
D_B *decoding*	Full HSI $\mathbf{d}^B_{\text{HSI}} = \mathbf{d}_A$ is combined with $\mathbf{d}_{AB}$ to decode $\mathbf{d}_B$.	Partial HSI $\mathbf{d}^{(B1)}_{\text{HSI}} = \mathbf{d}^{(1)}_A$ is combined with $\mathbf{d}^{(1)}_{AB}$ to obtain $\mathbf{d}^{(1)}_B$ and joined with $\mathbf{d}^{(2)}_B$ to get $\mathbf{d}_B$.

Table 10.1: Node operations in DF relaying scheme in perfect and partial HSI cases.

Available HSI	*Perfect/full*	*Imperfect/partial*
S_A, S_B *broadcast (step I)*	Sources S_A, S_B simultaneously broadcast their messages $\mathbf{d}_A, \mathbf{d}_B$ ($\lvert\mathbf{d}_A\rvert = \lvert\mathbf{d}_B\rvert = N_I r$) towards the relay and unintended destinations D_B, D_A with rate r.	
HSI channel capacity vs. source rate	$C(\gamma_2) \geq r$	$C(\gamma_2) < r$
D_A: *HSI processing*	Decodes perfectly the information message transmitted by the unintended source S_B, $\left\lvert\mathbf{d}_{\text{HSI}}^{A}\right\rvert = N_I r$.	Decodes only the partial HSI message, $\left\lvert\mathbf{d}_{\text{HSI}}^{(A1)}\right\rvert = N_I C(\gamma_2)$.
D_B: *HSI processing*	Decodes perfectly the information message transmitted by the unintended source S_A, $\left\lvert\mathbf{d}_{\text{HSI}}^{B}\right\rvert = N_I r$.	Decodes only the partial HSI message, $\left\lvert\mathbf{d}_{\text{HSI}}^{(B1)}\right\rvert = N_I C(\gamma_2)$.
JDF relay decoding	Decodes separate source data $\mathbf{d}_A, \mathbf{d}_B$ ($\lvert\mathbf{d}_A\rvert = \lvert\mathbf{d}_B\rvert = N_I r$) and combines them to form $\lvert\mathbf{d}_{AB}\rvert = N_I r$ (e.g. bit-wise XOR of the messages) [12].	Decodes separate source data $\mathbf{d}_A, \mathbf{d}_B$ ($\lvert\mathbf{d}_A\rvert = \lvert\mathbf{d}_B\rvert = N_I r$) and then splits each data message $\mathbf{d}_i$ ($i \in \{A,B\}$) into two separate parts, where $\left\lvert\mathbf{d}_i^{(1)}\right\rvert = N_I C(\gamma_2)$ and $\left\lvert\mathbf{d}_i^{(2)}\right\rvert = \lvert\mathbf{d}_i\rvert - \left\lvert\mathbf{d}_i^{(1)}\right\rvert = N_I(r - C(\gamma_2))$. Subsequently $\mathbf{d}_A^{(1)}$ and $\mathbf{d}_B^{(1)}$ are combined to form the hierarchical message $\mathbf{d}_{AB}^{(1)}$.
HDF relay decoding	Decodes directly the hierarchical data $\mathbf{d}_{AB}$ ($\lvert\mathbf{d}_{AB}\rvert = N_I r$).	Decodes directly the partial hierarchical data $\mathbf{d}_{AB}^{(1)}$ ($\left\lvert\mathbf{d}_{AB}^{(1)}\right\rvert = N_I C(\gamma_2)$) and separately the two remaining parts of individual source messages $\mathbf{d}_i^{(2)}$ ($i \in \{A,B\}$), where $\left\lvert\mathbf{d}_i^{(2)}\right\rvert = \lvert\mathbf{d}_i\rvert - \left\lvert\mathbf{d}_i^{(1)}\right\rvert = N_I(r - C(\gamma_2))$.
Relay broadcast (step II)	Broadcasts (after a potential re-encoding) the hierarchical message $\mathbf{d}_R = \mathbf{d}_{AB}$, $\lvert\mathbf{d}_R\rvert = N_I r$ with rate $r_R = C(\gamma_3)$ to both destinations.	Forms the output message as $\mathbf{d}_R = \left[\mathbf{d}_{AB}^{(1)}, \mathbf{d}_A^{(2)}, \mathbf{d}_B^{(2)}\right]$, $\lvert\mathbf{d}_R\rvert = N_I C(\gamma_2) + 2N_I(r - C(\gamma_2))$ and broadcasts it (after a potential re-encoding) with rate $r_R = C(\gamma_3)$ to both destinations.
D_A *decoding*	Full HSI $\mathbf{d}_{\text{HSI}}^{A} = \mathbf{d}_B$ is combined with $\mathbf{d}_{AB}$ to decode $\mathbf{d}_A$.	Partial HSI $\mathbf{d}_{\text{HSI}}^{(A1)} = \mathbf{d}_B^{(1)}$ is combined with $\mathbf{d}_{AB}^{(1)}$ to obtain $\mathbf{d}_A^{(1)}$ and joined with $\mathbf{d}_A^{(2)}$ to get $\mathbf{d}_A$.
D_B *decoding*	Full HSI $\mathbf{d}_{\text{HSI}}^{B} = \mathbf{d}_A$ is combined with $\mathbf{d}_{AB}$ to decode $\mathbf{d}_B$.	Partial HSI $\mathbf{d}_{\text{HSI}}^{(B1)} = \mathbf{d}_A^{(1)}$ is combined with $\mathbf{d}_{AB}^{(1)}$ to obtain $\mathbf{d}_B^{(1)}$ and joined with $\mathbf{d}_B^{(2)}$ to get $\mathbf{d}_B$.

Table 10.2: Node operations in JDF and HDF relaying schemes in perfect and partial HSI cases.

Proof. Step I is time-shared by both sources and hence the sources transmit separately their messages of $\frac{1}{2}N_I$ symbols to the relay. The optimal value of source rate r^{DF} which maximizes the sum-rate depends on the mutual relation between γ_1 and γ_2 and hence we split the proof into two disjunct γ_2 regions:

- *($\gamma_2 \geq \gamma_1$):* Source rate $r_{\max}^{DF^1} = C(\gamma_1)$ guarantees that both individual source messages can be decoded by the relay. Since $C(\gamma_2) \geq r_{\max}^{DF^1} = C(\gamma_1)$ in this region, source messages can be decoded also by the unintended destinations in step I and hence the perfect HSI processing can be applied according to Table 10.1. After decoding of source messages, the relay broadcasts the output message of size $|\mathbf{d}_R| = |\mathbf{d}_{AB}| = \frac{1}{2}N_I C(\gamma_1)$ with rate $r_R = C(\gamma_3)$ to ensure a decodability of this message at both destinations and hence the sum-rate (10.6) can be evaluated as:

$$R_{\text{sum}}^{DF^1} = \frac{\frac{1}{2}N_I C(\gamma_1) + \frac{1}{2}N_I C(\gamma_1)}{N_I + N_{II}} = \frac{N_I C(\gamma_1)}{N_I\left(1 + \frac{\frac{1}{2}C(\gamma_1)}{C(\gamma_3)}\right)}. \tag{10.8}$$

- *($\gamma_2 < \gamma_1$):* The HSI channels are the bottleneck of the system in this region. There are two possible solutions how to cope with this problem. If the source rate is decreased to $r_{\max}^{DF^2} = C(\gamma_2)$ we can still guarantee that perfect HSI is retrieved by destinations, which leads to the following sum-rate (similarly as in (10.8)):

$$R_{\text{sum}}^{DF^2} = \frac{\frac{1}{2}N_I C(\gamma_2) + \frac{1}{2}N_I C(\gamma_2)}{N_I + N_{II}} = \frac{N_I C(\gamma_2)}{N_I\left(1 + \frac{\frac{1}{2}C(\gamma_2)}{C(\gamma_3)}\right)}. \tag{10.9}$$

  The second option is to keep the source rate at $r_{\max}^{DF^{2'}} = r_{\max}^{DF^1} = C(\gamma_1)$, at the price of having only partial HSI. Since $C(\gamma_2) < r_{\max}^{DF^{2'}} = C(\gamma_1)$ in this region, only partial HSI can be received by destinations and the partial HSI processing must be applied according to Table 10.1. After decoding of source messages, the relay broadcasts the output message $\mathbf{d}_R = \left[\mathbf{d}_{AB}^{(1)}, \mathbf{d}_A^{(2)}, \mathbf{d}_B^{(2)}\right]$ of size $|\mathbf{d}_R| = \frac{1}{2}N_I C(\gamma_2) + 2\left(\frac{1}{2}N_I\left(C(\gamma_1) - C(\gamma_2)\right)\right)$ with rate $r_R = C(\gamma_3)$ to ensure a decodability of this message at both destinations and hence the sum-rate (10.6) can be evaluated as:

$$R_{\text{sum}}^{DF^{2'}} = \frac{\frac{1}{2}N_I C(\gamma_1) + \frac{1}{2}N_I C(\gamma_1)}{N_I + N_{II}} = \frac{N_I C(\gamma_1)}{N_I\left(1 + \frac{C(\gamma_1) - \frac{1}{2}C(\gamma_2)}{C(\gamma_3)}\right)}. \tag{10.10}$$

  Although it is possible to explicitly evaluate γ_2, γ_3 region where $R_{\text{sum}}^{DF^{2'}} > R_{\text{sum}}^{DF^2}$, for a better clarity of results we express the sum-rate for $\gamma_2 < \gamma_1$ simply as $\max\left[R_{\text{sum}}^{DF^2}; R_{\text{sum}}^{DF^{2'}}\right]$. This gives us finally (10.7).

□

Since perfect HSI can be received by both destinations whenever $\gamma_2 \geq \gamma_1$, WBN with DF strategy becomes equivalent to the 2-WRC scenario in this SNR region. Here the source-relay channels are the main bottleneck of the system and hence R_{sum}^{DF} does not depend on γ_2. Much more interesting situation occurs if $\gamma_2 < \gamma_1$, i.e. if the HSI channels are the bottleneck of the system. A straightforward approach is to reduce the source rate to $r^{DF} = C(\gamma_2)$ to guarantee a decodability of perfect HSI at destinations. Another option is to exploit the partial HSI processing (Table 10.1), while keeping the source rate at the maximum possible value for the given relaying strategy ($r^{DF} = C(\gamma_1)$ guarantees successful DF relay decoding).

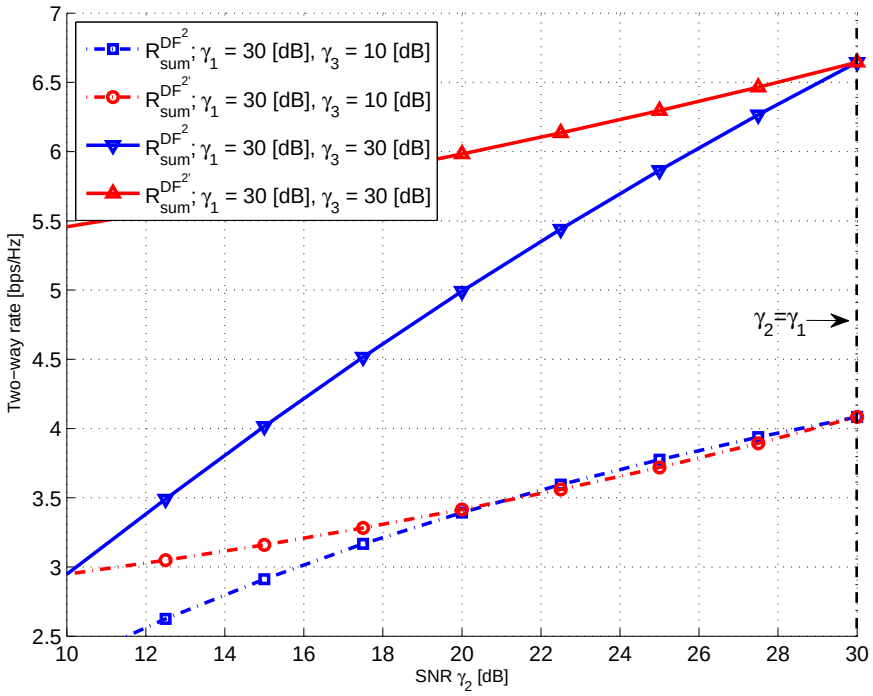

Figure 10.2: Comparison of the maximal DF sum-rates for perfect ($R_{\text{sum}}^{DF^2}$) and partial ($R_{\text{sum}}^{DF^{2'}}$) HSI processing in $\gamma_2 < \gamma_1$ region. Red curves correspond to the partial HSI processing (Table 10.1). Note that $R_{\text{sum}}^{DF^{2'}} > R_{\text{sum}}^{DF^2} \Leftrightarrow C(\gamma_3) > \frac{1}{2}C(\gamma_2)$.

It can be easily shown that the latter approach (i.e. the partial HSI processing) provides a higher sum-rate ($R_{\text{sum}}^{DF^{2'}} > R_{\text{sum}}^{DF^2}$) iff $C(\gamma_3) > \frac{1}{2}C(\gamma_2)$ and hence $\max\left[R_{\text{sum}}^{DF^2}; R_{\text{sum}}^{DF^{2'}}\right]$ in (10.7) can be further simplified according to this mutual relation between $C(\gamma_3)$ and $C(\gamma_2)$. An example comparison of $R_{\text{sum}}^{DF^{2'}}$ and $R_{\text{sum}}^{DF^2}$ is in Fig. 10.2.

Similar behaviour can be observed in the other relaying strategies (AF, JDF, HDF). When the HSI channels have sufficient capacity ($C(\gamma_2) \geq r$), perfect HSI is available at destinations and the system is equivalent to the 2-WRC. On the other hand, if the HSI channels become the bottleneck of the system (e.g. if $\gamma_2 < \gamma_1$ in DF), we can either decrease the source rate to retain the availability of perfect HSI at destinations or employ the partial HSI processing to avoid the potential performance reduction of the former method in the medium to low γ_2 region (see the rapid decrease of $R_{\text{sum}}^{DF^2}$ with γ_2 in Fig. 10.2).

10.3.3 2-step schemes

Both sources S_A, S_B are allowed to transmit simultaneously in step I of all the 2-step schemes and hence the relay has only a single compound observation of source signals in the Multiple-Access Channel (Fig. 10.1). Several 2-step relaying strategies can be distinguished in WBN according to a particular processing of this compound signal, including AF, JDF and HDF. More details on the individual strategies, together with their maximal sum-rate performance in WBN is provided in the following text.

10.3.3.1 Amplify & Forward

The AF relay always only amplifies the received signal prior to broadcasting it to both destinations [31, 70]. Since the AF relay does not decode the source messages from the received signal, it is not able to modify its output message (contrary to DF, JDF, HDF – see Tables 10.1,10.2) to respect the actual HSI observed at destinations. Each destination thus receives a mixture of source signals from the relay, having its desired data interfered by the data from the unintended source. This creates two equivalent channels $S_A \to D_A$, $S_B \to D_B$, where the particular equivalent SNR depends mainly on the destinations' ability to remove the interfering signal.

The interfering signal can be perfectly removed iff the destination is able to decode the unintended source message overheard on HSI channel, i.e. iff $r \leq C(\gamma_2)$. On the other hand, if the destination is not able to decode the HSI signal (i.e. if $r > C(\gamma_2)$), it can either estimate its value from the HSI channel observation (and subtract this estimate from the received relay signal) or completely ignore the HSI channel observation and treat the interfering signal as an additional noise. Note again that each received symbol is only re-transmitted by the relay, keeping the length of both communication steps in AF always equal ($N_I = N_{II}$). The maximal rate of AF strategy is proved in the following Theorem:

Theorem 26. *(AF sum-rate):* The maximal sum-rate in WBN with AF relaying strategy is:

$$R_{\text{sum}}^{AF} = \begin{cases} C\left(\frac{\gamma_1\gamma_3}{2\gamma_1+\gamma_3+1}\right), & \gamma_2 \geq \frac{\gamma_1\gamma_3}{2\gamma_1+\gamma_3+1} \\ C(\gamma_2), & \frac{\gamma_1\gamma_3}{2\gamma_1+\gamma_1\gamma_3+\gamma_3+1} \leq \gamma_2 < \frac{\gamma_1\gamma_3}{2\gamma_1+\gamma_3+1} \\ C\left(\frac{\gamma_1\gamma_3}{2\gamma_1+\gamma_1\gamma_3+\gamma_3+1}\right), & \gamma_2 < \frac{\gamma_1\gamma_3}{2\gamma_1+\gamma_1\gamma_3+\gamma_3+1} \end{cases} \tag{10.11}$$

Proof. In step I both sources transmit their messages of N_I symbols simultaneously to the relay. The relay has the following observation:

$$y_R = h_{S_AR}s_A + h_{S_BR}s_B + w_R. \tag{10.12}$$

After receiving (10.12), the relay simply multiplies it by the AF amplification factor β [31, 70]:

$$\beta = \sqrt{\frac{1}{|h_{S_AR}|^2 + |h_{S_BR}|^2 + N_0}} = \sqrt{\frac{1}{N_0(2\gamma_1+1)}}, \tag{10.13}$$

to keep the mean energy per symbol constant, and broadcasts the resulting signal $s_R = \beta y_R$ to destinations. In the following, we describe the destination D_A processing (D_B processing follows the same steps).

D_A receives the following signal from the relay:

$$\mathbf{y}_{D_A} = h_{RD_A}\mathbf{s}_R = \beta h_{RD_A}h_{S_AR}\mathbf{s}_A + \beta h_{RD_A}h_{S_BR}\mathbf{s}_B + (\beta h_{RD_A}\mathbf{w}_R + \mathbf{w}_{D_A}). \tag{10.14}$$

The interfering signal $\mathbf{s}_B$ can be completely removed from $\mathbf{y}_{D_A}$ iff perfect HSI is received in step I, resulting in an equivalent interference free $S_A \to D_A$ channel with SNR $\gamma_{AF}^{\text{perf-HSI}}$ (similarly also for $S_B \to D_B$):

$$\gamma_{AF}^{\text{perf-HSI}} = \frac{\beta^2 |h_{RD_A}|^2 |h_{S_AR}|^2}{N_0\left(\beta^2 |h_{RD_A}|^2 + 1\right)} = \frac{\gamma_1\gamma_3}{2\gamma_1+\gamma_3+1}.$$

The source rate $r_{\max}^{AF^1} = C\left(\gamma_{AF}^{\text{perf-HSI}}\right)$ guarantees that the desired message can be decoded from the equivalent channel and the sum-rate (10.5) can be evaluated as:

$$R_{\text{sum}}^{AF^1} = \frac{N_I C\left(\gamma_{AF}^{\text{perf-HSI}}\right) + N_I C\left(\gamma_{AF}^{\text{perf-HSI}}\right)}{N_I + N_{II}} = C\left(\gamma_{AF}^{\text{perf-HSI}}\right), \tag{10.15}$$

since $N_{II} = N_I$ in AF. Note that (10.15) can be achieved iff $C(\gamma_2) \geq C\left(\gamma_{AF}^{\text{perf}-\text{HSI}}\right)$, as perfect HSI must be available at destinations to allow a perfect removal of the interfering signal at destinations.

Now we have to analyse the sum-rate in the region where $C(\gamma_2) < C\left(\gamma_{AF}^{\text{perf}-\text{HSI}}\right)$, i.e. in the region where the HSI channels are the bottleneck of the system. Perfect HSI (and consequently a perfect cancellation of the interfering signal) can be guaranteed even in this region, simply by reducing the source rate to $r_{\max}^{AF^2} = C(\gamma_2)$. Since the equivalent source-destination channels still have SNR $\gamma_{AF}^{\text{perf}-\text{HSI}} = \frac{\gamma_1\gamma_3}{2\gamma_1+\gamma_3+1} > \gamma_2$ in this region, the desired source message can be decoded at each destination and hence the sum-rate (10.5) reduces to:

$$R_{\text{sum}}^{AF^2} = \frac{N_I C(\gamma_2) + N_I C(\gamma_2)}{N_I + N_{II}} = C(\gamma_2). \tag{10.16}$$

The other option in this region ($C(\gamma_2) < C\left(\gamma_{AF}^{\text{perf}-\text{HSI}}\right)$) is to keep the source rate at $r_{\max}^{AF'} = r_{\max}^{AF^1} = C\left(\gamma_{AF}^{\text{perf}-\text{HSI}}\right)$ and employ the AF equivalent of partial HSI processing. Since $C(\gamma_2) < r_{\max}^{AF'}$, D_A cannot perfectly decode the source S_B message from its HSI observation $y_{D_A}^{HSI} = h_{S_B D_A} s_B + w_{D_A}^{HSI}$. However, it can always try to estimate the value of HSI signal ($\hat{\mathbf{s}}_B$) and use it to (at least partially) remove the interfering signal $\mathbf{s}_B$ from (10.14). A particular implementation of this partial-HSI processing in AF (together with a particular method for partial HSI estimation) is a standalone research problem and hence it is beyond the scope of this analysis[39]. We assume that AF operates with full HSI in this region, keeping the sum-rate equal to (10.16). Note that this generally provides only a lower bound of the AF maximal sum-rate in $C(\gamma_2) < C\left(\gamma_{AF}^{\text{perf}-\text{HSI}}\right)$.

It is obvious that $R_{\text{sum}}^{AF^2} = C(\gamma_2)$ deteriorates rapidly with the quality of HSI channels. Fortunately, since each destination observes an analogue superposition of source messages from AF relay, it can completely ignore the unreliable HSI observation in low γ_2 region and try to decode the desired message directly from the relay signal (10.14). The resulting equivalent channel has SNR $\gamma_{AF}^{\text{zero}-\text{HSI}}$:

$$\gamma_{AF}^{\text{zero}-\text{HSI}} = \frac{\beta^2 |h_{RD_A}|^2 |h_{S_A R}|^2}{\beta^2 |h_{RD_A}|^2 |h_{S_B R}|^2 + N_0\left(\beta^2 |h_{RD_A}|^2 + 1\right)} = \frac{\gamma_1\gamma_3}{\gamma_1\gamma_3 + 2\gamma_1 + \gamma_3 + 1}.$$

The source rate $r_{\max}^{AF^3} = C\left(\gamma_{AF}^{\text{zero}-\text{HSI}}\right)$ guarantees a decodability of the desired source message from the interference channel (10.14) and hence the sum-rate (10.5) can be evaluated as:

$$R_{\text{sum}}^{AF^3} = \frac{N_I C\left(\gamma_{AF}^{\text{zero}-\text{HSI}}\right) + N_I C\left(\gamma_{AF}^{\text{zero}-\text{HSI}}\right)}{N_I + N_{II}} = C\left(\gamma_{AF}^{\text{zero}-\text{HSI}}\right). \tag{10.17}$$

Now it is straightforward to show that $R_{\text{sum}}^{AF^3} > R_{\text{sum}}^{AF^2}$ iff $\gamma_{AF}^{\text{zero}-\text{HSI}} > \gamma_2$ which gives us finally (10.11). □

10.3.3.2 Joint Decode & Forward

The JDF relay always decodes the individual source messages $\mathbf{d}_A, \mathbf{d}_B$ from MAC channel observation (see Fig. 10.1), regardless of the amount of HSI which can be gathered at destinations. Since we assume that the relay always knows the amount (and information content) of HSI received at destinations, it is always able to compose the output message $\mathbf{d}_R$ and then broadcast it to D_A, D_B (see Table 10.2). The maximal sum-rate of the JDF scheme can be evaluated as shown in the following Theorem:

[39] The optimal HSI estimator (and its performance) can generally depend also on the employed source modulation/coding strategy.

Theorem 27. *(JDF sum-rate):* The maximal sum-rate in WBN with JDF relaying strategy is:

$$R_{\text{sum}}^{JDF} = \begin{cases} \frac{C(2\gamma_1)C(\gamma_3)}{C(\gamma_3)+0.5C(2\gamma_1)}, & C(\gamma_2) \geq \frac{1}{2}C(2\gamma_1) \\ \max\left[R_{\text{sum}}^{JDF^2}; R_{\text{sum}}^{JDF^{2'}}\right], & C(\gamma_2) < \frac{1}{2}C(2\gamma_1) \end{cases} \tag{10.18}$$

where $R_{\text{sum}}^{JDF^2} = \frac{2C(\gamma_2)C(\gamma_3)}{C(\gamma_3)+C(\gamma_2)}$ and $R_{\text{sum}}^{JDF^{2'}} = \frac{C(2\gamma_1)C(\gamma_3)}{C(\gamma_3)+C(2\gamma_1)-C(\gamma_2)}$.

Proof. In step I both sources transmit their messages of N_I symbols simultaneously to the relay. The optimal value of source rate r^{JDF} which maximizes the sum-rate depends on the mutual relation of γ_1 and γ_2 and hence we split the proof into two disjunct γ_2 regions:

- *($C(\gamma_2) \geq \frac{1}{2}C(2\gamma_1)$):* Maximum symmetric source rate which guarantees that both individual source messages can be decoded by the relay is $r_{\max}^{JDF^1} = \frac{1}{2}C(2\gamma_1)$ [6]. Since $C(\gamma_2) \geq r_{\max}^{JDF^1} = \frac{1}{2}C(2\gamma_1)$ in this region, source messages can be decoded also by the unintended destinations in step I and hence the perfect HSI processing can be applied according to Table 10.2. After decoding of source messages, the relay broadcasts the output message of size $|\mathbf{d}_R| = |\mathbf{d}_{AB}| = N_I\frac{1}{2}C(2\gamma_1)$ with rate $r_R = C(\gamma_3)$ to ensure a decodability of this message at both destinations and hence the sum-rate (10.5) can be evaluated as:

$$R_{\text{sum}}^{JDF^1} = \frac{N_I\frac{1}{2}C(2\gamma_1)+N_I\frac{1}{2}C(2\gamma_1)}{N_I+N_{II}} = \frac{N_IC(2\gamma_1)}{N_I\left(1+\frac{\frac{1}{2}C(2\gamma_1)}{C(\gamma_3)}\right)}. \tag{10.19}$$

- *($C(\gamma_2) < \frac{1}{2}C(2\gamma_1)$):* The HSI channels are the bottleneck of the system in this region. There are two possible solutions how to cope with this problem. If the source rate is decreased to $r_{\max}^{JDF^2} = C(\gamma_2)$ we can still guarantee that perfect HSI is retrieved by destinations, which leads to the following sum-rate (similarly as in (10.19)):

$$R_{\text{sum}}^{JDF^2} = \frac{N_IC(\gamma_2)+N_IC(\gamma_2)}{N_I+N_{II}} = \frac{2N_IC(\gamma_2)}{N_I\left(1+\frac{C(\gamma_2)}{C(\gamma_3)}\right)}. \tag{10.20}$$

  The second option is to keep the source rate at $r_{\max}^{JDF^{2'}} = r_{\max}^{JDF^1} = \frac{1}{2}C(2\gamma_1)$, at the price of having only partial HSI. Since $C(\gamma_2) < r_{\max}^{JDF^{2'}} = \frac{1}{2}C(2\gamma_1)$ in this region, only partial HSI can be received by destinations and the partial HSI processing must be applied according to Table 10.2. After decoding of source messages, the relay broadcasts the output message $\mathbf{d}_R = \left[\mathbf{d}_{AB}^{(1)}, \mathbf{d}_A^{(2)}, \mathbf{d}_B^{(2)}\right]$ of size $|\mathbf{d}_R| = N_IC(\gamma_2)+2N_I\left(\frac{1}{2}C(2\gamma_1)-C(\gamma_2)\right)$ with rate $r_R = C(\gamma_3)$ to ensure a decodability of this message at both destinations and hence the sum-rate (10.5) can be evaluated as:

$$R_{\text{sum}}^{JDF^{2'}} = \frac{N_I\frac{1}{2}C(2\gamma_1)+N_I\frac{1}{2}C(2\gamma_1)}{N_I+N_{II}} = \frac{N_IC(2\gamma_1)}{N_I\left(1+\frac{C(2\gamma_1)-C(\gamma_2)}{C(\gamma_3)}\right)}. \tag{10.21}$$

  Although it is possible to explicitly evaluate γ_2, γ_3 region where $R_{\text{sum}}^{JDF^{2'}} > R_{\text{sum}}^{JDF^2}$, for a better clarity of results we express the sum-rate for $C(\gamma_2) < \frac{1}{2}C(2\gamma_1)$ simply as $\max\left[R_{\text{sum}}^{JDF^2}; R_{\text{sum}}^{JDF^{2'}}\right]$. This gives us finally (10.18).

□

It can be easily shown that for $C(\gamma_2) < \frac{1}{2}C(2\gamma_1)$ the partial HSI processing in JDF provides a better sum-rate than the perfect one ($R_{\text{sum}}^{JDF^{2'}} > R_{\text{sum}}^{JDF^2}$) iff $C(\gamma_3) > C(\gamma_2)$ and hence $\max\left[R_{\text{sum}}^{JDF^2}; R_{\text{sum}}^{JDF^{2'}}\right]$ in (10.18) can be further simplified according to the mutual relation between $C(\gamma_2)$ and $C(\gamma_3)$.

10.3.3.3 Hierarchical Decode & Forward

The fundamental idea of the HDF relaying strategies (see [12, 13, 65, 71] and references therein) is based on the fact that the intermediate relay node is not the final destination of communication and hence it does not have to decode *separate individual source messages*. This in turn allows to increase the source rates above the limits of the underlying relay *MAC capacity region* [6] (compare with JDF) and hence to further boost the sum-rate performance. However, a sufficient amount of HSI must be available at destinations to gather this potential performance benefit of HDF. In other words, HDF provides higher sum-rates than JDF only if HSI channels support the rates above the MAC capacity region (i.e. if $C(\gamma_2) \geq \frac{1}{2}C(2\gamma_1)$) This is illustrated in Fig. 10.3.

When sufficient HSI is available, the HDF relay decodes directly the hierarchical message $\mathbf{d}_{AB}$ from its observations[40], and hence the individual source messages $\mathbf{d}_A, \mathbf{d}_B$ are not necessarily decoded. Since we assume that the relay knows the amount (and information content) of HSI received at destinations, it is always able to compose the output message $\mathbf{d}_R$ and then broadcast it to D_A, D_B (see Table 10.2). The maximal sum-rate of the HDF scheme can be evaluated as shown in the following Theorem:

Theorem 28. *(HDF sum-rate):* The maximal sum-rate in WBN with HDF relaying strategy is:

$$R_{\text{sum}}^{HDF} = \begin{cases} \frac{2C(\gamma_1)C(\gamma_3)}{C(\gamma_1)+C(\gamma_3)}, & C(\gamma_2) \geq C(\gamma_1) \\ \frac{2C(\gamma_2)C(\gamma_3)}{C(\gamma_2)+C(\gamma_3)}, & \frac{1}{2}C(2\gamma_1) \leq C(\gamma_2) < C(\gamma_1) \\ \max\left[R_{\text{sum}}^{HDF^3}; R_{\text{sum}}^{HDF^{3'}}\right], & C(\gamma_2) < \frac{1}{2}C(2\gamma_1) \end{cases} \tag{10.22}$$

where $R_{\text{sum}}^{HDF^3} = \frac{2C(\gamma_2)C(\gamma_3)}{C(\gamma_3)+C(\gamma_2)}$ and $R_{\text{sum}}^{HDF^{3'}} = \frac{C(2\gamma_1)C(\gamma_3)}{C(\gamma_3)+C(2\gamma_1)-C(\gamma_2)}$.

Proof. In step I both sources transmit their messages of N_I symbols simultaneously to the relay. The optimal value of source rate r^{HDF} which maximizes the sum-rate depends on the mutual relation of γ_1 and γ_2 and hence we split the proof into three disjunct γ_2 regions:

- *($C(\gamma_2) \geq C(\gamma_1)$):* In the HDF strategy, the source rates are theoretically upper bounded only by the 1st order cut-set bound of the underlying MAC channel [6], i.e. by $r = C(\gamma_1)$. Even though the achievability of this rate has not been rigorously proved in general Gaussian channels (see e.g. [103]), we follow the conjecture from [31] and assume that hierarchical message $\mathbf{d}_{AB}$ can be successfully decoded by the relay if the sources transmit with the rate $r_{\max}^{HDF^1} = C(\gamma_1) - \varepsilon$. By setting $\varepsilon = 0$ we obtain the upper-bound of the maximal sum-rate of the HDF strategy. Since $C(\gamma_2) \geq r_{\max}^{HDF^1} = C(\gamma_1)$ in this region, source messages can be decoded by the unintended destinations in step I and hence the perfect HSI processing can be applied according to Table 10.2. After decoding of source messages, the relay broadcasts the output message of size $|\mathbf{d}_R| = |\mathbf{d}_{AB}| = N_I C(\gamma_1)$ with rate $r_R = C(\gamma_3)$ to ensure a decodability of this message at both destinations and hence the sum-rate (10.5) can be evaluated as:

$$R_{\text{sum}}^{HDF^1} = \frac{N_I C(\gamma_1) + N_I C(\gamma_1)}{N_I + N_{II}} = \frac{2N_I C(\gamma_1)}{N_I\left(1 + \frac{C(\gamma_1)}{C(\gamma_3)}\right)}. \tag{10.23}$$

- *($\frac{1}{2}C(2\gamma_1) \leq C(\gamma_2) < C(\gamma_1)$):* The HSI channels become the bottleneck of the system in this region. Perfect HSI can still be provided if the source rate is reduced to $r_{\max}^{HDF^2} = C(\gamma_2)$, which results in

[40] $\mathbf{d}_{AB}$ is generally some invertible function of source data. Each destination can decode its desired data from $\mathbf{d}_{AB}$ iff data from the unintended source (HSI) are also available [13].

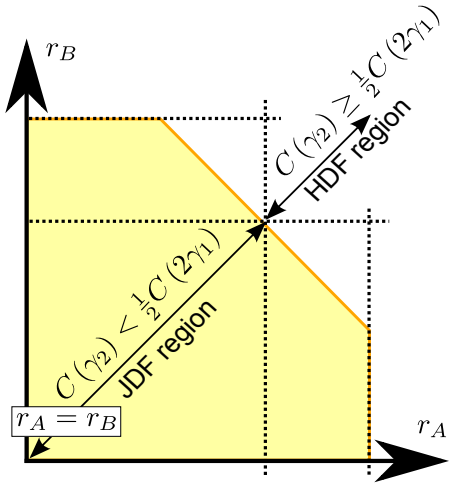

Figure 10.3: Operational regions of HDF strategy: impact of the relationship between the HSI channel capacity $C(\gamma_2)$ and relay MAC capacity region.

the following sum-rate:

$$R_{\text{sum}}^{HDF^2} = \frac{N_I C(\gamma_2) + N_I C(\gamma_2)}{N_I + N_{II}} = \frac{2N_I C(\gamma_2)}{N_I \left(1 + \frac{C(\gamma_2)}{C(\gamma_3)}\right)}. \tag{10.24}$$

- *($C(\gamma_2) \leq \frac{1}{2}C(2\gamma_1)$):* In this region the HSI channels cannot support the rates above the limits induced by the relay MAC capacity region and hence the HDF strategy becomes equivalent to JDF. Source rate can be set to $r_{\text{max}}^{HDF^3} = r_{\text{max}}^{JDF^1} = \frac{1}{2}C(2\gamma_1)$ and hence the maximal sum-rate is the same as in the JDF strategy, i.e. $R_{\text{sum}}^{HDF^3} = \max\left[R_{\text{sum}}^{JDF^2}; R_{\text{sum}}^{JDF^{2'}}\right]$, which gives us finally (10.22).

□

10.3.4 Performance comparison

Here we finally compare the performance of particular relaying schemes in WBN. Apart of the sum-rates we evaluate also the corresponding relative lengths of step II in all relaying strategies to emphasize the fact that WBN must operate with uneven lengths of steps I, II to achieve the sum-rates evaluated in the previous section. Since we are interested mainly in the impact of limited HSI, the sum-rate and relative length of step I are analysed as a function of the HSI channel SNR (γ_2).

10.3.4.1 Maximal sum-rates

Maximal sum-rates of the analysed relaying schemes are compared in Fig. 10.4 ($\gamma_1 = 10$dB, $\gamma_3 = 30$dB), Fig. 10.5 ($\gamma_1 = 30$dB, $\gamma_3 = 10$dB) and Fig. 10.6 ($\gamma_1 = \gamma_3 = 30$dB). The values of γ_2 where $C(\gamma_2)$ is equal to the 1st and 2nd order (symmetric rates) cut-set bounds of the underlying relay MAC channel are emphasized in all Figures. These cut-set bounds determine the HSI operating regions in most of the strategies (see equations (10.7), (10.18), (10.22)).

Many interesting observations can be made from Figs. 10.4, 10.5, 10.6. Similarly as in the 2-WRC scenario [31], the best sum-rate is provided by the HDF strategy in the whole range of channel SNRs[41)].

[41)] Note that in the low to medium γ_2 region only a lower bound on AF strategy sum-rate is provided (see proof of Theorem 26).

However, when $C(\gamma_2) \leq \frac{1}{2}C(2\gamma_1)$ the performance of HDF degrades theoretically to that of the JDF strategy, since the actual quality of HSI channels does not allow to increase the source rates above the conventional MAC capacity region (see Fig. 10.3).

As expected, the sum-rates depend strongly on the actual SNR of HSI channels (γ_2), and all the relaying strategies are capable to support non-zero sum-rates even when the HSI channels are very weak ($C(\gamma_2) \to 0$). On the other hand, when the HSI channels are sufficiently strong the sum-rates tend to saturate (for fixed γ_1, γ_3) as the HSI channels no longer limit the performance of the system. Similar behaviour can be observed in the low γ_2 region, where the impact of weak (unreliable) HSI channels on the maximal sum-rate becomes negligible. As it is obvious from Figs. 10.4, 10.5, 10.6, the particular regions of γ_2 where this saturation of sum-rates can be observed depend mainly on the applied relaying strategy and also on the actual values of γ_1, γ_3.

10.3.4.2 Relative length of communication steps

The WBN system must operate with uneven lengths of step I, II to achieve the sum-rates evaluated in (10.7), (10.18), (10.22). Since the relay itself is not a source of information (it does not have any own data to transmit) the length of step II is always proportional to the length of step I, i.e. $N_{II} = \delta N_I$ (note again that N_I is kept fixed in all strategies), where δ is the proportional coefficient. Both steps have a constant length ($N_I = N_{II}$, $\delta_{AF} = 1$) only in the AF strategy where the relay always only retransmits each received symbol [70]. .

The sum-rate in (10.5) can be evaluated as:

$$R_{\text{sum}}^{\text{2step}} = \frac{2r}{1+\delta} = 2rn_I, \tag{10.25}$$

where $n_I = \frac{N_I}{N_I+N_{II}} = \frac{1}{1+\delta}$ is the relative length of step I, and similarly for the 3-step strategy (10.6):

$$R_{\text{sum}}^{\text{3step}} = \frac{r}{1+\delta} = rn_I. \tag{10.26}$$

From (10.25), (10.26) is is obvious that the corresponding optimal relative lengths of step II ($n_{II} = 1 - n_I$) can be directly evaluated from the sum-rates proved in Theorems 25, 27, 28 and hence we omit a detailed derivation of n_{II} in this paper.

The optimal values of n_{II} which correspond to the sum-rates in Figs. 10.4, 10.5, 10.6 are compared in Fig. 10.7 ($\gamma_1 = 10$dB, $\gamma_3 = 30$dB), Fig. 10.8 ($\gamma_1 = 30$dB, $\gamma_3 = 10$dB) and Fig. 10.9 ($\gamma_1 = \gamma_3 = 30$dB). As it is obvious from these Figures, the lengths of step I, II must be always optimized to achieve the optimal sum-rate performance in WBN. For example, less resources are required in step II when $\gamma_1 < \gamma_3$, due to the superior quality of relay→destination channels (see Fig. 10.7). On the other hand, the length of step II must be increased relatively to step I when $\gamma_1 > \gamma_3$, i.e. when the relay→destination channels are weak (see Fig. 10.8). Quite surprisingly, the optimal lengths of steps I, II are not always equal ($n_{II} \neq \frac{1}{2}$) even if $\gamma_1 = \gamma_3$ (see Fig. 10.9). Note that the values of γ_2 where n_{II} curves change its derivative (in DF, JDF and HDF) in Fig. 10.8 correspond to the value of γ_2 where the partial HSI processing becomes superior than the perfect HSI processing (with reduced source rate, i.e. $r = C(\gamma_2)$). As noted in the previous discussion this corresponds to $C(\gamma_3) = \frac{1}{2}C(\gamma_2)$ in DF strategy and to $C(\gamma_3) = C(\gamma_2)$ in JDF and HDF strategies.

10.4 SC-based HDF scheme

In the previous text we assumed that the source coding strategy can guarantee that the relay node knows the information content of HSI received at destinations. This allows the relay to construct its output message and thus enables a successful decoding of desired data at both destinations. One particular

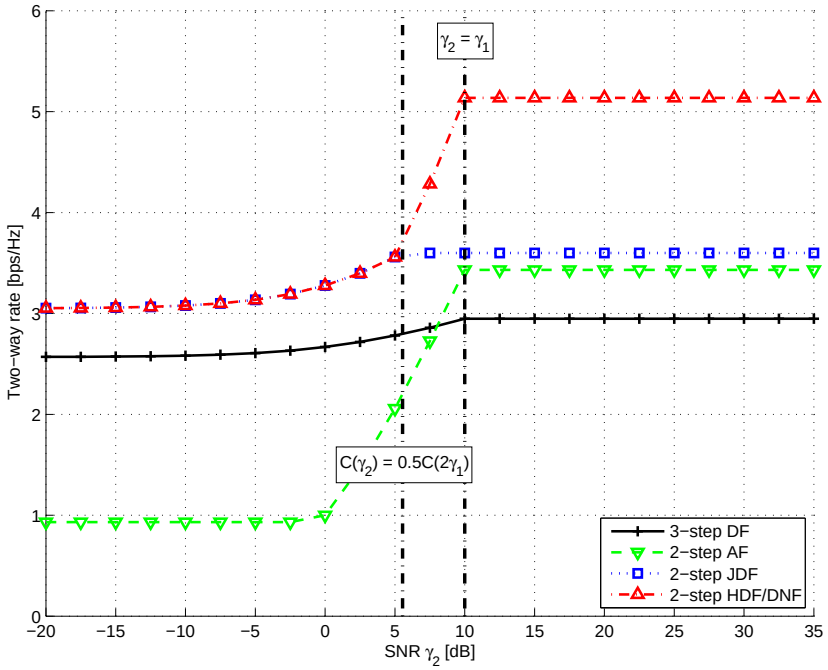

Figure 10.4: Comparison of the maximal sum-rates of DF, AF, JDF and HDF strategies in WBN ($\gamma_1 =$ 10 dB, $\gamma_3 = 30$ dB).

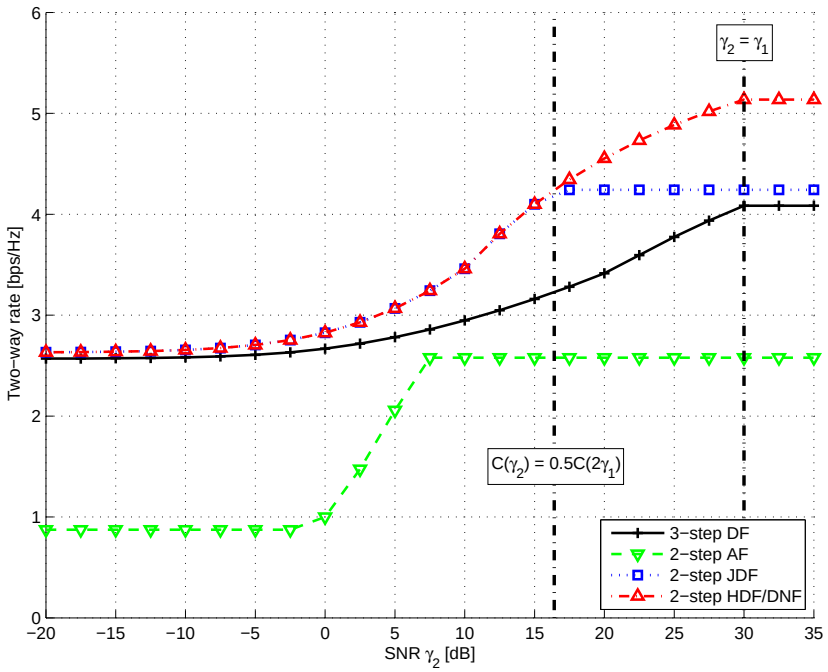

Figure 10.5: Comparison of the maximal sum-rates of DF, AF, JDF and HDF strategies in WBN ($\gamma_1 =$ 30 dB, $\gamma_3 = 10$ dB).

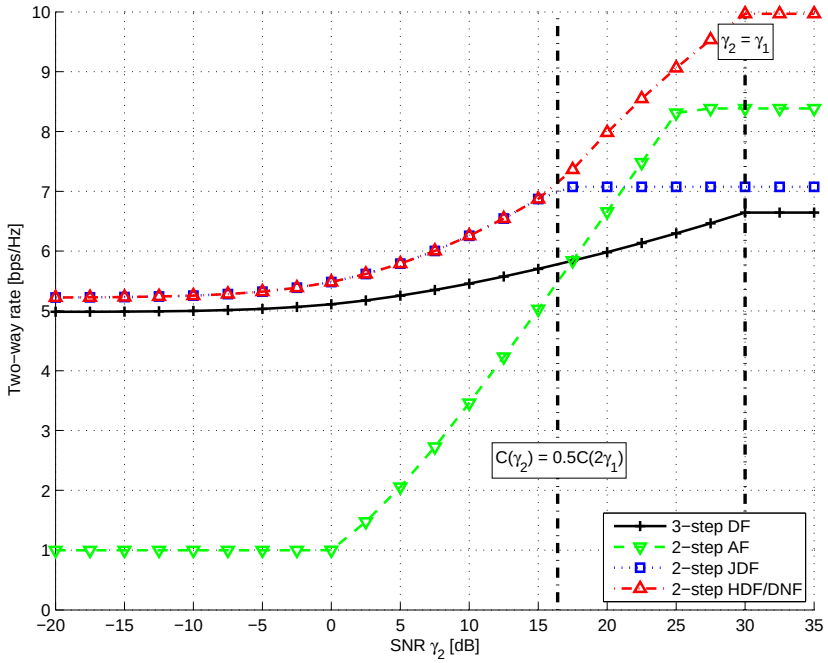

Figure 10.6: Comparison of the maximal sum-rates of DF, AF, JDF and HDF strategies in WBN ($\gamma_1 = 30$ dB, $\gamma_3 = 30$ dB).

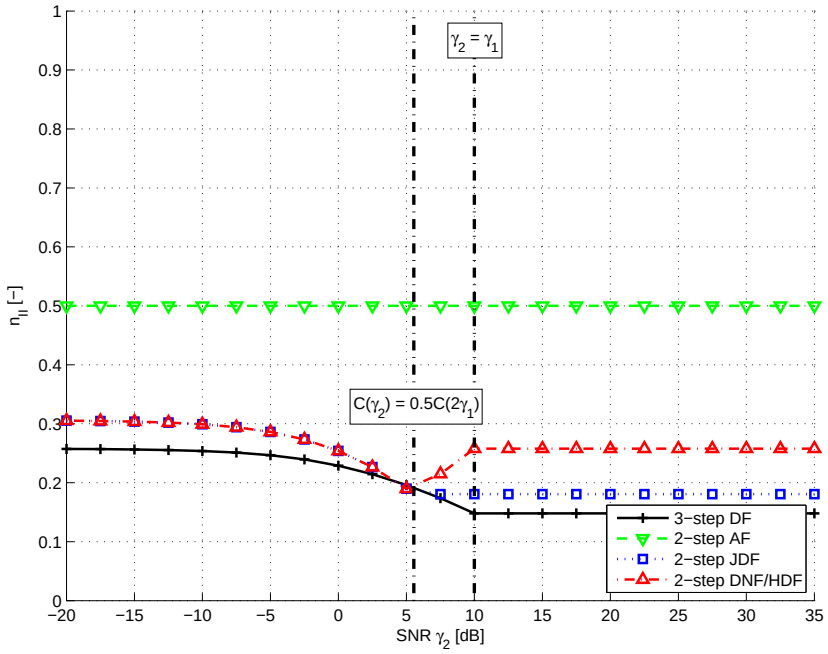

Figure 10.7: Comparison of the relative length of step II in DF, AF, JDF and HDF strategies in WBN ($\gamma_1 = 10$ dB, $\gamma_3 = 30$ dB).

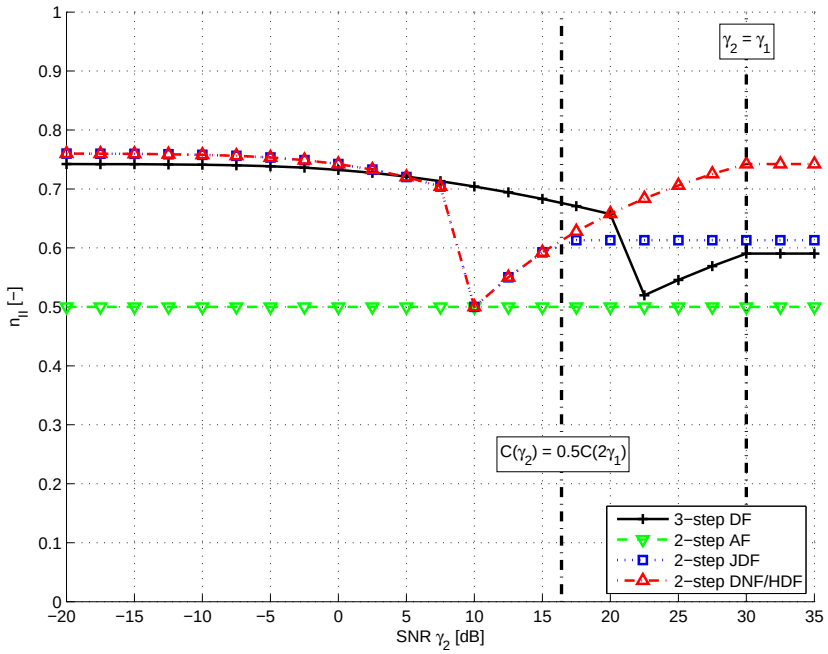

Figure 10.8: Comparison of the relative length of step II in DF, AF, JDF and HDF strategies in WBN ($\gamma_1 = 30$ dB, $\gamma_3 = 10$ dB).

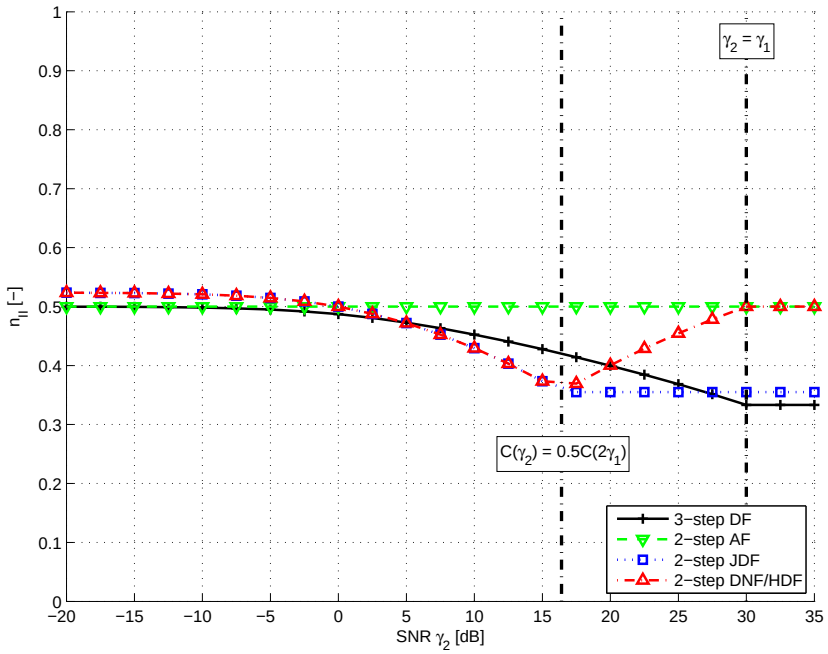

Figure 10.9: Comparison of the relative length of step II in DF, AF, JDF and HDF strategies in WBN ($\gamma_1 = 30$ dB, $\gamma_3 = 30$ dB).

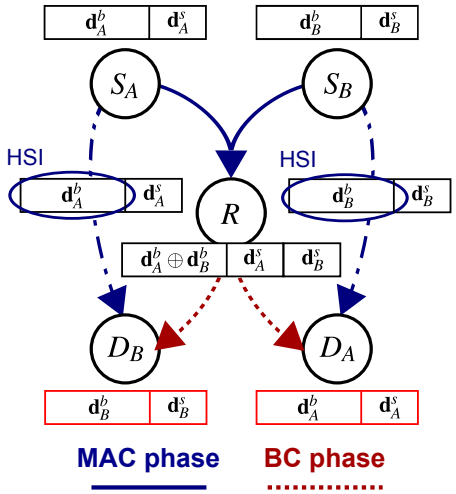

Figure 10.10: Principle of HDF_{SC} processing in WBN. Symbol $\oplus$ denotes a hierarchical function (e.g. bit-wise XOR).

coding strategy which can naturally guarantee the fulfilment of this assumption is SC [6, 27]. In the previosu Section we showed that HDF is capable to provide the best sum-rate performance among all the analysed WBN relaying strategies (for arbitrary γ_1, γ_3 and HSI channel quality (γ_2)). Hence, in the rest of this Chapter we focus on an implementation of the SC-based HDF relaying scheme (HDF_{SC}) in WBN[42]. The idea of HDF_{SC} strategy was originally proposed in [27].

10.4.1 Implementation of HDF_{SC} in WBN

Basic principle of HDF_{SC} processing is visualized in Fig. 10.10 (more details can be found in [27] or Chapter 9). Both sources S_i, $i \in \{A,B\}$ split their messages into two independent (basic & superposed) parts of potentially unequal length and broadcast them simultaneously in step I.

The fundamental idea of HDF_{SC} is to process only the basic messages as an *effective HSI* at destinations, treating the superposed messages on overheard source-destination channels purely and simply as an additional interference (with obvious consequences on the HSI channels capacity) [27]. Since the basic messages are decoded at both unintended destinations as HSI, it is sufficient to decode a hierarchical function of these basic messages (e.g. bit-wise XOR [12]) at the relay, while both individual superposed messages must be decoded separately. The relay then successively transmits (after a potential re-encoding) the hierarchical message and two individual superposed messages, forming a relay output message as

$$\mathbf{d}_R = \begin{bmatrix} \mathbf{d}_A^b \oplus \mathbf{d}_B^b \\ \mathbf{d}_A^s \\ \mathbf{d}_B^s \end{bmatrix}, \tag{10.27}$$

where $\oplus$ denotes a hierarchical function (e.g. bit-wise XOR [12]). It is obvious that each destination D_i, $i \in \{A,B\}$ is able to decode perfectly the desired message $\mathbf{d}_i^T = \left[\left(\mathbf{d}_i^b\right)^T, \left(\mathbf{d}_i^s\right)^T \right]$ iff both the relay message $\mathbf{d}_R$ and effective HSI (given by the basic message $\mathbf{d}_j^b$, $j \in \{A,B\}$, $j \neq i$) are correctly decoded (Fig. 10.10).

[42] Note that SC can be similarly implemented also in the DF, AF and JDF strategies.

The SC power division parameter α becomes obviously the crucial element of the HDF_{SC} system design. It introduces an additional degree of freedom to the system, which in turn allows an optimization of the rates of basic and superposed messages by a proper distribution of the power among them. The rate of basic messages hence can be matched to the actual quality of HSI channels, while still allowing to exploit the remaining capacity (if available) of the relay MAC channel for a transmission of superposed messages. As shown in the following Lemma, it is straightforward to evaluate the maximal sum-rate of the HDF_{SC} scheme as a function of the rates of superposed and basic messages.

Lemma 29. *(*HDF_{SC} *sum-rate):* In step I sources S_A, S_B transmit simultaneously their messages of N_I symbols with rate $r = r_b + r_s$. The maximal sum-rate rate of HDF_{SC} in WBN is then given by:

$$R_{\text{sum}}^{HDF_{SC}}(\gamma_1,\gamma_2,\gamma_3) \leq \frac{2C(\gamma_3)\left(r_b\left(\alpha_{\text{opt}}\right)+r_s\left(\alpha_{\text{opt}}\right)\right)}{C(\gamma_3)+r_b\left(\alpha_{\text{opt}}\right)+2r_s\left(\alpha_{\text{opt}}\right)}, \tag{10.28}$$

where α_{opt} is the optimal value of SC power division parameter maximizing the two-way rate for a given SNR triplet $\gamma_1,\gamma_2,\gamma_3$ and $r_b\left(\alpha_{\text{opt}}\right)$ (respectively $r_s\left(\alpha_{\text{opt}}\right)$) is the optimized rate of basic (respectively superposed) message.

Proof. Total of $N_I(r_A+r_B) = 2N_I r = 2N_I(r_b+r_s)$ bits are transmitted simultaneously from sources S_A, S_B in step I. The relay must send separately three independent messages (10.27) in step II through the relay→destination channel with capacity $C(\gamma_3)$, and hence step II will be at least $N_{II} = \frac{r_b N_I}{C(\gamma_3)} + \frac{2r_s N_I}{C(\gamma_3)}$ symbols long. Consequently, from (10.5) we have $R_{\text{sum}}^{HDF_{SC}} \leq \frac{2N_I(r_b+r_s)}{N_I+N_{II}}$, which gives us finally (10.28). □

As shown in [27], a numerical optimization of α must be performed to find the maximum sum-rate (10.28) of the SC-based strategy. We perform this optimization for HDF_{SC} and compare its maximal sum-rate with R_{sum}^{HDF} (evaluated in Theorem 28). The section is then concluded with an introduction of a $\text{HDF}_{\text{SC}}^{\text{IC}}$ scheme which nicely demonstrates how an inherent correlation of relay and source signals can be exploited to further improve the sum-rate performance in WBN.

10.4.1.1 HDF_{SC} relaying strategy

To provide a fair comparison with R_{sum}^{HDF} (see Theorem 28) we must follow the assumption of independent processing of HSI and relay channel observations (as stated in Section 10.3). Thus, in the basic HDF_{SC} strategy each destination D_i, $i \in \{A,B\}$ performs a decision on HSI (basic message $\mathbf{x}_j^b$, $j \in \{A,B\}$, $j \neq i$) immediately after step I, i.e. prior to the reception (and processing) of relay signal. A numerical optimization of α must be performed to find the rates r_b, r_s maximizing the sum-rate in (10.28). This optimization was performed already in [27] (see also Chapter 9) for a special case of relay processing which assumes a *specific interference cancellation* of the basic messages signal at the relay. However, since a feasibility of such processing has not been proved yet, we modify the relay processing in the HDF_{SC} strategy according to the results of the analysis in Section 10.3.

When $C(\gamma_2) \geq \frac{1}{2}C(2\gamma_1)$ we assume that the rate of superposed message is set to zero ($r_s = 0$) and only the basic messages are transmitted. Since the source rate $r = r_b = \min[C(\gamma_2), C(\gamma_1)]$ is kept bounded below the HSI channel capacity (i.e. $r \leq C(\gamma_2)$) in this region, a perfect HSI processing (see Table 10.2) is feasible. On the other hand (as noted in Section 10.3) we assume that the HDF operation is equivalent to JDF when $C(\gamma_2) < \frac{1}{2}C(2\gamma_1)$. Here, the relay decodes separately both basic and also both superposed messages, which corresponds to an equivalent four-user MAC decoding[43]. This, together with the assumption of destination's HSI decoding after step I (as mentioned above), provides a *set of rate upper-bounds* for basic and superposed messages, as summarized in the following Lemma:

[43] Note that hierarchical message $\mathbf{d}_A^b \oplus \mathbf{d}_B^b$ can be always constructed when both separate basic messages are decoded by the relay.

Lemma 30. *(*HDF_{SC} *messages rates):* If $C(\gamma_2) < \frac{1}{2}C(2\gamma_1)$ the HDF_{SC} relay operates in the JDF mode, and hence the rates of basic (r_b) and superposed messages (r_s) are bounded by the following:
1st order:

$$r_s(\alpha) \leq C(\alpha\gamma_1), \tag{10.29}$$
$$r_b(\alpha) \leq C((1-\alpha)\gamma_1), \tag{10.30}$$

2nd order:

$$2r_s(\alpha) \leq C(2\alpha\gamma_1), \tag{10.31}$$
$$2r_b(\alpha) \leq C(2(1-\alpha)\gamma_1), \tag{10.32}$$
$$r_b(\alpha) + r_s(\alpha) \leq C(\gamma_1), \tag{10.33}$$

3rd order:

$$2r_s(\alpha) + r_b \leq C((1+\alpha)\gamma_1), \tag{10.34}$$
$$r_s(\alpha) + 2r_b \leq C((2-\alpha)\gamma_1), \tag{10.35}$$

and 4th order cut-set bounds:

$$2(r_b(\alpha) + r_s(\alpha)) \leq (2\gamma_1). \tag{10.36}$$

The HSI (basic message) is decoded at destinations after step I from the interference channel, bounding the rate of basic messages as:

$$r_b(\alpha) \leq C\left(\frac{(1-\alpha)\gamma_2}{1+\alpha\gamma_2}\right). \tag{10.37}$$

Proof. Due to the symmetry of analysed WBN we can assume without loss of generality that $r_A = r_B = r = r_b + r_s$ and hence $\alpha_A = \alpha_B$. In step I the relay has the following observation:

$$y_R^{HSI} = h_{S_AR}\left(\sqrt{1-\alpha}s_A^b + \sqrt{\alpha}s_A^s\right) + h_{S_BR}\left(\sqrt{1-\alpha}s_B^b + \sqrt{\alpha}s_B^s\right) + w_R, \tag{10.38}$$

which forms an equivalent 4-user MAC channel. The maximal rates in this channel can be achieved using Successive Decoding – Interference Cancellation (SD-IC) technique [6]. Therefore, a set of upper-bounds of achievable rates for basic and superposed messages can be directly evaluated as a set of particular cut-set bounds [6] of the equivalent MAC channel (10.38). We can immediately evaluate the 1st order (10.29), (10.30), 2nd order (10.31), (10.32), (10.33), 3rd order (10.34), (10.35) and 4th order (10.36) cut-set bounds of this MAC channel. The last bound in Lemma 30 (10.37) corresponds to a decoding of effective HSI from the interference HSI channel $y_{D_i} = h_{S_jD_i}\left(\sqrt{1-\alpha}s_j^b + \sqrt{\alpha}s_j^s\right) + w_i$ at destination D_i, $i, j \in \{A, B\}$ and $i \neq j$. □

Based on the rate bounds evaluated in Lemma 30 a numerical optimization of α can be performed (see [27] for more details) to provide the optimal rates $r_b(\alpha_{\text{opt}})$, $r_s(\alpha_{\text{opt}})$ which maximize the HDF_{SC} sum-rate (10.28). An example of particular optimized values of α, r_b, r_s is evaluated for $\gamma_1 = \gamma_3 = 30\,\text{dB}$ in Fig. 10.11 as a function of γ_2 (compare the results with the proof of Theorem 28). A comparison of the maximal sum-rate of HDF_{SC} with the maximal sum-rate of HDF strategy R_{sum}^{HDF} (10.22) is available in Fig. 10.12. As expected, when $C(\gamma_2) \geq \frac{1}{2}C(2\gamma_1)$, the HDF_{SC} strategy can provide the same sum-rate as R_{sum}^{HDF}. The rates of superposed messages are set to zero (see Fig. 10.11) in this region, and hence a perfect HSI processing can always be performed (see Table 10.2). On the other hand, if $C(\gamma_2) < \frac{1}{2}C(2\gamma_1)$ the HDF_{SC} strategy does not achieve the maximal sum-rate R_{sum}^{HDF} in the whole range of observed channel SNRs $\gamma_1, \gamma_2, \gamma_3$(see Fig. 10.12). A similar information-theoretic sub-optimality of SC-processing was already observed in [120] for the conventional (one-way) relay channel.

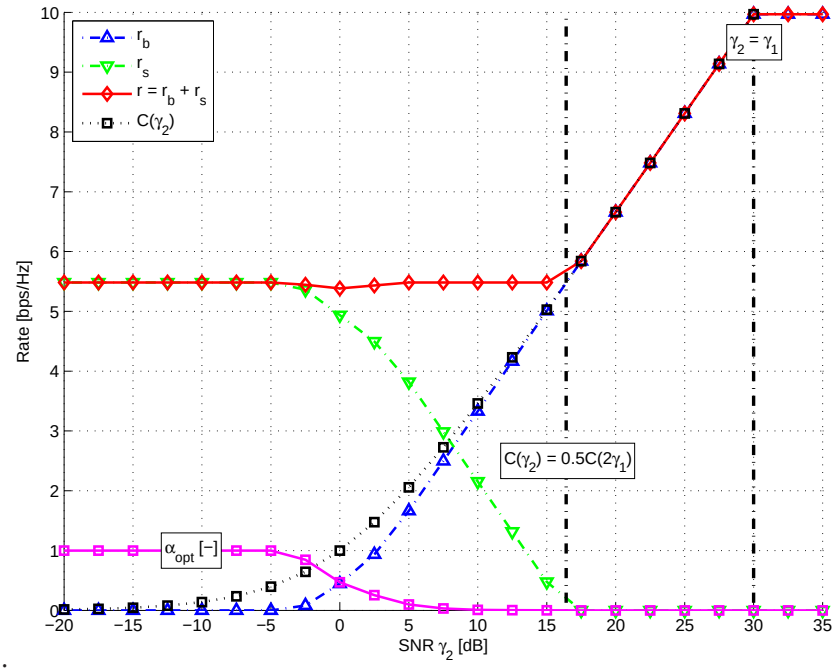

Figure 10.11: Optimized values of α, r_b, r_s as a function of γ_2 ($\gamma_1 = \gamma_3 = 30$ dB).

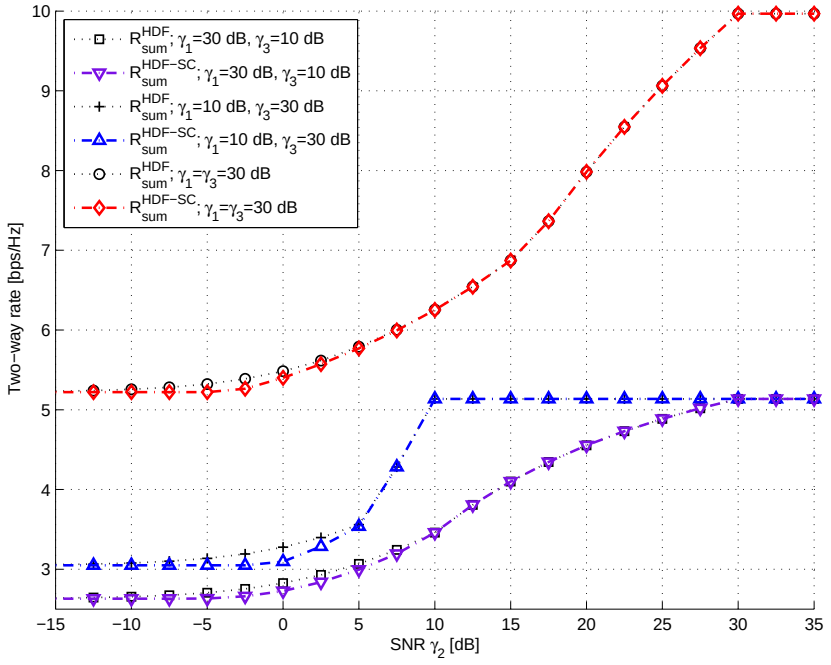

Figure 10.12: Comparison of the upper-bound of the HDF_{SC} sum-rates with R_{sum}^{HDF}.

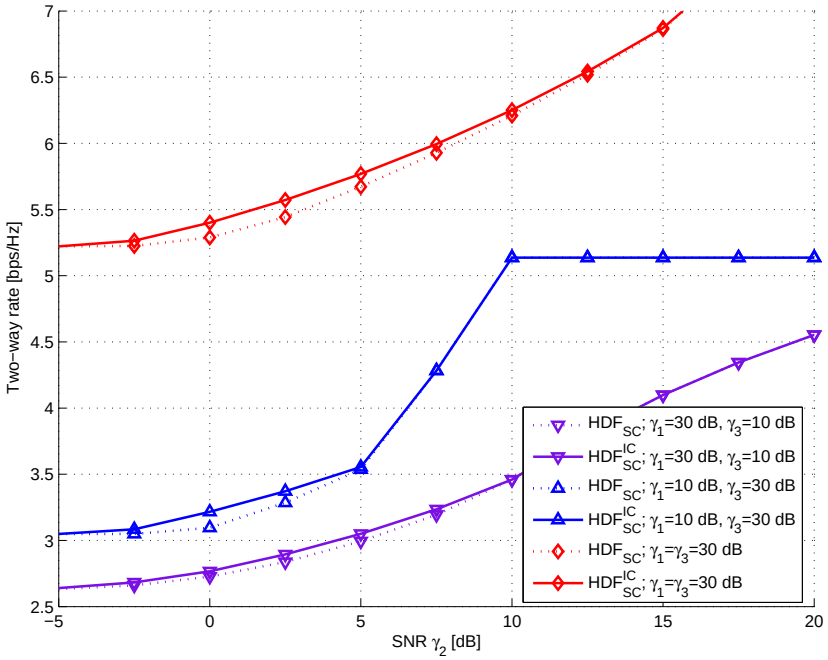

Figure 10.13: Comparison of the upper-bounds of sum-rates in $\mathrm{HDF}_{\mathrm{SC}}$ and $\mathrm{HDF}^{\mathrm{IC}}_{\mathrm{SC}}$.

10.4.1.2 $\mathrm{HDF}^{\mathrm{IC}}_{\mathrm{SC}}$ relaying strategy

Whenever a partial HSI processing is employed, the relay signal could become correlated with the signal transmitted on HSI channels. This happens obviously also in the $\mathrm{HDF}_{\mathrm{SC}}$ strategy, where the superposed messages influence both the relay signal (10.27) and signal on the HSI channels. Since the superposed message $\mathbf{d}^{\mathrm{s}}_j$, $j \in \{A,B\}$ is contained in the relay message $\mathbf{d}_R$ (decoded at both destinations), each destination D_i, $i \in \{A,B\}$, $i \neq j$ can remove the corresponding interfering superposed message signal from its HSI channel observation (see Fig. 10.10) to obtain an equivalent *interference free HSI channel* (see Chapter 9). This allows to further relax the last bound in Lemma 30 (10.37) to $r_b(\alpha) \leq C((1-\alpha)\gamma_2)$. We denote the strategy where this interference cancellation of superposed messages from HSI channel observations is performed as $\mathrm{HDF}^{\mathrm{IC}}_{\mathrm{SC}}$. A marginal sum-rate gain which can be achieved in $\mathrm{HDF}^{\mathrm{IC}}_{\mathrm{SC}}$ (when compared to $\mathrm{HDF}_{\mathrm{SC}}$) is visualized in Fig. 10.13. Note that the slight performance improvement over $\mathrm{HDF}_{\mathrm{SC}}$ can be achieved only when partial HSI processing is performed (i.e. when $r_s \neq 0 \wedge r_b \neq 0$ – compare with Fig. 10.11 for $\gamma_1 = \gamma_3 = 30$ dB).

10.5 Discussion of results

The impact of imperfect HSI on the sum-rate performance of WNC relaying strategies in WBN is analysed in this Chapter. An information-theoretic investigation was conducted to provide the maximal sum-rates of the WNC relaying strategies and the performance of all strategies was compared as a function of the quality of HSI channels. It was shown that all strategies are able to operate even with a limited (partial) HSI, if an appropriate modification of each strategy is applied. This partial HSI processing can usually provide a better sum-rate than the straightforward solution, where the perfect HSI operation is secured by a decrease of source transmission rates.

Apart of the sum-rates of particular strategies, the optimal distribution of time between the two communication steps was also analysed to stress that optimal sum-rate performance can be achieved only if unequal lengths of steps I, II are allowed. Since the performance of both perfect and partial HSI processing in all strategies greatly depends on the actual channel conditions in the system, it should be neccessary to implement some sort of feedback in WBN to match the strategy (perfect/partial), source rates and relay processing to the actual channel quality and thus to maximize the sum-rate performance of the system. The Chapter is concluded with an analysis of two novel SC-based HDF strategies, which provide a natural information theoretic tool for implementation of HDF in WBN, allowing to further improve the sum-rate performance by exploiting the natural correlation of source and relay signals (as demonstrated in the $\mathrm{HDF}_{\mathrm{SC}}^{\mathrm{IC}}$ strategy).

Chapter 11

Design of eXclusive mapper for wireless butterfly network

"Design is not just what it looks like and feels like. Design is how it works."

Steve Jobs

11.1 Introduction

As noted already in Section 8.1, one of the crucial steps in the HDF system design is the choice of a suitable eXclusive mapper at the relay. Simply speaking, this mapper defines how the separate data streams (from individual users) are mapped to the *hierarchical* (network-coded) data [71] stream at the relay node. The unreliable transmission of HSI in WBN can be overcome by increasing the cardinality of the relay output [71]. A design of this eXclusive mapping operation is quite simple for the *minimal mapping* (perfect HSI assumption) operation, where it is usually given by a simple bit-wise xor operation. However, in case of the *extended cardinality mapping* (see Fig. 3.10), a suitable eXclusive mapper must respect the amount of HSI at destinations to maximize the system throughput.

In this Chapter we focus on this problem. We introduce a systematic approach to the design of a *set of relay eXclusive output mappers* for relay output mapping in WBN. The scope is mainly on the relay processing and the subsequent BC phase of communication. In a numerical evaluation of the alphabet-constrained capacity (mutual information) we show how the performance of WBN can be controlled by a suitable choice (from a pre-designed set) of the relay eXclusive output mapper. These results pave the way for an idea of adaptive butterfly network, where the performance can be adapted to the actual channel conditions (and thus the quality of HSI).

11.2 Summary of definitions and assumptions

We adopt the general WBN model defined in Section 8.2. The main goal of this Chapter is the design of suitable relay *eXclusive mappers*, and hence we assume a perfect MAC phase (reliable decoding of arbitrary function $c_{AB} = f(c_A, c_B)$ is possible at the relay). Nevertheless, the proposed eXclusive mappers do not depend on the particular source alphabets and hence they are feasible also for the butterfly network with optimized parametric source alphabets (see Part II). For the purpose of this Chapter we evaluate the quality of HSI links by a number of "reliably" received channel symbol bits, i.e. c^A_{HSI} (for D_A) and c^B_{HSI} (for D_B), where $c^A_{\mathrm{HSI}}, c^B_{\mathrm{HSI}} \in \{0, 1, \ldots, \log_2 M_s\}$ and M_s is the source alphabet cardinality.

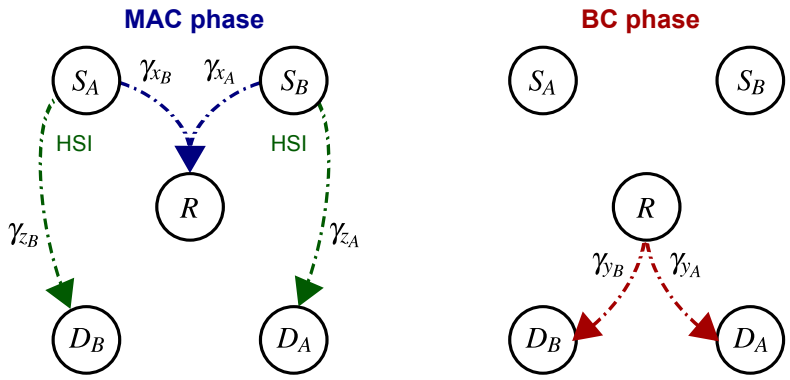

Figure 11.1: Signal-to-Noise Ratios (SNRs) of individual links in WBN with HDF strategy.

11.2.1 Relay output eXclusive mapping

In HDF systems the relay performs an eXclusive mapping operation (see [71] for details) to map the received signal to the relay output $s_R(c_R)$, where $c_R = c_{AB} = \mathscr{X}_c\left(c_A^i, c_B^j\right)$. This hierarchical symbol mapping is referred to as the *Hierarchical Network Code* (HNC map) in [119]. Note again that in principle the hierarchical (network-coded) output signal from the relay must jointly represent the data from both sources (S_A, S_B), while a knowledge of respective HSI at the destination is necessary for a successful decoding of the desired (separate) data stream [71].

For the purpose of this Chapter we assume that HNC mapping operation can be described directly on the signal-space symbol level $s_R^{k_{ij}} = \mathscr{X}_s\left(s_A^i, s_B^j\right)$. In this case it is suitable to describe the specific HNC mapping by the HNC matrix

$$X_s = \begin{bmatrix} k_{11} & \cdots & k_{1M_s} \\ \vdots & \ddots & \vdots \\ k_{M_s1} & \cdots & k_{M_sM_s} \end{bmatrix}, \tag{11.1}$$

where $k_{ij} = X_s(i,j)$, $i,j \in \{1,2,\ldots M_s\}$ is the index of the relay output (signal space) symbol $s_R^{k_{ij}} \in \mathscr{A}_s^R$. Note that for the cardinality of the relay output alphabet holds (see e.g. [71]):

$$|\mathscr{A}_s| = M_s \leq \left|\mathscr{A}_s^R\right| \leq M_s^2 = |\mathscr{A}_s|^2, \tag{11.2}$$

where $|\mathscr{A}_s| = \left|\mathscr{A}_s^A\right| = \left|\mathscr{A}_s^B\right| = M_s$ is the source alphabet cardinality (assumed identical at both sources). The equalities in (11.2) correspond to the minimal ($\left|\mathscr{A}_s^R\right| = |\mathscr{A}_s|$) and full ($\left|\mathscr{A}_s^R\right| = |\mathscr{A}_s|^2$) mapping (see [71, 96] or Section 3.2.2). More details about the relay output alphabet cardinality and corresponding required amount of the HSI are provided later. Assuming that a suitable HNC mapper has been used at the relay, destinations are able to decode the desired data from the relay signal and HSI.

11.3 The role of HSI

The amount of information on the complementary data stream (HSI) which is available at D_i (after the MAC phase) is given by a number of reliably received bits c_{HSI}^i, $i \in \{A,B\}$. This corresponds to a level of granularity at which the destination can distinguish particular symbols received on the HSI link, and consequently also to the partitioning of the HNC map (HNC matrix X_s). For the unambiguous decoding each destination needs to identify only the relay symbol inside the resulting subset of the HNC map

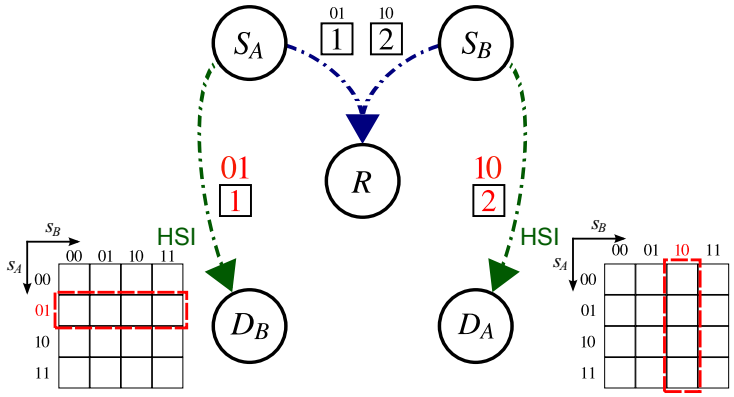

Figure 11.2: Butterfly network with perfect HSI links ($c^A_{\text{HSI}} = c^B_{\text{HSI}} = 2$).

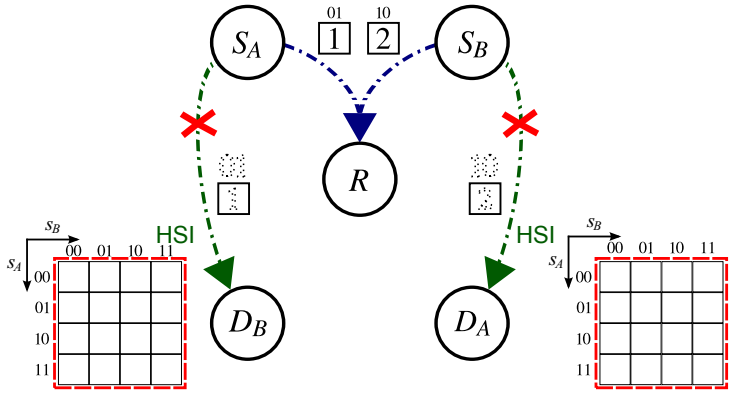

Figure 11.3: Butterfly network with unreliable/missing HSI links ($c^A_{\text{HSI}} = c^B_{\text{HSI}} = 0$).

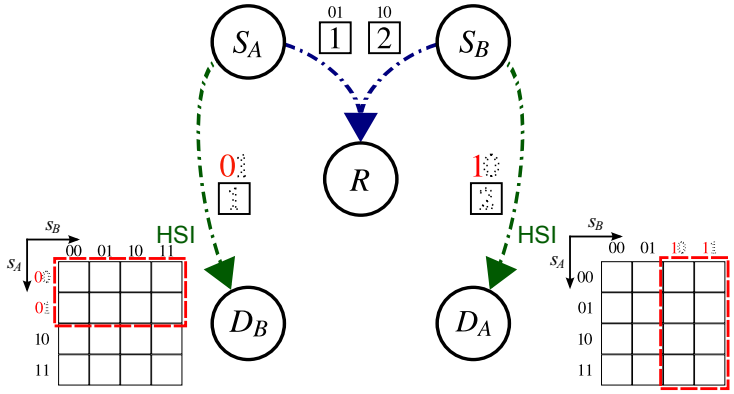

Figure 11.4: Butterfly network with imperfect HSI links ($c^A_{\text{HSI}} = c^b_{\text{HSI}} = 1$). Imperfection of the HSI links can be visualized as a loss of (several) least significant bits (only the last bit is lost in this example).

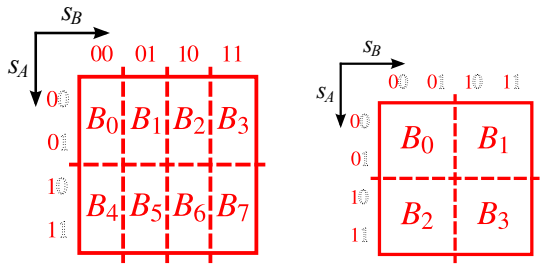

Figure 11.5: Examples of HNC matrix partitioning for $c^A_{\mathrm{HSI}} = 2$, $c^B_{\mathrm{HSI}} = 1$ and $c^A_{\mathrm{HSI}} = c^B_{\mathrm{HSI}} = 1$.

(submatrix of X_s). This is obvious from the example system with $|\mathscr{A}_s| = 4$ in Figs. 11.2, 11.3, 11.4 for perfect, zero and partial HSI (respectively).

As proved e.g. in [97], for unambiguous decoding in the presence of perfect HSI at each destination each particular relay output symbol can appear at most once on each row and in each column of the HNC map (see Fig. 11.2). This corresponds to the *minimal cardinality* relay output mapping ($\left|\mathscr{A}^R_s\right| = M_s$). Similarly (as also noted in [97]), for the case of partial/imperfect HSI each particular relay output symbol can appear at most once within a group of rows/columns (given by the HNC map partitioning – see Fig. 11.4). This corresponds to the *extended cardinality* relay output mapping. In the last case, i.e. in the butterfly network where the HSI links are completly missing (Fig. 11.3), the relay needs to deliver data to both sources without assistance of HSI and hence a *full cardinality* relay output mapping ($\left|\mathscr{A}^R_s\right| = M_s^2$) is required.

As it is obvious from the discussion above, HSI (overheard by destinations in the MAC phase) has a crucial impact on the overall system performance, since it determines a required minimal cardinality of the relay output alphabet $\left|\mathscr{A}^R_s\right|$ (as proved e.g. in [97]). This is obviously a direct consequence of the eXclusive law (see e.g. [71]). Accordingly, HSI introduces some preconditions on a suitable HNC matrix design. In the following section we introduce an algorithm for the design of a set of HNC matrices for arbitrary source alphabet cardinality M_s (and the corresponding range of permissible values of c^A_{HSI}, c^B_{HSI}).

11.4 HNC mapper design

As noted in the previous section, the quality of HSI links defines the partitioning of the HNC matrix X_s (see examples in Figs. 11.2, 11.3, 11.4), where unique relay output symbols are required in all the resulting submatrices (for a given c^A_{HSI}, c^B_{HSI}). In this way X_s can be partitioned into a set of (generally rectangular) blocks B_l (see examples in Fig. 11.5).

This observation leads to an idea of a systematic, block-based design of the HNC matrix. A suitable X_s must have unique symbols in each individual block B_l and also in all the respective subsets of blocks corresponding to the given partitioning (e.g. $\{B_0, B_1, B_2, B_3\}$, $\{B_4, B_5, B_6, B_7\}$ and $\{B_0, B_4\}$, $\{B_1, B_5\}$, $\{B_2, B_6\}$, $\{B_3, B_7\}$ in Fig. 11.5).

It is interesting to note that square building blocks B_l can be assumed without loss of generality (for arbitrary c^A_{HSI}, c^B_{HSI})[44]. Each individual block is hence a $\mathscr{B} \times \mathscr{B}$ submatrix of X_s. The block dimensionality is given by $\mathscr{B} = M_s/2^{c_{\mathrm{HSI}}}$, where $c_{\mathrm{HSI}} = \min\left\{c^A_{\mathrm{HSI}}, c^B_{\mathrm{HSI}}\right\}$. The HNC matrix designed for the source alphabet with cardinality M_s and CSI-links quality c_{HSI} will be denoted as $X^{(c_{\mathrm{HSI}})}_{M_s}$. The design algorithm

[44] The minimal required relay alphabet cardinality $\left|\mathscr{A}^R_s\right|$ is given by the weaker HSI link. To clarify this statement we can consider an example where one HSI link is fully unreliable (e.g. $c^A_{\mathrm{HSI}} = 0$). In this case the relay must use full cardinality relaying in order to guarantee successful decoding at D_A (even if D_B has a perfect HSI available). Hence for the purpose of the HNC mapper design we can assume the same level of partitioning given by $c_{\mathrm{HSI}} = \min\left\{c^A_{\mathrm{HSI}}, c^B_{\mathrm{HSI}}\right\}$, resulting in the square blocks B_l.

Algorithm 11.1 HNC matrix $X_{M_s}^{(m)}$ design ($M_s = |\mathscr{A}_s|$, $m = c_{\text{HSI}}$).

1. Assumptions:
   (a) Block dimensionality: $\mathscr{B} = {}^{M_s}/_{2^m}$
   (b) Number of unique blocks: $L = 2^m$
   (c) Input elements: $k \in \mathscr{K} = \left\{0, 1, 2, \ldots \left({}^{M_s^2}/_{L}\right) - 1\right\}$
2. Design the set of blocks $\{B_l\}_{l=0}^{L-1}$:
   (a) Partition the set $\mathscr{K}$ into L non-overlapping subsets $\mathscr{K}_l$, where $|\mathscr{K}_l| = \mathscr{B}^2$, $\forall l \in \{0, \ldots L-1\}$
   (b) Fill in successively (e.g. columnwise) the block B_l with unique elements from $\mathscr{K}_l$
3. Set up (block-by-block) the HNC matrix $X_{M_s}^{(m)}$:
   (a) $A_{i,j} = B_{i \oplus j}$, where $i, j \in \{0, 1, \ldots L-1\}$ and $\oplus$ is a bit-wise XOR
   (b) $X_{M_s}^{(m)} = \begin{bmatrix} A_{0,0} & \cdots & A_{0,L-1} \\ \vdots & \ddots & \vdots \\ A_{L-1,0} & \cdots & A_{L-1,L-1} \end{bmatrix}$

c_{HSI}	1	2
$X_4^{(c_{\text{HSI}})}$	$\left[\begin{array}{cc\|cc} 0 & 2 & 4 & 6 \\ 1 & 3 & 5 & 7 \\ \hline 4 & 6 & 0 & 2 \\ 5 & 7 & 1 & 3 \end{array}\right]$	$\left[\begin{array}{c\|c\|c\|c} 0 & 1 & 2 & 3 \\ \hline 1 & 0 & 3 & 2 \\ \hline 2 & 3 & 0 & 1 \\ \hline 3 & 2 & 1 & 0 \end{array}\right]$

Table 11.1: Example HNC matrices $X_4^{(1)}$ and $X_4^{(2)}$.

for HNC matrix $X_{M_s}^{(c_{\text{HSI}})}$ is summarized in Algorithm 11.1.

The complete set of HNC matrices $X_{M_s}^{(c_{\text{HSI}})}$ for given M_s and all permissible values of c_{HSI} ($0 \leq c_{\text{HSI}} \leq \log_2 M_s$) can be designed with Algorithm 11.1. This design algorithm is suitable even for the design of HNC mappers for minimal ($\mathscr{B} = 1, L = M_s$) and full cardinality ($\mathscr{B} = M_s, L = 1$) relaying. Some examples of the proposed HNC matrices are given in Tables 11.1, 11.2 for $M_s = 4$ and $M_s = 8$ (respectively). As it is also obvious from these tables, the cardinality of the relay output alphabet is given by

$$\left|\mathscr{A}_s^R\right| = |\mathscr{K}| = \frac{M_s^2}{L}. \tag{11.3}$$

11.4.1 Source alphabet partitioning

The HNC mapper design in Algorithm 11.1 is based on the assumption that each destination can identify (at least) first c_{HSI} bits from the constellation symbol received on the HSI link (except for the full cardinality case) – see examples in Figs. 11.2, 11.4. Interestingly, it is possible to increase the reliability of this (partial) HSI by a suitable partitioning (and corresponding constellation indexing) of both source alphabets $\mathscr{A}_s$.

c_{HSI}	1	2
$X_8^{(c_{\mathrm{HSI}})}$	$\left[\begin{array}{cccc\|cccc} 0 & 4 & 8 & 12 & 16 & 20 & 24 & 28 \\ 1 & 5 & 9 & 13 & 17 & 21 & 25 & 29 \\ 2 & 6 & 10 & 14 & 18 & 22 & 26 & 30 \\ 3 & 7 & 11 & 15 & 19 & 23 & 27 & 31 \\ \hline 16 & 20 & 24 & 28 & 0 & 4 & 8 & 12 \\ 17 & 21 & 25 & 29 & 1 & 5 & 9 & 13 \\ 18 & 22 & 26 & 30 & 2 & 6 & 10 & 14 \\ 19 & 23 & 27 & 31 & 3 & 7 & 11 & 15 \end{array}\right]$	$\left[\begin{array}{cc\|cc\|cc\|cc} 0 & 2 & 4 & 6 & 8 & 10 & 12 & 14 \\ 1 & 3 & 5 & 7 & 9 & 11 & 13 & 15 \\ \hline 4 & 6 & 0 & 2 & 12 & 14 & 8 & 10 \\ 5 & 7 & 1 & 3 & 13 & 15 & 9 & 11 \\ \hline 8 & 10 & 12 & 14 & 0 & 2 & 4 & 6 \\ 9 & 11 & 13 & 15 & 1 & 3 & 5 & 7 \\ \hline 12 & 14 & 8 & 10 & 4 & 6 & 0 & 2 \\ 13 & 15 & 9 & 11 & 5 & 7 & 1 & 3 \end{array}\right]$

Table 11.2: Example HNC matrices $X_8^{(1)}$ and $X_8^{(2)}$.

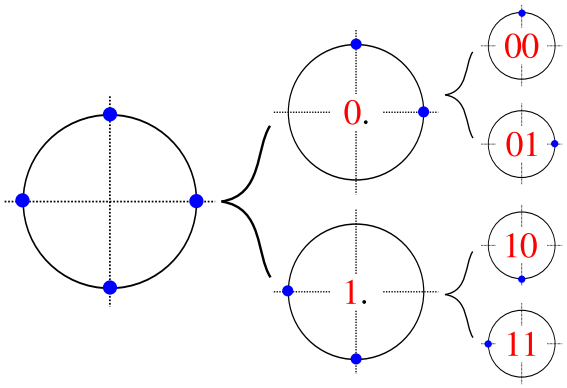

Figure 11.6: Partitioning of QPSK source constellation alphabet.

The idea is to partition the source constellation alphabet into smaller subsets (according to the principles similar to Ungerboeck mapping rules [123]) to increase the probability of successful (partial) HSI retrieval at the destination. Hence the intention is to maximize the distance between the particular subsets (not the particular symbols)[45]. The principle of the proposed source constellation alphabet partitioning is visualized in Figs. 11.6, 11.7 for QPSK and 8PSK (respectively).

11.5 Numerical evaluations

In this section we finally demonstrate a feasibility of the proposed HNC mapper design (Algorithm 11.1) for WBN. Without loss of generality, we focus on the D_B processing. Destination D_B has two channel observations – the relay (network-coded) signal $y_B(c_R)$ and HSI link $z_B(c_A)$.

Since the relay transmits a common signal to both destinations, the broadcast phase capacity region is *rectangular* [96] with maximum rate given by $I(c_B;y_B,z_B)$ (and similarly for D_A). The broadcast phase alphabet-constrained capacity [96] (mutual information) is given by

$$C_{\mathrm{HBC}} = I(c_B;y_B,z_B) = \mathscr{H}[y_B,z_B] - \mathscr{H}[y_B,z_B|c_B]. \tag{11.4}$$

[45] This should be clear e.g. from Fig. 11.4, where symbols 00 and 01 define the same subset of the HNC map and consequently the successful decoding would be possible even if the destination is unable to distinguish between these two symbols on the HSI link. Hence, these symbols should be grouped into one subset $\{00,01\}$ (and similarly for the other symbols).

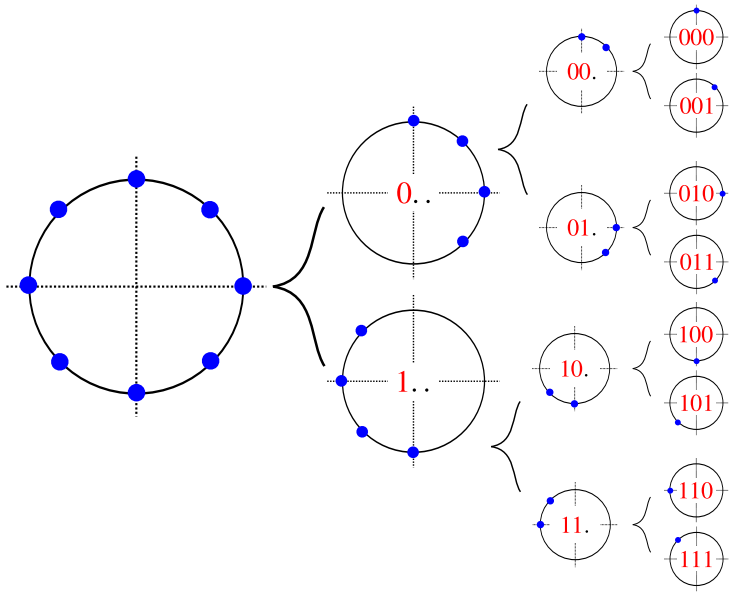

Figure 11.7: Partitioning of the 8PSK source constellation alphabet.

The pure HSI link capacity $C_{\mathrm{HSI}} = I(c_A; z_B)$ will be also evaluated (for a comparison)[46]. This capacity is simply a capacity of the Gaussian (alphabet constrained) channel [96].

The alphabet constrained capacities were evaluated numerically by the Monte-Carlo integral evaluation (for details see [96] and references therein). The broadcast phase capacity was evaluated as a function of the HSI link SNR (γ_{z_B}) for various relay-to-destination SNR (γ_{y_B}). The results are on Figs. 11.8, 11.9, 11.10 (QPSK source alphabet) and on Figs. 11.12, 11.13, 11.14, 11.16 (8PSK source alphabet). For all these results the source alphabets were partitioned according to the Figs. 11.6, 11.7 and the HNC mappers (matrices $X_{M_s}^{(c_{\mathrm{HSI}})}$) were designed using the Algorithm 11.1.

For the extended relaying scenarios we have evaluated also the capacities for source alphabets with Ungerboeck [123] mapping (see Figs. 11.11, 11.15, 11.17). Here a significant degradation of the broadcast phase capacity can be observed (see Figs. 11.10 and 11.11; Figs. 11.14 and 11.15; Figs. 11.16 and 11.17), although the HSI link capacity is identical for both compared source alphabet partitioning. Hence, it is obvious that Ungerboeck source alphabet partitioning is not appropriate for the proposed HNC mappers.

11.5.1 Adaptive butterfly network performance

As it is clear from the presented numerical results, the achievable broadcast phase capacity depends strongly on the employed HNC mapper. Obviously, by a suitable choice of the HNC mapper (according to the actual channel conditions) it would be possible to maximize the throughput of the system. Provided that the observed quality of the HSI link is delivered to the relay by both destinations D_A, D_B, a suitable HNC mapper can be chosen (from the predesigned set) to maximize the achievable capacity of the network.

To demonstrate a potential performance of such a system, we assume a genie-aided relay which

[46] It is important to note that some caution is necessary when interpreting the numerically evaluated HSI link capacity and the HSI link "quality indicator" c_{HSI} used in this Chapter. Obviously, the particular value of c_{HSI} does not directly correspond to the HSI link capacity and the proper relation between these quantities needs further investigation.

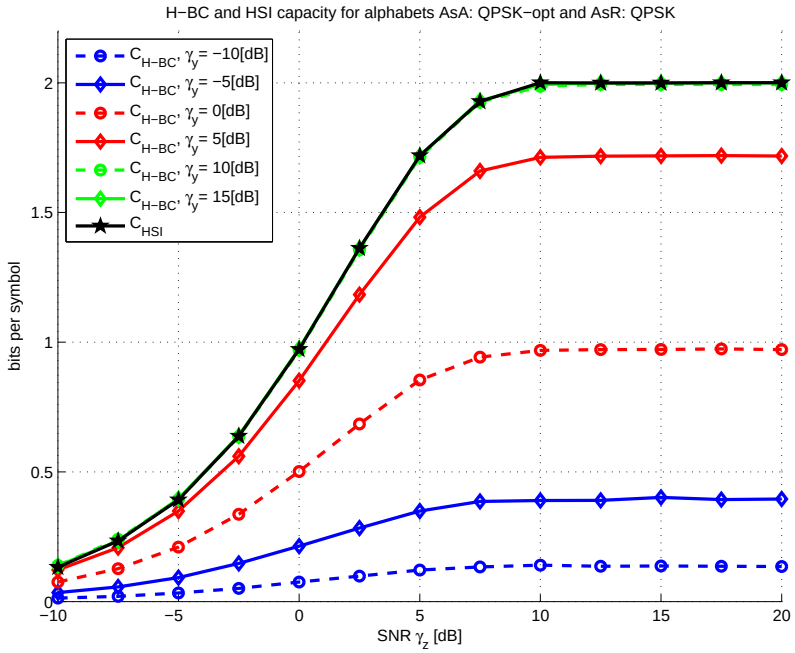

Figure 11.8: BC phase alphabet constrained capacity and capacity of the HSI link (minimal mapping, $\mathscr{A}_s = \text{QPSK}$, $\mathscr{A}_s^R = \text{QPSK}$).

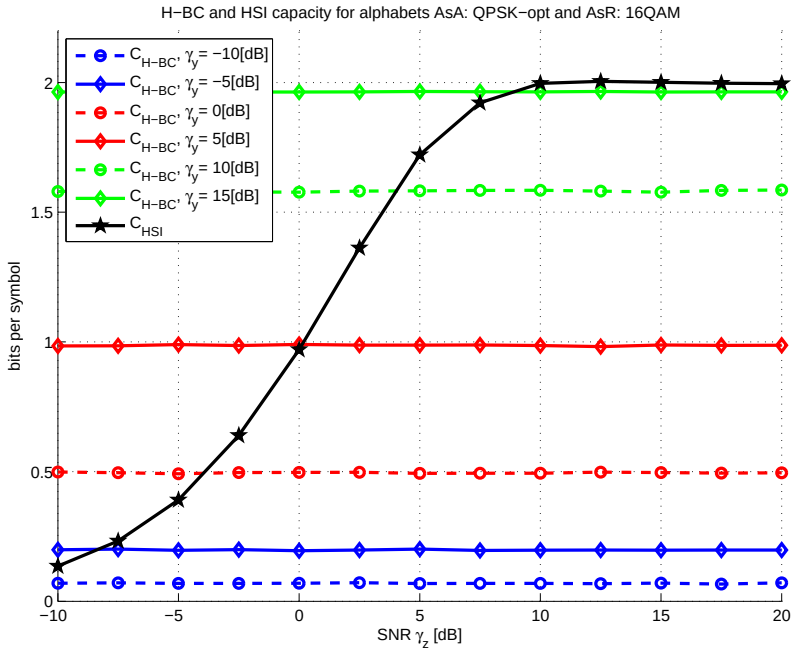

Figure 11.9: BC phase alphabet constrained capacity and capacity of the HSI link (full mapping, $\mathscr{A}_s = \text{QPSK}$, $\mathscr{A}_s^R = \text{16QAM}$).

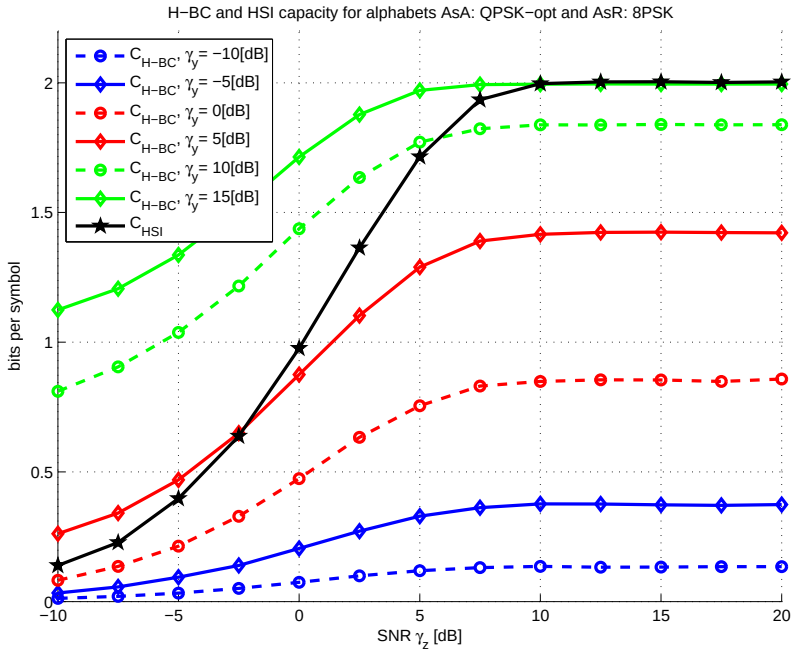

Figure 11.10: BC phase alphabet constrained capacity and capacity of the HSI link (extended mapping, $\mathscr{A}_s = \text{QPSK}$, $\mathscr{A}_s^R = \text{8PSK}$).

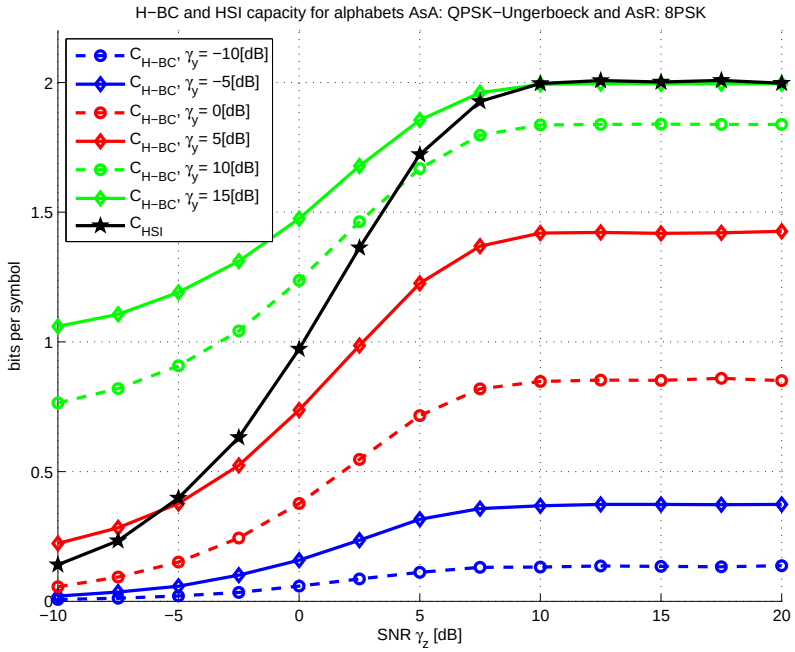

Figure 11.11: BC phase alphabet constrained capacity and capacity of the HSI link (extended mapping, $\mathscr{A}_s = \text{QPSK}$ with Ungerboeck mapping, $\mathscr{A}_s^R = \text{8PSK}$). Compare with Fig. 11.10.

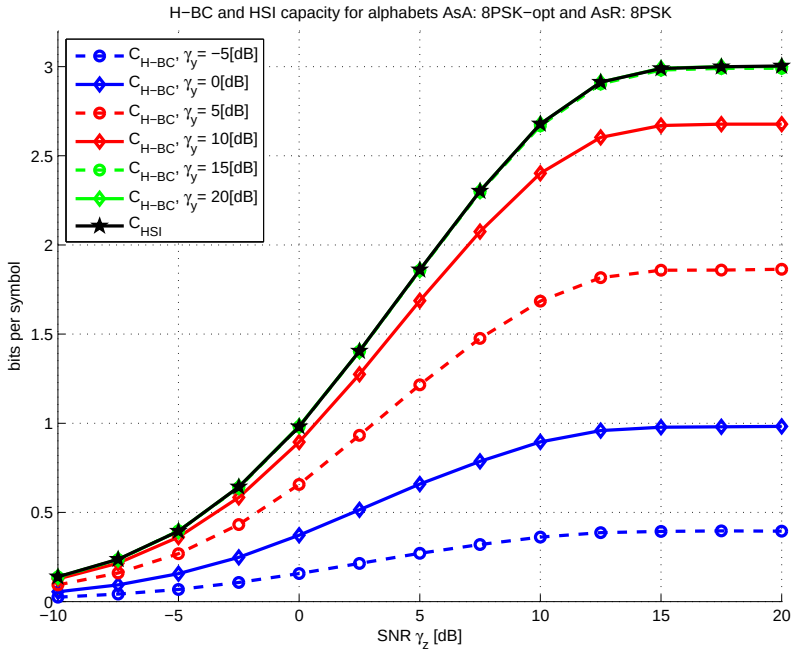

Figure 11.12: BC phase alphabet constrained capacity and capacity of the HSI link (minimal mapping, $\mathscr{A}_s = 8\text{PSK}$, $\mathscr{A}_s^R = 8\text{PSK}$).

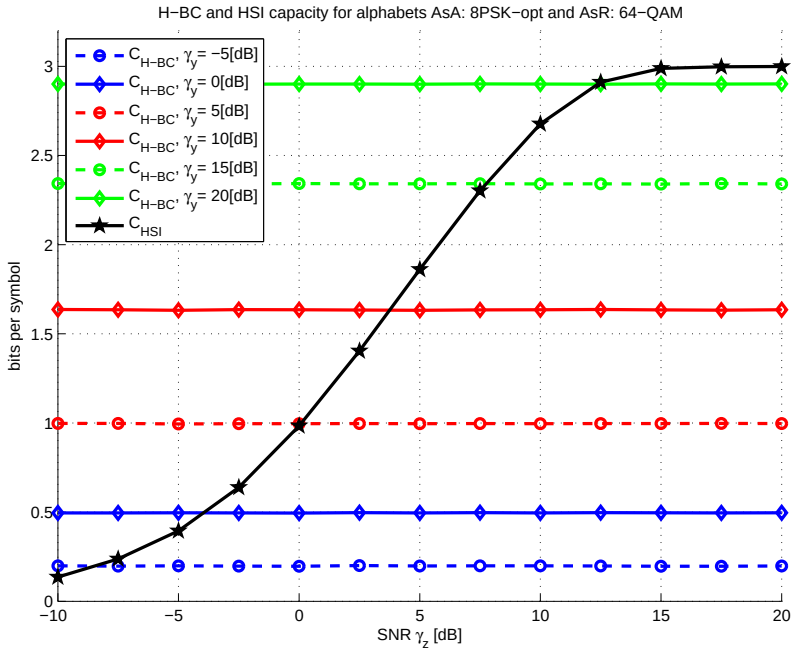

Figure 11.13: BC phase alphabet constrained capacity and capacity of the HSI link (full mapping, $\mathscr{A}_s = 8\text{PSK}$, $\mathscr{A}_s^R = 64\text{QAM}$).

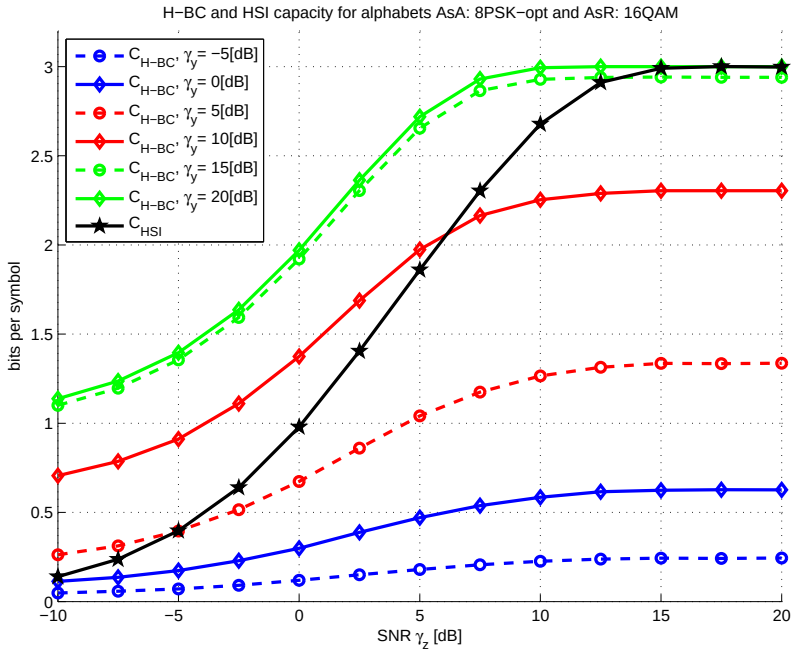

Figure 11.14: BC phase alphabet constrained capacity and capacity of the HSI link (extended mapping, $\mathscr{A}_s = 8\text{PSK}$, $\mathscr{A}_s^R = 16\text{QAM}$).

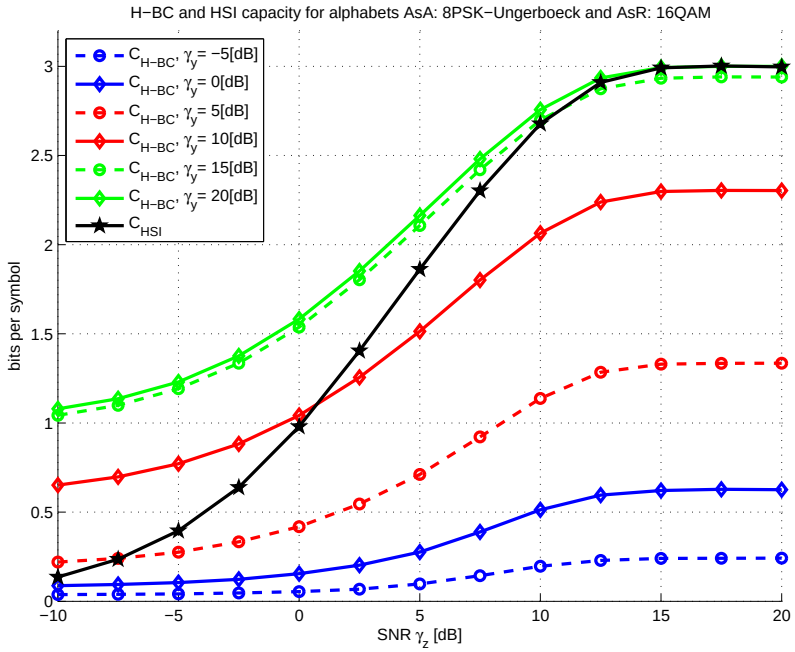

Figure 11.15: BC phase alphabet constrained capacity and capacity of the HSI link (extended mapping, $\mathscr{A}_s = 8\text{PSK}$ with Ungerboeck mapping, $\mathscr{A}_s^R = 16\text{QAM}$). Compare with Fig. 11.14.

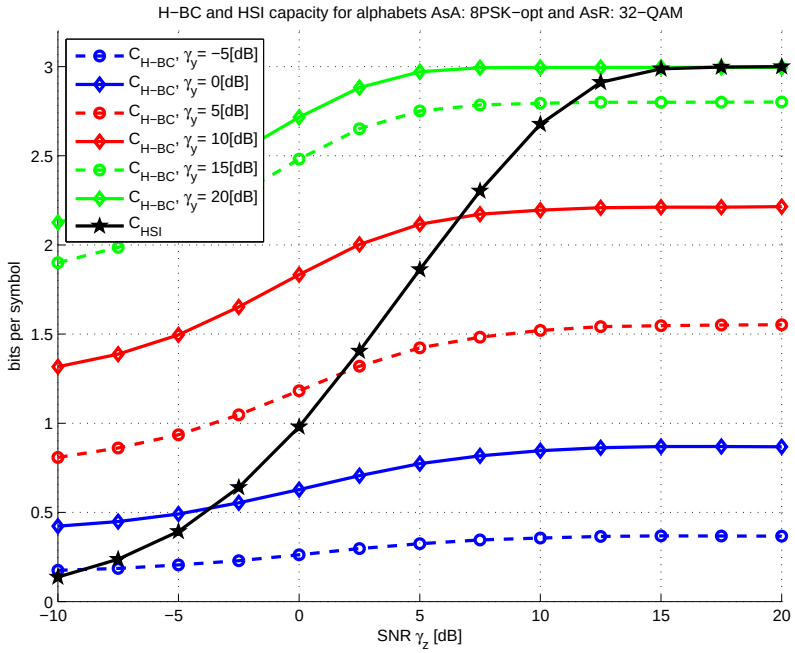

Figure 11.16: BC phase alphabet constrained capacity and capacity of the HSI link (extended mapping, $\mathscr{A}_s = 8\text{PSK}$, $\mathscr{A}_s^R = 32\text{QAM}$).

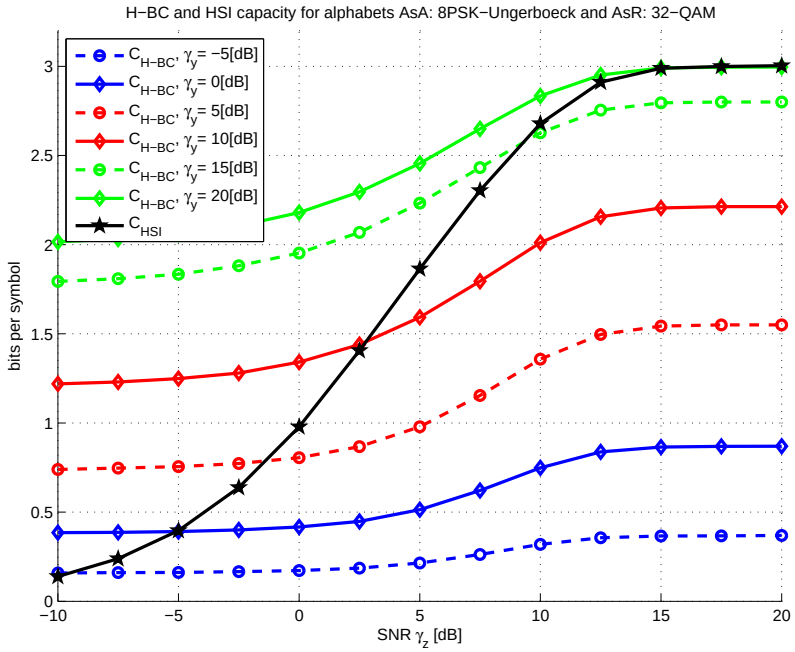

Figure 11.17: BC phase alphabet constrained capacity and capacity of the HSI link (extended mapping, $\mathscr{A}_s = 8\text{PSK}$ with Ungerboeck mapping, $\mathscr{A}_s^R = 32\text{QAM}$). Compare with Fig. 11.16.

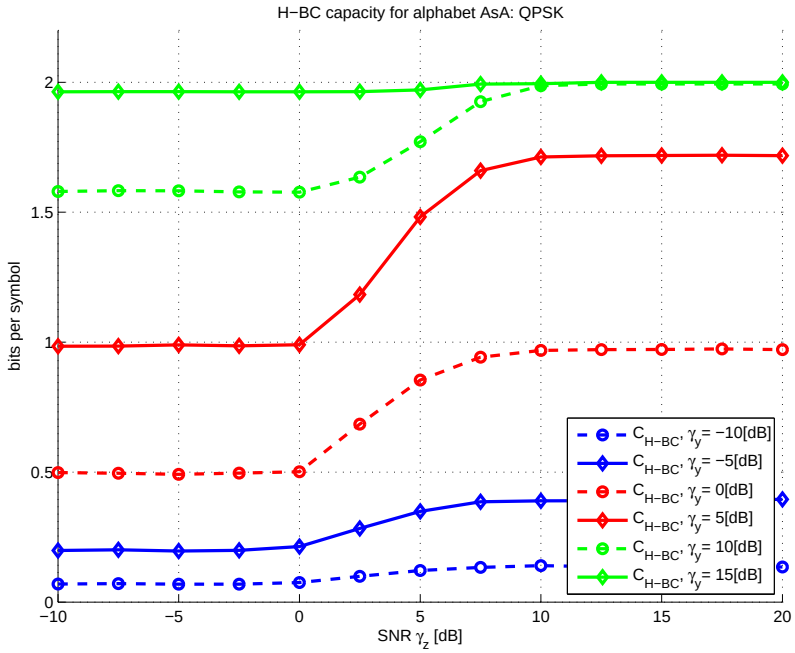

Figure 11.18: Maximum achievable BC phase (alphabet constrained) capacity for the adaptive butterfly network ($\mathscr{A}_S = \text{QPSK}$).

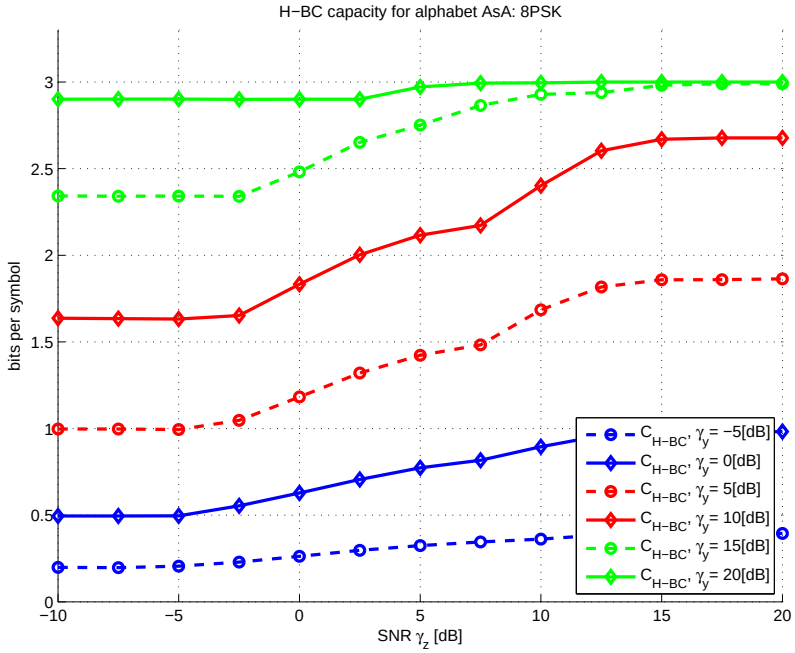

Figure 11.19: Maximum achievable BC phase (alphabet constrained) capacity for the adaptive butterfly network ($\mathscr{A}_S = \text{8PSK}$).

possess a perfect knowledge about the actual quality of the HSI links quality (γ_{z_A}, γ_{z_B}) and the respective relay to destination links (γ_{y_A}, γ_{y_B}). The achievable broadcast phase capacity of this (genie-aided) system is evaluated in Figs. 11.18, 11.19 for QPSK and 8PSK (respectively) source alphabets.

11.6 Discussion of results

A systematic algorithm for the HNC mapper design (see Algorithm 11.1) for relaying in WBN with HDF strategy is introduced in this Chapter. The feasibility of the proposed HNC mappers is demonstrated on the evaluation of the broadcast phase capacity. The fact that suitable *source alphabet partitioning* must be performed to increase the probability of successful (partial) HSI retrieval at destinations (to maximize the achievable capacity of the system) was also pointed out. The observed behaviour of the broadcast phase capacities encourages the idea of adaptive butterfly network, where the performance of the system can be adapted to the actual quality of the HSI and relay to destination links.

Chapter 12

NuT constellations for imperfect HSI relaying

"The only nice thing about being imperfect is the joy it brings to others."

Doug Larson

12.1 Introduction

Since 2-WRC can be viewed as the perfect HSI equivalent of WBN, the promising parametric channel performance of *NuT source alphabets* (see Chapter 7) can be likewise efficiently exploited in the WBN systems [17]. The non-uniform distribution of power between the two slots of the NuT constellation *super-symbol* can, however, degrade the performance on the HSI link (resulting in a significant performance loss). To avoid this performance degradation, we propose to employ the *extended cardinality relaying* (see Chapter 11), where only the stronger slot is harnessed as *partial HSI* (see Fig. 12.1), while the weaker slot can be discarded. Although an *increased cardinality* of the relay output is required to guarantee successful decoding at both destinations (see [24] for details), this approach can outperform the minimal cardinality case, where both slots of NuT constellation are utilized as HSI. The extended cardinality relaying hence offers an efficient trade-off between the amount of HSI (one/two slots of NuT constellation) and required relay output alphabet cardinality.

12.2 WBN with HDF strategy

We adopt again the general WBN model defined in Section 8.2 (see Fig. 12.2). The relay decodes only the *superimposed* (hierarchical) *symbol* in the MAC phase of the communication (instead of joint decoding of the two separate data streams). After receiving the MAC phase signal, the relay performs an eXclusive mapping operation to map the received *compound* symbol to the relay output symbol $s_R(c_{AB}) \in \mathscr{A}_s^R$, where $c_{AB} = \mathscr{X}_c\left(c_A^i, c_B^j\right)$ is the eXclusive mapping operation (HNC mapper [119]). More details on the cardinality of the relay output alphabet ($\left|\mathscr{A}_s^R\right| = M_R$) are be provided in the next section. In the following BC phase the relay output symbol is broadcast to both destinations. Assuming that a suitable HNC map is used by the relay (see Chapter 11), destinations are able to decode the desired data from the relay signal and HSI. The HSI and BC channels are (for the purpose of this Chapter) considered as pure Gaussian, whereas the MAC channel is considered to be parametric to embrace the detrimental effects of channel parametrization on the WNC processing (for details see [16] and references therein).

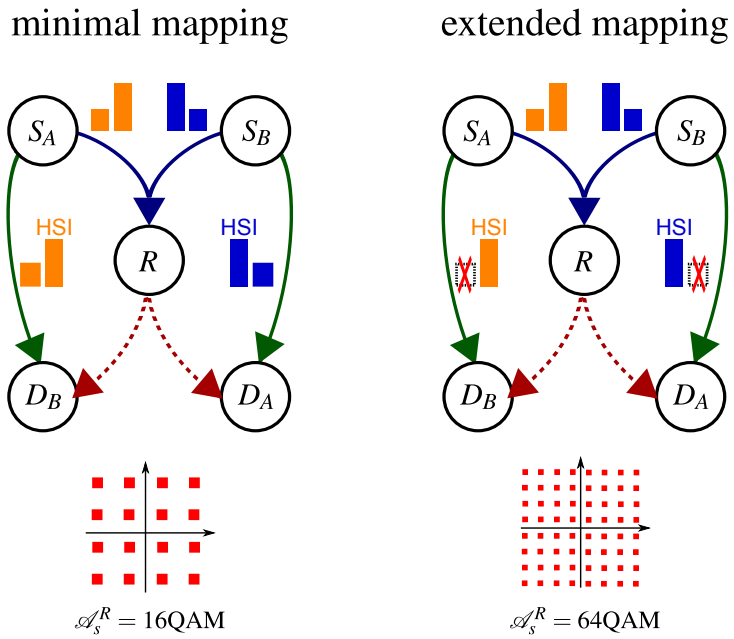

Figure 12.1: WBN with NuT source constellations and extended cardinality relaying.

12.2.1 Relay output alphabet cardinality

The cardinality of the relay output alphabet (M_R) can be bounded (see e.g. [71]) as:

$$M_s \leq M_R \leq M_s^2, \tag{12.1}$$

where M_s is the source alphabet cardinality (assumed identical at both sources). Note again that the equalities in (12.1) correspond to the *minimal* ($M_R = M_s$) and *full* cardinality ($M_R = M_s^2$) relaying (see Section 3.2.2). Obviously, the relay alphabet cardinality is affected by actual channel conditions, i.e. by the quality of HSI channels (e.g. full cardinality will be required if HSI is completely missing at one destination) [24]. An in-depth analysis of the mutual relation between the anticipated HSI link quality and the required relay alphabet cardinality is available in [24], where the systematic algorithm for the design of suitable HNC mapper is derived. The algorithm in [24] (see Algorithm 11.1) allows to design the HNC mapper for arbitrary source alphabet cardinality (and anticipated HSI link quality), i.e. including the extended cardinality case ($M_R > M_s$), which is discussed in the following sections.

12.3 Non-uniform 2-slot alphabets

A goal of the employed source constellations in WBN is twofold: first to deliver reliably source data to the relay; and second, within the same transmission, to secure (at least partially) the transfer of HSI to the respective destination (Fig. 12.1). We show that the NuT constellations are well suited to meet both these objectives, especially in case of the extended cardinality relaying.

The NuT constellations were originally proposed in [16] (see Chapter 7) to suppress the negative impact of *MAC channel parametrization* on the HDF relaying performance in 2-WRC. Being robust to channel parametrization effects, the NuT alphabets avoid the requirement of phase pre-rotation (or adaptive processing) while preserving the $\mathbb{C}^1$ (per symbol slot) dimensionality constraint (avoiding thereby

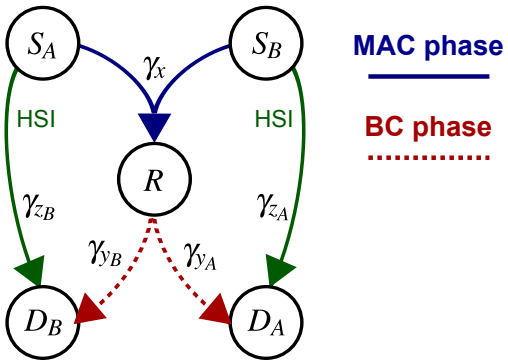

Figure 12.2: SNRs of individual links in WBN with HDF strategy.

the throughput reduction). This is achieved by a non-uniform re-allocation of power between the slots of the 2-slot *super-symbol* (formed by pairing of two subsequent source symbols), where a conventional linear modulation constellation is used as the base (per-slot) alphabet.

Distribution of output power within the 2-slot super-symbol is controlled by the *power scaling factor* $s_f \in (0,2)$ to guarantee the constant average power of the super-symbol. The NuT constellation $\left(\mathrm{NuT}\left(\mathscr{A}_s; s_f\right)\right)$ is hence a 2-source alphabet:

$$\mathscr{A}_s^A = \left[\sqrt{s_f}\cdot\mathscr{A}_s; \sqrt{2-s_f}\cdot\mathscr{A}_s\right], \tag{12.2}$$

$$\mathscr{A}_s^B = \left[\sqrt{2-s_f}\cdot\mathscr{A}_s; \sqrt{s_f}\cdot\mathscr{A}_s\right], \tag{12.3}$$

where the base alphabet $\mathscr{A}_s$ is a conventional linear modulation constellation (e.g. BPSK, QPSK).

Note that $\mathrm{NuT}\left(\mathscr{A}_s; 1\right)$ is a pure 2-slot extension of a conventional modulation with equal per-slot power. We use $\mathrm{NuT}\left(\mathscr{A}_s; 1\right)$ whenever a comparison with conventional linear modulation is required, since it has an identical performance. The cardinality of NuT constellation is obviously $M_s = |\mathscr{A}_s|^2$. An example $\mathrm{NuT}\left(\mathrm{QPSK}; 0.25\right)$ constellation with $M_s = 16$ is in Fig. 12.1 (for details see the NuT alphabet design Algorithm 7.1).

12.3.1 Performance as the HSI link alphabet

The NuT alphabets' robustness to the MAC channel parametrization is demonstrated in [16]. In WBN, the employed source alphabets are, however, also carriers of HSI (see Fig. 12.2), which rises some additional requirements on the alphabet properties/design. In this section we look on the secondary purpose of the alphabet, i.e. on its capability to deliver HSI (at least partial) to the respective destination.

Without loss of generality we focus solely on $\mathscr{A}_s^A$ part of the $\mathrm{NuT}\left(\mathrm{QPSK}; s_f\right)$ alphabets ($s_f \in \{1, 0.25\}$) and we analyze the alphabet-constrained capacity/mutual information as $C_{\mathrm{HSI}} = I(c_A; z_B)$ (for details on alphabet-constrained capacity evaluation see [96]). Comparison of mutual information performance of the observed alphabets is in Fig. 12.3.

Note that the non-uniform per-slot power ($s_f \neq 1$), required to improve the MAC phase performance [16], results in a deterioration of an aggregate (2-slot) C_{HSI} performance. However, as it is also obvious from Fig. 12.3, a significant SNR gain can be observed for the second slot of $\mathrm{NuT}\left(\mathrm{QPSK}; 0.25\right)$ constellation. This gain can be generally evaluated as

$$G_{\mathrm{NuT}}\left(s_f\right) = 10\log_{10}\left(\max\left(s_f, 2-s_f\right)\right), \tag{12.4}$$

which corresponds to the SNR gain of the "stronger" slot of the NuT alphabet (compared to conventional linear modulation). From (12.4) we have a gain of $G_{\mathrm{NuT}}\left(0.25\right) \approx 2.34\,\mathrm{dB}$ for the alphabet with $s_f = 0.25$.

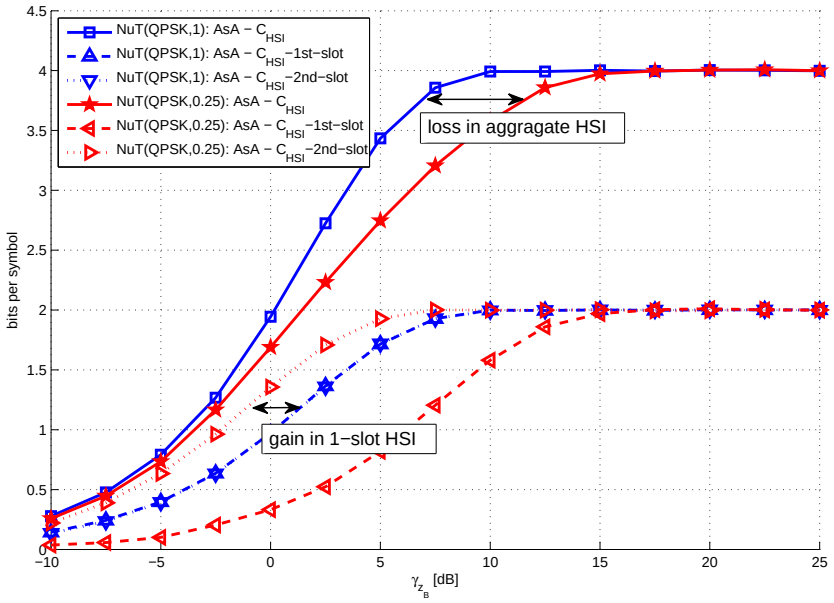

Figure 12.3: Mutual information of $\mathscr{A}_S^A$ for NuT$(\text{QPSK};1)$ & NuT$(\text{QPSK};0.25)$ alphabets. Per-slot mutual information is also evaluated to emphasize the 2-slot nature of NuT constellations. Note that NuT$(\text{QPSK};0.25)$ has better one-slot performance (for 2nd slot) than NuT$(\text{QPSK};1)$, although its aggregate 2-slot performance is worse.

As it is shown in the following section, this superior one-slot mutual information performance can be conveniently exploited in the extended cardinality relaying. Note again that in order to utilize this we need to use the extended relay output HNC map.

12.4 Numerical results

To demonstrate the feasibility of NuT constellation in WBN we evaluate the overall system BER. Without loss of generality we focus on the D_B processing. As it is obvious from Fig. 12.2, D_B has two channel observations – the relay (network-coded) signal $y_B(c_R)$ and HSI link $z_B(c_A)$.

The MAC channel is considered to be parametric (Rician fading channels h_{S_AR}, h_{S_BR} with a Rician factor $K = 10\,\text{dB}$ are assumed) to embrace the detrimental effects of channel parametrization on the WNC processing. The equivalent SNRs are evaluated on a per-slot basis. The average MAC channel SNR is defined as $\gamma_x = \frac{\overline{\varepsilon}}{2\sigma_{w_R}^2}\mathbb{E}\left[|h_A|^2 + |h_B|^2\right]$ and the individual links' SNRs are defined as $\gamma_{z_B} = \frac{\overline{\varepsilon}}{\sigma_{w'_B}^2}$, $\gamma_{y_B} = \frac{\overline{\varepsilon}}{\sigma_{w''_B}^2}$, where $\overline{\varepsilon} = 1$ is an equivalent one-slot alphabet mean symbol energy (mean symbol energy of the whole NuT super-symbol is equal to 2) and $\sigma_{w'_i}^2$ (respectively $\sigma_{w''_i}^2$) is a variance of the circularly symmetric complex Gaussian noise on the HSI (respectively relay$\rightarrow$destination) link. Particular bit mapping to constellation symbols and HNC maps are designed according to the design rules presented in [24] (see Chapter 11). For simplicity reasons we do not use error-correcting codes.

We observe an overall ($S_B \rightarrow D_B$) BER performance as a function of HSI link SNR (γ_{z_B}). The results are parametrized by $R \rightarrow D_B$ SNR (γ_{y_B}), while the average MAC channel SNR (γ_x) is supposed to be constant. In the following sections we introduce the observed BER performance results separately for minimal and extended cardinality relaying. To show a relevant comparison of the NuT and conventional

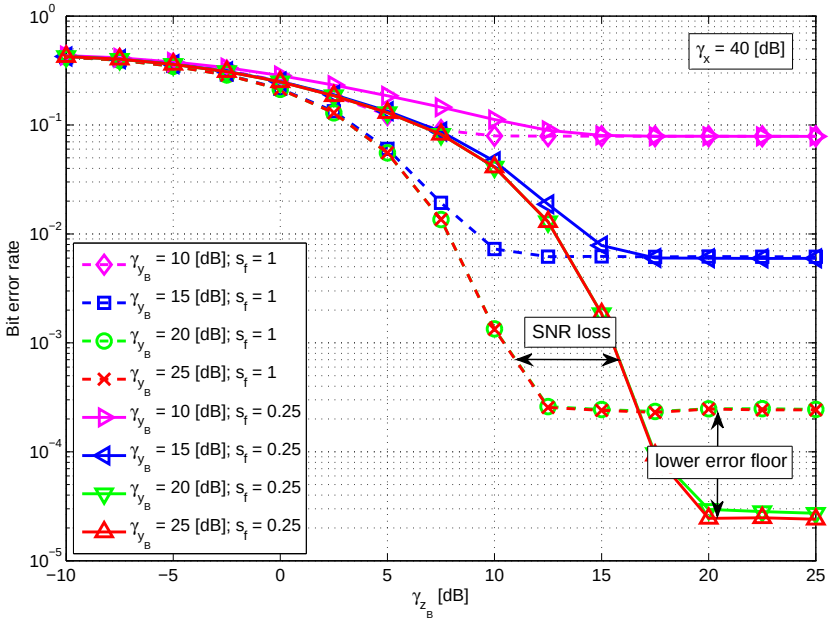

Figure 12.4: Minimal cardinality relaying ($M_R = 16$, $\mathscr{A}_s^R = 16$QAM), destination D_B BER (constellations NuT$(\mathrm{QPSK};1)$ & NuT$(\mathrm{QPSK};0.25)$). Note the error floor induced by MAC and $R \to D_B$ channel SNRs. Performance loss of NuT$(\mathrm{QPSK};0.25)$ due to the worse aggregate HSI (see Fig. 12.3) can be also observed.

linear modulation constellations, we always compare the performance of the $\mathscr{A}_s^A$ for NuT$(\mathrm{QPSK};1)$ and NuT$(\mathrm{QPSK};0.25)$ alphabets. Note again that the performance of NuT$(\mathrm{QPSK};1)$ is identical to that of the corresponding base-alphabet (i.e. QPSK in this case) [16].

12.4.1 Minimal cardinality relaying

In minimal cardinality HDF, both slots of NuT super-symbol are utilized as HSI to enable successful decoding of required data stream (from the received relay signal) at the destination. This allows to keep the cardinality of the relay output identical with the cardinality of individual source alphabets ($M_R = M_s$).

Before proceeding to the BER performance results, it is appropriate to briefly discuss the anticipated behavior. Since the MAC channel SNR is considered to be constant in BER evaluation, an error floor (given by the actual MAC and $R \to D_B$ channel SNRs) is expected. This is obviously given by the absence of the direct link ($S_B \to D_B$). If the relevant hierarchical data cannot be retrieved reliably by the relay in the MAC phase, the errors are propagated to destination (regardless of the HSI link quality). Note that this is true in general, i.e. even for the extended cardinality relaying. On the other hand, for the minimal cardinality case there should be some performance loss given by the worse aggregate HSI performance of the NuT$(\mathrm{QPSK};0.25)$ constellation (see Fig. 12.3). The simulated BER performance for the observed alphabets and minimal cardinality relaying ($M_R = 16$) is in Fig. 12.4.

12.4.2 Extended cardinality relaying

The superior MAC phase performance of the NuT$(\mathrm{QPSK};0.25)$ constellation results in the lower error floor (for sufficiently high γ_{y_B}). However, a significant performance loss can be observed for $\gamma_{z_B} \leq 17\,\mathrm{dB}$

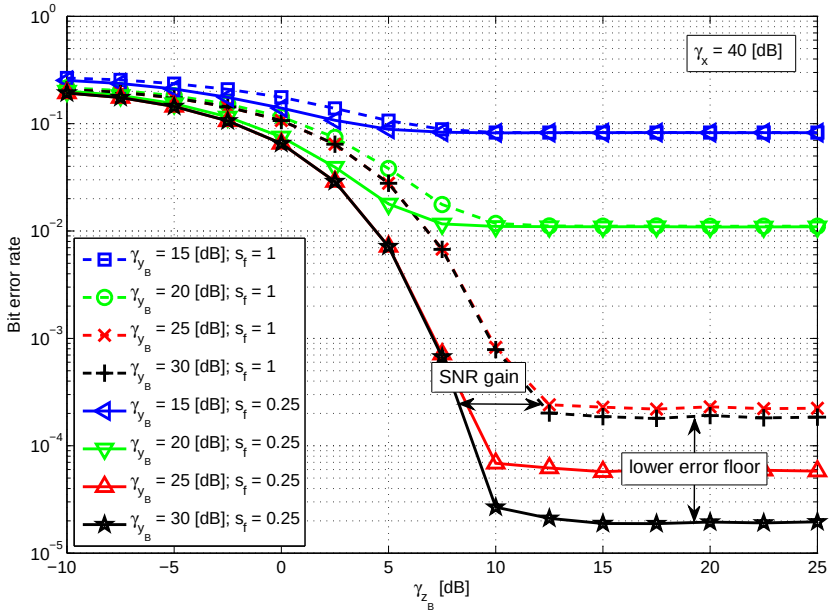

Figure 12.5: Extended cardinality relaying ($M_R = 64$, $\mathscr{A}_s^R = 64$QAM), destination D_B BER (constellations NuT$(\mathrm{QPSK};1)$ & NuT$(\mathrm{QPSK};0.25)$). Note the error floor induced by MAC and $R \to D_B$ channel SNRs. Performance gain of NuT$(\mathrm{QPSK};0.25)$ constellation induced by the better one-slot HSI performance (see Fig. 12.3) can be also observed.

as a consequence of the worse aggregate HSI performance of the NuT$(\mathrm{QPSK};0.25)$ constellation (see Fig. 12.3). Encouraged by potential performance gains of the extended cardinality relaying (see Chapter 11) and the superior one-slot mutual information performance (see Fig. 12.3) we propose to employ the extended cardinality relaying to overcome this behavior (see Fig. 12.1).

We assume that only the stronger slot carries the effective HSI (see Fig. 12.1). Since only partial HSI is available at destinations in this case, the cardinality of the relay output must be greater than the cardinality of individual source alphabets ($M_R > M_s$) to guarantee that both destination can reliably retrieve the desired data from their observations. The simulated BER performance of the extended cardinality relaying is in Fig. 12.5.

12.5 Discussion of results

Surpassing again the performance of conventional linear modulation schemes, the NuT constellations are shown to be a viable solution for HDF relaying in WBN. While their favorable parametric MAC channel performance (see [16]) induces a *lower error floor* in both minimal (Fig. 12.4) & extended (Fig. 12.5) cardinality relaying, the increased reliability of partial one-slot HSI (see Fig. 12.3) transforms into an *additional SNR gain* in the extended cardinality case (Fig. 12.5), where the worse aggregate HSI performance is compensated by an increased cardinality of the relay output alphabet (see [24]). Moreover, as it is obvious from comparison of Figs. 12.4, 12.5, for some specific SNR conditions the extended cardinality relaying outperforms the minimal one, suggesting the extended cardinality WNC to be a preferred solution for relaying in WBN with NuT source constellation alphabets.

Part IV

Conclusions

Chapter 13

Conclusions and future research directions

"Life was so much easier when Apple and Blackberry were just fruits!"

Anonymous

13.1 Summary of contributions

As already demonstrated in the literature (see e.g. [31, 59, 65, 71, 73, 101, 102]), the bidirectional relaying strategies based on a wireless-domain extension of traditional NC principles [14] offer a great potential to improve the performance of future wireless communication networks. Even in the very basic network scenarios (e.g. 2-WRC), these WNC relaying strategies (see e.g. [13, 65, 71]) can provide a two-fold increase of the communication rate, and even larger gains are envisaged in the research community for more complicated multi-source/multi-node network structures.

Unfortunately, even in the basic 2-WRC scenario, the performance of WNC strategies can be seriously degraded due to an inherent *wireless channel parametrization* [65, 71]). Several novel techniques were already introduced (including phase pre-rotation of source node transmissions [65, 68] and adaptation of the relay output symbol mapping [65]) to avoid this performance degradation, however, all these approaches face several drawbacks, including a practical infeasibility of (synchronized) multi-node transmission phase pre-rotation (in fading channels) or a sensitivity to channel estimation errors of adaptive solutions (inaccurate channel estimate results in an improper choice of relay output symbol mapper) [90]. Another research challenge arises when the scope is extended to more complex multi-node systems like WBN, where generally only *partial HSI* (required for WNC system decoding) can be delivered to destinations (due to an insuficcient capacity of corresponding wireless channels) and hence the WNC processing must be appropriately modified to cope with this situation (see e.g. [96, 97]). These two particular research challenges, namely the *WNC processing in parametric channels* (Part II) and implementation of *WNC in networks with partial side information* (Part III) form together the *core of this thesis*.

Our contributions to the design of linear modulation schemes for *parameteric HDF systems* are summarized in Part II. Even though the design of multi-dimensional constellations in $\mathbb{C}^2$ (Chapter 5) appears to be the most simple solution, the increased alphabet cardinality is inherently accompanied with a reduction of achievable througput. Hence, the natural goal of the follow-up work was to find a suitable constellations in $\mathbb{C}^1$ to avoid this inherent drawback of multi-dimensional constellations. However, based on the analysis of Euclidean distance (Chapter 6), it was proved that the detrimental effects of channel

parametrization (eXclusive law failures) cannot be prevented in case of conventional modulation schemes in $\mathbb{C}^1$ (excepting the binary alphabets). Fortunatelly, it is possible to at least suppress this harmful behaviour of channel parametrization by a design of novel *NuT* constellation alphabets (Chapter 7), if the 2-WRC system operates in *Rician fading channels*. The proposed NuT alphabets are robust to channel parametrization effects in Rician channels, outperforming the traditional linear modulation schemes (in the sense of SER performance) without sacrificing the overall system throughput.

Part III of the thesis summarizes our original contributions in the field of *partial/imperfect HSI processing* in WNC networks. The *SC-based scheme* (Chapter 9) for relaying in WBN is capable to adapt to arbitrary amount of HSI and hence it provides a natural information theoretic tool for the implementation of HDF strategy in WBN. Moreover, all conventional bi-directional 3-step (DF) and 2-step (AF, JDF and HDF) WNC strategies can be modified to guarantee that successful decoding at destinations is made possible even if only partial HSI is available (Chapter 10). The (modified) HDF strategy provides the *best performance* among all the WNC strategies, even under the partial HSI condition. Another crucial step in the design of *practical HDF processing* for partial HSI systems is the choice of suitable eXclusive mapping operation at the relay. The design of the *set of eXclusive relay output mappers* (Chapter 11) provides a systematic tool for a construction of relay output mapping for WBN with arbitrary source alphabet cardinality and HSI link quality. Finally, the promising parametric channel performance of NuT constellations is rediscovered in WBN, where the increased reliability of *partial one-slot HSI* transforms into an *additional SNR gain* in BER performance of the system (Chapter 12).

13.2 Future research directions

A huge progress was achieved in the field of physical layer algorithms research during the last few decades. Linear, nonlinear and multi-carrier modulation schemes, sophisticated coding principles (e.g. turbo codes, LDPC codes etc.), together with iterative decoding principles and space-time coding for multi-antenna terminals has introduced a giant leap in performance of wireless communication networks. However, most of these results are relatively tightly connected with a traditional (point-to-point) understanding of the physical layer.

While the point-to-point communication is already covered by a relatively mature theory, only limited results are still available for general *multi-node, multi-source* wireless network scenarios. Here the concepts of cooperative communications (e.g. relaying, NC, WNC etc.) are becoming more and more important. Although the complexity of research in this area is greatly increased (as compared to the conventional single-link physical layer), appealing performance gains are envisaged in the research community, with some promising initial results being already available. The paradigm shift of physical layer research focus from point-to-point to general multi-source, multi-node networks is hence a logical evolutionary step. However, it is evident that the research in this area is still only at its very beginning. There are very few rigorous research results available up to this day, and a vast number of challenging research problems still remains to be solved, but it is clear that only a perpetual progress in this cutting-edge research area can guarantee that the ever-growing requirements of *fast and reliable communication* and *omnipresent connectivity* in future wireless networks could be met.

In this thesis we focus on *two specific research problems* in the design of WNC networks. The results presented in this thesis have a reasonable potential to push the state-of-the-art beyond the limits induced by the conventional point-to-point interpretation of the physical layer. Implementation of these novel PHY concepts, algorithms and results can help to significantly improve the performance and reliability (robustness) of future cooperative wireless communication systems, including the mobile or wireless sensor networks.

Numerous challenging research questions are yet to be answered to enable a *practical implementation of WNC* in real-world wireless systems, and moreover, the extension of WNC-based processing to *general*

(random) multi-source, multi-node networks also represents a very intricate and demanding research area [28]. Nevertheless, being encouraged by the results of our research efforts in the field of WNC, we are very keen to focus our future research endeavour on these interesting (but challenging) WNC research problems.

Bibliography

[1] R. Axelrod, *The Evolution of Cooperation*. Basic Books, 1984.

[2] F. P. Fitzek and M. D. Katz, *Cooperation in Wireless Networks: Principles and Applications*. Springer, 2006.

[3] M. Dohler and Y. Li, *Cooperative Communications: Hardware Channel and PHY*. John Wiley & Sons, 2010.

[4] V. Tarokh, *New Directions in Wireless Communications Research*. Springer, 2009.

[5] C. E. Shannon, "A mathematical theory of communication," *The Bell System Technical Journal*, vol. 27, pp. 379–423, 623–656, 1948.

[6] T. M. Cover and J. A. Thomas, *Elements of Information Theory*. John Wiley & Sons, 1991.

[7] A. E. Gamal and Y.-H. Kim, *Network Information Theory*. Cambridge University Press, 2011.

[8] E. van der Meulen, "Three-terminal communication channels," *Advances in Applied Probability*, no. 3, pp. 120–154, 1971.

[9] T. M. Cover and A. A. E. Gamal, "Capacity theorems for the relay channel," *IEEE Trans. Inf. Theory*, vol. IT-25, pp. 572–584, Sept. 1979.

[10] B. Nazer and M. Gastpar, "Reliable physical layer network coding," *Proc. IEEE*, vol. 99, no. 3, pp. 438–460, 2011.

[11] A. Goldsmith, M. Effros, R. Koetter, M. Médard, A. Ozdaglar, and L. Zheng, "Beyond Shannon: The quest for fundamental performance limits of wireless ad hoc networks," *IEEE Communications Mag.*, vol. 49, pp. 195–205, May 2011.

[12] S. Zhang, S.-C. Liew, and L. Lu, "Physical-layer network coding: Tutorial, survey, and beyond," *Physical Communication*, vol. 2012, pp. 1–39, 2012. doi:10.1016/j.phycom.2012.05.002.

[13] B. Nazer and M. Gastpar, "Compute-and-forward: Harnessing interference through structured codes," *IEEE Trans. Inf. Theory*, vol. 57, no. 10, pp. 6463–6486, 2011.

[14] R. W. Yeung, S.-Y. R. Li, N. Cai, and Z. Zhang, *Network Coding Theory*. NOW Publishers, 2006.

[15] T. Uricar and J. Sykora, "Design criteria for hierarchical exclusive code with parameter-invariant decision regions for wireless 2-way relay channel," *EURASIP J. on Wireless Comm. and Netw.*, vol. 2010, pp. 1–13, 2010. doi:10.1155/2010/921427.

[16] T. Uricar and J. Sykora, "Non-uniform 2-slot constellations for bidirectional relaying in fading channels," *IEEE Commun. Lett.*, vol. 15, no. 8, pp. 795–797, 2011.

[17] T. Uricar and J. Sykora, "Non-uniform 2-slot constellations for relaying in butterfly network with imperfect side information," *IEEE Commun. Lett.*, vol. 16, no. 9, pp. 1369–1372, 2012.

[18] T. Uricar, "Parameter-invariant hierarchical eXclusive alphabet design for 2-WRC with HDF strategy," *Acta Polytechnica*, vol. 50, no. 4, pp. 79–86, 2010.

[19] T. Uricar, B. Qian, J. Sykora, and W. H. Mow, "Wireless (physical layer) network coding with limited side-information: Maximal sum-rates in 5-node butterfly network," Submitted for publication.

[20] T. Uricar and J. Sykora, "Extended design criteria for hierarchical eXclusive code with pairwise parameter-invariant boundaries for wireless 2-way relay channel," in *COST 2100 MCM*, (Vienna, Austria), pp. 1–8, Sept. 2009. TD-09-952.

[21] T. Uricar, J. Sykora, and M. Hekrdla, "Example design of multi-dimensional parameter-invariant hierarchical eXclusive alphabet for layered HXC design in 2-WRC," in *COST 2100 MCM*, (Athens, Greece), pp. 1–8, Feb. 2010. TD-10-10088.

[22] T. Uricar and J. Sykora, "Hierarchical eXclusive alphabet in parametric 2-WRC - Euclidean distance analysis and alphabet construction algorithm," in *COST 2100 MCM*, (Aalborg, Denmark), pp. 1–9, June 2010. TD-10-11051.

[23] T. Uricar and J. Sykora, "Hierarchical network code mapper design for adaptive relaying in butterfly network," in *COST IC1004 MCM*, (Barcelona, Spain), pp. 1–9, Feb. 2012. TD-12-03048.

[24] T. Uricar and J. Sykora, "Systematic design of hierarchical network code mapper for butterfly network relaying," in *Proc. European Wireless Conf. (EW)*, (Poznan, Poland), pp. 1–8, Apr. 2012.

[25] T. Uricar and J. Sykora, "Non-uniform 2-slot constellations: Design algorithm and 2-way relay channel performance," in *COST IC1004 MCM*, (Lyon, France), pp. 1–7, May 2012. TD-12-04041.

[26] T. Uricar and J. Sykora, "Wireless (Physical Layer) Network Coding in 5-node butterfly network: Superposition coding approach," in *COST IC1004 MCM*, (Malaga, Spain), pp. 1–9, Feb. 2013. TD-13-06026.

[27] T. Uricar, B. Qian, J. Sykora, and W. H. Mow, "Superposition coding for wireless butterfly network with partial network side-information," in *Proc. IEEE Wireless Commun. Network. Conf. (WCNC)*, (Shanghai, China), pp. 1–6, Apr. 2013.

[28] T. Uricar, T. Hynek, P. Prochazka, and J. Sykora, "Wireless-aware network coding: Solving a puzzle in acyclic multi-stage cloud networks," in *Proc. Int. Symp. of Wireless Communication Systems (ISWCS)*, (Ilmenau, Germany), pp. 612–616, Aug. 2013.

[29] Y. Zhang, H.-H. Chen, and M. Guizani, *Cooperative Wireless Communications*. CRC Press, 2009.

[30] E. van der Meulen, *Transmission of information in a T-terminal discrete memoryless channel*. Phd thesis, Dept. of Statistics, University of California, Berkeley, 1968.

[31] P. Popovski and H. Yomo, "Physical network coding in two-way wireless realy channels," in *Proc. IEEE Internat. Conf. on Commun. (ICC)*, 2007.

[32] R. Ahlswede, N. Cai, S.-Y. R. Li, and R. W. Yeung, "Network information flow," *IEEE Trans. Inf. Theory*, vol. 46, pp. 1204–1216, July 2000.

[33] C. Fragouli, J.-Y. L. Boudec, and J. Widmer, "Network coding: An instant primer," *Computer Communication Review (ACM SIGCOMM)*, vol. 36, pp. 63–68, Jan. 2006.

[34] Y. Chen, S. Kishore, and J. T. Li, "Wireless diversity through network coding," in *Proc. IEEE Wireless Commun. Network. Conf. (WCNC)*, 2006.

[35] D. H. Woldegebreal and H. Karl, "Multiple-access relay channel with network coding and non-ideal source-relay channels," in *Proc. Int. Symp. of Wireless Communication Systems (ISWCS)*, pp. 732–736, Oct. 2007.

[36] S. Zhang, Y. Zhu, S.-C. Liew, and K. B. Letaief, "Joint design of network coding and channel decoding for wireless networks," in *Proc. IEEE Wireless Commun. Network. Conf. (WCNC)*, 2007.

[37] C. Hausl, F. Schreckenbach, and I. Oikonomidis, "Iterative network and channel decoding on a Tanner graph," in *Proc. Annual Allerton Conf. on Commun., Cont., and Comp.*, (Monticello, Illinois, USA), Sept. 2005.

[38] D. J. MacKay, *Information Theory, Inference, and Learning Algorithms*. Cambridge University Press, 2005.

[39] C. Hausl and P. Dupraz, "Joint network-channel coding for the multiple-access relay channel," in *Proc. International Workshop on Sensor and Ad Hoc Communications and Networks (SECON)*, (New York, USA), June 2006.

[40] S. Katti, D. Katabi, W. Hu, H. Rahul, and M. Medard, "The importance of being opportunistic: Practical network coding for wireless environments," in *Proc. Annual Allerton Conf. on Commun., Cont., and Comp.*, (Monticello, Illinois, USA), Sept. 2005.

[41] S. Katti, H. Rahul, W. Hu, D. Katabi, M. Médard, and J. Crowcroft, "XORs in the air: Practical wireless network coding," *IEEE/ACM Transactions on Networking*, vol. 16, pp. 497–510, June 2008.

[42] R. W. Yeung, *Information Theory and Network Coding*. Springer-Verlag, 2008.

[43] C. Fragouli and E. Soljanin, *Network coding applications*. NOW Publishers, 2007.

[44] C. Fragouli and E. Soljanin, *Network coding fundamentals*. NOW Publishers, 2007.

[45] T. Ho and D. S. Lun, *Network Coding: An Introduction*. Cambridge University Press, 2008.

[46] A. S. Avestimehr, S. N. Diggavi, and D. N. Tse, "A deterministic model for wireless relay networks an its capacity," in *Proc. IEEE Information Theory Workshop on Information Theory for Wireless Networks*, pp. 1–6, 2007.

[47] A. S. Avestimehr, S. N. Diggavi, and D. N. Tse, "Approximate capacity of gaussian relay networks," in *Proc. IEEE Internat. Symp. on Inf. Theory (ISIT)*, pp. 474–478, 2008.

[48] A. S. Avestimehr and T. Ho, "Approximate capacity of the symmetric half-duplex gaussian butterfly network," in *Proc. IEEE Inf. Theory Workshop (ITW)*, pp. 311–315, 2009.

[49] A. S. Avestimehr, S. N. Diggavi, and D. N. Tse, "Wireless network information flow: A deterministic approach," *IEEE Trans. Inf. Theory*, vol. 57, no. 4, pp. 1872–1905, 2011.

[50] M. A. Khojastepour, *Distributed Cooperative Communications in Wireless Networks*. Phd thesis, Rice University, Dept. of Electrical and Computer Engineering, 2004.

[51] G. Kramer, M. Gastpar, and P. Gupta, "Cooperative strategies and capacity theorems for relay networks," *IEEE Trans. Inf. Theory*, vol. IT-51, pp. 3037–3063, Sept. 2005.

[52] A. Nosratinia, T. E. Hunter, and A. Hedayat, "Cooperative communication in wireless networks," *IEEE Communications Mag.*, vol. 42, pp. 74–80, Oct. 2004.

[53] A. Chakrabarti, E. Erkip, A. Sabharwal, and B. Aazhang, "Code designs for cooperative communication," *IEEE Signal Process. Mag.*, vol. 24, Sept. 2007.

[54] J. Castura and Y. Mao, "Rateless coding and relay networks," *IEEE Signal Process. Mag.*, vol. 24, Sept. 2007.

[55] M. Luby, "LT codes," in *Proc. Annual IEEE Symposium on Foundations of Computer Science (FOCS)*, (Vancouver, Canada), 2002.

[56] A. Shokrollahi, "Raptor codes," *IEEE Trans. Inf. Theory*, vol. IT-52, pp. 2551–2567, June 2006.

[57] J. Castura and Y. Mao, "Rateless coding for wireless relay channels," *IEEE Trans. Wireless Commun.*, vol. 6, pp. 1638–1642, May 2007.

[58] S. Katti, S. Gollakota, and D. Katabi, "Embracing wireless interference: Analog network coding," in *Proc. Annual SIGCOMM Conference*, (Kyoto, Japan), 2007.

[59] P. Larsson, N. Johansson, and K.-E. Sunell, "Coded bi-directional relaying," in *Proc. IEEE Vehicular Technology Conf. (VTC)*, pp. 851–855, Spring 2006.

[60] Y. Wu, P. A. Chou, and S.-Y. Kung, "Information exchange in wireless networks with network coding and physical-layer broadcast," in *Proc. Conference on Information Sciences and Systems (CISS)*, March 2005.

[61] C. Hausl and J. Hagenauer, "Iterative network and channel decoding for the two-way relay channel," in *Proc. IEEE Internat. Conf. on Commun. (ICC)*, 2006.

[62] P. Popovski and H. Yomo, "Bi-directional amplification of throughput in a wireless multi-hop network," in *Proc. IEEE Vehicular Technology Conf. (VTC)*, Spring 2006.

[63] S. Zhang, S.-C. Liew, and P. P. Lam, "Hot topic: Physical layer network coding," in *Proc. Annual International Conference on Mobile Computing and Networking (MobiCom)*, (Los Angeles, CA, USA), 2006.

[64] B. Rankov and A. Wittneben, "Achievable rate regions for the two-way relay channel," in *Proc. IEEE Internat. Symp. on Inf. Theory (ISIT)*, July 2006.

[65] T. Koike-Akino, P. Popovski, and V. Tarokh, "Optimized constellations for two-way wireless relaying with physical network coding," *IEEE J. Sel. Areas Commun.*, vol. 27, pp. 773–787, June 2009.

[66] P. Popovski and H. Yomo, "The anti-packets can increase the achievable throughput of a wireless multi-hop network," in *Proc. IEEE Internat. Conf. on Commun. (ICC)*, 2006.

[67] S. Zhang, S.-C. Liew, and L. Lu, "Physical layer network coding schemes over finite and infinite fields," in *Proc. IEEE Global Telecommunications Conf. (GlobeCom)*, 2008.

[68] S. Zhang and S.-C. Liew, "Applying physical-layer network coding in wireless networks," *EURASIP J. on Wireless Comm. and Netw.*, vol. 2010, pp. 1–12, 2010. doi:10.1155/2010/870268.

[69] J. N. Laneman, D. N. C. Tse, and G. W. Wornell, "Cooperative diversity in wireless networks: Efficient protocols and outage behavior," *IEEE Trans. Inf. Theory*, vol. 50, no. 12, pp. 3062–3080, 2004.

[70] B. Rankov and A. Wittneben, "Spectral efficient protocols for half-duplex fading relay channels," *IEEE J. Sel. Areas Commun.*, vol. SAC-25, pp. 379–389, Feb. 2007.

[71] J. Sykora and A. Burr, "Layered design of hierarchical exclusive codebook and its capacity regions for HDF strategy in parametric wireless 2-WRC," *IEEE Trans. Veh. Technol.*, vol. 60, pp. 3241–3252, Sept. 2011.

[72] J. Liu, M. Tao, and Y. Xu, "Pairwise check decoding for LDPC coded two-way relay block fading channels," *IEEE Trans. Commun.*, vol. 60, no. 8, pp. 2065–2076, 2012.

[73] S. J. Kim, P. Mitran, and V. Tarokh, "Performance bounds for bidirectional coded cooperation protocols," *IEEE Trans. Inf. Theory*, vol. 54, Nov. 2008.

[74] T. J. Oechtering, C. Schnurr, I. Bjelakovic, and H. Boche, "Broadcast capacity region of two-phase bidirectional relaying," *IEEE Trans. Inf. Theory*, vol. 54, Jan. 2008.

[75] A. Li, Y. Yan, and H. Kayama, "An enhanced denoise-and-forward relaying scheme for fading channel with low computational complexity," *IEEE Signal Process. Lett.*, vol. 15, 2008.

[76] B. Nazer and M. Gastpar, "Compute-and-forward: Harnessing interference with structured codes," in *Proc. IEEE Internat. Symp. on Inf. Theory (ISIT)*, pp. 772–776, 2008.

[77] K. Narayanan, M. P. Wilson, and A. Sprintson, "Joint physical layer coding and network coding for bi-directional relaying," in *Proc. Annual Allerton Conf. on Commun., Cont., and Comp.*, 2007.

[78] B. Hern and K. Narayanan, "Multilevel coding schemes for compute-and-forward," in *Proc. IEEE Internat. Symp. on Inf. Theory (ISIT)*, pp. 1713–1717, 2011.

[79] T. Koike-Akino, P. Popovski, and V. Tarokh, "Denoising maps and constellations for wireless network coding in two-way relaying systems," in *Proc. IEEE Global Telecommunications Conf. (GlobeCom)*, 2008.

[80] V. T. Muralidharan and B. S. Rajan, "Performance analysis of adaptive physical layer network coding for wireless two-way relaying," *IEEE Trans. Wireless Commun.*, vol. 12, no. 3, pp. 1328–1339, 2013.

[81] V. T. Muralidharan, V. Namboodiri, and B. S. Rajan, "Wireless network-coded bidirectional relaying using latin squares for M-PSK modulation," *IEEE Trans. Inf. Theory*, in press.

[82] Z. Faraji-Dana and P. Mitran, "On non-binary constellations for channel-coded physical-layer network coding," *IEEE Trans. Wireless Commun.*, vol. 12, no. 1, pp. 312–319, 2013.

[83] S. Zhang and S.-C. Liew, "Channel coding and decoding in a relay system operated with physical-layer network coding," *IEEE J. Sel. Areas Commun.*, vol. 27, pp. 788–796, June 2009.

[84] U. Bhat and T. M. Duman, "Decoding strategies at the relay with physical-layer network coding," *IEEE Trans. Wireless Commun.*, vol. 11, no. 12, pp. 4503–4513, 2012.

[85] S. Wang, Q. Song, L. Guo, and A. Jamalipour, "Constellation mapping for physical-layer network coding with M-QAM modulation," in *Proc. IEEE Global Telecommunications Conf. (GlobeCom)*, pp. 4429–4434, 2012.

[86] J. Sykora and A. Burr, "Hierarchical alphabet and parametric channel constrained capacity regions for HDF strategy in parametric wireless 2-WRC," in *Proc. IEEE Wireless Commun. Network. Conf. (WCNC)*, (Sydney, Australia), pp. 1–6, Apr. 2010.

[87] T. Koike-Akino, P. Popovski, and V. Tarokh, "Denoising strategy for convolutionally-coded bidirectional relaying," in *Proc. IEEE Internat. Conf. on Commun. (ICC)*, 2009.

[88] R. Zamir, "Lattices are everywhere," in *Proc. IEEE Inf. Theory and Applications Workshop (ITA)*, pp. 392–421, 2009.

[89] J. Liu, M. Tao, and Y. Xu, "Pseudo exclusive-OR for LDPC coded two-way relay block fading channels," in *Proc. IEEE Internat. Conf. on Commun. (ICC)*, pp. 1–5, 2011.

[90] K. Yasami, A. Razi, and A. Abedi, "Analysis of channel estimation error in physical layer network coding," *IEEE Commun. Lett.*, vol. 15, pp. 1029 –1031, Oct. 2011.

[91] D. Fang and A. Burr, "Rotationally invariant coded modulation for physical layer network coding in two-way relay fading channel," in *Proc. European Wireless Conf. (EW)*, pp. 1–6, 2012.

[92] V. T. Muralidharan and B. S. Rajan, "Distributed space time coding for wireless two-way relaying," *IEEE Trans. Signal Process.*, vol. 61, no. 4, pp. 980–991, 2013.

[93] M. Hekrdla and J. Sykora, "Design of uniformly most powerful alphabets for HDF 2-way relaying employing non-linear frequency modulations," *EURASIP J. on Wireless Comm. and Netw.*, vol. 128, pp. 1–18, Oct. 2011.

[94] M. Hekrdla and J. Sykora, "Uniformly most powerful alphabet for HDF two-way relaying designed by non-linear optimization tools," in *Proc. Int. Symp. of Wireless Communication Systems (ISWCS)*, pp. 594 –598, Nov. 2011.

[95] T. Uricar, "Constellation alphabets for hierarchical relaying in multiple-access relay channel," in *Proc. POSTER 2011 - 15th International Student Conference on Electrical Engineering*, (Prague, Czech Republic), pp. 1–5, May 2011.

[96] J. Sykora and A. Burr, "Network coded modulation with partial side-information and hierarchical decode and forward relay sharing in multi-source wireless network," in *Proc. European Wireless Conf. (EW)*, (Lucca, Italy), 2010.

[97] A. Burr and J. Sykora, "Extended mappings for wireless network coded butterfly network," in *Proc. European Wireless Conf. (EW)*, (Vienna, Austria), 2011.

[98] T. Koike-Akino, P. Popovski, and V. Tarokh, "Adaptive modulation and network coding with optimized precoding in two-way relaying," in *Proc. IEEE Global Telecommunications Conf. (GlobeCom)*, 2009.

[99] V. T. Muralidharan and B. S. Rajan, "Wireless network coding for MIMO two-way relaying," *IEEE Trans. Wireless Commun.*, vol. 12, no. 7, pp. 3566–3577, 2013.

[100] U. Erez and R. Zamir, "Achieving $1/2\log(1+\mathrm{SNR})$ on the AWGN channel with lattice encoding and decoding," *IEEE Trans. Inf. Theory*, vol. 50, pp. 2293–2314, Oct. 2004.

[101] I.-J. Baik and S.-Y. Chung, "Network coding for two-way relay channels using lattices," in *Proc. IEEE Internat. Conf. on Commun. (ICC)*, 2008.

[102] W. Nam, S.-Y. Chung, and Y. H. Lee, "Capacity bounds for two-way relay channels," in *Proc. Int. Zurich Seminar on Communications*, 2008.

[103] W. Nam, S.-Y. Chung, and Y. H. Lee, "Capacity of the gaussian two-way relay channel to within $1/2$ bit," *IEEE Trans. Inf. Theory*, vol. 56, pp. 5488–5494, Nov. 2010.

[104] S. Zhang, S.-C. Liew, and P. P. Lam, "On the synchronization of physical-layer network coding," in *Proc. IEEE Inf. Theory Workshop (ITW)*, pp. 404–408, 2006.

[105] F. Rossetto and M. Zorzi, "On the design of practical asynchronous physical layer network coding," in *Proc. IEEE Workshop on Signal Processing Advances in Wireless Communications*, pp. 469–473, 2009.

[106] D. Wang, S. Fu, and K. Lu, "Channel coding design to support asynchronous physical layer network coding," in *Proc. IEEE Global Telecommunications Conf. (GlobeCom)*, pp. 1–6, 2009.

[107] Y. Huang, S. Wang, Q. Song, L. Guo, and A. Jamalipour, "Synchronous physical-layer network coding: A feasibility study," *IEEE Trans. Wireless Commun.*, in press.

[108] M. H. Firooz, Z. Chen, S. Roy, and H. Liu, "Wireless network coding via modified 802.11 MAC/PHY: Design and implementation on SDR," *IEEE J. Sel. Areas Commun.*, vol. 31, no. 8, pp. 1618–1628, 2013.

[109] L. Lu, T. Wang, S. C. Liew, and S. Zhang, "Implementation of physical-layer network coding," in *Proc. IEEE Internat. Conf. on Commun. (ICC)*, pp. 4734–4740, 2012.

[110] "Ettus inc. universal software radio peripheral." `http://www.ettus.com`

[111] W. Pu, C. Luo, B. Jiao, and F. Wu, "Natural network coding in multi-hop wireless networks," in *Proc. IEEE Internat. Conf. on Commun. (ICC)*, pp. 2388–2392, 2008.

[112] M. Noori and M. Ardakani, "On symbol mapping for binary physical-layer network coding with PSK modulation," *IEEE Trans. Wireless Commun.*, vol. 11, no. 1, pp. 21–26, 2012.

[113] H. J. Yang, Y. Choi, and J. Chun, "Modified high-order PAMs for binary coded physical-layer network coding," *IEEE Commun. Lett.*, vol. 14, no. 8, pp. 689–691, 2010.

[114] J. Liu, M. Tao, Y. Xu, and X. Wang, "Superimposed XOR: A new physical layer network coding scheme for two-way relay channels," in *Proc. IEEE Global Telecommunications Conf. (GlobeCom)*, pp. 1–6, 2009.

[115] J. Sykora and A. Burr, "Hierarchical exclusive codebook design using exclusive alphabet and its capacity regions for HDF strategy in parametric wireless 2-WRC," in *COST 2100 MCM*, (Vienna, Austria), pp. 1–9, Sept. 2009. TD-09-933.

[116] J. Sykora, "Design criteria for parametric hierarchical exclusive constellation space code for wireless 2-way relay channel," in *COST 2100 MCM*, (Valencia, Spain), pp. 1–6, May 2009. TD-09-855.

[117] T. Uricar, "Parameter-invariant hierarchical eXclusive alphabet design for 2-WRC with HDF strategy," in *Proc. POSTER 2010 - 14th International Student Conference on Electrical Engineering*, (Prague, Czech Republic), pp. 1–8, May 2010.

[118] C. D. Meyer, *Matrix Analysis and Applied Linear Algebra*. SIAM: Society for Industrial and Applied Mathematics, 2001.

[119] J. Sykora and E. A. Jorswieck, "Network coded modulation with hdf strategy and optimized beamforming in 2-source 2-relay network," in *Proc. IEEE Vehicular Technology Conf. (VTC)*, pp. 1–6, Fall 2011.

[120] P. Popovski and E. de Carvalho, "Improving the rates in wireless relay systems through superposition coding," *IEEE Trans. Wireless Commun.*, vol. 7, pp. 4831–4836, Dec. 2008.

[121] S. Boyd and L. Vandenberghe, *Convex Optimization*. New York, NY, USA: Cambridge University Press, 2004.

[122] J. Sykora and A. Burr, "Tutorial: Advances in Wireless Network Coding - The future of cloud communications," in *Proc. IEEE Int. Symp. on Personal, Indoor and Mobile Radio Communications (PIMRC)*, Sept. 2013.

[123] G. Ungerboeck, "Channel coding with multilevel/phase signals," *IEEE Trans. Inf. Theory*, vol. 28, pp. 55–67, Jan. 1982.

Appendix I: IEEE Reviewer Appreciation